Studies of the flow of a fluid with density differences caused by turbidity. August 1973.

Author:
Jenkins, B. S.

Publication details:
Commissioning Body: Electricity Commission of New South Wales
Report No. UNSW Water Research Laboratory Report No. 133
0858241056 (ISBN)

Publication Date:
1973

DOI:
https://doi.org/10.4225/53/579ae7aed0736

THE UNIVERSITY OF NEW SOUTH WALES

water research laboratory

Manly Vale, N.S.W., Australia

Report No.133

STUDIES OF THE FLOW OF A FLUID WITH DENSITY DIFFERENCES CAUSED BY TURBIDITY

by

B.S.Jenkins

August 1973

The University of New South Wales
WATER RESEARCH LABORATORY

STUDIES OF THE FLOW OF A FLUID WITH DENSITY DIFFERENCES CAUSED BY TURBIDITY.

by

B.S. Jenkins

Report No. 133

August 1973.

https://doi.org/10.4225/53/579ae7aed0736

Key Words

Sediment Load
Suspension
Computer
Programmes
Eddies
Turbulence
Settling Velocity
Density Currents
Flow
Turbidity
Model Studies

0/85824/105/6

Preface

This work is part of a programme of research concerned with the suspension of sediment in turbulent flow and the related problem of the behaviour of turbidity currents. The work was supported financially by the Electricity Commission of New South Wales.

The study was undertaken by Brian S. Jenkins, lecturer in Civil Engineering and essentially constitutes his thesis presented for the degree of Doctor of Philosophy. The work was supervised by I.R. Wood, formerly Associate Professor in Civil Engineering at the University of New South Wales and now Professor of Civil Engineering at the University of Canterbury, Christchurch, New Zealand.

Printing and publication is by permission of the author through service facilities provided by the Water Research Laboratory.

D.N. Foster,
Officer-in-Charge.

Acknowledgements

The investigation described in this thesis was sponsored by the Electricity Commission of New South Wales.

The author wishes to acknowledge the assistance given by the staff of the Water Research Laboratory of the University of New South Wales, and in particular the advice and encouragement of Professor I.R.Wood (now Professor of Civil Engineering in the University of Canterbury, Christchurch, New Zealand).

The author is indebted to Mrs. P. Decent for the typing of the manuscript, and to Mr. J.A.Reizes of the School of Mechanical and Industrial Engineering of the University of New South Wales for many helpful discussions.

ABSTRACT

The mechanism of suspension of a non-buoyant particle in a turbulent flow has been examined, from the viewpoint of the history of an individual particle.

A computer program developed for the purpose has been employed to compute trajectories of a non-buoyant particle within a field of eddies. The computed trajectories have indicated that the particle may be suspended indefinitely within an individual eddy of the eddy field, or may fall through the eddy field with a fall velocity which differs from the settling velocity of the particle in the quiescent fluid.

A criterion for the suspension of a particle within an eddy has been established. The criterion takes the form of a limiting value of the ratio between a characteristic fluid velocity within the eddy field and the settling velocity of the particle in the quiescent fluid.

The quantitative results are specific to the particular conditions examined. The investigation has, however, demonstrated that in a flow in which the net vertical motion of the fluid is zero the time-averaged fall velocity of a non-buoyant particle may differ from the settling velocity of the particle in the quiescent fluid and may be reduced to zero.

In a series of laboratory experiments, rates of entrainment of fluid across a density discontinuity between two fluid layers have been measured. In these experiments, the turbulent flow of a fluid layer has been simulated by the motion induced by an oscillating grid.

Density discontinuities due to temperature differences, salinity differences and the presence in one layer of suspended particles have been examined. The measured entrainment rates are consistent with the hypothesis that under given conditions the rate of entrainment is dependent upon the molecular diffusivity of the property causing the density discontinuity.

Table of Contents

Table of Contents (cont'd.)

APPENDICES

List of Figures

List of Figures (cont'd.)

List of Tables.

Notation

All symbols are defined within the text. For convenience, the more commonly occurring symbols are defined in the list below. Definitions of symbols and subscripts which are not listed will be found in the text, immediately following the use of the symbol or subscript concerned. Symbols used in appendices are defined within the text of the appendices.

a	=	acceleration
A	=	dimensionless acceleration
A	=	area
$\underset{\sim}{c}$	=	concentration
C_D	=	drag coefficient
d	=	particle diameter
D	=	molecular diffusivity
F	=	force
g	=	gravitational acceleration
h	=	depth of a fluid layer
k	=	added-mass coefficient
K	=	Boltzman's constant
l	=	length
L	=	dimensionless length
m	=	mass
m_p	=	particle mass
m_a	=	added mass
P	=	particle-fluid parameter (PART) $= \frac{\sqrt{gd^3}}{\nu}$
$\mathbb{R}$	=	Reynolds Number
s	=	ratio of density of particle to density of surrounding fluid
t	=	time
T	=	dimensionless time
T	=	absolute temperature
u	=	velocity; velocity component in the x coordinate direction
U	=	dimensionless velocity; dimensionless velocity component in the x coordinate direction
U_e	=	dimensionless characteristic velocity in the model eddy field
U_{ec}	=	limiting value of U_e, for suspension of a particle in an eddy
U_{max}	=	dimensionless maximum velocity in the model eddy field
v	=	velocity; velocity component in the y coordinate direction

Notation (cont'd.)

v_e	=	entrainment velocity
v_s	=	settling velocity of particle in quiescent fluid
V	=	dimensionless velocity; dimensionless velocity component in the y coordinate direction
V_f	=	dimensionless fall velocity of a particle in the model eddy field or in a turbulent flow
V_s	=	dimensionless settling velocity of a particle in quiescent fluid
$\forall$	=	volume
x, y, z	=	Cartesian position coordinates
X, Y	=	dimensionless Cartesian position coordinates
X_c, Y_c	=	dimensionless spacing of eddy centres in the x and y coordinate directions
ν	=	kinematic viscosity
ψ	=	stream function
ρ	=	density
τ	=	time
ξ	=	vorticity

Some of the FORTRAN Variables to which reference is made in the text are defined in the following list. Other variables are defined in Chapter 4, and Table III.1, p.III. 12 - III.14.

PART	=	Particle-Fluid Parameter(P) = $\frac{\sqrt{gd^3}}{\nu}$
GRAV	=	Gravitational Parameter = (s-1.0)
XCNTR	=	dimensionless spacing of eddy centres in the x coordinate direction (X_c)
YCNTR	=	dimensionless spacing of eddy centres in the y coordinate direction (Y_c)
UEDDY	=	dimensionless characteristic velocity in the model eddy field (U_e)

1. Introduction

In contemporary engineering practice, increasing attention is being paid to the significance of density stratification in the phenomena of fluid flow. Increased awareness of environmental considerations has directed attention towards a class of fluid phenomena in which density stratification is invariably of obvious importance. Continuing investigations have served to indicate, furthermore, that the significance of density stratification extends to situations in which its role has not previously been fully acknowledged. The identification of fine-scale density structures in the ocean, for example, has led to an increased recognition of the significance of density stratification in phenomena within the oceans.

A difference between the densities of two adjoining strata of fluid may occur when one or more of the following conditions exists:-

(i) The fluid in one stratum differs in its chemical composition from the fluid in the adjoining stratum.

(ii) The temperature of the fluid in one stratum differs from that of the (otherwise similar) fluid in the adjoining stratum.

(iii) The fluid in one stratum contains dissolved substances, in concentrations different from those applying in an adjoining stratum.

(iv) Particulate material (of a density different from that of the fluid) is present in one fluid stratum, in a concentration different from that applying in an adjoining stratum.

In this dissertation, the terms "density current" and "turbidity current" are used, in referring to the motion of density-stratified fluids. The meanings assigned to these terms are as follows: When a fluid stratum moves (in response to gravitational forces) in relation to an adjacent fluid stratum of a different density, then the flow is termed a "density current". In the particular case of such a flow in which the density difference is due to the presence of suspended particles of solid material (turbidity), the flow is termed a "turbidity current"; this term was introduced by D.W. Johnson (26).

In general, the common situation in which water or other liquid flows in an open channel could be regarded as a density-stratified flow (that is, as a density current) if it is viewed as the flow of a stratum of liquid beneath a stratum of gas (the atmospheric air). In practice, however, the significance of the atmospheric air in such a situation is usually negligible, and the flow is viewed as the motion of a single (liquid) stratum. The effects of density stratification are of significance in those situations in which the difference between the densities of the fluids in adjoining strata is small, in relation to the density of either fluid.

The investigation to be described presently is concerned with certain aspects of the flow of a turbidity current.

Turbidity currents have been observed to occur in situations where a stream bearing a relatively high concentration of suspended material enters a lake or artificial reservoir containing water which is relatively free of suspended material. After flowing to a region of the lake or reservoir in which a sufficient depth of water exists, the suspension-laden water has been observed to descend steeply to the lake bed, and to flow along the bed beneath the relatively clear ambient water of the lake. The zone of descent is characterised by intense large-scale turbulence, and by the presence of floating debris entrapped in its eddies.

Phenomena of this type have been observed at the entry of the Rhine into Lake Constance, and at the entry of the Colorado River into Lake Mead (the reservoir impounded by the Hoover Dam, U.S.A.). In Lake Mead, turbidity currents have been observed to flow for distances in excess of 100 miles without loss of identity through mixing - Bell (4). The Lake Mead turbidity currents consist primarily of suspensions of silt and clay particles of less than 20 microns (20.10^{-3}mm.) in diameter, the ratio of the submerged specific weight of the fluid in the turbidity current to the specific weight of the ambient fluid being of the order of 0.0005, as reported by the A.S.C.E. Task Committee on Sedimentation (1). The suspended material is reported to originate from erosion of the land surface within the catchment area, rather than from erosion of the stream bed.

It has been hypothesised that turbidity currents may be significant agents in the distribution of sediments on the ocean floor, and in the shaping of submarine topography - Daly (12). In a series of small-scale experiments, Kuenen (28) has demonstrated qualitatively the erosive power of a turbidity current and the tendency of a turbidity current to follow a depression in the bed over which it moves. Sediments whose deposition is attributed to turbidity current action are identified by the geological term "turbidites". Middleton (34) has studied the deposition of sediments from turbidity currents.

During the present century, several turbidity currents of sufficient magnitude to be of geological significance have been reported. These have included the Messina Turbidity Current of 1908, described by Ryan and Heezen (42), and the Grand Banks Turbidity Current of 1929. The fracture by the Grand Banks Turbidity Current of a series of telephone cables has permitted the estimation of the velocity and size of the current, as the distances between the cables were known and the times of failure were observed. The estimates finally arrived at must be regarded as somewhat tentative, in view of uncertainties surrounding the original observations and the further assumptions which must be made. A phenomenon of very large scale is however indicated: the thickness of the turbidity current has been estimated as several hundred metres - Kuenen (29), Johnson (27) - its breadth as several hundred kilometres, and the extent of its movement as about 1000 kilometres - Kuenen (29), Charnock (9). The estimated velocities of the current have ranged from about 30 $m.sec^{-1}$ (in a region in which the slope of the ocean bed is about 1 in 170) to about 6 $m.sec^{-1}$ in a region in which the bed slope is about 1 in 1500.

Certain motions of the atmosphere appear to be essentially turbidity currents. Bell (4) has drawn attention to the similarity between turbidity currents in liquids and atmospheric phenomena such as dust storms, volcanic dust clouds and "nuées ardentes" (clouds of glowing volcanic ash). Avalanches of the "powder-snow" type appear to be essentially turbidity currents.

All known evidence of prototype turbidity currents refers to currents of the "underflow" type, in which a suspension of a solid particulate material having a density greater than that of the suspending fluid flows underneath a stratum of fluid which is relatively free of suspended material. Thistlethwayte (44) has drawn attention to the possibility that a suspension of a material such as oil or grease, dispersed as fine droplets in water, could form a turbidity current of the "overflow" type, the lighter suspension flowing over the surface of the denser clear fluid.

It has been suggested that the turbidity current phenomenon could be of practical significance in the submarine disposal of inert particulate material of small grain size - such as boiler fly ash and mineral ore residues. It is hypothesised that a suspension of such material in water, discharged onto the ocean bed, would form a turbidity current which would flow down the slope of the ocean bed. The diminishing slope of the ocean bed, together with the progressive dilution of the turbidity current as a result of the entrainment of ambient fluid, would cause the transporting power of the turbidity current to be progressively reduced. Consequently, the material would eventually be deposited on the ocean bed. Under favourable conditions, however, the motion of the turbidity current might be sustained until the material had been transported into such a depth of water that after its deposition no significant redisturbance of the material by wave action would occur. If the turbidity current is sufficiently persistent, the zone of eventual deposition might be at such depths that even a volume of material which might be very large, by terrestrial standards, would be small in relation to the submarine volume which could be filled with material before any effect upon the near-surface or coastal environment became evident.

Investigations into the proposed disposal of fly ash in this manner have been described by Harwood and Wilson (21), Greslou (19), Foster and Stone (17) and The Electricity Commission of New South Wales (14). In the last reference, some large-scale experiments on the formation of turbidity currents in the ocean are described. Experiments (of smaller scale) in the ocean have also been described by Buffington (8).

In general, a turbidity current could be an "eroding" current (removing material from the bed over which it flows), a "steady-state" current, or a "depositing" current. In this context, the term "steady-state" is used in the Lagrangian sense (referring to the temporal invariance of conditions at a point which is stationary within a frame of reference which moves with the turbidity current) and refers to conditions pertaining to the suspension of particles within the current. The phenomenon of entrainment of ambient fluid is excluded from the present discussion, but is discussed later.

The known prototype evidence is insufficient to firmly establish the existence of a steady-state turbidity current. If a steady state is to be attained within a turbidity current which consists of a suspension of non-buoyant material of grain size larger than the colloidal limit, then it is evidently necessary that the flow within the turbidity current should be turbulent. In the absence of turbulent motion (or some other - as yet unrecognised - mechanism of suspension of the non-buoyant material) the progressive settlement of the suspended material towards the bed would cause the progressive decay of the turbidity current. Similarly, it would be necessary that the flow within a hypothetical overflow-type turbidity current should be turbulent.

The presence of suspended material imparts to the fluid within an underflow-type turbidity current an effective density greater than the density of the clear ambient fluid. The difference between the effective density of the suspension and the density of the ambient fluid causes the establishment of a pressure gradient which in turn causes the forward motion of the turbidity current. Settlement of suspended material to the bed (under the action of gravity) will tend to reduce the effective density of the suspension and hence to reduce the driving force of the turbidity current. If the forward velocity of the current is sufficiently great, the motion within the current will be turbulent. Turbulent motion within the turbidity current could evidently tend to maintain the material in suspension and to inhibit the settlement of the suspended material towards the bed.

The existence of steady-state conditions within a turbidity current will imply that a balance must exist between the tendency of the suspended material to settle towards the bed, and the effect of the turbulent motion (or some other mechanism) in tending to inhibit settlement. This balance represents the condition of "auto-suspension" - Bagnold (2), Middleton (33). When this condition of equilibrium prevails, the presence of suspended material causes a density difference which induces the forward motion of the current; the forward motion causes turbulent motion within the current and the turbulence, in turn, maintains the material in suspension and inhibits its tendency to settle.

Similar considerations would apply in the case of a hypothetical overflow-type turbidity current. In this case, the buoyant suspended material would tend to rise to the surface. If steady-state conditions are to be maintained, it is necessary that the material should be maintained in a state of effective suspension within the current, by the turbulent motion within the current or by some other mechanism.

The stability or persistence of a density current, and (in particular) of a turbidity current, will also be affected by the entrainment of ambient fluid into the current. In general, when turbulent motion occurs within a density current, entrainment of ambient fluid will occur across the interface between the density current and the adjoining fluid stratum. The entrained fluid will be (in general) initially at rest, or moving with a velocity less than that of the fluid within the density current. In some cases, the entrained fluid may have a velocity in the sense opposite to that of the motion of the density current. The incorporation of entrained fluid into the density current will accordingly cause a reduction in the momentum per unit volume of the current. Furthermore, the incorporation of entrained fluid into the density current will cause a reduction in the difference between the density of the fluid within the current and the density of the ambient fluid. As a result, the magnitude of the force available to sustain the forward motion of the density current will be reduced.

The investigation to be described herein is accordingly directed to the examination of two aspects of the behaviour of flows in which the presence of suspended material within a stratum of fluid imparts to the fluid within that stratum an effective density different from the density of the (otherwise similar) fluid within an adjoining stratum. The aspects to be examined are:-

(i) the mechanism of suspension of a non-buoyant rigid particle within a turbulent flow. The investigation of this aspect of the subject is described in Chapters 2 - 6 inclusive;

(ii) the process of turbulent mixing across a density discontinuity between two fluid strata, as a result of the turbulent motion of one or both of the strata. The investigation of this aspect is described in Chapter 7.

2. The Suspension of Non-buoyant Particles in a Turbulent Fluid

2.1 Introduction

In the context of the present discussion, a particle is understood to be suspended in a fluid when the time-averaged vertical velocity of the particle approaches the net vertical velocity of the body of fluid which surrounds the particle. (The particle is assumed to be remote from fluid-solid boundaries and from interfaces between bodies of fluid of differing properties). If the fluid has zero net motion in the vertical direction, then the time-averaged vertical velocity of a suspended particle will approach zero.

A particle of a size greater than the upper limit of the colloidal range, and of a density different from that of the surrounding fluid, will move through a quiescent fluid with a non-zero vertical velocity. The sense of the motion of the particle will depend upon the relative magnitudes of the gravitational force and the buoyant force acting on the particle. If such a particle is to be suspended in a fluid, it is implied that the time-averaged vertical velocity of the particle must, by some mechanism or agency, be modified from that value of the velocity which applies in the quiescent fluid. In the investigation to be described below, a postulated mechanism of such modification is examined.

The particles considered are specified to be spherical in form, and composed of a rigid, solid material. The particles are assumed to be so small, and present in such low concentrations, that their presence within the fluid has no effect on the overall or detailed properties of the fluid motion. At the same time, the particles are assumed to be sufficiently large to permit forces and motions on molecular scales to be neglected. The materials of engineering significance which may substantially satisfy these criteria will include silt, fly ash and coal dust.

The phrasing of the discussion will be oriented towards a non-buoyant particle - that is, a particle which has a density greater than that of the surrounding fluid, and which will consequently tend to move downwards through the quiescent fluid, the gravitational force on the particle being of greater magnitude than the buoyant force. In general, however, with suitable modification, the argument will be equally relevant to the case of a buoyant particle which has a density less than that of the surrounding fluid and which consequently tends to move upwards through the quiescent fluid.

The discussion is concerned with particles which are "discovered" within a body of fluid, remote from fluid-solid boundaries and from free liquid surfaces; the consideration of processes such as the disturbance of a non-buoyant particle from its position of rest on a stream bed, and its movement towards the interior of the body of fluid, is excluded.

It is generally recognised that a non-buoyant particle of solid material can, under certain conditions, be transported for a considerable distance in a turbulent flow in which the mean fluid motion is in a horizontal (or nearly horizontal) direction. Fluvial hydraulics and physical geology provide numerous examples of the operation of such transport phenomena, whilst a practical engineering application is found in the field of hydraulic pipeline conveyance of granular materials. The existence of such phenomena implies that the time-averaged fall velocity of a non-buoyant particle in the turbulent flow is smaller (in absolute magnitude) than the settling velocity of the same particle in the quiescent fluid. On the other hand, there is some experimental evidence that particles have fallen through turbulent flows at velocities which have exceeded (in absolute magnitude) the settling velocity of the same particle in quiescent fluid. Jobson and Sayre (25) have reported such results for sand particles and glass beads settling through water; the increase in fall velocities in the turbulent flow (as compared with settling velocities in quiescent water) was more marked for smaller particles than for larger particles.

It is appropriate at this stage to examine the general implications, and then to consider some possible models of the process of particle suspension. Lift forces (forces acting in a direction perpendicular to that of the velocity of the fluid relative to the particle) do not appear to play any significant part in determining the motion of a solid particle in a fluid, except in the immediate vicinity of a solid boundary - as discussed in Section 2.2.4 below. Accordingly, it appears that the modification of a particle's fall velocity in a turbulent flow is primarily associated with the vertical velocity components of the turbulent motion.

If the fluid motion is such that net motion of fluid occurs only in a horizontal direction, then the principle of continuity implies that a balance must exist, at any given time, between the vertical transport of fluid in the two opposing senses, by the vertical components of velocity associated with the turbulent motion. In the case of an incompressible fluid, this balance will imply an equality between the rates of transport of fluid volume in the upward and downward directions, and will imply that

$$\int_A v.dA = 0 \qquad (2.1)$$

where v = the vertical component of fluid velocity

A = an area (in plan) of the flow

Previous investigators have in general examined the problem of particle suspension by consideration of statistical parameters associated with assemblages of large numbers of particles, rather than by consideration of the behaviour of an individual particle. The approach adopted by Rouse (39), Hunt (23) and others leads to the conclusion that a steady state can exist only if a gradient of particle concentration exists within the flow: The particles are assumed to be non-buoyant spheres, of uniform diameter and density. The movement, as part of the turbulent motion of the fluid, of an element of fluid from an initial elevation y_1 to an elevation y_2 is examined (Figure 1). It is specified that $|(y_2 - y_1)|$ should be small; no assumptions concerning the fluid velocities at y_1 or at y_2 are necessary, and hence this specification implies no assumption concerning the nature of the fluid motion. The fluid element is assumed to be of unit area in plan. Continuity requires that the transport of a fluid element from elevation y_1 to elevation y_2 should be accompanied by a net transport of an equal volume of fluid from elevation y_2 to elevation y_1.

The concentration of particles within the element of fluid which was initially located at elevation y_1 may be expressed in terms of a Taylor Series expansion:

$$c_{y1} = c_y - \frac{dc}{dy}\frac{(y_2 - y_1)}{2} + \frac{1}{2}\frac{d^2c}{dy^2}\frac{(y_2 - y_1)^2}{2^2} + \ldots\ldots.$$

where c_y = the particle concentration at $y = \frac{1}{2}(y_1 + y_2)$

$\frac{dc}{dy}$ = the gradient of particle concentration at $y = \frac{1}{2}(y_1 + y_2)$,

or, neglecting the higher-order terms, as $(y_2 - y_1)$ has been specified to be small:

$$c_{y1} = c_y - \frac{dc}{dy}\frac{(y_2 - y_1)}{2}$$

and similarly the concentration of particles within the element of fluid which was initially located at elevation y_2 may be written as

$$c_{y2} = c_y + \frac{dc}{dy}\frac{(y_2 - y_1)}{2}$$

If the transfer of fluid volume across the plane at elevation $y = \frac{1}{2}(y_1 + y_2)$ takes place at a rate q (per unit area in plan) then the transfer of fluid results in a net upward transport of suspended particles at a rate (per unit area in plan) of

$$\left[c_y - \frac{dc}{dy} \cdot \frac{(y_2 - y_1)}{2}\right] . q - \left[c_y + \frac{dc}{dy} \cdot \frac{(y_2 - y_1)}{2}\right] . q$$

$$= - \frac{dc}{dy} \cdot (y_2 - y_1) . q$$

$$= - \frac{dc}{dy} \cdot \Delta y . q \qquad \text{where} \quad \Delta y = (y_2 - y_1)$$

The net rate of the simultaneous downward movement of particles through the plane $y = \frac{1}{2}(y_1 + y_2)$, as a result of the settlement of particles through the fluid, is represented by

$c_y . w$ per unit area in plan

where c_y = the particle concentration at $y = \frac{1}{2}(y_1 + y_2)$

w = the settling velocity of the particles.

If steady-state conditions are to be maintained, an equality must exist between the net rate of downward movement of particles and the net rate of upward transport of particles, and hence

$$c_y . w = - \frac{dc}{dy} \cdot \Delta y . q \tag{2.2}$$

If c_y and w have non-zero values, Equation (2.2) can be satisfied only if $\frac{dc}{dy}$ is non-zero - that is, only if a gradient of particle concentration exists within the flow.

Rouse (39) has suggested that the product $\Delta y.q$ may be replaced by $\beta.v'.l$ where v' is the time-averaged absolute value of the turbulent velocity fluctuations, l is the "mixing length" or the distance through which a small element of fluid is transported (as part of the turbulent motion) before it loses its identity by mixing with the surrounding fluid, and β is a dimensionless coefficient representing a postulated ratio between the transfer characteristics of suspended particles on the one hand and of momentum on the other.

Integration of Equation (2.2) then leads to an expression for the distribution of particle concentration:

$$c = c_o.\exp\left[-\frac{w}{\beta}\int_{y_o}^{y}\frac{dy}{v'l}\right] \tag{2.3}$$

where c_o is a reference concentration at a reference elevation y_o.

If v' and l are assumed to be sensibly constant throughout the greater part of the body of fluid, then the concentration distribution represented by Equation (2.3) implies that the particle concentration must decrease with increasing elevation above the bed. Rouse (39) has reported that such a trend has been confirmed by experiments in which turbulence has been simulated by the fluid motions induced by oscillating metal grids.

The model described above of the mechanism of suspension of non-buoyant particles implies a balance between the net upward transport of particles (due to the interaction of the turbulent fluid motion and the distribution of particle concentration) on the one hand, and the downward settlement of particles under the action of gravitational forces on the other. The argument on which the model is based is, however, untenable when examined from the viewpoint of an individual particle.

It appears to be empirically established that a single particle can, under appropriate conditions, be suspended in a turbulent flow for a period of time of sufficient duration to permit the transport of the particle over a considerable distance. If one single particle alone is present in the flow, then no distribution of particle concentration can exist, except as a discontinuous function with the condition "particle present" applying at a single point and the condition "particle absent" applying at all other points. The argument outlined in the preceding paragraphs then breaks down. Even in the presence of other suspended particles, and in the presence of a distribution of concentration, an individual particle at a given instant is as likely to be located within a downward-moving fluid stream as it is to be located within an upward-moving fluid stream. Accordingly, the net effect of the turbulent fluid motion on the fall velocity of the individual particle is expected to be zero. The particle would therefore be expected to fall towards the bed with a time-averaged velocity equal to its settling velocity in quiescent fluid.

If the role of fluid turbulence in the suspension of a non-buoyant particle is to be modelled by a system of upward- and downward-moving fluid streams, a realistic model will evidently involve the specification, in one form or another, of criteria governing the transition of the particle from an upward stream to a downward stream, and vice versa. The simplest forms of such criteria are:

(i) a spatial criterion

(ii) a temporal criterion

In a model designed on the basis of a spatial criterion, a particle, after having travelled for a specified vertical distance in an upward stream, would then move into a downward stream. After having travelled a specified vertical distance in the downward stream, the particle would then move into an upward stream, and so on.

A model of this type, however, imposes unacceptable constraints on the behaviour of the particle. If the particle moves downward in the downward-moving fluid streams, and upward in the upward-moving fluid streams, then its behaviour is substantially specified as soon as the distances to be traversed in the upward and downward streams are specified: if these distances are specified to be equal to one another, then the net fall velocity of the particle will be zero. If the distance to be traversed in downward streams is greater than that to be traversed in upward streams, the particle will have a net velocity downward, whilst if the distance to be traversed in upward streams is greater than that in downward streams, the particle will have a net upward velocity. If the particle moves downward in both upward- and downward-moving fluid streams, then it will in all cases have a net downward velocity; the relative distances traversed in upward and downward streams can affect only the magnitude of the velocity.

The alternative temporal criterion involves the specification of the time that a particle spends in upward- and downward-moving fluid streams. If it be specified that the particle is to spend equal periods of time in upward and downward streams, this model coincides in principle with the models of Field (16) and of Ho (22). These investigators have measured the fall velocity of a particle in a column of fluid which is oscillated in simple harmonic motion along a vertical axis. Field has measured the fall velocities of non-buoyant particles of plastic, glass and sand in an oscillating water column, and has compared the measured values with those derived from a computer model of the motion. The measured and computed values of the fall velocities were in approximate agreement. In all cases, the fall velocity of a particle in the oscillating fluid column was observed (and computed) to be less than the settling velocity of the particle in the quiescent fluid. No increase in fall velocity as a consequence of the fluid motion was observed.

2.2 The Motion of a Rigid Particle in a Fluid

The limitations of the models outlined above having been recognised, the present investigation has been directed towards the development of a less restrictive model of the mechanism of suspension of a non-buoyant particle in a turbulent flow.

With this objective in view, the process of particle suspension is examined by consideration of the behaviour of an individual particle. In this respect, the present investigation is to be contrasted with most earlier investigations, which have been based on the consideration of statistical parameters associated with large numbers of particles.

Prior to the description, in Chapter 3, of the model which has been developed to form the basis of the present investigation, it is appropriate to review the environment of a rigid particle suspended in a fluid, and to examine the forces which act on the particle. This review is presented as follows:-

2.2.1 Introduction

2.2.2 The Concept of Added Mass

2.2.3 Gravitational and Buoyant Forces

2.2.4 Lift Forces

2.2.5 Drag Forces

2.2.6 Pressure-Gradient Forces

2.2.7 The Inertial Reaction of the Particle

2.2.8 The Role of the History of the Motion of a Particle within a Fluid.

2.2.9 Sign Convention

2.2.10 The Equation of Motion

2.2.1 Introduction

A rigid spherical particle of diameter d, volume V_p and density ρ_p is assumed to be located, remote from any solid boundaries, within a body of fluid which is in motion. It is assumed that the volume and mass of the particle are so small that the flow is not affected by the presence of the particle. It is also assumed that the velocity and acceleration of the fluid immediately surrounding the particle can be taken to be equal to the velocity and acceleration which would occur, in the absence of the particle, at the point (x_o, y_o, z_o), where (x_o, y_o, z_o) is the point at which the geometric centre of the particle is located.

If the particle be located at a given time t_o at a point whose rectangular Cartesian position coordinates are (x_o, y_o, z_o), then the velocity and acceleration of the particle at this instant are respectively denoted by:

$$v_p(x_o, y_o, z_o, t_o) = v_p$$

and

$$a_p(x_o, y_o, z_o, t_o) = a_p$$

Also, the velocity and acceleration of the fluid immediately adjacent to the surface of the particle, at the same time t_o, are respectively denoted by:

$$v_f(x_o, y_o, z_o, t_o) = v_f$$

and $a_f(x_o, y_o, z_o, t_o) = a_f$

In general, v_p will differ from v_f and a_p will differ from a_f.

2.2.2 The Concept of Added Mass

When a rigid particle undergoes an acceleration relative to a fluid which surrounds the particle, then the acceleration of the particle imparts a disturbance to the motion (or state of rest) of the fluid. The extent of the disturbance is unlimited, but its magnitude decreases with increasing distance from the boundaries of the particle. At the surface of the particle, the motion of the fluid conforms to the motion of the particle, rather than to the motion of the fluid as a whole. As the distance from the particle becomes very large, the magnitude of the disturbance becomes infinitesimally small.

As a consequence of the generation of such disturbances, the response of a rigid particle to an impressed force (this response taking the form of an acceleration of the particle) does not conform to the familiar relationship

$$F = m_p . a_p$$

where F = the impressed force

m_p = the mass of the particle

a_p = the acceleration of the particle

but to a relationship

$$F = m_v . a_p$$

where m_v = the "virtual" mass of the particle

and $m_v = m_p + m_a$

where m_a = the "added" (or "induced") mass of the particle.

As the disturbance due to the acceleration of the particle extends throughout the full extent of the body of fluid, it is not practicable to identify the contribution made by specific fluid elements to the added-mass effect. It is nevertheless convenient to attribute the added-mass effect to a hypothetical body of fluid, the motion of which is assumed to conform to that of the rigid particle. This hypothetically-identified body of fluid is hereafter referred to as the "appendant" fluid.

A coefficient k may now be defined by the relationship

$$\forall_f = k.\forall_p$$

where $\forall_f$ = the volume of the "appendant" fluid

k = the added-mass coefficient

$\forall_p$ = the volume of the rigid particle

The mass of the appendant fluid is then given by the expression

$$m_a = k.\forall_p.\rho_f$$

$$= \frac{k}{s}.m_p \qquad (2.4)$$

where ρ_f = the density of the fluid surrounding the particle

m_p = the mass of the particle

s = the ratio of the density of the particle to the density of the fluid surrounding the particle.

Accordingly, the virtual mass of the rigid particle is given by

$$m_v = m_p + m_a$$

$$= \mathbb{V}_p . \rho_p + k . \mathbb{V}_p . \rho_f$$

or, for the particular case of a spherical particle, by

$$m_v \doteq \frac{\pi d^3 .}{6} (\rho_p + k . \rho_f) \qquad (2.5)$$

where d = the diameter of the particle

ρ_p = the density of the particle

Theoretical analysis of the irrotational flow of an inviscid fluid around a sphere yields a value of 0.5 for the added-mass coefficient k (Robertson, 38). The analysis of Basset (3) indicates that if, as a first approximation, the "history" term be omitted from the equation of motion of a sphere in a viscous fluid, then k is to be assigned a value of 0.5. Experiments on spheres accelerated in viscous fluids have indicated values of k somewhat greater than 0.5 (Iversen and Balent, 24). The sum of the data available at this stage, however, does not appear to have established any basis for a more refined estimate of the value of the added-mass coefficient for a sphere in a viscous fluid (Robertson, 38, p. 206). Accordingly, in the present investigation the added-mass coefficient k has been assigned a value of 0.5.

Examination of Equation (2.4) indicates that the effect of the added mass will be most significant when s is small - that is, when the density of the accelerating particle is small in comparison with the density of the surrounding fluid. The potentially large magnitude of the effect has been pointed out by Birkhoff (6) and by Robertson (38). In the case, for example, of a small air-filled balloon submerged in water at a depth of about 1 foot below the water surface, the ratio s will have a value of about 1/800. If the effect of added mass is neglected, the expected value of the initial acceleration of the balloon upon its release will be about 799g. When the effect of added mass is taken into account, however, the expected value of the initial acceleration is about 2g.

If the density ratio s has a relatively large value (of the order of 2, for example, as in the case of siliceous materials) the effect of the added mass will be less significant. Furthermore, the effects of possible variations in the value of the added mass coefficient k from the assumed value of 0.5 will be expected to be of correspondingly small significance.

2.2.3 Gravitational and Buoyant Forces

When a particle is submerged in a fluid, the effective weight of the particle is the vector sum of the gravitational force on the particle and the buoyant force exerted on the particle by the surrounding fluid.

In the present context, the buoyant force acting on the particle is calculated on the assumption that a hydrostatic pressure distribution exists within the fluid. The effects of departures from the condition of a hydrostatic pressure distribution are considered in Section 2.2.6.

With this specification, the effective weight of a particle immersed in a fluid is

$$\vec{F}_G = \forall_p (\rho_p - \rho_f)\vec{g}$$

or, for the particular case of a spherical particle

$$\vec{F}_G = \frac{\pi d^3}{6}(\rho_p - \rho_f)\vec{g} \tag{2.6}$$

where $\vec{g}$ = the gravitational acceleration vector.

2.2.4 Lift Forces

A component of force which acts on a rigid particle, in a direction perpendicular to that of the velocity of the fluid relative to the particle, is termed a lift force.

The distribution of pressures at the surface of a sphere, located within a fluid in which a velocity gradient exists, has been measured by Chepil (10). From the measured pressure distribution, the components of force acting on the sphere can be calculated. Chepil's measurements have indicated that the lift force component is of comparable magnitude to the drag force component only when the particle is in contact with a rigid boundary. As the distance from the boundary increases, the magnitude of the lift force component diminishes sharply.

The results of experiments described by Young (50) are also consistent with the occurrence of a rapid reduction in the magnitude of the lift force as the particle moves away from a rigid boundary. These results are discussed in Appendix I, in conjunction with a hypothesis concerning the modification of lift forces as a result of the ability of a freely-suspended particle to spin.

As the present investigation is confined to regions which are remote from rigid boundaries, it has been concluded in the light of the available evidence that lift force components will not be of magnitudes comparable to those of the fluid drag force or the gravitational force. Accordingly, the lift force component has not been included in the formulation of the equation of motion of the particle.

2.2.5 Drag Forces

When relative motion occurs between a fluid and a rigid particle which is immersed in the fluid, a drag force is exerted on the particle. The drag force acts in the direction and sense of the motion of the fluid relative to the particle.

The drag force may be related to the properties of the flow and of the particle by the expression

$$F_D = C_D . A_p \frac{\rho_f . u^2}{2} \tag{2.7}$$

where F_D = the drag force on the particle

C_D = a dimensionless "drag coefficient"

A_p = the cross-sectional area of the particle, projected onto a plane perpendicular to the direction of the velocity of the fluid relative to the particle

ρ_f = the density of the fluid

u = the velocity of the fluid, relative to the particle

For spherical particles under steady-state conditions, values of the drag coefficient as a function of the Reynolds Number $u.d/\nu$ describing the motion of the fluid relative to the particle have been firmly established by experiment (Schlichting, 43). When, however, the velocity of the fluid relative to the particle is not steady, but varies with time, the concept of the drag coefficient must be modified in the light of the effect of the added mass of the particle (Section 2.2.2) and the effect of the "history" of the motion (Section 2.2.8). Consequently, steady-state drag coefficients cannot in general be assumed to be applicable to unsteady situations. Experiments on solid bodies accelerated (by external driving forces) through fluids have indicated that instantaneous drag coefficients differ somewhat in such cases from the corresponding steady-state values.

In the circumstances of the present investigation, conditions are essentially unsteady: even if the fluid motion relative to a frame of reference fixed outside the fluid body be steady, the motion of the fluid relative to the particle will in general be unsteady.

Davies (13) has discussed the use of steady-state drag coefficients in the calculation of particle trajectories, and has suggested that the use of such coefficients is not likely to be significantly in error, provided that the Reynolds Number describing the motion of the fluid relative to the particle does not exceed a certain limit. This limit is not clearly defined but is reported to lie well above the upper limit of the range of validity of Stokes' Law. Davies has suggested that the limiting condition will apply at lower values of the Reynolds Number as the difference between the particle density and the fluid density is reduced. It should be noted, however, that the smaller this density difference, the more closely will the motion of the particle conform to the motion of the surrounding fluid, and hence the smaller will be the magnitude of the velocity of the fluid relative to the particle. Accordingly, for particles of a given diameter, the Reynolds Number describing the motion of the fluid relative to the particle is expected to be smaller, as the density of the particle approaches that of the suspending fluid.

In the present investigation, it has been concluded that the best available estimate of drag forces will be provided by the use of the established values of the steady-state drag coefficient, in the anticipation that the Reynolds Number describing the motion of the fluid relative to the particle will be less than the limit of validity of Stokes' Law - that is, less than 0.1. The calculation of the drag coefficient has been based on values presented by Rouse (40; p. 122) which correspond closely to those presented by Schlichting (43). The relevant values are tabulated in Appendix II.

Equation (2.7) may conveniently be written in vector form, for the particular case of a spherical particle, as

$$\vec{F}_D = \tfrac{1}{2} C_D \cdot \frac{\pi . d^2}{4} \cdot \rho_f \cdot |u_{rel}| \cdot \vec{u}_{rel} \tag{2.8}$$

where u_{rel} = the velocity of the fluid, relative to the particle.

2.2.6 Pressure-Gradient Forces

In an accelerating body of fluid, a gradient of pressure will, in general, exist in the direction of the acceleration. If a fluid element of volume V_f has its centroid (at time t_o) at the point (x_o, y_o, z_o), then the surrounding fluid will exert on this element a net pressure force F_P which is just sufficient to impart to the element the local fluid acceleration $a_f(x_o, y_o, z_o, t_o)$. The force F_P acts in the direction and sense of the fluid acceleration:

$$\vec{F}_P = V_f \; \rho_f \vec{a}_f \tag{2.9}$$

where $\vec{F}_P$ = the force exerted on the fluid element by the surrounding fluid

V_f = the volume of the fluid element

ρ_f = the density of the fluid

$\vec{a}_f$ = the local fluid acceleration

= $\vec{a}_f(x_o, y_o, z_o, t_o)$

If the fluid element be now replaced by a rigid particle of the same volume, and if it be assumed that the presence of the particle causes no significant alteration in the properties of the flow field, then an unchanged force $\vec{F}_P$ will act on the particle. If, however, the mass of the particle differs from that of the fluid element which it has replaced, then the acceleration of the particle will differ from that of the replaced fluid element. Hence, a relative acceleration will occur, between the particle and the surrounding fluid. As pointed out in Section 2.2.2 above, however, the acceleration of a rigid particle relative to a surrounding fluid will give rise to a disturbance which will be propagated throughout the full extent of the fluid. It is assumed here that such disturbance does not cause a significant alteration in the overall properties of the fluid motion. The propagation of such a disturbance will be manifested by each fluid element's experiencing a force $\vec{F}_P'$ which may be expressed as

$$\vec{F}_P' = V_f \rho_f \vec{a}_f' \tag{2.10}$$

where $\vec{a}_f'$ = the disturbance in the local fluid acceleration.

A complete examination of the effect of replacement of a fluid element by a rigid particle would require the integration of Equation (2.10) over the full extent of the fluid. As discussed in Section 2.2.2 above, it is convenient to identify the added mass of a rigid particle with the mass of a hypothetically-identified body of fluid (the "appendant" fluid), the motion of which conforms to that of the particle. The magnitude of the disturbance resulting from the acceleration of a rigid particle relative to the surrounding fluid will diminish rapidly with increasing distance from the particle (Robertson, 38). This is consistent with the assumption that the added mass of the particle may be represented by a body of appendant fluid of the appropriate volume and located adjacent to the particle. Accordingly, it is now assumed that the force which will act on a rigid particle within an accelerating fluid, due to the pressure gradient within the fluid, may be considered (as a first approximation) to be equal to the force which would act on a fluid element, of volume equal to that of the rigid particle together with its appendant fluid, located in a flow in which the fluid acceleration conforms to that in the undisturbed flow at the point to be occupied by the centroid of the particle.

This force is

$$\vec{F}_P = V_p\,(1+k)\,\rho_f \vec{a}_f$$

or, for the particular case of a spherical particle

$$\vec{F}_P = \frac{\pi d^3}{6}\,(1+k)\,\rho_f \vec{a}_f \qquad (2.11)$$

2.2.7 The Inertial Reaction of the Particle

A non-zero resultant force acting on the particle-appendant fluid system will impart to the system (which has a virtual mass of m_v) an acceleration $\vec{a}_p$. In order to formalise the equation of motion, the product of mass and acceleration may be identified as a force - the "inertial reaction" $\vec{F}_R$.

Accordingly, the inertial reaction of the particle-appendant fluid system is

$$\vec{F}_R = m_v \vec{a}_p$$

$$= V_p(\rho_p + k \cdot \rho_f)\vec{a}_p$$

or, for the particular case of a spherical particle

$$\vec{F}_R = \frac{\pi d^3}{6}(\rho_p + k.\rho_f)\vec{a}_p \qquad (2.12)$$

2.2.8 The Role of the History of the Motion of a Particle within a Fluid

Basset (3) has derived the following equation:

$$\frac{\pi d^3}{6}(\rho_p + \tfrac{1}{2}\rho_f)a_p + 3\pi d\,\rho_f\left\{\nu v_p + \frac{d}{2}\sqrt{\frac{\nu}{\pi}}\int_o^t \frac{F'(t-\tau)\,d\tau}{\sqrt{\tau}}\right\} = \frac{\pi d^3}{6}g(\rho_p - \rho_f) \qquad (2.13)$$

where d = the diameter of a spherical particle

ρ_p = the density of the particle

ρ_f = the density of the surrounding fluid

ν = the kinematic viscosity of the surrounding fluid

v_p = the velocity of the particle = $F(t)$

a_p = the acceleration of the particle

t = time

τ = time; $\tau \leq t$

g = the gravitational acceleration

Equation (2.13) represents the equation of motion of a spherical particle which

(i) has started from rest, in an infinite fluid which is at rest, and

(ii) has moved in a straight line in the direction and sense of the gravitational force, for a considerable time, with a velocity which is obviously a function of time.

In Equation (2.13) the term $3\pi d \rho_f \nu v_p$ represents the "Stokes' Law" drag force on the particle; this may be verified by substituting in Equation (2.7), p. 28, the value of the drag coefficient for laminar flow. This value is $C_D = \frac{24\nu}{v_p d}$ (Rouse, 40).

The term $\frac{3}{2}d^2 \rho_f \sqrt{\nu\pi}\int_0^t \frac{F'(t-\tau)\, d\tau}{\sqrt{\tau}}$ represents a component of fluid resistance related to the time-history of the motion, and has accordingly become known as Basset's History Term, (Brush, Ho and Yen, 7). If, at large values of the time t, the motion tends to attain a steady state, then the value of the integral will approach a limiting constant value. This is consistent with the concept of steady-state drag coefficients, the values of which are substantially independent of the mode of establishment of the steady state.

The case of a particle which has not started from rest is less amenable to analysis, and Basset has presented approximate solutions for some such motions of a spherical particle. In the context of the present investigation, the particle cannot be considered as starting from rest, as the commencement of its motion is outside the range of the investigation. Furthermore, the fluid surrounding the particle is not at rest, the direction of motion of the particle does not coincide (in general) with that of the gravitational force, and the motion of the particle is not in general rectilinear. Accordingly, it appears that the formulation of an expression corresponding to Basset's History

Term and appropriate to the motion at present under consideration would be extremely difficult.

Mockros and Lai (35) have experimentally examined the motion of spherical particles accelerated (by gravitational force) through a body of quiescent viscous fluid. The experimental results have been compared with the behaviour predicted by an equation of motion corresponding to Equation (2.13). Figure 2, which is reproduced from Figure 2 of Mockros and Lai, illustrates the effect of neglecting -

(i) the history term, and

(ii) the history term and the Stokes' Law drag term

in Equation (2.13), for the case of a spherical particle with a density approximately 9 times that of the surrounding fluid. This figure illustrates that neglect of the history term will become significant (in this particular case) after the particle has travelled, from its position of rest, a distance of the order of one-half the particle diameter.

It is considered impracticable to formulate, within the scope of the present investigation, any expression corresponding to Basset's history term which would be appropriate to the fluid and particle motions involved in the present investigation. Accordingly, it is proposed to assume that the interaction between the fluid and the particle, arising from the motion of one relative to the other, may be adequately deduced from the steady-state drag coefficients, as discussed in Section 2.2.5. It is proposed to seek empirical confirmation that the assumptions made will not significantly prejudice the validity of the computed particle trajectories.

2.2.9 Sign Convention

The present discussion is limited to two dimensions, and a rectangular Cartesian coordinate system is employed. The coordinate axis parallel to the horizontal direction is designated the x axis, and the coördinate axis parallel to the vertical direction is designated the y axis.

The algebraic signs associated with components of force, acceleration, velocity and distance are allocated as follows:-

Components parallel to the x (horizontal) coordinate axis, acting from left to right: positive

Components parallel to the x (horizontal) coordinate axis, acting from right to left: negative

Components parallel to the y (vertical) coordinate axis, acting upwards: positive

Components parallel to the y (vertical) coordinate axis, acting downwards: negative.

2.2.10 The Equation of Motion

In the light of the preceding discussion, it is assumed that the forces which are of significance in determining the motion of a particle moving within a fluid, in a region remote from fixed boundaries, are as follows:

(i) The effective weight of the particle $\vec{F}_G$ - that is, the resultant of the gravitational and buoyant forces acting on the particle;

(ii) The fluid drag force $\vec{F}_D$;

(iii) The force $\vec{F}_P$ which results from the existence of a pressure gradient within the fluid.

It is implied that lift forces are assumed to be of negligible significance, in the present context. Furthermore, the effects of the history of the motion have not been taken into consideration, as no practicable basis for taking account of such effects is available at this stage. As stated above, it is proposed to seek empirical confirmation that the assumptions made will not significantly prejudice the validity of the particle trajectories which are to be computed.

With the inclusion of the intertial reaction $\vec{F}_R$ of the particle, the following equation results:

$$\vec{F}_G + \vec{F}_D + \vec{F}_P = \vec{F}_R \tag{2.14}$$

For the particular case of a spherical particle, substitution from Equations (2.6), (2.8), (2.11) and (2.12) - from pages 27, 31, 33 and 34 respectively - leads to the equation

$$\frac{\pi d^3}{6}(\rho_p - \rho_f)\vec{g} + \tfrac{1}{2}C_D \frac{\pi d^2}{4}\rho_f \left|u_{rel}\right| \vec{u}_{rel} + \frac{\pi d^3}{6}(1+k)\rho_f \vec{a}_f = \frac{\pi d^3}{6}(\rho_p + k\rho_f)\vec{a}_p \tag{2.15}$$

As each term is dimensionally equivalent to a force, Equation (2.15) is conveniently made non-dimensional in a manner similar to that adopted by Field (16), by dividing throughout by the magnitude of the weight of a fluid element having a volume equal to that of the particle - that is, dividing by $\frac{\pi d^3}{6} \rho_f g$:

$$\left(\frac{\rho_p}{\rho_f} - 1\right)\hat{g} + \frac{0.75\, C_D |u_{rel}| \overrightarrow{u_{rel}}}{gd} + (1+k)\frac{\vec{a}_f}{g} = \left(\frac{\rho_p}{\rho_f} + k\right)\frac{\vec{a}_p}{g} \tag{2.16}$$

$$\text{or } (s-1)\hat{g} + \frac{0.75 C_D |u_{rel}|\ \overrightarrow{u_{rel}}}{gd} + (1+k)\frac{\vec{a}_f}{g} = (s+k)\frac{\vec{a}_p}{g}$$

and hence

$$(s-1)\,\hat{g} + 0.75\, C_D\, |U_{rel}|\ \vec{U}_{rel} + \frac{(1+k)}{(s+k)}\vec{A}_f = \vec{A}_p \tag{2.17}$$

where U_{rel} = a non-dimensional velocity

$$= \frac{u_{rel}}{\sqrt{dg}} \tag{2.18}$$

A_f = a non-dimensional fluid acceleration

$$= (s+k)\frac{a_f}{g} \tag{2.19}$$

A_p = a non-dimensional particle acceleration

$$= (s+k)\frac{a_p}{g}$$

s = the ratio of the density of the particle to the density of the surrounding fluid

$\hat{g}$ = a unit vector, in the direction of the gravitational force.

From the relationships between dimensional and non-dimensional quantities for velocities and accelerations - Equations (2.18) and (2.19) -

the corresponding relationships for lengths and times follow:

$$\frac{L}{l} = \frac{U^2/A}{u^2/a}$$

$$= \left(\frac{1}{\sqrt{dg}}\right)^2 \frac{g}{(s+k)}$$

$$= \frac{1}{(s+k)\ d}$$

and hence $$L = \frac{1}{(s+k)d} \qquad (2.20)$$

$$\frac{T}{t} = \frac{(U/A)}{(u/a)}$$

$$= \frac{1}{\sqrt{dg}} \quad \frac{g}{(s+k)}$$

and hence $$T = \frac{t}{(s+k)} \sqrt{\frac{g}{d}} \qquad (2.21)$$

If a non-dimensional parameter P is defined by

$$P = \frac{\sqrt{gd^3}}{\nu} \qquad (2.22)$$

where g = the gravitational acceleration

d = the particle diameter

ν = the kinematic viscosity of the fluid

and a non-dimensional velocity U by

$$U = \frac{u}{\sqrt{gd}} \qquad (2.23)$$

then the product PU will have the value of the Reynolds Number

$\frac{ud}{\nu}$, for

$$PU = \frac{\sqrt{gd^3}}{\nu} \cdot \frac{u}{\sqrt{gd}}$$

$$= \frac{ud}{\nu} \qquad (2.24)$$

In particular, if $U_{rel} = \frac{u_{rel}}{\sqrt{gd}}$ where u_{rel} is the velocity of the fluid relative to the particle, then the product $P.U_{rel}$ will have the value of the Reynolds Number $\frac{u_{rel} \cdot d}{\nu}$, describing the motion of the fluid relative to the particle. Hence, the drag coefficient C_D will be a function of the product $P.U_{rel}$.

The relationship between force, mass and acceleration is linear, as is the relationship between acceleration, time and velocity. Consequently, Equation (2.17) may be separated into its components in the several coordinate directions. As the present discussion is limited to two dimensions, components in the x (horizontal) and the y (vertical) directions are to be considered.

In the x direction, the vector $\hat{g}$ has zero component, and hence the relevant component of Equation (2.17) becomes

$$(0.75\ C_D \left|U_{rel}\right| \left|U_{rel}\right| \ \cos\theta + \frac{(1+k)}{(s+k)} A_{fx} = A_{px}$$

where θ = the angle between $\overrightarrow{U}_{rel}$ and the x coordinate axis

A_{fx} = the component of fluid acceleration in the x coordinate direction

A_{px} = the component of particle acceleration in the x coordinate direction

which may be written as

$$0.75\ C_D \left|U_{rel}\right| U_{relx} + \frac{(1+k)}{(s+k)} A_{fx} = A_{px} \qquad (2.25)$$

where U_{relx} = the component, in the x coordinate direction, of the velocity of the fluid relative to the particle.

In the y coordinate direction, the vector $\hat{g}$ has an absolute value of unity and its sense is downwards, which has been defined in Section 2.2.9 as the negative y direction. Hence, the component in the y coordinate direction of Equation (2.17) becomes

$$(s-1)(-1) + (0.75\ C_D \left|U_{rel}\right| \left|U_{rel}\right|)\sin\theta + \frac{(1+k)}{(s+k)}\ A_{fy} = A_{py}$$

or
$$0.75\ C_D \left|U_{rel}\right|\ U_{rely} + \frac{(1+k)}{(s+k)}\ A_{fy} - (s-1) = A_{py} \qquad (2.26)$$

where A_{fy} = the component of fluid acceleration in the y coordinate direction

A_{py} = the component of particle acceleration in the y coordinate direction

U_{rely} = the component, in the y coordinate direction, of the velocity of the fluid relative to the particle.

3. The Eddy Model of Turbulent Flow

3.1 General Considerations

It has been postulated in Section 2.1 that the modification of fall velocity of a non-buoyant particle in a turbulent flow (as compared with the fall velocity of the same particle in quiescent fluid) is associated with the fluctuating vertical velocity components which exist in a fluid which is in turbulent motion, even when the net motion of the fluid in the vertical direction is zero. It is now further postulated that these vertical velocity components, in conjunction with the fluctuating horizontal velocity components associated with the turbulent motion, may be identified with a field of eddies or vortices. Townsend (46) has described a turbulent flow as "an intricate and irregular eddying motion of the fluid". It is accordingly proposed that a turbulent flow will be modelled by a field of eddies, and that the process of suspension of a particle within the flow will be examined by the computation of the trajectory of the particle within the eddy field. In order that such a model may be formulated, it becomes necessary to determine the appropriate characteristics to be assigned to the model eddy field.

The available experimental data on the statistical properties of turbulence yield very little insight into the physical characteristics to be attributed to such an eddy field, or into the nature of the velocity distribution within an individual eddy of the field. In the present state of knowledge, it appears that the assignment of the characteristics of the model eddy field can be placed on no firmer basis than a set of plausible assumptions.

It is proposed that the turbulent flow should be modelled by a single field of eddies; this is recognised as being no more than a first approximation to a real turbulent flow, in which conditions probably correspond more closely to a superposition of a number of eddy fields, with interaction between the superimposed eddies. It is also proposed to specify that conditions within the model eddy field should be invariant with time.

In an actual turbulent flow, periods of time would probably occur during which the fluid motion in the vicinity of a suspended particle is determined primarily by one predominant eddy. During such a period (or portion thereof) the characteristics of the dominant eddy may remain substantially constant. In these circumstances, conditions within the flow would substantially conform to the specified characteristics of the proposed model eddy field, as outlined in the preceding paragraph. Hence, it is anticipated that the proposed approach should permit a valid examination of portions of the history of the motion of a rigid particle in the turbulent flow.

If the flow in a region within a two-dimensional turbulent flow is to be modelled by a field of eddies as proposed, then physical plausibility will require that the definition of the eddy field should satisfy the following general conditions:-

(i) The eddies should be two-dimensional.

(ii) The equation of continuity should be satisfied at all points within the field.

(iii) If the region of the flow which is to be modelled is remote from fixed boundaries, then no velocity discontinuities should exist within the eddy field.

(iv) Each eddy should be surrounded by other eddies which are of approximately the same size.

(v) The definition of the eddy field should be continuous over the entire flow field.

It is necessary to acknowledge that the lack of information concerning the physical characteristics of the eddy motions within actual turbulent flows places, at this stage of knowledge, a substantial obstacle in the way of the present approach to the examination of the process of particle suspension. It is anticipated, however, that, notwithstanding the existence of this obstacle, the present approach may yield some insight into the behaviour of a suspended particle and may demonstrate the utility, in principle, of the eddy model.

3.2 Definition of the Model Eddy Field

An eddy field which substantially satisfies the criteria outlined in Section 3.1 results when the periodic eddy field of infinite extent described by Townsend (46) is particularised to two dimensions. The two-dimensional eddy field is defined by the stream function

$$\psi = -\cos(l_1 x)\ \cos(l_2 y) \tag{3.1}$$

where ψ = the stream function

l_1 and l_2 are "shape factors"

x and y are Cartesian position coordinates.

The shape factors l_1 and l_2 may be expressed as

$$l_1 = \frac{\pi}{X}$$

$$l_2 = \frac{\pi}{Y}$$

where X = the spacing of eddy centres, in the x coordinate direction

Y = the spacing of eddy centres, in the y coordinate direction

Then $$\psi = -\cos\left(\frac{\pi x}{X}\right)\ \cos\left(\frac{\pi y}{Y}\right) \tag{3.2}$$

and expressions for the components of the fluid velocity at any point (x, y) are derived by differentiation:

$$u(x, y) = \frac{\partial \psi}{\partial y}$$

$$= \frac{\pi}{Y} \cos\left(\frac{\pi x}{X}\right) \sin\left(\frac{\pi y}{Y}\right)$$

$$v(x, y) = -\frac{\partial \psi}{\partial x}$$

$$= -\frac{\pi}{X} \sin\left(\frac{\pi x}{X}\right) \cos\left(\frac{\pi y}{Y}\right)$$

where u(x, y) = the component, in the x coordinate direction, of the fluid velocity at the point (x, y)

$v(x, y)$ = the component, in the y coordinate direction, of the fluid velocity at the point (x, y)

The expressions for the components of velocity may be written in terms of a characteristic velocity U_e:

$$u(x, y) = U_e \cos(\frac{\pi x}{X}) \sin(\frac{\pi y}{Y}) \tag{3.3}$$

$$v(x, y) = - U_e \frac{Y}{X} \sin(\frac{\pi x}{X}) \cos(\frac{\pi y}{Y}) \tag{3.4}$$

where U_e = a characteristic velocity within the eddy field.

Examination of Equations (3.3) and (3.4) indicates that the eddy field consists of an unbounded array of eddies, with centres spaced at intervals of X in the direction parallel to the x coordinate axis and at intervals of Y in the direction parallel to the y coordinate axis. Alternate eddies, encountered in moving in a direction parallel to either coordinate axis, will rotate in opposite senses.

The eddy field is illustrated diagrammatically in Figure 3. A number of streamlines in a single eddy of a square array (that is, a field in which $X = Y$) is shown in Figure 4. Some velocity distributions in a similar eddy are shown in Figure 5.

Townsend has defined two other eddy structures, having the form of a single isolated eddy and of a finite row of simple eddies, respectively. The unbounded eddy field described above, however, will permit a particle to move from a given eddy into a neighbouring eddy without constraint in any direction. For this reason, the unbounded eddy field has been selected as the basis of the present investigation. The selected eddy field is restrictive in that all eddies within the field are of the same size, whereas it is to be expected that in an actual turbulent flow, eddies of varying sizes will be present. It is expected, however, that in an actual flow the sizes of neighbouring dominant eddies will not vary greatly, and hence this restriction is not expected to be a serious one, provided that a particle trajectory does not traverse more than a few eddies.

Some further properties of the fluid motion within the model eddy field are as follows:-

(i) Within each eddy, the streamlines form closed curves. The streamline pattern is symmetrical about lines which pass through the eddy centre and which are parallel to the x or y coordinate axes. In a square array of eddies (that is, in a field in which $X = Y$) the streamline pattern will also be symmetrical about lines passing through the eddy centre at angles of 45° with the coordinate axes.

(ii) The maximum absolute value $|U_{max}|$ of the fluid velocity within the eddy field is related to the characteristic velocity U_e thus:

$$|U_{max}| = |U_e| \quad \text{if } X \geq Y \tag{3.5}$$

$$|U_{max}| = \frac{Y}{X}|U_e| \quad \text{if } X < Y \tag{3.6}$$

(iii) The equation of continuity is satisfied at all points, as

$$\frac{\partial u}{\partial x} + \frac{\partial v}{\partial y} = 0 \quad \text{for all values of x and y.}$$

(iv) The vorticity at any point (x, y) is given by:-

$$\xi(x,y) = -\pi U_e \frac{(X^2+Y^2)}{X^2 Y} \cos\left(\frac{\pi x}{X}\right) \cos\left(\frac{\pi y}{Y}\right) \tag{3.7}$$

Hence, $\xi(x, y)$ is, in general, non-zero, except on the lines defined by $x = \pm (n+\frac{1}{2})X$ and by $y = \pm (n+\frac{1}{2})Y$ where n has integral values.

When X = Y, (that is, when the eddy field consists of a square array):

$$\xi(x,y) = -2\pi \frac{U_e}{X} \cos\left(\frac{\pi x}{X}\right) \cos\left(\frac{\pi y}{Y}\right) \tag{3.8}$$

(v) With the specification that U_e, the characteristic velocity within the eddy field, does not vary with time, the components of the fluid acceleration at a point (x, y) are given by:-

$$\begin{aligned} a_{fx} &= a_{fx}(x,y) \\ &= -\pi \frac{1}{X} u^2(x,y) \tan\left(\frac{\pi x}{X}\right) - \pi \frac{X}{Y^2} v^2(x,y) \cot\left(\frac{\pi x}{X}\right) \end{aligned} \tag{3.9}$$

and

$$\begin{aligned} a_{fy} &= a_{fy}(x,y) \\ &= -\pi \frac{Y}{X^2} u^2(x,y) \cot\left(\frac{\pi y}{Y}\right) - \pi \frac{1}{Y} v^2(x,y) \tan\left(\frac{\pi y}{Y}\right) \end{aligned} \tag{3.10}$$

where $a_{fx}(x,y)$ = the component, in the x coordinate direction, of the fluid acceleration at the point (x, y)

$a_{fy}(x,y)$ = the component, in the y coordinate direction, of the fluid acceleration at the point (x, y).

4. Description of the Computer Program for the Computation of Particle Trajectories

4.1 General Description

The examination of the process of suspension of a particle in the model eddy field involves the step-by-step computation of the trajectory of the particle after it has passed through an arbitrarily-specified starting point within the specified velocity field.

The digital computer program developed for this purpose is described below. The program, written in the FORTRAN IV language, was developed for use on the IBM 360/50 System at the University of New South Wales Computing Centre. The program consists of a main program and three sub-programs; a further subroutine is used for timing the execution of the program.

The FORTRAN program developed for the computation of the trajectory of a particle in the model eddy field, together with the associated sub-programs, is listed in Appendix III. A flow chart for the program is shown in Figure III.1. The variables which are to be read in as data in order to operate the program are listed and defined in Table III.A, Appendix III.

The remainder of Chapter 4 is devoted to a description of the operation of the program. Familiarity with the material contained within this chapter is not essential for an understanding of the results of the computations, which are described in Chapters 5 and 6.

4.2 The Computational Procedure

The computational procedure is essentially one of prediction and correction. The basis of the process is shown diagrammatically in Figure 6. The procedure is described below; it is, however, convenient to first describe the three sub-programs:

The subroutine VEL defines the velocity field. The components (in each of the two coordinate directions) of the fluid velocity at any point in space and time - as defined by coordinates (x, y, t) - are calculated. The components (in each of the two coordinate directions) of the fluid acceleration at (x, y, t) are also calculated. (In the model eddy field defined in Chapter 3 above, fluid velocities have been specified to be independent of time. In the interests of generality, however, provision has been made in the development of the program for the specification of fluid velocities as functions of time. The application of the program to a time-dependent velocity distribution is described in Chapter 5).

The subroutine VELID causes an identification of the velocity distribution (as defined by the accompanying subroutine VEL) to be printed in the output.

The subroutine DRAG carries out the computation of the components (in each of the two coordinate directions) of the fluid drag force on the particle at a given point in space, for given values of the components of the fluid velocity and the particle velocity at that point.

One aspect of the program - concerned with the calculation of the energy interchange between fluid and particle - is described in Section 4.4 below. In the interests of clarity, it is considered expedient to separate the description of this aspect from the description of the more significant operations within the main program.

In the following description, the variable names correspond to those used in the FORTRAN program; the algebraic expressions which occur in the description are, however, written in the ordinary notation of algebra, rather than in the notation of the FORTRAN language. Variables which are read in as data are defined in Table III.A.

The computational procedure within the main program is as follows:-

(a) In order to avoid instability in the computation, an arbitrary limit (defined by a parameter STEP) is placed upon the distance that the particle may travel during one step of the computation. This spatial limit, which is read in as data at the commencement of program execution, is converted to a basic limiting time interval (DTBAS) by dividing the spatial limit by the maximum fluid velocity which can occur within the eddy field (namely, the characteristic velocity UEDDY if XCNTR $\geq$ YCNTR, or UEDDY. YCNTR/XCNTR if XCNTR $<$ YCNTR). If UEDDY has a zero value, as in the case of the settlement of a particle through a quiescent fluid, then DTBAS is set equal to $\sqrt{2.\,\mathrm{STEP}}$: In the development of Equation (2.17) p. 39, the gravitational acceleration has been reduced to the form of the vector $\hat{g}$, which is of unit magnitude, and hence the above value of DTBAS is consistent with the equation

$$y = \tfrac{1}{2}gt^2$$

for the initial motion of a particle settling (under the action of gravity) through a quiescent fluid.

(b) The particle is assumed to pass through an arbitrarily selected starting point, with coordinates (XSTART, YSTART), at an arbitrarily selected time (TSTART). The components (UFL, VFL) of the fluid velocity, and the components (FFAX, FFAY) of the force on the particle due to the fluid acceleration, at this point and time are calculated (in the subroutine VEL) in accordance with Equations (3.3) and (3.4), p. 47, and Equations (3.9) and (3.10), p. 49, respectively.

(c) Specified values of the components of particle velocity at the starting point may be read in as data (if the parameter KSTART - which is itself read in as data- has been assigned a value of unity). Alternatively (if KSTART has been assigned a value of 2) the components of particle velocity at the starting point are set equal to the corresponding components of the fluid velocity at the starting point. (Note vii, Section 4.3 below).

(d) The components FDRX, FDRY of the drag force acting on the particle at the starting point are calculated (in the subroutine DRAG). These force components represent the first terms in Equations (2.25) and (2.26) pp. 41 and 42 respectively. (If the particle velocity components and the fluid velocity components at the starting point have been set equal, the components of drag force are of course zero).

(e) A time increment DT is calculated:

(i) If the components of the particle velocity in the two coordinate directions are both equal to zero, then the time increment DT is set equal to the basic time step DTBAS.

(ii) Otherwise, the time increment DT is set equal to the result of dividing the spatial limit STEP by the absolute value of that component of the particle velocity which has the greater absolute value.

(f) The components of the forces (due to fluid drag and to the pressure gradient) acting on the particle are summed, for the two coordinate directions, the sums being denoted by FXT and FYT respectively.

(g) The corresponding components of particle acceleration in the two coordinate directions are calculated (including, in the case of the y coordinate direction, the effect of the net gravitational force) by expressions corresponding to Equations (2.25) and (2.26) pp. 41 and 42 respectively.

(h) On the assumption that the components of particle acceleration acting throughout the time increment DT have constant values equal to those calculated in step (g) above, the following are calculated:-

D1X, the distance travelled in the x coordinate direction by the particle during the time increment DT.

D1Y, the distance travelled in the y coordinate direction by the particle during the time increment DT.

(i) If the condition $(D1X^2 + D1Y^2) \leq (STEP)^2$ be not satisfied, then the value of the time increment DT is reduced to 70 per cent of its former value, and step (h) is repeated. Successive reductions of DT (to 70 per cent of its immediately preceding value) and subsequent repetitions of step (h) continue until the condition $(D1X^2 + D1Y^2) \leq (STEP)^2$ is satisfied.

(j) Then, the following are calculated:-

$$\left.\begin{aligned} X1 &= XT + D1X \\ Y1 &= YT + D1Y \end{aligned}\right) \begin{array}{l} \text{At the starting point, } XT = XSTART \\ \text{and } YT = YSTART \end{array}$$

UPT1 = the component, in the x coordinate direction, of the velocity of the particle at the end of the time increment DT - that is, at the point (X1, Y1)

VPT1 = the component, in the y coordinate direction, of the velocity of the particle at the end of the time increment DT - that is, at the point (X1, Y1).

The point (XT, YT) is a point which has been determined as lying on the trajectory - arbitrarily, in the case of the starting point, or, in the case of subsequent cycles in the computation, as a result of the preceding computations. The point (X1, Y1) represents a first estimate of the next point on the trajectory after the point (XT, YT).

(k) The components (UFL1, VFL1) of the fluid velocity, and the components (FFAX, FFAY) of the force on the particle due to the fluid pressure gradient, at the point (X1, Y1) are calculated, in the subroutine VEL. The components (FDRX, FDRY) of the drag force on the particle at the point (X1, Y1) are calculated in the subroutine DRAG.

The components of the forces on the particle due to fluid drag and to the pressure gradient at the point (X1, Y1) are summed, for the two coordinate directions, the sums being denoted by FX1 and FY1 respectively.

(l) The components (FX, FY) of the average force (due to fluid drag and to the pressure gradient) acting on the particle throughout the time interval DT - that is, during the particle's traverse of that segment of its trajectory which lies between the point (XT, YT) and the next computed point on the trajectory - are then estimated by:

$$FX = (W.FXT + FX1) / (W + 1) \tag{4.1}$$

and

$$FY = (W.FYT + FY1) / (W + 1) \tag{4.2}$$

where FXT = the component, in the x coordinate direction, of the sum of the forces due to fluid drag and to the pressure gradient acting on the particle at the point (XT, YT)

FYT = the corresponding component of force, in the y coordinate direction

W = a weighting factor

FX1 and FY1 are as defined in the preceding paragraph.

The weighting factor W has been assigned a value of 2.0 throughout the computations (Note(v), Section 4.3 below).

Using the estimates of the force components furnished by Equations (4.1) and (4.2), the corresponding values of the components of particle acceleration are calculated, by expressions corresponding to Equations (2.25) and (2.26), pp. 41 and 42 respectively.

(m) Using the values of the components of particle acceleration calculated in step (l) above, displacements D2X and D2Y are calculated; the definitions of D2X and D2Y correspond (respectively) to those associated with D1X and D1Y in step (h).

(n) If the condition $(D2X^2 + D2Y^2) \leq (STEP)^2$ be not satisfied, then the value of the time increment DT is reduced to 70 percent of its former magnitude, and the computation returns to step (h).

(o) When the condition $(D2X^2 + D2Y^2) \leq (STEP)^2$ is satisfied, the quantities X2, Y2, UPT2 and VPT2 are calculated. The definitions of these quantities correspond (respectively) to those of X1, Y1, UPT1 and VPT1 in step (j). The point (X2, Y2) represents a second estimate of the next point on the particle trajectory after the point (XT, YT).

(p) The components (UFL2, VFL2) of the fluid velocity, and the components (FFAX, FFAY) of the force on the particle due to the pressure gradient, at the point (X2, Y2) are calculated in the subroutine VEL. The components (FDRX, FDRY) of the fluid drag force on the particle at the point (X2, Y2) are calculated in the subroutine DRAG.

The components of the forces due to fluid drag and to the pressure gradient acting on the particle at the point (X2, Y2) are summed for each of the two coordinate directions, the sums being denoted by FX2 and FY2 respectively.

(q) A new estimate of the components (FX, FY) of the average force (due to fluid drag and to the pressure gradient) acting on the particle throughout the time increment DT is made:

$$FX = \tfrac{1}{2}\,(FXT + FX2) \tag{4.3}$$

$$FY = \tfrac{1}{2}\,(FYT + FY2) \tag{4.4}$$

The corresponding values of the components of particle acceleration are calculated, by expressions corresponding to Equations (2.25) and (2.26) pp. 41 and 42 respectively.

(r) Using the values of the components of particle acceleration calculated in step (q) above, displacements D3X and D3Y are calculated; the definitions of D3X and D3Y correspond (respectively) to those associated with D1X and D1Y in step (h).

(s) If the condition $(D3X^2 + D3Y^2) \leq (STEP)^2$ be not satisfied, then the value of the time increment DT is reduced to 70 percent of its former magnitude, and the computation returns to step (h).

When the condition $(D3X^2 + D3Y^2) \leq (STEP)^2$ is satisfied, the quantities X3, Y3, UPT3 and VPT3 are calculated. The definitions of these quantities correspond (respectively) to those of X1, Y1, UPT1 and VPT1 in step (j). The point (X3, Y3) represents a third estimate of the next point on the particle trajectory after the point (XT, YT).

The components (UFL3, VFL3) of the fluid velocity, and the components (FFAX, FFAY) of the force on the particle due to the pressure gradient, at the point (X3, Y3) are calculated in the sub-routine VEL.

(t) The components (FDRX, FDRY) of the fluid drag force on the particle at the point (X3, Y3) are calculated in the subroutine DRAG.

The computation returns to step(q), the point (X3, Y3) having been renamed as (X2, Y2) - that is, X2 is now assigned the value which was previously assigned to X3, and similarly for other quantities.

(u) The computation having re-arrived at the end of step (s), a quantity DELXY is calculated: DELXY is the distance between the current point (X3, Y3) and the current point (X2, Y2).

(v) If DELXY exceeds (in absolute value) an arbitrarily specified value DELSCR, the calculation returns to step (t).

(w) When DELXY does not exceed (in absolute value) the value DELSCR, it is assumed that a point lying midway between the current point (X2, Y2) and the current point (X3, Y3) lies on the trajectory. The components of the particle velocity at this point are assumed to be equal to the averages of the corresponding components at the points (X2, Y2) and (X3, Y3).

The components (UFL, VFL) of the fluid velocity, and the components (FFAX, FFAY) of the force on the particle due to the pressure gradient, at the newly-determined point on the trajectory are calculated in the subroutine VEL, and the components (FDRX, FDRY) of the fluid drag force on the particle at this point are calculated in the subroutine DRAG.

The computation then returns to step (e), the newly-determined point on the trajectory now being designated as the point (XT, YT).

4.3 Explanatory Notes

(i) Operation of the program necessitates the assignment of values to a number of parameters which are not part of the definition of the eddy field or of the definition of the particle characteristics, but which serve to control various phases of the computation. These parameters are STEP, DELSCR, and W, and they are discussed in Notes (ii), (iii) and (v) below respectively. In the determination of the values to be assigned to these parameters - as in all phases of the investigation - the limited availability of computer time has been a dominant factor. Restrictions on the amount of machine time available have precluded a complete investigation of the effects of variations in the values assigned to these parameters. In order to make the most effective use of the machine time available, the values to be assigned to these parameters have been determined pragmatically, on the basis of limited numbers of trials.

(ii) Trial computations with various values of the parameter STEP (the maximum distance that the particle may travel between two successive computed points on the trajectory) have indicated that values of STEP of the order of 0.10 (expressed in the non-dimensional length units of the program) may cause instability in the computation, and are likely to require an excessively large number of trials before the criterion established by a given value of the parameter DELSCR - Note (iii) below - is satisfied. A value of STEP of the order of 0.02, on the other hand, has produced no evidence of instability and has not in general involved an excessive number of trials before the DELSCR criterion is satisfied. Accordingly, STEP has been assigned a value of 0.02 throughout the majority of the computations. In the case of some computations involving very small and very large eddies, the value of STEP has been arbitrarily varied in order to maintain a somewhat consistent ratio between the value of this parameter and the eddy size.

(iii) The value to be assigned to the parameter DELSCR has also been determined on the basis of trials. The value of DELSCR represents the displacement of the latest estimate of the next point on the particle trajectory from the preceding estimate when the prediction-correction procedure is to be terminated. Trial runs have indicated that no sensible change in the computed trajectory occurs as the value of DELSCR is reduced below 10^{-7} (expressed in the non-dimensional length units of the program) and this value has been adopted throughout the computations.

(iv) The parameters STEP and DELSCR are to some extent inter-related in their effect on the efficiency of the computation - that is, on the length of trajectory computed in a given amount of machine time. If STEP is relatively large, the number of computational steps necessary to cover a given length of trajectory will be correspondingly small, but the number of trial points required at each step to satisfy the criterion established by a given value of DELSCR may become very large. In some cases the overall efficiency of the computation has been enhanced by reducing the value of STEP and thereby reducing the number of trial points required at each step to satisfy a given DELSCR criterion.

As stated in Note (i) above, no attempt has been made to investigate completely the effects of variations in the values of the parameters STEP and DELSCR. The values which have been adopted are such that the validity of the computed particle trajectories does not appear to be prejudiced by them, whilst at the same time reasonable efficiency in computation is achieved.

(v) A weighting factor W is included in the expressions - Equations (4.1) and (4.2) - employed in the calculations described in step (1), Section 4.2. The force components FXT and FYT which appear in these expressions have been computed at a point (XT, YT) which has been determined as lying on the particle trajectory. The force components FX1 and FY1, on the other hand, have been computed at a point which is no more than a first estimate of the next point on the trajectory. Accordingly, in the estimation of the mean values of the components of force acting on the particle during its traverse of that segment of its trajectory which lies between the point (XT, YT) and the succeeding point (which is yet to be determined), it is considered that greater weight should be placed upon FXT and FYT than upon (respectively) FX1 and FY1. This is effected by the assignment to W of a value greater than unity.

The weighting factor W has been arbitrarily assigned a value of 2.0 throughout the computations. It is to be noted that the value assigned to W influences only the first estimate of the next point on the trajectory, and has no influence in the subsequent process of refinement of this estimate. Accordingly, the value assigned to W is expected to have no effect upon the final form of the computed trajectory. Some early trial computations in which W was varied over a small range have tended to confirm this hypothesis. Variations in the value of W could evidently affect the efficiency of the computation; this effect has not been investigated.

(vi) The point within the eddy field at which the computations were commenced was initially selected arbitrarily as the point (0.0, 0.3Y) - with an eddy centre located at the point (0.0, 0.0) and the spacing of eddy centres in the vertical direction being Y. This point was selected in the expectation that with this starting point, a particle which was tending to fall through the eddy field would relatively quickly move into the high-velocity zones of an eddy. Accordingly, the fate of the particle (that is, whether it would become suspended within a given eddy, or would continue to fall through the eddy field) could be determined relatively quickly, without the possible necessity of tracing the trajectory of the particle through the low-velocity zones in the outer regions of several eddies, before it traversed the higher-velocity zones of an eddy.

The effect of adopting alternative starting points within the eddy field has been examined, as described in Chapter 6 below.

(vii) In the majority of the computations, the components (in the two coordinate directions) of the velocity of the particle at the starting point have been set respectively equal to the corresponding components of fluid velocity at the same point. In the case, however, of a computation which is a continuation of an earlier computation, the last computed point of the earlier computation becomes the starting point of the restarted computation, and the components of particle velocity at this point (as calculated in the earlier computation) are available for use as the components of particle velocity at the starting point of the re-started computation.

In a few cases, the components of particle velocity at the starting point have been specified as follows: the horizontal component of the particle velocity has been set equal to the horizontal component of fluid velocity at the starting point (as determined by a separate previous calculation), and the vertical component of particle velocity has been set equal (in magnitude and sense) to the settling velocity of the particle in quiescent fluid (as determined in a separate calculation) - in all such cases, the vertical component of the fluid velocity at the starting point has been zero.

In the computed trajectories described in Chapter 6 below, the effects of two alternative sets of starting conditions may be compared, under otherwise identical conditions. The absence of any significant difference between the computed trajectories indicates that relatively minor variations in the starting conditions are quickly "forgotten" by the particle, which rapidly attains a state of quasi-equilibrium with the flow.

(viii) The program is written in "double-precision" FORTRAN; each non-integral variable is allotted 8 bytes (64 bits) of core storage.

(ix) The development of the program was carried out on the WATFOR Compiler at the University of New South Wales Computing Centre. Once the development of the program had been completed, substantial economies in machine time were effected by the use of a compiled machine-language card deck.

(x) The subroutine TEME is employed to control the termination of execution of the program. In order to satisfy the administrative requirements of the Computing Centre, it is necessary to specify a time limit on the execution of the program. If the execution of the program is terminated as a result of the expiration of this time limit, a certain amount of computed information (which is contained, at the time of termination, in the machine buffer store) will be lost. Furthermore, the data required for the re-starting of the computation will not be available, to the desirable degree of precision. With the use of the subroutine TEME, however, a time-limiting parameter (ITIME) may be specified. The value of the parameter ITIME must be less than the time limit referred to above; the value assigned to ITIME has usually been equivalent to one minute less than the relevant time limit. If the program has not completed the specified number (NSTEP) of computational steps when the expired machine time reaches the value defined by the parameter ITIME, then a flag set up by the subroutine TEME causes termination of the program.

The subroutine TEME was developed by Dr. R.W. Thomas of the School of Mechanical and Industrial Engineering, University of New South Wales.

4.4 Calculation of the Energy Interchange between Fluid and Particle

In order to permit an examination of the interaction between the fluid and the particle, the program has been adapted to include the estimation of the work done by the fluid on the particle, or the work done by the particle on the fluid, within each segment of the particle trajectory. If the direction of energy transfer (fluid to particle, or particle to fluid) varies systematically throughout the trajectory of a particle suspended within an eddy, then the motion of the particle could cause a redistribution of energy and vorticity within the eddy.

This aspect of the investigation is concerned with a particle which is suspended within an individual eddy of the model eddy field, and is designed to examine the transfer of energy, by the particle, between different zones of the eddy located at varying radii from the eddy centre. Accordingly, the work done on or by the particle has been evaluated in the form of a "Moment of Work" defined as follows:-

$$M = \oint r(F.ds) \tag{4.5}$$

where M = the "moment of work"

F = the average force exerted by the fluid on the particle during the particle's traverse of an element ds of its trajectory.

$r = (x_m^2 + y_m^2)^{\frac{1}{2}}$

x_m and y_m are the coordinates (with the eddy centre as origin) of the average position of the particle during its traverse of the segment ds of its trajectory

$\oint$ implies that the integral is to be taken along the particle trajectory.

As the system to be examined represents an interchange of energy between the particle and the fluid, it is convenient to formulate the examination from the viewpoint of one member: the particle has been selected for this purpose. Work done on the particle (by the fluid) has been allotted a positive sense. Work done by the particle (on the fluid) has been allotted a negative sense. In this context, it is to be understood that if, in the course of a certain process, the energy of the particle increases, then work is done on the particle during that process; if, on the other hand, the energy of the particle decreases, then work is done by the particle during the process.

With the above convention, it follows that if the total fluid force (that is, the fluid drag force, together with the force due to the pressure gradient within the fluid) acting on the particle, throughout a given time interval, acts in the same sense as the sense of the motion of the particle, then the work done during that time interval is to be allotted a positive sign. If, on the other hand, the total fluid force acting on the particle acts in the sense opposite to that of the particle motion, then the work is to be allotted a negative sign.

As before, it is convenient to consider separately the two coordinate directions. A given element of work dW may be considered as the sum of two terms, each of which is the product of the component (in a given coordinate direction) of a force and the component (in the same coordinate direction) of the displacement of the point of action of the force:

$$dW = dW_x + dW_y$$

$$= F_x dx + F_y dy \tag{4.6}$$

where F_x and F_y are the components, in the x and y coordinate directions respectively, of a force F

dx and dy are the components, in the x and y coordinate directions respectively, of the displacement of the point of action of the force F.

The "moment", about the eddy centre, of the element of work dW is then given by:

$$dM = (F_x dx + F_y dy).(x_m^2 + y_m^2)^{\frac{1}{2}} \tag{4.7}$$

Although the components dx and dy of the displacement of the point of action of the force F may have positive or negative senses within the coordinate system, it is convenient to consider the displacement of the particle (and hence the displacement of the point of action of the force acting on the particle) as inherently positive, in the context of the particle trajectory. Then, with the convention of signs defined above in this section, together with the previously defined convention of signs for forces and velocities (Section 2.2.9 above), dM in Equation (4.7) will have the appropriate sign if the force components F_x and F_y are replaced (respectively) by components of "signed force" F_{xs} and F_{ys} given by:-

$$F_{xs} = \pm 1.\,(F_{Dx} + F_{Px}) \tag{4.8}$$

$$F_{ys} = \pm 1.\,(F_{Dy} + F_{Py}) \tag{4.9}$$

where F_D = the force acting on the particle due to fluid drag

F_P = the force acting on the particle due to the pressure gradient within the fluid

the subscripts x and y denote components in the x and y coordinate directions, respectively, and the factor of unity is to be allotted the same sign as that associated with the component, in the relevant coordinate direction, of the velocity of the particle.

The allocation of the appropriate sign to the unit factors in Equations (4.8) and (4.9) is conveniently effected by the FORTRAN (double-precision) function DSIGN(A, B). This function yields a parameter which bears the same sign as B, and which has an absolute value equal to the absolute value of A. If A has been previously assigned a value of unity, then DSIGN(A,UPT) will yield the required factor when

UPT is the component, in the appropriate coordinate direction, of the particle velocity.

The computation is carried out as follows:-

(i) The components (FXSIGO, FYSIGO) of the "signed force" at the starting point are calculated, in expressions corresponding to Equations (4.8) and (4.9) respectively.

(ii) After the computation of the position coordinates of the next computed trajectory point, the coordinates (XM, YM) of the average position of the particle, during its traverse of this latest segment of its trajectory, are calculated. The x coordinate (XM) of the average position is taken to be the mean of the x coordinates of the initial point and the final point of the segment, and YM is calculated similarly.

(iii) The components (FXSIGN, FYSIGN) of the "signed force" at the final point of the trajectory segment are evaluated, in expressions corresponding to Equations (4.8) and (4.9) respectively.

(iv) A quantity corresponding to the first term on the right-hand side of Equation (4.6) is evaluated, being the product of $\frac{1}{2}$(FXSIGO+FXSIGN) and the absolute value of the length of the projection, onto the x coordinate axis, of the trajectory segment.

(v) A quantity corresponding to the second term of the right-hand side of Equation (4.6) is evaluated, being the product of $\frac{1}{2}$(FYSIGO+FYSIGN) and the absolute value of the length of the projection, onto the y coordinate axis, of the trajectory segment.

(vi) The "moment" of the work done during the particle's traverse of this segment of its trajectory is then evaluated, in an expression corresponding to Equation (4.7).

(vii) The moment thus evaluated is added to a "sum of moment of work" (WMSUM) - which is assigned an initial value of zero at the starting point.

(viii) For subsequent segments of the trajectory, the computation proceeds in the same fashion. Components of force evaluated for the final point of each segment become the corresponding components for the initial point of the succeeding segment.

(ix) The algebraic sum of the "moment of work" is accumulated, segment by segment along the particle trajectory.

4.5 Organisation of the Output and Trajectory Identification

4.5.1 Organisation of the Output

The printed output furnished by the program includes:-

(i) an identification of the card deck employed in the computation;

(ii) a tabulation of all the parameters which have been read in as data;

(iii) an identification of the velocity distribution.

The following information is then printed, in respect of points on the computed trajectory:-

(a) Time Parameter (that is, the non-dimensional time at which the particle passes through the given point on the trajectory)

(b) Position Coordinates (in the x and y coordinate directions)

(c) Components of the Fluid Velocity (in the two coordinate directions)

(d) Components of the Particle Velocity (in the two coordinate directions)

(e) Reynolds Number (describing the motion of the fluid relative to the particle)

(f) Integral of the "Moment of Work" (as described in Section 4.4 above)

(g) The number of trials involved in the computation of the point.

This information is printed in tabulated form for each of the first 50 computed points on the trajectory, and thereafter at intervals as specified by the value of the parameter IPRNT (which is read as data). The information (items (a) to (g) above) which is printed as the last line of each page is again printed as the first line of the tabulation on the following page.

On the termination of the computation - after the computation of a specified number (NSTEP) of points on the trajectory, or upon the expiration of the specified time (Note (x), Section 4.3 above) - the time parameter, position coordinates and particle velocity components in respect of the last computed point on the trajectory are printed, to the full precision of the machine. This information is accordingly available for the re-starting of the computation, if required.

An example of the printed output from one computation is included in Appendix III.

If the parameter KPUNCH is assigned a value other than zero, output cards are punched as follows:-

(i) An identifcation of the trajectory, and the values of all parameters which have been read in as data.

(ii) For computed points on the trajectory, at intervals as specified by the value of the parameter IPUNCH:

(a) The trajectory identification number.

(b) A number identifying the card.

(c) A number identifying the computed point.

(d) The time parameter.

(e) The position coordinates of the computed point.

The card output described above is intended for use in the plotting of the computed particle trajectory. In addition, the information required for the re-starting of the computation is punched onto cards, for incorporation into the set of data cards for the re-started computation.

The computed particle trajectories were plotted on the "Calcomp" Plotter at the University of New South Wales Computing Centre. A FORTRAN program was developed for the plotting of the trajectories, using the punched cards described above as the input data. This program is listed in Appendix IV.

4.5.2 Identification of the Computed Trajectories

Each computer run is allotted an identifying number (IDENT) which is read as data. Within a given run, up to 99 distinct sets of data may be read in. The number of such sets (NSET) is read after IDENT.

Within a data set, up to 5 values of the Eddy Velocity Parameter UEDDY may be read. The number of such values to be read is itself read in as NV, and the individual values of the Eddy Velocity Parameter are read as UEDDS(NN), where $1 \leq NN \leq NV$. The combination of a given data set and a given value of the velocity parameter has been termed a data subset.

Each data subset, and hence each computed trajectory, has a unique identifying number of 5, 6 or 7 digits, of the form: ZKLMN, YZKLMN, or XYZKLMN,

where Z, YZ, or XYZ is the number identifying the run, with a value within the range 1 - 999.

KL identifies the data set, and has a value within the range 01 - 99.

MN identifies the data subset, and has a value within the range 01 - 05.

Within any one computer run, data sets with differing values of KL may have different values for the parameter KSTART and for all the parameters which follow KSTART in Table III. A.

Data subsets whose identifications differ only in MN will have the same values for all parameters except the Eddy Velocity Parameter UEDDY.

5. Verification of the Computer Program for the Computation of Particle Trajectories

5.1 Introduction

The equation of motion which is to be used in the computation of the trajectories of particles within the model eddy field has been formulated in Chapter 2 above. The formulation of the equation has involved the following assumptions:

(i) that the lift force component acting on the particle may be neglected (Section 2.2.4),

(ii) that the effect of the history of the motion of the particle relative to the fluid need not be specifically taken into account (Section 2.2.8),

(iii) that the drag force component acting on the particle may be estimated by use of the steady-state drag coefficients (Section 2.2.5),

(iv) that the value of the added-mass coefficient for the particle will not differ significantly from 0.50 (Section 2.2.2),

(v) that the effect of the forces, due to the existence of a pressure gradient within the fluid, which act on the particle-appendant fluid system may be estimated, to within a reasonable degree of approximation, by the method described in Section 2.2.6.

Further assumptions are involved in the development of the computer program, as described in Chapter 4. At this stage, it remains to be confirmed that the computational scheme described in Section 4.2 will yield a convergent solution for the successive computed points on the particle trajectory, and that the accumulation of numerical errors will not significantly affect the form of the computed trajectory. It is also implicitly assumed that the values assigned, in the operation of the program, to the parameters STEP, DELSCR, and W - (as discussed in Notes(ii), (iii) and (v) respectively in Section 4.3) - are such that the validity of the computed trajectories will not be prejudiced.

In general, no a priori justification of the assumptions made is available. The assumptions involved in the development of the equation of motion have been dictated by necessity, in the absence of definitive evidence on the issues involved. The selection of the values of the program parameters has been based on the results of limited numbers of trials. Consequently, reliance will be placed upon a pragmatic verification of the program in order to justify the assumptions which have been made.

A preliminary check on the performance of the program has been effected by confirming that it will predict the fall velocity of a particle settling in a quiescent fluid. This was carried out by computing the trajectories (and, more particularly, the velocities at the successive points on the trajectories) of non-buoyant particles in an eddy field in which the characteristic fluid velocity was specified to be zero. Under these conditions, the particle trajectory took the form of a straight line, directed vertically downward. The particle velocity approached a constant value, which represented the settling velocity of the particle in the quiescent fluid. This check, however, verifies the performance of the program under steady-state conditions only. It is of little significance in the context of the unsteady conditions involved in the computation of the trajectory of a particle within a field of non-zero fluid velocities.

Verification of the program depends, in principle, upon a comparison between particle trajectories as computed by the program and the corresponding trajectories as indicated by deduction or by experimental measurement. It is impractical to experimentally generate a velocity distribution which is precisely of the form specified to exist within the model eddy field. Furthermore, the facilities necessary for the measurement of the properties of experimentally-realisable velocity distributions of generally similar form were not available. Hence, a comparison of computed and experimental particle trajectories within such a velocity distribution is not available. Accordingly, in order to effect verification of the computer program, recourse has been had to

(i) comparison of computed and deduced trajectories of neutrally-buoyant particles within the model eddy field (Section 5.2 below), and

(ii) comparison of computed and experimentally-determined trajectories of non-buoyant particles falling through water in the presence of gravity-wave motion (Section 5.3 below).

5.2 The Trajectories of Neutrally-buoyant Particles within the Model Eddy Field

The fluid streamlines within an individual eddy of the model eddy field defined by Equation (3.2), p. 46, consist of a series of closed curves, as shown in Figure 4. Accordingly, if any point within the eddy field (other than the singular points comprising the eddy centres and the nodes, at which the two components of fluid velocity are zero) be selected as a starting point, and if an infinitesimal element of fluid, passing through that point at any instant of time, could be "tagged", then the tagged element will periodically return to the starting point. During each of the intervening intervals of time, the fluid element will execute a circuit of one of the eddies of the model eddy field. Its trajectory throughout each circuit will (by definition, since the fluid motion within the model eddy field is steady) coincide with the streamline which passes through the starting point.

The trajectory of such a fluid element is, in general, curved in form. The curvature of the trajectory at any point is a function of the relative magnitudes of the local components, in the two coordinate directions, of the acceleration of the fluid element. The components of acceleration are, in turn, functions of the components of force which act on the fluid element at the given point. The force components are due to the existence of pressure gradients within the fluid. If the trajectory of the fluid element forms a closed curve, it is implied that the integrated effect of the local curvatures of the trajectory (integrated along the trajectory) is such as to cause the trajectory to return to its starting point.

If the fluid element (of infinitesimally small size) which is under consideration is now instantaneously replaced, at the starting point, by a neutrally-buoyant rigid particle of the same size, then the force which acts on the rigid particle at the starting point will be unchanged from the force which acted, at the same point, on the fluid element. The mass of the rigid particle will be equal to that of the fluid element which it has replaced. Accordingly, the response of the rigid particle to the force acting upon it at the starting point will be identical to the response of the fluid element to the same force. The components of the acceleration of the rigid particle at the starting point will consequently be respectively equal to the corresponding components of the acceleration of the fluid element at the starting point. Extension of the argument from point to point along the trajectory indicates that the trajectory of the rigid, neutrally-buoyant particle will coincide with the trajectory of the fluid element - that is, the particle trajectory will coincide with the fluid streamline which passes through the starting point.

The argument of the preceding paragraph is applicable to particles of infinitesimally small size. In the case of particles of finite size, however, recognition must be given to the deformable nature of a fluid particle, contrasting with the inherently non-deformable nature of a rigid particle. If a fluid particle of finite size is located within a non-uniform velocity field, then the fluid velocity at the boundary of the particle will, in general, vary from point to point on the boundary. In the absence of discontinuities between the velocities of fluid elements within the particle and the velocities of fluid elements outside the particle, deformation of the particle will occur. The corresponding rigid particle is, however, inherently incapable of deformation. Conditions within the fluid immediately adjacent to the boundary of the rigid particle will, in general, vary from point to point on the boundary. The response of the rigid particle to the forces exerted on it by the surrounding fluid will represent the outcome of a process of averaging or integration (of the elemental forces exerted by the various fluid elements surrounding the particle). This response must be invariant from point to point on the particle. Consequently, the velocity of the boundary of the particle will, in general, tend to differ from that of the immediately adjacent fluid elements, and acceleration of the rigid particle, relative to the surrounding fluid elements, will tend to occur. Under these conditions, in the absence of slip at the particle boundary, the diffusion of shear stresses from the boundary will cause a readjustment of fluid velocities within a zone extending outwards from the particle boundary. Accordingly, the phenomenon of added mass will come into operation, in the case of a rigid particle of finite size. The concept of added mass appears to have no meaning, however, in the context of a fluid particle.

A series of computations of trajectories of neutrally-buoyant particles within the model eddy field (as defined in Chapter 3) has been carried out. The values of the parameters defining the characteristics of the particle-fluid systems, and the characteristics of the model eddy field, are tabulated in Table 1. It is to be noted that in the case of a neutrally-buoyant particle, the gravitational parameter GRAV assumes a value of zero, since

$$GRAV = (s - 1.0)$$

where s = the ratio of the density of the particle to the density of the fluid surrounding the particle.

= 1.0 in the case of a neutrally-buoyant particle.

The significance of the parameter values, in terms of the properties of actual particle-fluid systems of practical engineering interest, is discussed in Section 6.1 below. From the values shown in Table 5, it may be deduced that the parameter values in Table 1 correspond to a neutrally-buoyant particle 50.10^{-3}mm in diameter, the surrounding fluid being water. In the computations of the first three trajectories listed in Table 1, the spacing of eddy centres within the model eddy field corresponds to a value employed in computations which are described subsequently in Chapter 6. Within these computations, variations in the parameter values occur only in the values of the ordinate (Y_O or YSTART) of the starting points of the respective trajectories. In the case of the remaining trajectory (identified as Number 1.4) the spacing of the eddy centres within the eddy field is smaller and the curvature of the streamlines is consequently sharper. The starting point of this trajectory is at (almost) the same point, relative to the eddy centres, as is the starting point of Trajectory 1.2.

The printed results of the computation of Trajectory 1.2 are included in Appendix III. The results of the several computations are indicated in Figures 7 and 8, and in the final column of Table 1. In

Figures 7 and 8, the curves represent the computed particle trajectories, and the crosses indicate representative points on the streamlines which pass through the starting points of the trajectories. No deviation which is discernible at the scale of the diagrams exists, between the computed particle trajectories and the corresponding fluid streamlines. In the final column of Table 1 is listed, for each computed particle trajectory, the value of Y_1 (the ordinate of the point in which the computed trajectory intersects the line X = 0.0, after the execution of one circuit of the eddy). For each trajectory, the value of Y_1 has been calculated by the application of the Lagrange Interpolation Formula to four computed points: the two computed points (for which results are printed) which lie closest to, and to the left of, the line X = 0.0, and the two computed points (for which results are printed) which lie closest to, and to the right of, the line X=0.0. The tabulated values of Y_1 confirm that any accumulated deviation, throughout one circuit of the eddy, of the computed particle trajectory from the streamline which passes through its starting point is very small in relation to the overall dimensions of the trajectory. The deviation is in fact not discernible within the four decimal places to which the computed position coordinates of points on the computed trajectory have been printed.

The investigation described in this section has involved the examination of the trajectories, within the model eddy field, of neutrally-buoyant particles with diameters which are small, in comparison with the dimensions of the eddy field. It is concluded that, at least under conditions similar to those applying in the investigation described, the computer program may be expected to yield a reasonably accurate estimate of the overall form of a particle trajectory.

5.3 The Trajectories of Non-buoyant Particles Falling through Waves

The distribution of fluid velocities within a body of water in which two-dimensional surface gravity waves are present is mathematically definable, and such a velocity distribution can be created experimentally without undue difficulty. A velocity distribution of this type has accordingly been employed in securing further verification of the computer program.

This section of the investigation has involved the comparison of experimentally-determined particle trajectories and the corresponding trajectories as determined by the computer program. In each case, the experimental particle trajectory was determined by photographing successive positions of the particle as it fell through the wave field. Subsequently, a section of the particle trajectory was selected from the photographic record and the reproduction, by means of the computer program, of this section of the trajectory was attempted.

Appendix V contains a description of the non-buoyant particles which were used in the investigation described in the following paragraphs. The characteristics of the particles are listed in Table 3, and the characteristics of the experimental wave fields are listed in Table 2. It is to be noted that the particle diameters were relatively large, in comparison with the dimensions of the trajectories of the particles. The relative magnitudes of the particle diameters and the excursions of the particles are indicated in Figures 9 to 15. In this respect, the investigation at present under discussion is to be contrasted with those described in Section 5.2 and Chapter 6, where the particle diameters were small in comparison with the overall dimensions of the particle trajectories. In the present investigation, some minor discrepancies have been observed between the experimentally-determined trajectory and the computed trajectory of a given particle, as discussed below. The existence of such discrepancies may be partially attributable to the relatively large size of the particles.

The wave field which was employed comprised a system of standing waves, generated within a laboratory wave flume. The experimental procedure employed in the determination of the particle trajectories is described in detail in Appendix V. The computation of the computed particle trajectories was carried out by means of the computer program developed for the computation of trajectories of particles within the model eddy field (as described in Chapter 4 and Appendix III) with certain modifications which were necessary to adapt the program to the present purpose. The modified program, and the procedure adopted in the computation of the particle trajectories, is described in Appendix VI. A computer program was developed, by adaptation of the program described in Appendix IV, for the purpose of plotting the computed trajectory of a particle within the wave field.

In a few experiments, anomalous results were obtained, apparently as a result of the particle's encountering debris or air bubbles in the water within the flume. Such results were rejected, as were the results of experiments which showed evidence of undue horizontal drift of the particle (that is, undue net motion of the particle in the direction of the length of the flume). Some horizontal drift is in evidence in the trajectory illustrated in Figure 9.

Corresponding segments of experimentally-determined and computed particle trajectories are illustrated in Figures 9 to 15 inclusive. Figure 16 is a reproduction of the original photographic record of the trajectory of the particle numbered 36. Trajectory 1250201 is the reproduction, by the computer program, of a section of the trajectory shown in Figure 16; its starting point is indicated by the small white cross. The characteristics of the wave systems are tabulated in Table 2, together with the corresponding dimensionless parameters used in the computations. The characteristics of the particles, and the corresponding dimensionless parameters, are shown in Table 3. In Figures 9 to 15 the lines designated as the experimentally-determined trajectories have been derived by joining, with straight lines, the successive photographed positions of the particle. The experimental and computed trajectories coincide at the starting points - no relative translation of the trajectories, such as might improve the overall fit, has been carried out.

Examination of Figures 9 to 15 indicates that general qualitative agreement exists, between each experimental trajectory and the corresponding computed trajectory. In general, fairly close quantitative agreement between the experimental trajectory and the corresponding computed trajectory has been maintained throughout approximately one wave period, with varying degrees of divergence being in evidence at later stages. The divergence generally takes the form of a difference between the "wave lengths" of the experimental and computed trajectories - that is, a difference between the vertical distance traversed by the particle during one wave period as indicated by the experimental trajectory and the corresponding distance as indicated by the computed trajectory. These discrepancies may be attributable, at least in part, to the relatively large diameter of the experimental particles. The computation of the particle trajectories is based upon the assumption that the particles are so small that the presence of a particle has no effect upon the local fluid velocity field. The experimental particles are, however, relatively large in comparison with the overall dimensions of the particle trajectories, and hence this assumption will be to some extent violated.

The comparison of the experimental and computed trajectories is quantified in Table 4, in terms of the particle fall velocity and of the horizontal excursions of the particle. Table 4 indicates that the fall velocity of a given particle within the wave field, as indicated by the computed particle trajectory, has generally differed little from the settling velocity of the particle in quiescent water. The relationship between the fall velocity of a given particle as indicated by the computed trajectory, and the fall velocity of the same particle as indicated by the experimental trajectory, is represented by the value of the ratio V_c / V_e, which is shown in Table 4. For the seven trajectories under consideration, the discrepancies between the computed and experimental fall velocities have magnitudes corresponding to 0, 3, 11, 15, 16, 18 and 23 per cent of the experimental fall velocities.

It is of some interest to note that there is little evidence to indicate that a standing-wave field is likely to cause the fall velocity of a given particle to be significantly less (in absolute magnitude) than the settling velocity of the particle in the quiescent fluid. As pointed out above, the computed particle trajectories generally indicate that the fall velocity of a given particle within the wave field will differ little from the settling velocity of the particle in quiescent water, whilst only one of the experimental trajectories (No. 1090101) indicates that the fall velocity within the wave field will be less than the settling velocity in quiescent water.

The horizontal excursions of the particles within the waves, as tabulated in Table 4, have been measured from the plotted trajectories, at about the mid-depth of the section of the trajectory over which the particle fall velocity was determined. In the case of the experimental trajectories, some degree of estimation has been involved, where interpolation of the form of the trajectory between the successive photographed particle positions has been necessary. The experimental and computed particle excursions as tabulated are in reasonably close agreement, with the exception of those associated with Trajectory 1120101. In the case of Trajectory 1280101, which is illustrated in Figure 15, the horizontal excursions of the particle are so small in relation to the overall (combined horizontal and vertical) excursions that a comparison between the experimental and computed values of the horizontal excursion alone is not considered relevant. Examination of Figure 15 indicates, however, that reasonably close agreement exists between the overall excursions of the particle as indicated by the experimental and computed trajectories respectively.

In view of the probability that the fall velocity of a given particle within the wave field does not differ substantially from the settling velocity of the given particle in quiescent water, comparison of the experimental and computed results in respect of the excursions of the particle is probably more significant, from the viewpoint of verification of the computer program, than is the consideration of particle fall velocities. It is concluded that the reasonably close agreement which is in evidence, in six of the seven trajectories under consideration, between the excursions of the particle in experimentally-determined and computed trajectories respectively offers a substantial degree of verification of the computer program.

5.4 Conclusion concerning the Verification of the Computer Program

In view of the results of

(i) the comparison of computed and deduced trajectories of neutrally-buoyant particles within the model eddy field (Section 5.2), and

(ii) the comparison of experimentally-determined and computed trajectories of particles falling through waves (Section 5.3), it is concluded that verification of the computer program developed for the computation of particle trajectories has been established, at least to the extent of justifying the use of the program in an examination of the eddy model of turbulent flow, and in an examination of the behaviour of a rigid non-buoyant particle within the model eddy field.

6. The Results of the Computations of Trajectories of Particles within the Model Eddy Field

6.1 The Relationship between the Parameter Values used in the Computations and the Physical Properties of Actual Particle-Fluid Systems

In the early stages of the investigation, it became evident that it would not be practicable to extend the investigation to cover a wide range of particle and fluid properties. Accordingly, it was decided that the investigation should be directed towards the examination of certain specific particle-fluid systems which are of practical engineering interest.

This approach was intended to yield insight into the behaviour of the specific systems examined, and to furnish the basis for an overall assessment of the eddy model of suspension of a non-buoyant particle within a turbulent flow. Some limitation was, however, thereby imposed upon the generality of the results.

The stimulus for the present investigation originated in an examination of the feasibility of the disposal of fly ash from power station boilers by the formation of a suspension of fly ash in water, and the discharge of the ash-water suspension into the ocean. The prediction of the behaviour of the suspension within the ocean is dependent upon an understanding of the process of suspension of the ash particles in the water. Accordingly, in the present investigation, emphasis has been placed upon the examination of a system consisting of a typical fly ash particle in water. The significant properties of such a particle have been abstracted from the Electricity Commission of New South Wales Research Note No. 30, "Report on the Ocean Disposal of Fly Ash"- Reference (14). For the present purpose, a representative significant particle diameter has been taken to be 50.10^{-3}mm (the particles are essentially spherical in form, and 90 percent by weight of a typical fly ash is reported to be of this or lesser diameter). The particle specific gravity is approximately 2.0.

In order to gain some insight into the effects of particle density, computations were also carried out - as described in Section 6.3.2 - with parameter values corresponding to systems consisting of particles of the same diameter (50.10^{-3}mm) with specific gravities of 2.65 and 11.40, suspended in water. The smaller of these values of specific gravity corresponds to that of the common siliceous materials; a particle of the given diameter would fall within the size range designated as silt. The larger value of specific gravity corresponds to that of lead, and is assumed to lie at the upper limit of the range of common engineering interest.

A further set of parameter values was selected, to represent a typical dust particle in air. The particle diameter was assumed to be 5.10^{-3}mm, and the particle specific gravity 2.65.

The properties of the various particle-fluid systems are tabulated in Table 5. This table shows the particle diameter and specific gravity, the ratio (s) between the particle density and the fluid density, the dimensionless parameters PART and GRAV, and the ratios between dimensional and dimensionless quantities in respect of length, velocity and time. Also tabulated is the settling velocity of the particle in the quiescent fluid, together with the corresponding dimensionless velocity and the associated Reynolds Number.

When the Reynolds Number describing the settlement of a particle in quiescent fluid is within the range of validity of Stokes' Law (that is, $\mathbb{R} \leq 0.1$) then the velocity of settlement is given by

$$v_s = \frac{(s-1.0)\, gd^2}{18\, \nu} \tag{6.1}$$

where v_s = the velocity of settlement of the particle

s = the ratio of the density of the particle to the density of the surrounding fluid

g = the gravitational acceleration

d = the particle diameter

ν = the kinematic viscosity of the fluid

The corresponding dimensionless velocity V_s is then given, in accordance with Equation (2.23), p.40, by

$$V_s = \frac{v_s}{\sqrt{gd}}$$

Substituting from Equation (6.1)

$$V_s = \frac{(s-1.0)}{18} \frac{\sqrt{gd^3}}{\nu}$$

$$= \frac{(s-1.0)}{18} \cdot (PART) \tag{6.2}$$

The associated Reynolds Number is given by

$$\mathbb{R} = \frac{v_s d}{\nu} = \frac{(s-1.0)}{18} \cdot \frac{gd^3}{\nu^2}$$

$$= \frac{(s-1.0)}{18} (PART)^2 \tag{6.3}$$

which is as indicated by Equation (2.24), p. 40.

For those cases in which the Reynolds Number describing the settlement of the particle is beyond the range of validity of Stokes' Law, the settling velocity of the particle has been calculated by an iterative procedure, using an IBM "MATH" terminal facility which was available during portion of the investigation.

Listed below Table 5 are the values which have been adopted for certain physical quantities. The values have been adopted on the basis of numerical convenience, rather than on the basis of precise correspondence to any given physical situation, but all values correspond to conditions which are attainable within the range of ordinary engineering interest. The value adopted for the specific gravity of air, for example, differs by only 1.9 per cent from the corresponding value at sea-level in the ICAO Standard Atmosphere, and leads to the convenient value of 2200 for the gravitational parameter GRAV when the particle specific gravity is 2.65.

In the course of the investigation, it became evident that the spacing of eddy centres within the model eddy field is not a significant variable, insofar as the suspension of a particle is concerned. The actual values of the eddy spacings employed in the computations are essentially relics of the first approaches to the investigation; the extent of the modification of these values in the course of the investigation was deliberately limited, in order to facilitate the comparison of results obtained at successive stages. The value of 135 dimensionless units for the spacing of eddy centres corresponds to an actual physical spacing of about 17 mm, in the case of a particle of diameter 50.10^{-3}mm, a density ratio (s) of 2.0 and an added mass coefficient of 0.5. With a spacing of eddy centres of 135 units, the ordinate of the starting point of the particle trajectory was selected as 40 units - for the reasons discussed in Section 4.3. A larger eddy spacing and a trajectory starting point at the same relative position with respect to the eddy centres, was determined by simply doubling the above values, to 270 and 80 units respectively. In determining a smaller eddy spacing, the ordinate of the starting point of the particle trajectory was assigned the convenient integral value 15.0, and the spacing of the eddy centres was assigned the value 50.625, in order to maintain the same relative position of the starting point with respect to the eddy centres.

In most of the computations representing particles in water, the spacing of eddy centres within the model eddy field has been assigned the value 50.625. In some such cases, however, and in the case of computations which represent a particle in air, this value has been varied in such a way as to maintain an approximate constancy of the corresponding physical spacing of eddy centres - as shown in Table 6. It is to be noted that the results of the investigation to be described below indicate that the spacing of the eddy centres within the model field is not a significant quantity, insofar as the suspension of a particle within the model eddy field is concerned.

In all cases, it has been assumed that the spacing of the eddy centres is the same, in each of the two coordinate directions - that is, it has been assumed that the eddy centres form a square array within the model eddy field. This assumption has been made in the absence of any evidence to suggest that the model eddies should be other than "square".

The object of the investigation described in the succeeding sections is to determine the conditions under which a given particle will be suspended within the model eddy field. With the characteristics of the particle and the other characteristics of the model eddy field fixed, it remains to determine - by trial, as described below - that value of the characteristic fluid velocity within the model eddy field which will cause the given particle to be suspended within the eddy field.

A complete listing of the values assigned to the parameters in the various computations of the trajectories of particles within the model eddy field is shown in Tables 7, 8, 9, 10 and 11.

6.2 The Computed Trajectories of Neutrally-Buoyant Particles

The computed trajectories of neutrally-buoyant particles within the model eddy field have been described within Chapter 5, and specifically in Section 5.2, in the context of the significance of these computations in the verification of the computer program. No further description of these trajectories is necessary, except by way of comparison with certain features of the computed trajectories of non-buoyant particles. Such comparisons will be made, where appropriate, in the course of the following discussion of the trajectories of non-buoyant particles.

6.3 The Computed Trajectories of Non-Buoyant Particles

6.3.1 General Observations

Examination of the computed trajectories of non-buoyant particles within the model eddy field leads immediately to the following empirical conclusions:

(i) The trajectories fall into two general categories. The first category consists of trajectories which form virtually-closed curves, each encircling an individual eddy centre, as typified by the Trajectory No. 610101-620101 which is shown in Figure 17. The second category consists of open curves, such as are typified by Trajectory No. 380101 which is shown in Figure 18.

(ii) The particle trajectories do not, in general, conform closely to the shape of fluid streamlines within the model eddy field.

(iii) Certain symmetries are in evidence in the computed particle trajectories, although the particle trajectories do not in general share the simple symmetry associated with the fluid streamlines within the individual eddies.

As stated above, a proportion of the computed particle trajectories form curves which are virtually closed and which encircle an eddy centre. In such a case, if the coordinates of the starting point are (X_O, Y_O), the particle trajectory after one circuit of the eddy passes through a point $(X_O, Y_O + \Delta Y)$ where ΔY is a small positive quantity. This tendency for the particle trajectory to be spiral in form is discussed in Section 6.3.7 and Appendix VIII. The occurrence of a trajectory which forms a (virtually) closed curve implies that the particle is suspended within the eddy; so long as the identity of the eddy persists and its properties remain constant, the particle will execute successive circuits of the eddy. After each circuit the particle will pass through a point which (virtually) coincides with the starting point. Under these conditions, the temporal mean fall velocity of the particle will approach zero. The occurrence of computed particle trajectories of this form is probably the most significant result of the present investigation. The formulation of a criterion for the definition of the conditions under which a particle will be suspended within an individual eddy of the model eddy field is discussed in Section 6.3.2.

When the trajectory forms an open curve, such as that shown in Figure 18, the particle is not suspended but falls through the eddy field. The behaviour of the particle under these conditions is discussed in Section 6.3.4 below.

The symmetry of the computed particle trajectories is discussed in Section 6.3.8 below and in Appendix IX.

More detailed examination of the numerical results of the computations, such as the results of the computation of Trajectory No. 610101-620101 as presented in Appendix III, leads to the following empirical conclusions.

(i) At all points, the vertical component of the particle velocity differs from the vertical component of the local fluid velocity by a quantity which is sensibly equal in magnitude to, and is of the same sense as, the settling velocity of the particle in the quiescent fluid. Hence, the vertical component of the velocity of the particle at any point is sensibly equal to the algebraic sum of the vertical component of the fluid velocity at that point and the settling velocity of the particle in the quiescent fluid.

(ii) At any given point, the magnitude of the difference between the horizontal component of the particle velocity and the horizontal component of the fluid velocity is small, in comparison with the magnitude of the settling velocity of the particle in the quiescent fluid.

These conclusions are in agreement with the theoretical results of Manton (30) concerning the motion of a particle in a cylindrical vortex with a horizontal axis, and lead to some further inferences concerning the forces acting on the particle. It is implied that the horizontal component of the velocity of the fluid relative to the particle will be small in magnitude, in comparison with the vertical component of the velocity of the fluid relative to the particle. It follows that the resultant vector velocity of the fluid relative to the particle will be approximately equal in magnitude to the vertical component of that relative velocity, and virtually independent of the magnitude of the (small) horizontal component of that relative velocity. The first of the conclusions enumerated above implies that the vertical component of the velocity of the fluid relative to the particle is sensibly invariant from point to point, and is equal in magnitude to, and opposite in sense from, the settling velocity of the particle in the quiescent fluid. It is accordingly implied that at all points the vector velocity of the fluid relative to the particle is expected to be approximately equal in magnitude to the settling velocity of the particle in the quiescent fluid.

This conclusion is empirically confirmed by examination of the computed values of the Reynolds Number describing the motion of the fluid relative to the particle, as shown in the results of the computation of Trajectory No. 610101-620101 in Appendix III. As shown in Table 5, the value of the Reynolds Number associated with the settlement of the particle in the quiescent fluid is 0.0681. Examination of the computed values of the Reynolds Number as tabulated in Appendix III confirms that after the first few computed points (at which conditions are influenced by the arbitrarily-imposed starting conditions) the Reynolds Number varies little from this value.

The magnitude of a component of the fluid drag force acting on the particle at any point is in general dependent upon the vector velocity of the fluid relative to the particle and upon the component, in the given coordinate direction, of that relative velocity - as indicated by the initial terms of Equations (2.25) and (2.26), pp. 41 and 42. The empirical inferences discussed above, however, indicate that the vector velocity of the fluid relative to the particle is sensibly invariant from point to point. It is consequently implied that the magnitudes of the horizontal and vertical components of the fluid drag force acting on the particle at any point will be nearly proportional (respectively) to the magnitudes of the horizontal and vertical components of the velocity of the fluid relative to the particle at that point.

The existence of a sensibly constant difference between the vertical components of fluid velocity and particle velocity leads to the inference that, for the conditions applying in the computation of trajectory No. 610101-620101 (where the ratio of particle density to fluid density is 2.0) the force on the particle due to the existence of a pressure gradient within the fluid is small, in comparison with the net gravitational force and the force due to fluid drag. The net gravitational force on the particle is constant in magnitude and sense at all points on the trajectory, acting in the negative (downward) sense. It has been noted that at all points on the trajectory the vertical component of the velocity of the fluid relative to the particle has a positive (upward) sense, as consequently has the vertical component of the fluid drag force on the particle. The vertical component of force on the particle due to the existence of a pressure gradient within the fluid varies, in magnitude and sense, from point to point on the trajectory. This force component has at each point the sense of the vertical component of the local fluid acceleration - that is, negative (downward) in the upper half of an eddy and positive (upward) in the lower half. As pointed out above, however, the magnitude of the vertical component of the velocity of the particle relative to the fluid tends to be constant from point to point on the trajectory, and differs little from the settling velocity of the particle in quiescent fluid. It is accordingly implied that the vertical component of the force on the particle due to the existence of a pressure gradient within the fluid must be small, in comparison with the net gravitational force and the fluid drag force.

6.3.2 The Suspension of a Non-Buoyant Particle in the Model Eddy Field

As pointed out in Section 6.3.1, the computed particle trajectories fall into two categories. A trajectory of the first category takes the form of a virtually-closed curve and encircles an eddy centre- as typified by the Trajectory No. 610101-620101 shown in Figure 17. The occurrence of a trajectory of this form implies that the particle is suspended within the eddy whose centre is encircled by the trajectory. A trajectory of the second category takes the form of an unclosed curve, as typified by the trajectory illustrated in Figure 18, and it is implied in such a case that the particle is not suspended but falls through the eddy field.

With the object of the demarcation of the conditions which will cause a particle to be suspended within an eddy (rather than falling through the eddy field) the results of a number of trajectory computations have been plotted as shown in Figure 19. The values of the parameters involved in these computations are listed in Table 7. It is to be noted that the following parameter values are common to all the computations at present under discussion:

$$\text{Particle-fluid parameter} \quad PART = \frac{\sqrt{gd^3}}{\nu} = 1.1068$$

$$\text{Gravitational parameter} \quad GRAV = (s-1.0) = 1.00$$

where g = gravitational acceleration

d = particle diameter

ν = kinematic viscosity of the fluid

s = the ratio of the density of the particle to the density of the fluid.

In all cases, the starting point of the trajectory is at the point ($X = 0.0$, $Y = 0.3\ Y_c$) where Y_c is the spacing of the eddy centres in the Y direction (which is equal to the spacing in the X direction). The computations have been carried out for various values of the characteristic fluid velocity in the model eddy field, and for a number of different values of the spacing of the eddy centres within the eddy field.

In Figure 19, each plotted point represents a trajectory computation (or a series of computations, where re-starting of the computation has been necessary). The abscissa of each point is proportional to the spacing of the eddy centres, and the ordinate is proportional to the dimensionless characteristic fluid velocity within the eddy field (U_e). Points which are designated by circles represent those cases in which the computed trajectory indicates that the particle will be suspended within an eddy. Points designated by triangles represent those cases in which the particle is not suspended, but falls through the eddy field. The reference number of the trajectory, as shown in Table 7, is indicated alongside each point. In the case of points representing those trajectories in which the particle is not suspended but falls through the eddy field, the figure (in brackets) alongside each point represents the value of the ratio, V_f/V_s

where V_f = the dimensionless fall velocity of the particle, calculated over one "wavelength" of the computed trajectory, which is typified by that shown in Fig. 18

V_s = the dimensionless settling velocity of the particle in the quiescent fluid.

Examination of Figure 19 leads to the following conclusions, for the particular conditions applying to the computations which are represented therein:

(i) Suspension of the particle occurs when the dimensionless characteristic fluid velocity in the eddy field (U_e) is equal to, or greater than, about 0.17.

(ii) The critical value (U_{ec}) of the characteristic fluid velocity necessary for suspension of the particle does not appear to depend, to any significant extent, upon the eddy size.

(iii) The value of the ratio $\frac{V_f}{V_s}$ depends upon the value of the characteristic fluid velocity U_e, but (for a given value of U_e) the value of $\frac{V_f}{V_s}$ does not appear to depend, to any significant extent, upon the eddy size.

(iv) With increasing values of the characteristic fluid velocity U_e, the value of the ratio $\frac{V_f}{V_s}$ at first increases slowly, from a value of unity when U_e is zero, to a maximum of about 1.4 and then decreases rather rapidly to a value of zero as U_e approaches the critical value of approximately 0.17.

The variations of the ratio $\frac{V_f}{V_s}$ are discussed in greater detail in Section 6.3.4.

In order to examine the effects of variations in the properties of the particle and the fluid upon U_{ec} (the critical magnitude of the characteristic fluid velocity within the eddy field which is necessary for the suspension of a particle) some less extensive series of computations were carried out with the following values of the significant parameters:

PART= $\frac{\sqrt{gd^3}}{\nu}$	1.1068	1.1068	0.00234
GRAV=(s-1.0)	1.65	10.40	2200

The physical properties of particles to which the above parameter values would apply are shown in Table 5.

Complete lists of the parameter values employed in these computations are shown, for the three groups indicated above, in Tables 8, 9 and 10 respectively. In carrying out these computations, it has been implicitly assumed, in the light of the results shown in Figure 19, that the value of U_{ec} is not dependent upon the spacing of eddy centres within the eddy field. In all cases, the trajectory was assumed to pass through the point (X=0.0, Y = $0.3Y_c$) where Y_c is the spacing of the eddy centres.

The object of each set of computations was to determine the minimum value of the characteristic fluid velocity within the eddy field which would lead to the suspension of the particle. It is evident that the result of each trajectory computation (that is, whether the particle is suspended within an eddy or falls through the eddy field) is determined by the form of the trajectory within that region in which the point of inflection occurs in the case of a trajectory of the unclosed form. Accordingly, in order to reduce the total amount of machine time involved in the computations, several computations have been carried out, with a point ($X = 0.0$, $Y = -0.3Y_c$) as starting point. These have been designated as "partial trajectories" in the tabulations. The results of such computations have provided guidance in the selection of values of the characteristic fluid velocity within the eddy field, for the subsequent computations.

The significant results of the computations listed in Tables 8, 9 and 10 are represented in Figure 20. The reference numbers shown alongside the plotted points are the Trajectory Reference Numbers as listed in Tables 8, 9 and 10. Also shown in Figure 20 are points (marked 2.10 and 2.16) which represent the corresponding trajectories of Table 7. The abscissa of each point in Figure 20 is proportional to V_s, the dimensionless settling velocity of the particle in the quiescent fluid. Each point designated by a circle has an ordinate which represents the smallest value of U_e for which the computed trajectories have indicated that suspension of the given particle will occur. Each point designated by a triangle has an ordinate which represents the next (smaller) value of U_e for which a trajectory has been computed - that is, the ordinate of a point designated by a triangle represents the largest value of U_e for which a computed trajectory has indicated that suspension of the given particle will not occur.

Figure 20 indicates that, for the specific conditions associated with the particle trajectories at present under discussion, the relationship between U_{ec}, the critical magnitude of the dimensionless characteristic velocity within the eddy field for suspension of the particle, and V_s, the dimensionless settling velocity of the particle in the quiescent fluid, may be expressed as

$$U_{ec} = 2.7\ V_s \tag{6.4}$$

In other words, it is indicated that, for the specific conditions considered and for the specific velocity distribution of the model eddy field, a particle will be suspended within an eddy of the field provided that the characteristic fluid velocity within the eddy field is equal to, or greater than, about 2.7 times the settling velocity of the particle in the quiescent fluid.

It is to be noted that this conclusion is based upon the assumption that the particle trajectory passes through a specific point within an eddy - namely, the point ($X = 0.0$, $Y = 0.3\ \dot{Y}_c$) where Y_c is the spacing of the eddy centres within the eddy field, the origin of co-ordinates coinciding with an eddy centre. This assumption is examined more closely in Section 6.3.3.

6.3.3 The Effect on the Computed Trajectory of the Initial Velocity and Location of the Particle

As pointed out in Note vii, Section 4.3, the components of the particle velocity at the starting point have been set respectively equal to the corresponding components of the local fluid velocity, in the majority of the computations of trajectories of particles within the model eddy field. The empirical conclusions concerning particle velocities set down in Section 6.3.2 justify this artifice insofar as the horizontal component of particle velocity is concerned. The conclusion concerning the vertical component of particle velocity, however, indicates that a more appropriate procedure would evidently be to impart to the particle at the starting point a vertical velocity component, relative to the vertical component of the local fluid velocity, equal in magnitude and sense to the settling velocity of the particle in the quiescent fluid.

In order to examine the effect on the form of the computed trajectory of these alternative conditions at the starting point, the trajectory computed in Computation No. 3360101 (and identified as Trajectory No. 4.7 in Table 9) has been compared with the result of Computation No. 3350101. The parameter values employed in the two computations are identical, and are as shown for Trajectory No. 4.7 in Table 9. In the case of the former computation (Trajectory No. 4.7) the components of the particle velocity at the starting point have been set respectively equal to the corresponding components of the local fluid velocity. In the case of the latter computation, the horizontal component of the particle velocity at the starting point has been set equal to the horizontal component of the local fluid velocity, as estimated in a separate, previous calculation. The vertical component of the particle velocity at the starting point has been set equal, in magnitude and sense, to the settling velocity of the particle in the quiescent fluid as previously determined and as is shown in Table 5. (The vertical component of the fluid velocity at the starting point was zero).

The results of the computations are indicated in Figure 21. The crosses denote representative points on Trajectory No. 4.7 (Computation 3360101) whilst the continuous line represents the result of Computation 3350101. No significant difference between the forms of the two trajectories is in evidence, and it is concluded that a state of quasi-equilibrium between the motion of the particle and the motion of the fluid is established within a relatively short distance from the starting point, small variations in conditions at the starting point being relatively quickly "forgotten".

In the computation of the partial trajectories listed in Table 9 the second of the alternative sets of starting conditions was employed; the horizontal component of the particle velocity at the starting point was set equal to the horizontal component of the local fluid velocity and the vertical component was set equal to the settling velocity of the particle in the quiescent fluid, the vertical component of the local fluid velocity being in all cases zero. (These computations were employed in estimating the value of the characteristic fluid velocity necessary for the suspension of a particle, as described in Section 6.3.2).

The trajectories of non-buoyant particles within the model eddy field, described in the preceding sections of Chapter 6, have had their starting points at a fixed position, relative to the eddy centres, within the eddy field - namely, at the point ($X = 0.0$, $Y_O = 0.3Y_c$) where Y_c is the spacing of eddy centres in the Y coordinate direction. The selection of this point was made arbitrarily, having in mind the considerations which are outlined in Note vi, Section 4.3. Most of the conclusions drawn in the preceding sections of Chapter 6 are, as pointed out, specific to this particular starting point.

In an actual turbulent flow, the conceptual starting point of a particle trajectory (relative to a given eddy) will be a function of the processes of generation, migration and decay of eddies, and of the possibility of a particle's falling into an eddy.

In order to examine the effect of the specification of different starting points within the model eddy field, the series of computations listed in Table 11 has been carried out. All the parameter values involved in the computations listed in Table 11 coincide with those which apply in the computation of Trajectory No. 2.16, with the exception of the ordinate (YSTART) of the starting point of the trajectory. Accordingly, the computed trajectories are those traversed by a given particle, with different starting points within a given eddy field.

The computed trajectories are shown in Figure 22. They fall into three categories:

1. Trajectories which indicate that the particle will be suspended, within the eddy which has its centre at the point (0.0, 0.0), the particle travelling clockwise around the eddy.

2. Trajectories which indicate that the particle is not suspended, but falls through the eddy field.

3. Trajectories which indicate that the particle will be suspended within the eddy which has its centre at the point $(0.0, Y_c)$ where Y_c is the spacing of eddy centres in the Y coordinate direction. The particle travels around the eddy in an anti-clockwise sense.

The ordinates (Y_o) of the starting-points of trajectories of the three categories lie within intervals (on the line X = 0.0) defined as follows:

Category 1: $0 \leq |Y_o| \leq 0.35\ Y_c$ (approximately)

Category 2: $0.35\ Y_c \leq |Y_o| \leq 0.65\ Y_c$ (approximately)

Category 3: $0.65\ Y_c \leq |Y_o| \leq 1.35\ Y_c$ (approximately)

This last definition will include the trajectories of particles which are suspended within the eddy which has its centre at the point $(0.0, -Y_c)$.

The above results are clearly dependent upon the specific properties of the model eddy field, and upon the constancy (with respect to time) and uniformity (from eddy to eddy) of the eddy properties. The results imply that if the particle is, at any time, located within the zone which is traversed by trajectories of Category 1 (this zone being referred to below as Zone 1) then it will remain suspended within that zone, so long as the properties of the eddy field remain constant. If the particle is at any time located within Zone 3 (similarly defined) it will remain suspended within that zone. Furthermore, if the particle is at any time located within Zone 2, it will continue to fall indefinitely through the eddy field.

The broken line in Figure 22 denotes the approximate boundary of Zone 1 - that is, of the zone within which the particle (of the given properties) will become suspended within the eddy which has its centre at the point (0.0, 0.0). The area enclosed by the broken line is almost exactly 50 per cent of the area of the individual eddy, this latter area being defined as $X_c . Y_c$ where X_c and Y_c are the spacings of the eddy centres in the respective coordinate directions. Accordingly, a "probability factor" of about 0.50 is to be associated with the criterion established in Section 6.3.2 above. This is to be interpreted as meaning that the criterion of Section 6.3.2 (defining the conditions under which a given particle will be suspended within an individual eddy) holds, provided that the trajectory of the particle is located (at any time) within a given zone which has an area which is 50 per cent of that of the eddy.

In this context, it is of interest to note that the empirical conclusions set out in Section 6.3.2 imply that a non-buoyant particle whose trajectory passes through the point $(0.0,\ 0.5Y_c)$ cannot be suspended within an individual eddy of the model eddy field, irrespective of the magnitude of the characteristic fluid velocity within the eddy field. The conclusions (in Section 6.3.8) concerning symmetry of the particle trajectories imply that, if the particle trajectory passes through the point $(0.0,\ 0.5Y_c)$ it will also pass through the point $(0.0,\ -\ 0.5Y_c)$. At this point, the vertical component of the local fluid velocity is zero. It has been empirically concluded that the vertical component of the velocity of the particle relative to the fluid is at all points equal in magnitude and sense to the settling velocity of the particle in the quiescent fluid. It is accordingly implied that, after passing through the point $(0.0,\ -\ 0.5Y_c)$ the particle will move into a zone in which the vertical component of the fluid velocity is directed in the negative sense. The particle will consequently continue to fall through the eddy field. This conclusion is clearly dependent upon the specific properties of the model eddy field.

6.3.4 The Fall Velocity of a Particle which Falls Through the Model Eddy Field

The computed particle trajectories indicate that, for given properties of the particle and the fluid, the particle may be suspended within an eddy of the model eddy field, provided that the characteristic fluid velocity within the model eddy field (U_e) has a magnitude which is equal to, or greater than, a certain critical value.

If, on the other hand, the characteristic fluid velocity is less than the critical value, the particle will fall through the model eddy field. Under these conditions, the computed trajectory of the particle takes the form of an essentially-periodic curve of serpentine shape, as discussed in Section 6.3.2. and typified by the trajectory identified as 380101 and illustrated in Figure 18.

The results of the computations described in Section 6.3.3 have indicated that a particle can fall through the model eddy field within the zone designated (in Section 6.3.3) as Zone 2, even when the characteristic fluid velocity within the eddy field exceeds the critical value established in Section 6.3.2. The existence of such a zone of descent is however dependent upon the specific properties of the model eddy field, and in particular upon the temporal constancy of such properties. It accordingly seems unlikely that such zones of descent could exist - except perhaps as transitory phenomena - in an actual turbulent flow.

It is to be expected, on the other hand, that a relatively common phenomenon in an actual turbulent flow will be the descent of a particle through the flow, as a result of the characteristic fluid velocities within the flow becoming too small to maintain the particle in suspension. Such circumstances could arise as a result of spatial or temporal variations in the mean flow velocity, or when a particle has been lifted to some distance above the bed by a phenomenon such as the 'kolke' - a localised intense vortex to which is attributed the lifting of material from river beds - Matthe (31).

It is accordingly of some interest to examine the behaviour of a particle, initially located within the zone designated in Section 6.3.3 as Zone 1, when the characteristic fluid velocity within the model eddy field is less than the critical value necessary for suspension of the particle. The mean vertical velocity at which the particle falls through the eddy field has been calculated, for each of a number of such cases. In each case, the following parameter values applied:

$$\text{Particle-fluid parameter} \quad \text{PART} = \frac{\sqrt{gd^3}}{\nu} = 1.1068$$

$$\text{Gravitational parameter} \quad \text{GRAV} = (s - 1.0) = 1.00$$

$$\text{Spacing of eddy centres} \quad \text{XCNTR} = 50.6250$$

and the starting point of the trajectory was at the point which has coordinates (0.0, 15.0) with respect to an eddy centre as origin.

The result is presented in Figure 23, in which values of the ratio V_f/V_s are plotted against values of the ratio U_e/V_s. The velocity V_f is the (dimensionless) velocity at which the particle falls through the model eddy field, calculated as the average fall velocity of the particle throughout one "wave length" of the particle trajectory. The velocity V_s is the (dimensionless) settling velocity of the particle in quiescent fluid, and U_e is the (dimensionless) characteristic fluid velocity in the model eddy field.

Inspection of Figure 23 indicates that the ratio V_f/V_s has a value greater than unity, for almost the entire range of values of the characteristic fluid velocity U_e from zero to the critical value at which the particle will be held in indefinite suspension within an eddy. Under these conditions (V_f/V_s greater than unity) the mean fall velocity of the particle within the model eddy field will be greater than the settling velocity of the particle in quiescent fluid.

There is no indication that the curve of Figure 23 is sharply peaked; the ratio V_f/V_s appears to have a maximum value of about 1.4, at a value of the characteristic velocity U_e of some 70 per cent of the critical value necessary for suspension of the particle.

6.3.5 A Comparison between the Results of the Present Study and the Results of some Previous Investigations

In Section 6.3.2 it has been inferred that, under the specific conditions which apply to the investigation described therein, a non-buoyant particle will be suspended within an eddy of the model eddy field if the characteristic fluid velocity within the eddy field is equal to, or greater than, 2.7 times the settling velocity of the particle in the quiescent fluid. It is instructive to compare this criterion with some results derived by previous investigators.

A comparison can be made with the results of some experiments on plumes. A plume is the flow which is formed by the discharge of fluid into a body of ambient fluid of a different density, and of a considerable depth. The discharged fluid flows through the ambient fluid in an essentially vertical direction. The sense of the motion of the plume will be upward if the discharged fluid is less dense than the ambient fluid, downward if the discharged fluid is denser than the ambient fluid. The difference between the density of the fluid within the plume and the density of the ambient fluid may be due to a temperature difference, a salinity difference, the presence in either fluid of suspended material, or to the other (less common) causes enumerated in Chapter 1.

Tsang (47) has experimentally determined the distribution of fluid velocities within a two-dimensional "starting plume" of salt water descending through fresh water. The results of Tsang's experiments indicate that, in the eddy which forms one half of the "cap" of the plume, the extreme values of the vertical components of fluid velocity (relative to an observer travelling with the plume cap) are of magnitude 1.6 V_c, as shown in Figure 24, where V_c is the vertical velocity of the plume cap relative to a fixed external frame of reference. The horizontal components of fluid velocity tend to be smaller in magnitude than the vertical components; the magnitude of the maximum horizontal velocity component is about one third of the magnitude of the maximum vertical component.

Gray (18) has experimentally examined two-dimensional descending plumes formed by the discharge, into clear water, of water containing non-buoyant particles. It has been found that, in those cases in which the velocity of the plume cap exceeded a velocity representative of the settling velocity (in quiescent fluid) of the particles within the plume - that is, when $V_c > V_s$ - the behaviour of the turbid plume was generally similar to that of a salt-water plume of similar properties (although the turbid plume was somewhat more slender than the corresponding salt-water plume). When, however, a turbid plume commenced to descend with a velocity less than the representative quiescent-fluid settling velocity of the particles within the plume - that is, with $V_c < V_s$ - the plume did not maintain its identity. The particles fell through the plume cap, and descended as a turbid cloud which lacked the characteristic form of a plume and which fell at the quiescent-fluid settling velocity of the particles.

If the velocity distribution within Gray's turbid plumes conformed to the distribution determined by Tsang, then the results of Gray's experiments would imply that a non-buoyant particle could be suspended within an eddy only if the maximum vertical component of the fluid velocity within the eddy were equal to, or greater than, 1.6 times the settling velocity of the particle in the quiescent fluid - that is, if $U_e/V_s \geqq 1.6$. It cannot be validly assumed that the velocity distribution within the turbid plumes conformed exactly to that derived by Tsang, particularly in view of the fact that the turbid plumes are "driven" by the suspended particles themselves. Furthermore, the conditions prevailing in the plume experiments do not conform to the conditions which apply in the present investigation, and it is for these latter specific conditions that the criterion of Section 6.3.2 has been established. Some measure of agreement does exist, however, (at least as to order of magnitude) between the value (2.7) of the numerical coefficient in Equation (6.4), p. 109, which defines the criterion for particle suspension established in the present investigation, and the corresponding value (1.6) which is indicated by the results of the plume experiments referred to above.

Woodward (49) has experimentally determined the distribution of velocities in a three-dimensional cloud of salt water descending through fresh water. By analogy, the measured velocity distribution has been assumed to apply in a buoyant "thermal" - a body of heated air ascending through cooler air. The experimental velocity distributions have indicated that the extreme values of the vertical components of the velocity of the fluid relative to the plume cap have magnitudes of about $1.6V_c$, where V_c is the velocity of the cap. This result is in close agreement with that of Tsang, discussed earlier in this section.

Woodward has concluded, apparently on the basis of numerical computation of particle trajectories, that a particle which is overtaken by such a plume, or which falls into the plume, may be entrapped within the plume and suspended indefinitely within it, if the settling velocity of the particle in the quiescent fluid is less than 1.6 times the velocity of the plume cap. This conclusion, together with the observed ratio between the extreme magnitudes of the vertical fluid velocities and the velocity of the cap, as described in the preceding paragraph, implies a value of unity or more for the coefficient in Equation (6.4), p. 109 - that is, it implies that $U_e \geqq 1.0\ V_s$ if suspension of the particle is to occur. As before, direct comparison of the results is not valid, in view of the differing specific conditions applying in the different investigations. Once again, however, the order of magnitude of the numerical coefficient in Equation (6.4) is confirmed.

Jobson and Sayre (25) have compared the experimentally-determined fall velocities of particles falling through turbulent flows with the settling velocities of the particles in quiescent fluid. The experimental particles consisted of sand grains and glass beads. The sand grains had a representative diameter of 0.39 mm, a specific gravity of 2.65 and a settling velocity in quiescent water (at 24^{o}C) of about 63 mm. sec.$^{-1}$. The glass beads were 0.12 mm in diameter, with a specific gravity of 2.42 and a settling velocity in quiescent water (at 24^{o}C) of about 11 mm. sec.$^{-1}$. The fall velocities of the particles were determined in turbulent water flows in which the mean velocities were approximately 290, 570 and 880 mm. sec.$^{-1}$.

In all three of the experimental flows, suspension of the particles failed to occur, and the particles fell through the flow. Direct comparison of this result with the criterion expressed in Equation 6.4, p. 109 is not possible. The criterion of Equation 6.4 is restricted to the specific conditions which applied in the computations from which the criterion was derived. Accordingly, it is restricted to the specific velocity distribution which existed in the model eddy field, and to particle trajectories with a specific starting point, relative to the eddy centres. There is no evidence that similar conditions existed within the experimental flows. The relationship between the known parameters of the experimental flows and the quantity corresponding to U_e (the characteristic velocity within the model eddy field) is unknown. The possibility of agreement, at least as to orders of magnitude, is not, however, precluded. The application of the criterion of Equation 6.4 would indicate values of U_{ec} (the critical value of the characteristic velocity within the model eddy field, for suspension of the particle) of about 170 mm sec.$^{-1}$ for the sand grains, and about 30 mm. sec.$^{-1}$ for the glass beads. The most extreme of the experimental results, in which the glass beads were not suspended in a flow with a mean velocity of 880 mm. sec^{-1}, indicates that the quantity corresponding to U_e had a magnitude less than about 3 per cent of the mean velocity. This result is within (albeit perhaps towards the lower end of) the range of credibility.

The experiments of Jobson and Sayre indicated that the ratio of the fall velocity in the turbulent flow to the settling velocity in quiescent water (V_f/V_s) had, for the sand grains, values of 1.06, 1.03 and 1.04 in the three flows, which had mean velocities of 290, 570 and 880 mm. sec^{-1} respectively. For the glass beads, the corresponding values of the ratio V_f/V_s were 1.39, 1.65 and 1.40 respectively. In common with the other results of the present investigation, Figure 23 is specific to the particular conditions which applied in the trajectory computations on which it is based, and no claim as to its general validity can be made. If, however, Figure 23 is compared with the experimental values of the ratio V_f/V_s, some measure of agreement is in evidence. For a given value of U_e, the ratio U_e/V_s for the glass beads will be some six times as great as the corresponding value for the sand grains. Accordingly, values of U_e/V_s for the sand grains might be expected to lie towards the left of Figure 23. Values of U_e/V_s for the glass beads might be expected to lie towards the right (but short of the zone denoting suspension of the particle). Under these conditions, the values of the ratio V_f/V_s, as indicated by the curve of Figure 23, would be in some measure of agreement with the experimental results of Jobson and Sayre, as quoted above.

6.3.6 The Interchange of Energy between a Suspended Particle and the Surrounding Fluid

In the development of the computer program for the computation of the trajectories of particles within the model eddy field (as described in Chapter 4 above) provision was made for the examination of the interchange of energy between the particle and the fluid. This feature of the program is described in detail in Section 4.4.

A particle trajectory such as that illustrated in Figure 17 is markedly asymmetric about the line X = 0.0. When a particle traverses such a trajectory, it is evidently possible that the particle will effect a net transfer of energy between different zones of the eddy - that is, between annular zones located at varying radii from the eddy centre. While the particle is falling (that is, while the vertical component of its velocity is directed in the negative sense) the particle will contribute energy, at the expense of its potential energy, to the fluid. Conversely, while the vertical component of the particle velocity is directed in the positive sense, the potential energy of the particle will be augmented at the expense of the energy of the fluid. Examination of Figure 17 indicates that, in general, the particle tends to be closer to the eddy centre while traversing those segments of its trajectory in which it contributes a portion of its potential energy to the fluid, than while traversing those segments of its trajectory in which it gains potential energy from the fluid. Accordingly, it is implied that a transfer of fluid energy towards the eddy centre will occur, during a particle's traverse of a trajectory such as that illustrated in Figure 17.

The results of the calculation of particle-fluid energy interchange are discussed in detail in Appendix VII. The results confirm that a particle's traverse of a trajectory such as that shown in Fig. 17 will effect a net transfer of energy between different annular zones of the eddy.

The quantitative results, and the sense of the net energy transfer (towards the eddy centre, in the case of a trajectory such as that shown in Fig. 17) are specific to the particular conditions which applied in the computations carried out. The results are, in particular, dependent upon the form of the velocity distribution specified within the model eddy field. They lead, however, to the general conclusion that, in any case in which a non-buoyant particle is suspended within an eddy, the particle will acquire energy from the fluid in zones of the eddy in which the fluid energy is relatively high, and will contribute energy to the fluid in zones of the eddy in which the fluid energy is relatively low. In a real fluid, the process of energy transfer (in either sense) will not be a completely efficient one. When energy is transferred from the fluid to the particle, some energy will be transformed into thermal energy, within the wake of the particle. A similar transformation of energy into thermal energy will occur when a transfer of energy from the particle to the fluid occurs. Accordingly, a particle's traverse of a closed trajectory within an eddy will cause a reduction in the available energy of the fluid within the eddy. This conclusion is consistent with the body of empirical evidence which indicates that the presence of suspended material accelerates the degradation of the energy of a flowing fluid.

6.3.7 The Spiral Form of the Trajectory of a Non-Buoyant Particle Suspended within an Eddy

In the preceding discussion of the computed particle trajectories, it has been noted that when a non-buoyant particle appears to be suspended within an individual eddy of the model eddy field, the computed particle trajectory does not return precisely to its starting point, Such a trajectory, with its starting point at the point (X_O, Y_O), after executing one circuit of the eddy passes through a point $(X_O, Y_O + \Delta Y)$ where ΔY is a small quantity which is positive if Y_O is greater than zero. In other words, the trajectory forms a spiral, rather than a closed curve. In order to illustrate this effect, reference may again be made to the trajectory No. 610101-620101 (Appendix III). The starting point of this trajectory is at the point (0.00, 15.00) and after one circuit of the eddy the trajectory passes through the point (0.0000, 15.0174) - as indicated by interpolation between the computed points which lie closest to, and one each side of, the line X = 0.0. It is evident that the spiral effect is of relatively small magnitude: it is scarcely discernible in the plot of this trajectory in Figure 17.

The spiral form of a particle trajectory has been examined analytically by Manton (30) for cases in which the particle trajectory deviates little from the streamline which passes through its starting point. If the density of the particle differs from that of the fluid, then the local curvature of the particle trajectory at any point will differ from the curvature of the fluid streamline at that point, as discussed in Section 5.2. The forces which act on an elemental body of fluid are just sufficient to cause that element of fluid to follow a path which (for steady flow) conforms to the local streamline pattern. If the element of fluid is now replaced by a rigid particle of a density different from that of the fluid, and if it is assumed that the forces acting on the rigid particle are unchanged from those which acted on the fluid element, then the curvature of the trajectory of the rigid particle will differ from the curvature of the streamlines. In such a case, an acceleration of the particle relative to the surrounding fluid will occur. In these circumstances, the response of the particle to the forces acting on it, and hence the curvature of the particle trajectory, will also be affected by the added mass of the particle. If the density of the particle is greater than that of the fluid, the curvature of the particle trajectory will be less than that of the streamlines. Accordingly, in the case of a non-buoyant particle whose trajectory deviates only slightly from the streamline which passes through the starting point, the trajectory will at all points be of lesser curvature than the local streamline pattern, and hence the particle trajectory will spiral outwards.

The present investigation is concerned with a non-buoyant particle which is subject to the action of gravity. Since the density of the particle is greater than that of the fluid, the particle trajectory may be expected to be everywhere of lesser curvature than the local streamlines. The effect of the gravitational force, however, causes the particle trajectory to deviate from the streamline which passes through the starting point of the trajectory - as illustrated by comparison of Figure 17 with Figure 4. Consequently, the comparison of curvature of the trajectory with local streamline curvature is inconclusive, insofar as prediction of the spiral form of the trajectory is concerned.

The spiral form of the computed particle trajectories is further discussed in Appendix VIII. The spiral phenomenon appears to be of no more than secondary significance, in the examination of the trajectories of particles within the model eddy field - except perhaps in the case of a particle which follows a trajectory of very sharp curvature, close to an eddy centre. The spiral effect will be of even less significance in the case of a real turbulent flow - the effect appears unlikely to be important unless the properties of the fluid motion remain constant for periods of time which are at least several times as great as the time taken for the particle to execute one circuit of the eddy. It appears unlikely that this condition would be realised in an actual turbulent flow.

6.3.8 The Symmetry of the Computed Particle Trajectories

The computed trajectories of particles within the model eddy field exhibit certain symmetries in their overall forms. The spiral form of the trajectories, discussed in Section 6.3.7, introduces a measure of asymmetry. The deformations of the trajectories due to the spiral phenomenon are however small in comparison with the overall dimensions of the trajectories, and if this effect is disregarded clearly defined overall symmetries are in evidence.

The computed trajectories of neutrally-buoyant particles within the model eddy field (as described in Section 5.2) conform closely to the form of the streamlines of the model eddy. The overall form of these trajectories consequently exhibits the inherent symmetry of the streamline pattern. Of greater interest, however, are the trajectories of non-buoyant particles within the model eddy field (as described in Section 6.3.2). Overall symmetries are in evidence in trajectories of both the closed and open forms.

In a computed trajectory of the closed form, as typified by the trajectory illustrated in Figure 17, that section of the trajectory which is located within the second quadrant is essentially a reflection, in the line Y = 0.0, of the section of the trajectory which is located within the first quadrant. The section of the trajectory which is located within the fourth quadrant is essentially a reflection, in the line Y = 0.0, of the section located within the third quadrant. In this context, the quadrants are numbered clockwise, in the order in which the particle traverses them during its circuit of the eddy. The quadrant in which both X and Y have positive values is designated as the first.

No symmetry about the line X = 0.0 is in evidence. In fact, Figure 17 indicates a marked assymetry about this line.

In the case of a computed trajectory of the unclosed form - that is, the trajectory of a particle which is falling through the model eddy field - as typified by the trajectory shown in Figure 18, similar symmetries are in evidence. The first two sections of the trajectory are reflections in the line $Y = 0.0$, and the following two sections are reflections in the line $Y = -Yc$ - that is, in the line which is parallel to the x coordinate axis and which passes through the centre of the eddy located next below the eddy on which the first two sections of the particle trajectory are centred. Hence, the trajectory of a particle falling through such a field (of uniformly-spaced eddies, of uniform and constant properties) will form a curve which is essentially periodic in nature. The long-term average fall velocity of a particle falling through such an eddy field will, accordingly, be closely approximated by the particle's average velocity of fall through one "wave length" of the trajectory - that is, by the average fall velocity between the particle's starting point at $(0.0, Y_o)$ and the point $(0.0, -(2Y_c - Y_o))$ where Y_c is the spacing of the eddy centres in the y coordinate direction.

Further discussion of the symmetry of the computed particle trajectories is presented in Appendix IX.

7. Experiments on the Process of Turbulent Entrainment across a Density Discontinuity

7.1 Introduction

As pointed out in Chapter 1, it appears that the flow within a turbidity current must be turbulent, if the turbidity current is to maintain its identity throughout an extended period of time. Unless the flow is turbulent, the non-buoyant particulate material within the current will progressively be removed from suspension by settlement to the bed, with a concurrent progressive loss of identity of the turbidity current. The occurrence, however, of turbulent flow within the turbidity current will be accompanied by the phenomenon of turbulent entrainment. In general, with turbulent flow within the current, ambient fluid will be entrained across the interface and will be incorporated into the moving turbidity current. The entrained elements of ambient fluid will, in general, possess less momentum (per unit volume) than will the fluid within the turbidity current, and hence the process of entrainment will lead to a reduction in the momentum (per unit volume) of the turbidity current. At the same time, the process of entrainment of ambient fluid will tend to reduce the difference between the density of the fluid within the turbidity current and that of the ambient fluid. Consequently, the forces which sustain the motion of the turbidity current will be diminished.

Accordingly, it is evident that the process of turbulent entrainment will be one of the factors which affect the persistence or stability of a turbidity current. The experiments to be described within this chapter were designed to provide some insight into the phenomenon of turbulent entrainment, in the context of the behaviour of a turbidity current. These experiments chronologically preceded the investigation described in Chapters 2 to 6 above, and it was the outcome of such experiments which led to the conclusion that a more complete understanding of the process of suspension of a non-buoyant particle within a turbulent flow was a pre-requisite to a full insight into the behaviour of a turbidity current.

Previous laboratory investigations of the phenomenon of turbulent entrainment have been concerned with non-suspension density currents - that is, with density currents in which the density differences were due to temperate differences, or to differences in the concentrations of dissolved salts - Ellison and Turner (15), Turner (48). The difficulties involved in forming and maintaining model turbidity currents in the laboratory have discouraged the performance of experiments which might yield insight into the phenomenon of turbulent entrainment as applying to a turbidity current. One of the objectives of the investigation at present under discussion was the examination of the validity with which data derived from experiments on non-suspension density currents might be applied in the prediction of rates of turbulent entrainment of ambient fluid into a turbidity current.

In the experiments to be described, a turbulent density current was simulated, in the laboratory, by a layer of fluid in which no mean motion existed, but which was stirred by the motion of an oscillating metal grid within the fluid layer. The stirred layer was one of a series of stably density-stratified fluid layers. The experiments involved the measurement of the rates at which fluid was entrained across the density discontinuity which separated the stirred layer from the adjoining layer.

In the present investigation, a comparison has been made between rates of turbulent entrainment across density discontinuities in which the density differences were due to temperate differences, salinity differences, and to the presence of suspended material within a fluid layer. Similar experiments, with density differences due to differences in temperature and salinity, have been described by Rouse and Dodu (41), Cromwell (11) and Turner (48). Thompson (45) has examined the fluid motions induced by oscillating grids in density-stratified systems. The experiments of Rouse (39) on the mechanics of particle suspension - referred to in Chapter 2 above - were carried out in apparatus of a generally similar type.

7.2 The Experimental Apparatus

The apparatus in which the experiments were carried out is shown schematically in Figure 25. It consisted essentially of a cylindrical tank, constructed of rigid PVC plastic. The internal diameter of the tank was 200 mm. Its depth was originally 500 mm, but a false floor was subsequently added, reducing the working depth to 429 mm. The tank was fitted with a baffled inlet at the top, and an outlet which permitted the withdrawal of fluid from the lower part of the tank.

Turbulent flow in a layer of fluid was simulated within the tank by the fluid motions induced by the motion of an oscillating metal grid. The grid consisted of brass bars, 10 mm wide and approximately 3 mm (actually, 0.125 inches) in thickness, forming a square grid with the centres of the bars spaced at 50 mm in each direction. The grid was mounted on a central vertical shaft, and was oscillated vertically in simple harmonic motion. The mid-stroke position of the grid relative to the floor of the tank was adjustable. The grid was driven by an electric motor, power transmission being by means of a variable-speed belt drive system which permitted variation of the frequency of oscillation of the grid. Provision was made for variation of the amplitude of oscillation (stroke) of the grid, but in the experiments to be described the stroke was maintained constant at 10 mm. Provision was made for the fitting of additional grids, with the addition of shaft extensions of length equal to the required distance between the grids.

The tank was fitted, at its original mid-depth, with a sliding horizontal partition. The partition consisted of a sheet of rigid

PVC plastic 1 mm in thickness. It could be moved across the tank to separate the upper half from the lower, or could be completely withdrawn from the tank as required. The partition was moved manually, by means of a rack and pinion drive. The partition was employed in the establishment of the density-stratified system prior to the start of each experiment, as described in Section 7.3 below.

The tank was fitted with a removable insulating jacket of polyurethane foam, in order to eliminate the effects of heat transfer to or from the surroundings.

7.3 The Experimental Procedure

Before the start of each experiment, it was necessary to set up in the tank a density-stratified system consisting of two layers of fluid, of different densities. It was required that the density within each fluid layer should be (as nearly as possible) constant throughout the depth of the layer, and that a sharp density discontinuity should occur at the interface between the layers.

In the case of a density difference which is due to the presence of non-buoyant suspended material within a fluid layer, the establishment of the density-stratified system is complicated by the tendency of the non-buoyant material to settle towards the bottom of the tank. The horizontal sliding partition fitted at the mid-depth of the tank was designed to overcome this difficulty, as described in the following paragraphs.

The fluid which was to comprise the lower, more dense, layer was first pumped into the tank, until its surface reached an elevation just above that of the sliding partition. The partition was then closed across the tank, and the small amount of fluid which remained above it was removed, by means of a sponge. In those cases in which the lower fluid layer consisted of a suspension of non-buoyant particles, stirring of the suspension by means of the oscillating grid was carried out during these operations.

The less dense fluid which was to form the upper layer was then pumped into the tank, above the partititon. The apparatus was allowed to stand for about one hour, in order to permit the dissipation of most of the fluid motion (in the unstirred layer) arising from the placing of the fluid into the tank. The sliding partition was then withdrawn. The withdrawal of the partition was carried out slowly, and as smoothly as possible, in order to minimise the disturbances created at the interface.

In the case of experiments in which the density difference was due to the presence of suspended material within the lower layer, stirring was continued during the withdrawal of the partition, and entrainment of fluid across the interface commenced as soon as the partition was withdrawn. In the case of experiments in which the density difference was due to a salinity difference or to a temperature difference, stirring was not commenced until after the partition had been withdrawn.

After withdrawal of the partition, adjustment of the elevation of the interface was possible by the addition of fluid to one layer and the simultaneous displacement of fluid from the other layer. Such additions and withdrawals of fluid were made at a carefully regulated rate, in order to minimise the generation of disturbances at the interface. Alternatively, the elevation of the interface could be adjusted by permitting the stirred layer to increase in volume, and the unstirred layer to decrease in volume, as a result of the process of turbulent entrainment.

The basic working fluid in all experiments was distilled water. In those experiments in which the density difference was due to a salinity difference, sodium chloride was dissolved in the water which was to form the lower layer. In the experiments involving a density difference due to a temperature difference, the lower layer consisted of melted ice, the upper layer being at ambient temperature. The particle suspensions consisted of suspensions of bentonite, manually dispersed in distilled water. In the experiments with density differences due to salinity differences and temperature differences, the position of the interface was made visible by the addition of dye to one of the fluid layers, or (occasionally) the addition of dyes of different colours to the two layers. The cloudy appearance of the bentonite suspensions rendered the interface visible, without the addition of dyes.

When one layer was stirred by means of the oscillating grid, fluid from the adjacent unstirred layer was entrained into the stirred layer. As a result, the stirred layer tended to increase in volume, and the unstirred layer tended to decrease in volume. The interface accordingly tended to move away from the mid-stroke position of the oscillating grid. By pumping into the unstirred layer (at a regulated rate) additional fluid of the same density as the fluid already within that layer, and displacing (at an equal rate) fluid from the stirred layer, it was possible to maintain the interface at a constant elevation within the tank. In this way, the distance between the interface and the mid-stroke position of the grid was kept constant throughout each experiment. Measurement of the rate at which fluid was displaced from the stirred layer then provided a direct measure of the rate at which fluid was entrained across the interface.

Throughout each experiment, the interface was maintained as closely as possible at a predetermined elevation (marked by a line on the tank wall) by manually regulating a valve which controlled the rate at which fluid was admitted to the unstirred layer. Small apertures in the insulating jacket allowed the interface and the reference line to be observed.

The basic quantity which was to be determined was the rate at which fluid was entrained across the interface. If it is assumed that the entrainment of fluid occurs uniformly over the full area (in plan) of the interface, then the rate of entrainment may be expressed as a velocity. This entrainment velocity is equal in magnitude to the velocity with which the interface would move away from the mid-stroke position of the oscillating grid if no fluid was added to or withdrawn from the tank during the experiment. When the experiment is conducted as described in the preceding paragraphs, with the addition of fluid to (and displacement of fluid from) the tank, then the entrainment velocity is given by

$$v_e = \frac{1}{A_i} \cdot \frac{dV}{dt} \tag{7.1}$$

where v_e = the entrainment velocity

A_i = the area of the interface, in plan

dV = an incremental volume of fluid displaced from the tank

dt = an element of time

The fluid which was displaced from the stirred layer was collected in a graduated measuring cylinder. At successive times throughout the course of an experiment, the volume of fluid collected up to that time was recorded. From this record, a curve of cumulative volume against time (as shown in Figure 26) was prepared. The value of entrainment velocity v_e at any given time during the experiment could accordingly be calculated, by means of Equation (7.1).

Throughout each experiment, the density of the unstirred layer remained constant, whilst the density of the stirred layer progressively approached that of the unstirred layer - that is, the difference between the densities of the two layers approached zero. At intervals throughout each experiment, the density of the stirred layer was measured and recorded. In the case of experiments in which the density difference was due to a temperature difference, the density was deduced from the layer temperature as measured by the thermometer fitted to the tank, on the basis of the temperature-density data for water contained within Reference (20). In the case of salinity differences, the density of the stirred layer was determined by measuring the electrical conductivity of the fluid within the layer, a correlation between conductivity and density having been established in the course of the investigation. The densities of particle suspensions were determined by withdrawing small samples of the suspension from the tank and (after weighing the sample) evaporating the water content. With the mass of the water content of a sample - represented by the loss of mass in drying - and the mass of the solid residue determined, the density of the suspension could be calculated.

A second estimate of the entrainment rate was deducible, from the rate of change of the density of the stirred layer:

$$v_e = - \frac{h}{\Delta\rho} \cdot \frac{d(\Delta\rho)}{dt} \qquad (7.2)$$

where v_e = the entrainment velocity

h = the depth of the stirred layer

$\Delta\rho$ = the difference between the density of the stirred layer and that of the unstirred layer

t = time

Equation (7.2) was used to check values of the entrainment velocity calculated from Equation (7.1). In general, close agreement was obtained, except in the case of determinations made in the later stages of an experiment when the rate of entrainment was high and the control of the experiment became increasingly difficult.

A typical set of experimental results is shown in Figure 26. The data plotted represent the experimental observations of the cumulative volume of fluid displaced from the stirred layer, and the measured difference between the density of the stirred layer and that of the unstirred layer. These quantities are plotted against a time base. Also shown are the two sets of values of entrainment velocity, derived from the volumetric measurements by means of Equation 7.1 and from the measurements of the density difference by means of Equation 7.2, respectively. As stated above, the values of entrainment velocity are in close agreement, except in the later stages of the experiment.

7.4 Dimensional Analysis of the Process of Turbulent Entrainment

With the benefit of some insight into the entrainment process which was obtained only in the course of the experimental investigation at present under discussion, it was concluded that the significant variables in the process of entrainment across a density discontinuity by grid-induced fluid motions are as follows:-

v_e	the entrainment velocity
ρ	the density of the stirred layer
$\Delta\rho$	the difference between the density of the stirred layer and that of the unstirred layer
D	the molecular diffusivity of the property causing the density difference
d_i	the distance between the mid-stroke position of the grid and the interface
u	a velocity scale of the fluid motion
l	a length scale of the fluid motion
and g	the gravitational acceleration

It is to be noted that the fluid viscosity has not been included in the list of significant variables. The omission of viscosity is consistent with the conclusions of Turner (48) who has examined the significance of viscosity in connection with his experiments on turbulent entrainment across density discontinuities which were due to temperature differences and salinity differences. In the experiments carried out in the course of the present investigation, variations in the viscosity were small, and the hypothesis that viscosity is not a significant variable has been confirmed as described in the following paragraphs.

As discussed in Section 7.6 below, the experimental results which are presented in Figure 27 indicated that, under given conditions, the rate of entrainment across a density discontinuity which was due to a bentonite suspension would be less than that across a density discontinuity due to a salinity difference. If the difference between the entrainment rates was caused by a difference in viscosity, it would be expected that the difference (in entrainment rates) would be enhanced, if the distance between the grid and the interface was increased. A series of supplementary experiments indicated, however, that this was not the case.

In order to gain further insight into this aspect, an additional experiment was carried out, with stirring in each of two fluid layers. The lower layer was a bentonite suspension, and the upper layer was clear water. The driving shaft was fitted with two grids, one of which stirred each layer. Experiments with stirring in two layers have been discussed by Turner (48). Preliminary experiments carried out in the course of the present investigation confirmed that, in essence, the two entrainment systems (one of which is associated with each grid) are superimposed. Under these conditions, entrainment takes place across the interface in both senses. In the experiment at present under discussion, the interface was initially closer to the lower grid than to the upper. During the course of the experiment, however, the interface moved to a position midway between the grids, and subsequently remained in that position. It was accordingly concluded that the rates of entrainment in the two directions were dependent upon the respective grid-interface distances and that any difference between the viscosities of the fluids in the two layers had no significant effect.

Accordingly, it was concluded that the fluid viscosity is not a significant variable in the process of turbulent entrainment, in the context of the experiments at present under discussion (in which viscosity variations were small).

It is assumed that, for a grid of given geometry, the velocity scale u and the length scale l of the relevant fluid motion depend upon the stroke of the grid, the frequency of oscillation n of the grid and the grid-interface distance d_i. Under these conditions, if the grid stroke and the grid-interface distance d_i have constant values, as was the case in the series of experiments whose results are represented in Figure 27, then the independent, non-constant dimensionless parameters into which the relevant variables may be grouped are as follows:-

a Richardson Number $\frac{\Delta\rho}{\rho} \cdot \frac{g\,l}{u^2}$

a Peclet Number $\frac{ul}{D}$ and

a velocity ratio $\frac{v_e}{u}$

7.5 The Results of the Experiments

7.5.1 Qualitative Observations

Prior to the discussion of the quantitative results of the experiments, it is appropriate to record some observations concerning the qualitative nature of the process of entrainment across a density discontinuity, as demonstrated in the experiments at present under discussion.

Throughout the course of each experiment, the rate of entrainment across the density discontinuity was observed to increase progressively. Concurrently, the difference between the density of the stirred layer and that of the unstirred layer progressively diminished, as indicated in Figure 26. Accordingly, it was concluded that under given conditions the rate of turbulent entrainment across a density discontinuity will depend upon the difference between the densities of the fluids in the two adjacent layers. The rate of entrainment will increase as the density difference decreases.

The experiments demonstrated that a density discontinuity constitutes a spectacularly effective barrier to the transfer of fluid momentum. The fluid motions induced by the oscillating grid were almost entirely confined to the stirred layer. By extension, the density discontinuity at the interface between a turbidity current and the ambient fluid might be expected to constitute a similarly effective barrier to the diffusion of turbulence generated by the motion of the fluid within the turbidity current.

The effectiveness of the density discontinuity as a barrier to momentum transfer was demonstrated by dropping small crystals of potassium permanganate through the two layers of fluid within the tank. In the stirred layer, the resulting dye streaks were dispersed within a few seconds of their formation. In the unstirred layer, on the other hand, the streaks persisted almost indefinitely. Whilst the motion within the stirred layer was relatively vigorous, the dye streaks indicated that within the unstirred layer no significant motion occurred, except in the immediate vicinity of the interface. Within this region of the unstirred layer, some motion was in evidence, and was apparently associated with the distortion of the interface.

The effectiveness of a density discontinuity as a barrier to the transfer of fluid momentum is of significance in the context of the persistence or stability of a turbidity current. It leads to the inference that the maintenance of non-buoyant material in suspension within a turbidity current must be dependent primarily upon turbulence generated within the turbidity current itself. The effectiveness of the interface as a barrier to momentum transfer may render relatively ineffective (insofar as the suspension of material within the turbidity current is concerned) fluid motions which might be transmitted into the turbidity current from a source outside the current.

With two fluid layers in the tank, one being stirred and the other unstirred, the interface was observed to be distorted into a series of wave-like "domes" or "billows" which were concave to the stirred layer. The domes were transitory; a recognisable form might persist for a period of the order of one second. A typical dimension (in plan) of a dome was of the order of some tens of millimetres.

With stirring in one fluid layer, the entrainment of fluid across the interface was observed to be essentially a one-way process. Any elements of fluid from the stirred layer which penetrated into the unstirred layer (beyond the general level of the interface) appeared to move back into the stirred layer without evidence of any significant mixing. On the other hand, fluid from the unstirred layer was observed to be entrained into the stirred layer in a process which appeared to conform closely to the description presented by Phillips (36). From cusps at the extremities of the domes or billows on the interface, streamers or sheets of fluid from the unstirred layer were observed to be drawn down into the stirred layer. A portion of the fluid within such a streamer was entrained into the stirred layer; the remainder returned to the interface under the action of gravitational and buoyant forces.

7.5.2 The Effect of Intermediate Layers on the Entrainment Process

In some preliminary trials, the apparatus was operated without the insulating jacket which was designed to minimise the effects of heat transfer to or from the surroundings. On a number of occasions, in the absence of the insulating jacket, it was found that a well-defined intermediate layer of fluid was formed, adjacent to the original interface. In each case, the layer was of a density intermediate between the densities of the original fluid layers. A typical intermediate layer was a few millimetres (up to about 10 mm) in thickness.

The formation of such intermediate layers has been attributed to the mechanism postulated by Mendenhall and Mason (32). This mechanism is dependent upon the existence of a horizontal temperature gradient across the interface, and the existence of a gradient of density in the vicinity of the interface, rather than a sharp density discontinuity. In the experiments at present under discussion, the first of these conditions could have arisen as a result of the location within the laboratory of the experimental apparatus: one side of the apparatus was more intensely illuminated (and hence more intensely heated) by sky radiation than was the other side. The second condition could have arisen as a result of the disturbances inevitably generated at the interface during the establishment of the density-stratified system within the apparatus.

The presence of an intermediate layer appeared to have the effect of reducing the rate of entrainment of fluid into the stirred layer. In one experiment in which an intermediate layer of about 10 mm in thickness was observed, the rate of entrainment in the presence of the intermediate layer was reduced to about 25 per cent of the rate which would have been expected in the absence of the intermediate layer, on the basis of the given experimental conditions and the density difference which existed between the top and bottom fluid layers. A priori, it might be expected that the intermediate layer would be relatively rapidly entrained into the stirred layer, as the density difference between the stirred (bottom) layer and the intermediate layer would be less than that between the bottom layer and the top layer. The experimental observations indicated, however, that this expectation was not realised.

7.5.3 The Quantitative Results of the Experiments

The significant quantitative results of the experiments at present under discussion are shown in Figure 27. This diagram shows the results of a series of experiments with density differences due to temperature differences, salinity differences and particle (bentonite) suspensions, carried out with a constant grid stroke (10 mm) and a fixed distance (60 mm) between the interface and the midstroke position of the grid. The scales of Figure 27 correspond to those used by Turner (48); the abscissa is proportional to the Richardson Number.

It is evident that, under given conditions, the rate of entrainment is greatest in the case of a temperature difference, somewhat less in the case of a salinity difference, and less again in the case of a bentonite suspension.

The present results for density differences due to temperature differences and salinity differences may be compared with the results of similar experiments described by Turner (48). In the experiments of Turner, the distance between the grid and the interface was 90 mm, and entrainment rates were consequently generally less than those measured in the experiments at present under discussion. The slopes of the lines fitted by Turner to his sets of experimental points were 1.0 and 1.5, for points associated with density differences due to temperature differences and salinity differences respectively. These values correspond closely to the slopes (0.9 and 1.5 respectively) of the lines fitted by least-squares regression to the arrays of points associated with density differences due to temperature differences and salinity differences in Figure 27. The asterisk in Figure 27 denotes the point of intersection of the lines fitted to Turner's sets of experimental points.

Turner (48) has postulated that the observed difference between the entrainment rates (under given conditions) associated with density discontinuities due to a temperature difference on the one hand, and to a salinity difference on the other, is related to the differing molecular diffusivities of the properties causing the density differences. The molecular diffusivity of heat (temperature) has a value of about 10^{-7} $m^2.sec^{-1}$, and that of salinity a value of about 10^{-9} $m^2. sec^{-1}$. In the case of a suspension of small particles, a property analogous to the molecular diffusivity may be estimated by the use of the Stokes-Einstein (Nernst-Einstein) Equation - Reference (5)

$$D = \frac{K\,T}{3\pi\,\mu\,d}$$

where D = the "molecular diffusivity" of a particle suspension

K = Boltzmann's constant

T = the temperature

μ = the viscosity of the suspending fluid

d = the particle diameter.

If a typical diameter of the bentonite particles is taken to be 2 microns (2.10^{-6}m), then the molecular diffusivity of the bentonite suspension is estimated to be of the order of $10^{-12}\ m^2.sec^{-1}$. Accordingly, the results presented in Figure 27 are seen to be in general qualitative agreement with the hypothesis that the dependence of entrainment rates upon molecular diffusivity (of the property causing the density difference) extends to the case of particle suspensions.

The results of Turner (48) for density differences due to temperature differences and salinity differences conform to the relationship

$$\frac{v_e}{u} = R_i^{-1}\ (C + (R_i\ P_e)^{-\frac{1}{2}}) \qquad (7.3)$$

where v_e = the entrainment velocity

u = the velocity scale of the fluid motion

C = a constant

R_i = the Richardson Number, as defined in Section 7.4

P_e = the Peclet Number, as defined in Section 7.4.

The results of the experiments at present under discussion in which density differences were due to particle suspensions do not, however, conform to the relationship of Equation (7.3).

7.6 Inferences Drawn from the Results of the Experiments on Turbulent Entrainment

The results of the experiments carried out on the entrainment of fluid across density discontinuities have indicated that, in general, it is to be expected that differences will exist between the behaviour of thermal density currents, salt-water density currents and turbidity currents, at least insofar as the phenomenon of turbulent entrainment is concerned.

The experimental results are in agreement with the hypothesis that, under given conditions, the rate of entrainment across a density discontinuity is dependent upon the molecular diffusivity of the property causing the density difference. The significance of molecular diffusivity in the process of turbulent entrainment is apparently associated with diffusion from the sheets or streamers of fluid which, as described in Section 7.5.1 above, were observed to be drawn into the stirred layer. The process of turbulent entrainment proceeds at rates which are, in general, considerably higher than those associated with the molecular diffusion of properties in fluids which are at rest. In the latter case, the process of diffusion itself tends to diminish the sharpness of concentration gradients, and hence the diffusion process is self-retarding. In the case of turbulent entrainment, on the other hand, fluid motions within the turbulent fluid can evidently sharpen the concentration gradient at the boundaries of these streamers to such an extent that diffusion from the streamers, and the process of turbulent entrainment as a whole, can proceed at relatively high rates.

The experimental results have indicated that it is to be expected that a turbidity current will be more resistant to dilution, under given conditions, than will a thermal density current or a salt-water density current. It has also been indicated that the rate of dilution of a density current or a turbidity current may be affected by the presence of intermediate layers adjacent to the interface.

The demonstrated effectiveness of a density discontinuity as a barrier to the transfer of fluid momentum has indicated that the maintenance of non-buoyant material in suspension within a turbidity current will be primarily dependent upon fluid motions generated within the turbidity current itself.

8. Conclusion

The investigation described in the preceding chapters has confirmed that the mechanism of suspension of non-buoyant material in a turbulent flow can be examined by consideration of the history of an individual particle. The potential usefulness for this purpose of the "eddy" model of turbulent flow has been demonstrated. Consideration of the history of an individual particle provides an alternative to the statistical examination of the behaviour of large assemblages of particles.

The eddy model of turbulent suspension has demonstrated that the fall velocity of a non-buoyant particle may be modified by the action of vertical components of fluid velocity, even when the net vertical motion of the fluid is zero. As a result of such modification, the particle may exhibit a fall velocity which differs from the settling velocity of the particle in the quiescent fluid. The resultant fall velocity may be smaller, in absolute magnitude, than the quiescent-fluid settling velocity, and may approach zero, in which case the condition of indefinite suspension of the particle is approached. On the other hand, the resultant fall velocity may, under certain conditions, be greater (in absolute magnitude) than the settling velocity of the particle in the quiescent fluid.

The model has demonstrated that an interchange of energy will occur, between a suspended particle and the surrounding fluid. The sense of the energy transfer (from particle to fluid, or from fluid to particle) will vary periodically. The transfer of energy in either sense will, however, be accompanied by the transformation of some energy into thermal energy. Accordingly, when a non-buoyant particle is suspended within an eddy, the presence of the particle will accelerate the degradation of the energy of the fluid within the eddy.

These effects have been demonstrated for particles whose trajectories pass through a specific relative position within a model eddy which lies within an unbounded array of similar eddies. It has not been established that the effects described are independent of the particular velocity distribution which has been specified to exist within the model eddy field, and no claim is made that the specified velocity distribution represents more than a first approximation to a realistic picture of the fluid motions within an actual turbulent flow.

For the specified conditions within the model eddy field, a criterion for the condition of indefinite suspension of a non-buoyant particle within an individual eddy has been established. The criterion takes the form of a limiting value of the ratio between a characteristic velocity within the eddy field and the settling velocity of the particle in the quiescent fluid. The limiting value of this ratio, for the suspension of a particle within an eddy, does not appear to depend upon the spacing of the eddy centres within the eddy field. Although the established domain of validity of this criterion is restricted to the specific conditions applying in the investigation as described, the limiting value of the ratio is of the same order of magnitude as that indicated by experiments on plumes.

The results of the examination of the process of entrainment across density discontinuities have indicated that, under given conditions, the rate of entrainment of fluid across the density discontinuity will be dependent upon a characteristic of the property which causes the density of one fluid layer to differ from that of the adjoining layer. Rates of entrainment have been compared, for cases in which the density differences have been due to temperature differences, to salinity differences and to turbidity. If the concept of molecular diffusivity is extended to particle suspensions by the application of the Stokes-Einstein Equation, the experimental results are in general agreement with the hypothesis that the rate of entrainment is dependent upon the molecular diffusivity of the property causing the difference in the densities of the adjoining fluid layers.

The investigation of the entrainment process has indicated that a turbidity current will be less susceptible to dilution as a result of the entrainment of ambient fluid than a non-suspension type density current under similar conditions. Accordingly, it is to be expected that a turbidity current will tend to be more stable and persistent, under given conditions, than a thermal or saline density current.

9. References

1. American Society of Civil Engineers, Task Committee on Preparation of Sedimentation Manual: Progress Report, A.S.C.E. Proc. v.89 (J. Hydraulics Divn) n. HY5 Sept. 1963 pt 1 p. 77-87.

2. Bagnold R.A. "Auto-suspension of Transported Sediment; Turbidity Currents" Royal Society, London Proc. ser. A v. 265 1962 p. 315-319.

3. Basset A.B. "A Treatise on Hydrodynamics" Dover Publications Inc. New York U.S.A. 1961 (vol. 2).

4. Bell H.S. "Density Currents as Agents for Transporting Sediments" J. of Geology v. 50 n. 5 July-Aug. 1942 p. 512-547.

5. Bird R.B., Stewart W.E., Lightfoot E.N., "Transport Phenomena" John Wiley and Sons, New York U.S.A., 1960.

6. Birkhoff G. "Hydrodynamics" Princeton University Press, Princeton New Jersey U.S.A. 1960.

7. Brush L.M., Ho H.W., Yen B.C. "Accelerated Motion of a Sphere in a Viscous Fluid" American Soc. of Civil Engineers Proc. v. 90 (J. Hydraulics Divn) n. HY1 Jan. 1964 p. 149-160.

8. Buffington E.C. "Experimental Turbidity Currents on the Sea Floor" Amer. Assoc. of Petroleum Geologists Bul. v.45 1961 p. 1392-1400.

9. Charnock H. "Turbidity Currents" Nature v. 183 March 7, 1959, p. 657-659.

10. Chepil W.S., "The Use of Spheres to Measure Lift and Drag on Wind-eroded Soil Grains" Soil Science Soc. of America Proc. v. 25 1961 p. 243-245.

11. Cromwell T. "Pycnoclines Created by Mixing in an Aquarium Tank" J. of Marine Research v. 18 n. 2 1960 p. 73-82.

12. Daly R.A. "Origin of Submarine Canyons" American J. of Science, ser. 5 v. 31 n. 186 p. 401-420.

13. Davies C.N. "The Particle Resistance/Inertia Parameter" Appendix to "Aerodynamic Capture of Particles" - Proc., Conf. at British Coal Utilisation Research Assoc., Leatherhead Surrey 1960 Richardson E.G. ed., Pergamon Press Oxford 1960.

14. Electricity Commission of New South Wales, The; "Report on the Ocean Disposal of Fly Ash" Research Note n.30 December 1962.

15. Ellison T.H., Turner J.S. "Turbulent Entrainment in Stratified Flows" J. of Fluid Mechanics v. 6 pt 3 1959 p.423-448.

16. Field W.G. "Some Effects of Density Ratio on Sedimentary Similitude" Ph.D. Thesis, The University of Newcastle, New South Wales, 1967.

17. Foster D.N., Stone D.M. "Ocean Disposal of Ash" University of New South Wales, Water Research Laboratory Report n.65, Sydney, N.S.W. 1963.

18. Gray W.A. "Comparative Study of Behaviour of Two-dimensional Plumes formed by Salt Water or Turbid Water" M.E. Thesis, The University of New South Wales 1970.

19. Greslou L. "Rejet de matériaux a la mer par refoulement hydraulique risques de pollution des plages" 7th Conf. on Coastal Engrg, The Hague 1960 Proc. v.1 p.455-484. (An English translation, in which the author's name appears as Creslom, is contained in Appendix A3 to Electricity Commission of New South Wales Research Note n.30 "Ocean Disposal of Fly Ash".)

20. "Handbook of Chemistry and Physics" 44th ed., The Chemical Rubber Publishing Co., Cleveland Ohio U.S.A.

21. Harwood F.L., Wilson K.C., "An Investigation into a Proposal to Dispose of Power Station Ash by Discharging it into the Sea at Low Water" Institution of Civil Engineers Proc. v.8 Sept. 1957 p.53-70.

22. Ho H.W. "Fall Velocity of a Sphere in a Field of Oscillating Fluid" Ph.D. Thesis, State University of Iowa, Iowa U.S.A. 1964.

23. Hunt J.N. "The Turbulent Transport of Suspended Sediment in Open Channels" Royal Society, London Proc. ser. A v.224 1954 p. 322-335.

24. Iversen H.W., Balent R. "A Correlating Modulus for Fluid Resistance in Accelerated Motion" J. of Applied Physics v.22 n.3 March 1951 p.324-328.

25. Jobson H.E., Sayre W.W. "An Experimental Investigation of the Vertical Mass Transfer of Suspended Sediment" International Assoc. for Hydraulic Research, XIIIth Congress, Tokyo 1969 Proc. v.2 paper B11 p.111-120.

26. Johnson D.W. "The Origin of Submarine Canyons" Columbia Univ. Press New York U.S.A. 1939.

27. Johnson M.A. "Physical Oceanography: Turbidity Currents" Science Progress v.L n.198 April 1962 p.257-273.

28. Kuenen Ph. H. "Experiments in Connection with Daly's Hypothesis on the Formation of Submarine Canyons" Leidse Geol. Mededelingen, deel 8, 1936-37, p.327-351.

29. Kuenen Ph. H. "Estimated Size of the Grand Banks Turbidity Current" American J. of Science v.250 Dec. 1952 p.874-884.

30. Manton M.J. "On the Motion of a Small Spherical Particle within a Steady Viscous Flow" Univ. of Sydney, Dept. of Mechanical Engrg., Charles Kolling Research Lab. Tech. Note F-28, July 1971.

31. Matthe G.H. "Macroturbulence in Natural Stream Flow" American Geophysical Union Trans. v. 28 n. 2 April 1947 pp 255-265.

32. Mendenhall C.E., Mason M. "The Stratified Subsidence of Fine Particles" National Academy of Sciences Proc. v.9 1923 pp. 199-202; also Mason M., Mendenhall C.E. "Theory of the Settling of Fine Particles" ibid pp. 202-207.

33. Middleton G.V. "Small-scale Models of Turbidity Currents and the Criterion for Auto-Suspension" J. of Sedimentary Petrology v.36 n.1 March 1966 p. 202-208.

34. Middleton G.V. "Experiments on Density and Turbidity Currents III: Deposition of Sediment" Canadian J. of Earth Sciences v.4 1967 p.475-505.

35. Mockros L. F., Lai R.Y.S. "Validity of Stokes Theory for Accelerating Spheres" American Soc. of Civil Engineers Proc. v.95 (J. of Eng. Mech. Divn) n.EM3 June 1969 p.629-640.

36. Phillips O.M. "The Dynamics of the Upper Ocean" University Press Cambridge 1966.

37. Deleted.

38. Robertson J.M. "Hydrodynamics in Theory and Application" Prentice-Hall Inc. Englewood Cliffs New Jersey U.S.A. 1965.

39. Rouse H. "Experiments on the Mechanics of Sediment Suspension" Proc. 5th Int. Congress for Appl. Mechanics. New York U.S.A. 1938.

40. Rouse H. "Engineering Hydraulics" Rouse H. ed. John Wiley and Sons Inc. New York U.S.A. 1950.

41. Rouse H., Dodu J. "Turbulent Diffusion across a Density Discontinuity" La Houille Blanche v.10 n.4 Aug.-Sept. 1955 pp 522-532.

42. Ryan W.B.F., Heezen B.C. "Ionian Sea Submarine Canyons and 1908 Messina Turbidity Current" Geological Soc. of America Bul. v.76 n.8 Aug. 1965 p.915-932.

43. Schlichting H. "Boundary Layer Theory" Kestin J. trans. 6th ed. McGraw Hill New York U.S.A. 1968.

44. Thistlethwayte D.K.B., late of School of Civil Engrg., University of New South Wales - personal communication.

45. Thompson S.J. "Turbulent Interfaces Generated by an Oscillating Grid in a Stably Stratified Fluid" Ph.D. Thesis, University of Cambridge, 1969.

46. Townsend A.A. "The Structure of Turbulent Shear Flow" Cambridge Monographs on Mechanics and Applied Mathematics, University Press Cambridge 1956.

47. Tsang Gee "Two-dimensional Plume Studies" M. Tech. Thesis, The University of New South Wales 1965.

48. Turner J.S. "The Influence of Molecular Diffusivity on Turbulent Entrainment across a Density Interface" J. of Fluid Mechanics v.33 pt 4 1968 p.639-656.

49. Woodward B. "The Motion in and around Isolated Thermals" Royal Meteorological Soc., Quarterly J. v.85 1959 p.144-151.

50. Young D.F. "Drag and Lift on Spheres within Cylindrical Tubes" American Soc. of Civil Engineers Proc. v.86 (J. of Hydraulics Divn) n.HY6 June 1960 p.47-57.

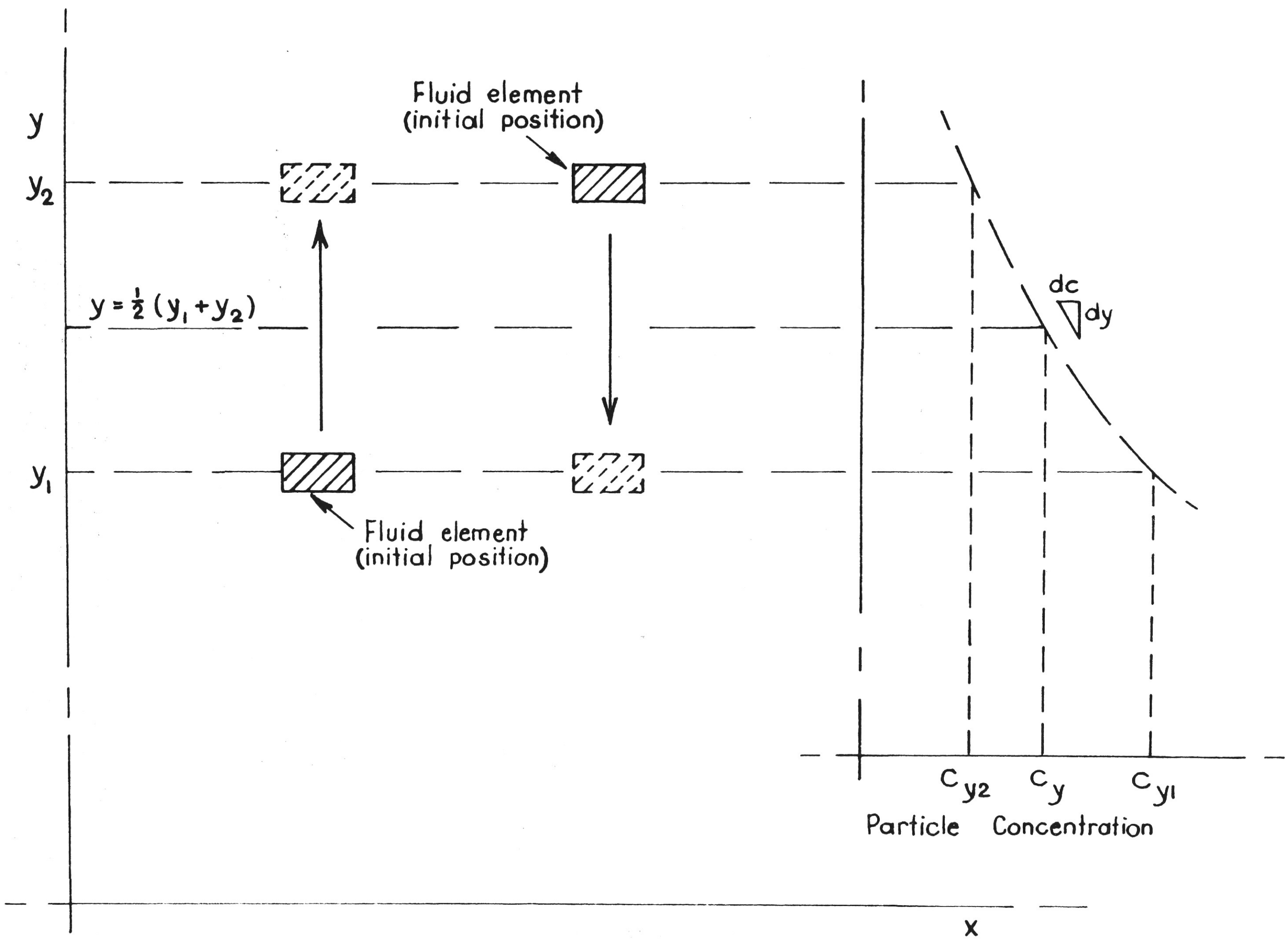

FIGURE I : THE NET UPWARD TRANSPORT OF PARTICLES BY EXCHANGE OF FLUID VOLUMES, IN THE PRESENCE OF A GRADIENT OF PARTICLE CONCENTRATION

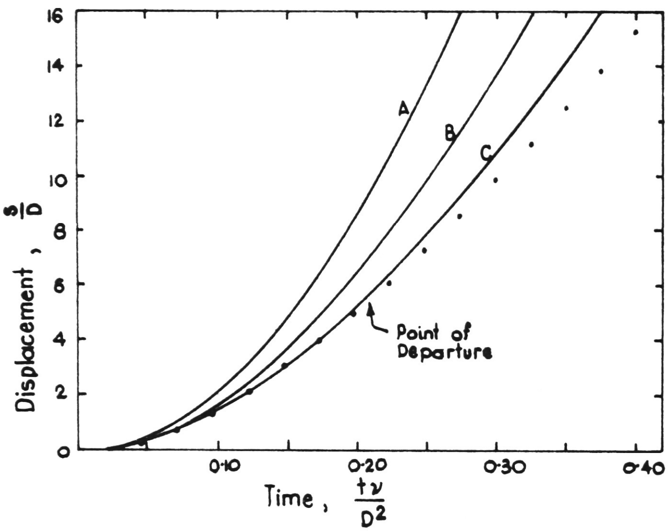

S = The particle displacement
D = The particle diameter
• Experimental results
A Theory ; History Term and Viscous Drag neglected
B Theory ; History Term neglected
C Theory ; Complete Equation of Motion

FIGURE 2 : THE MOTION OF SPHERICAL PARTICLES SETTLING THROUGH A QUIESCENT VISCOUS FLUID - MOCKROS AND LAI, REF.(35).

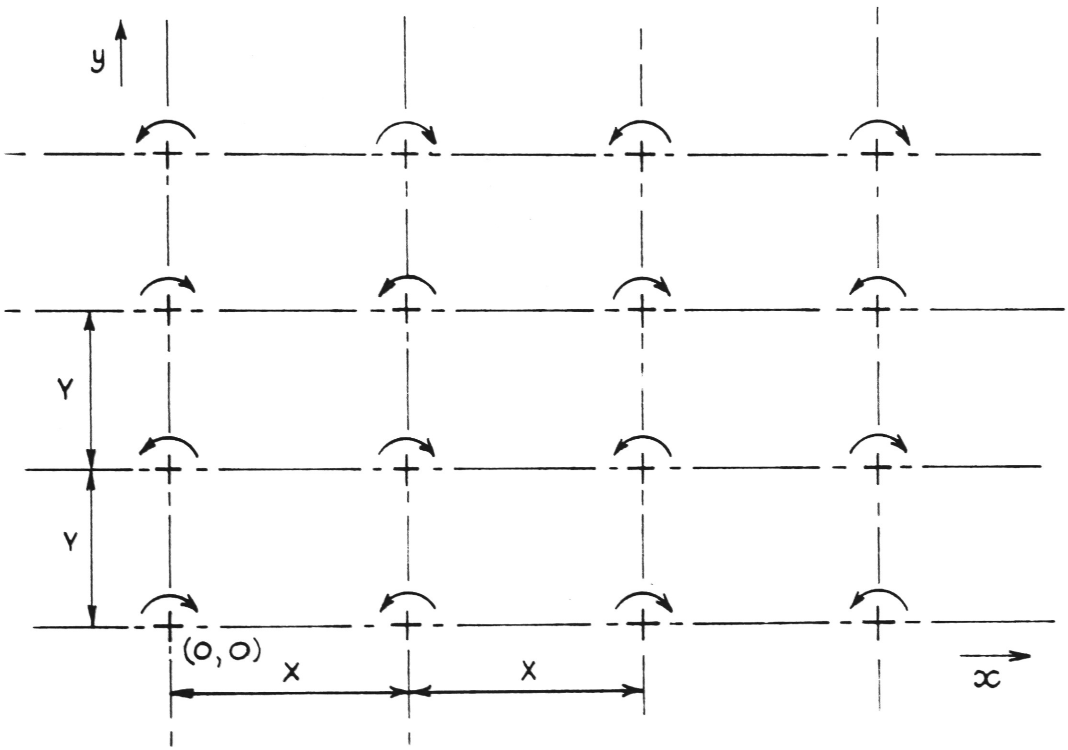

FIGURE 3 : THE MODEL EDDY FIELD

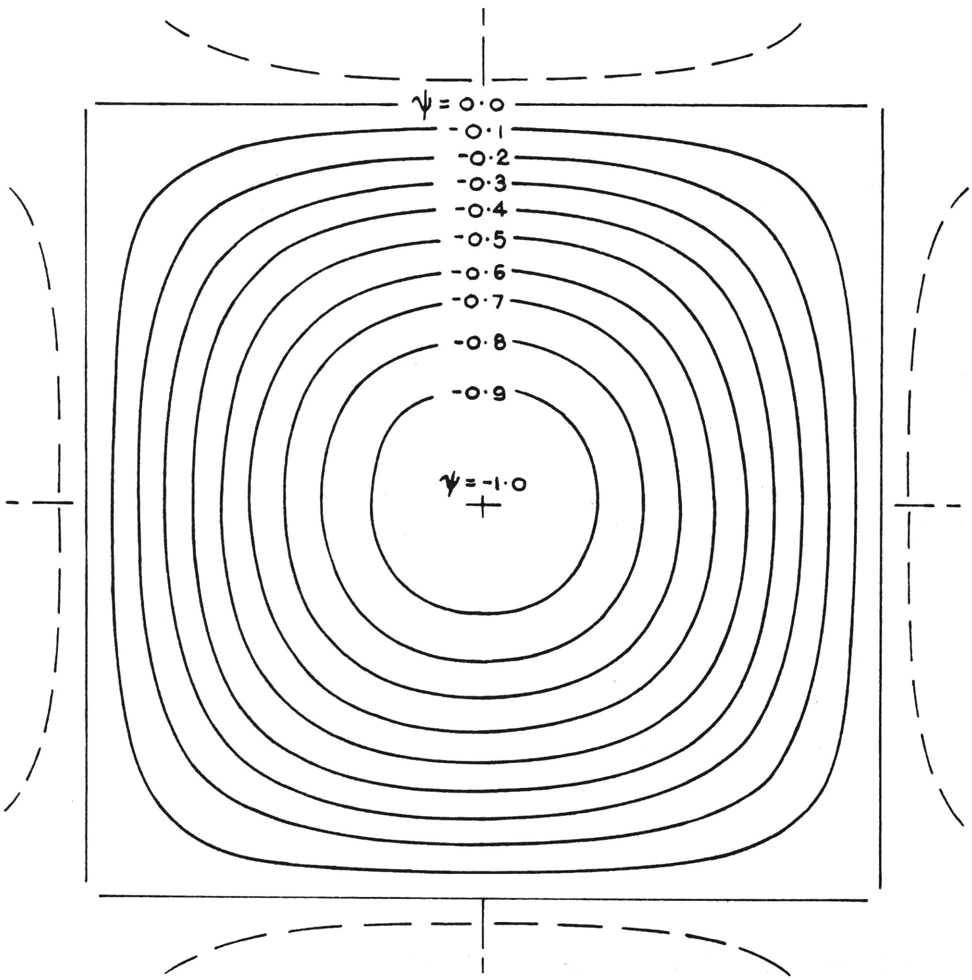

FIGURE 4 : THE STREAMLINE PATTERN WITHIN AN EDDY IN A FIELD OF SQUARE EDDIES

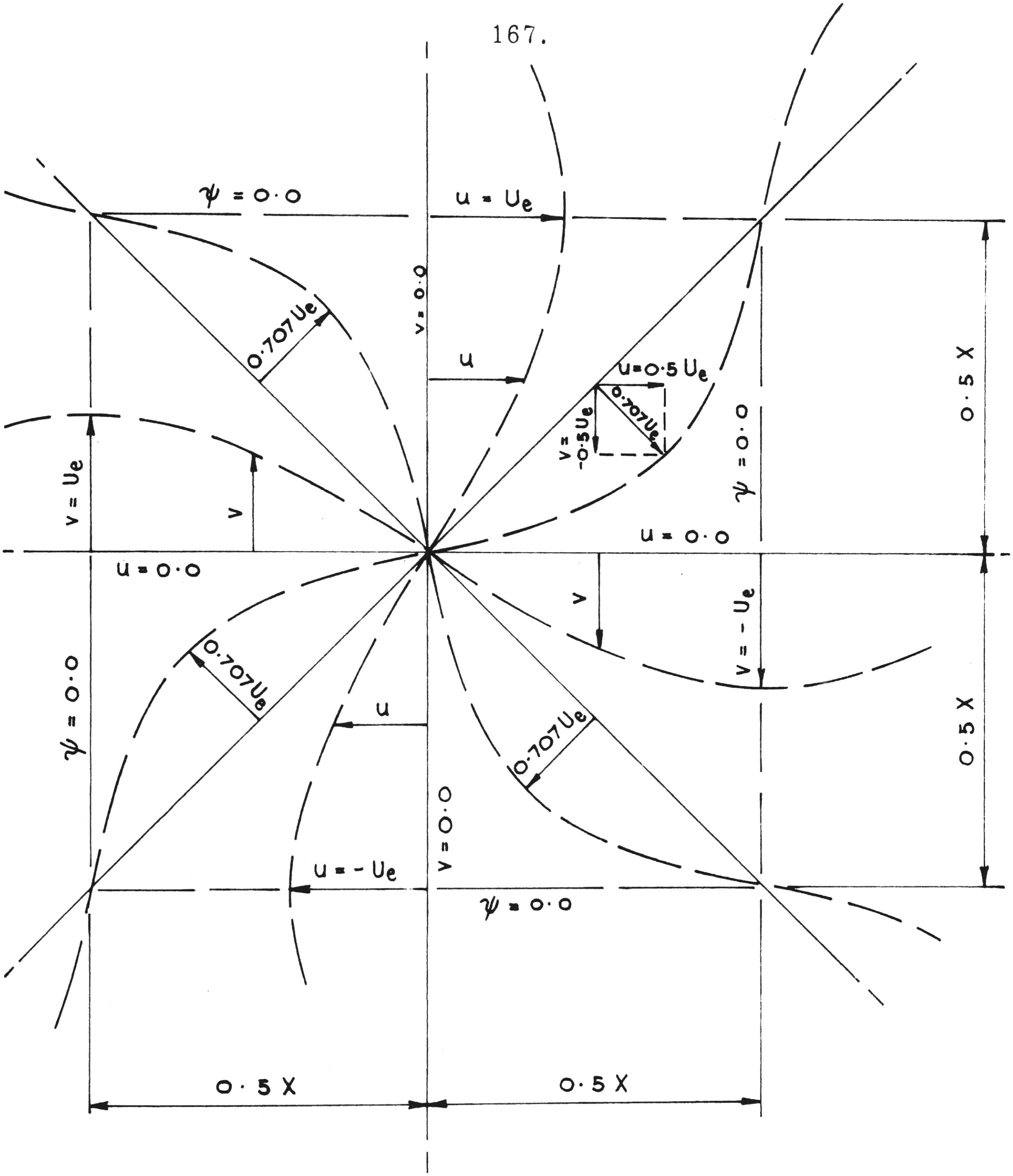

FIGURE 5 : VELOCITY DISTRIBUTIONS WITHIN THE EDDY SHOWN IN FIGURE 4

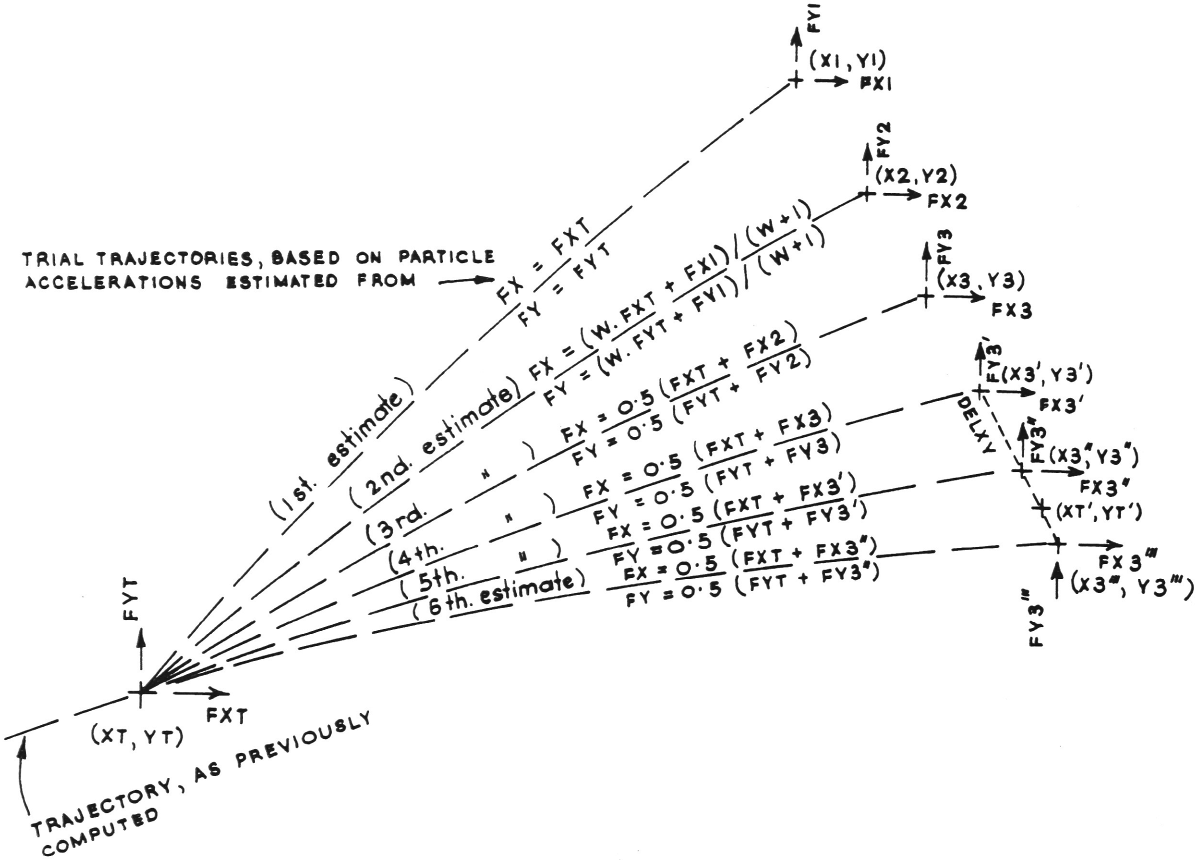

Note : The relative positions of the points (X1, Y1), (X2, Y2) etc. as shown are diagrammatic only - the points have been displaced to illustrate the order of their computation.
The procedure is described in Section 4·2 of the text.

FIGURE 6 : A DIAGRAMMATIC REPRESENTATION OF THE PROCEDURE FOR THE COMPUTATION OF A POINT ON THE PARTICLE TRAJECTORY

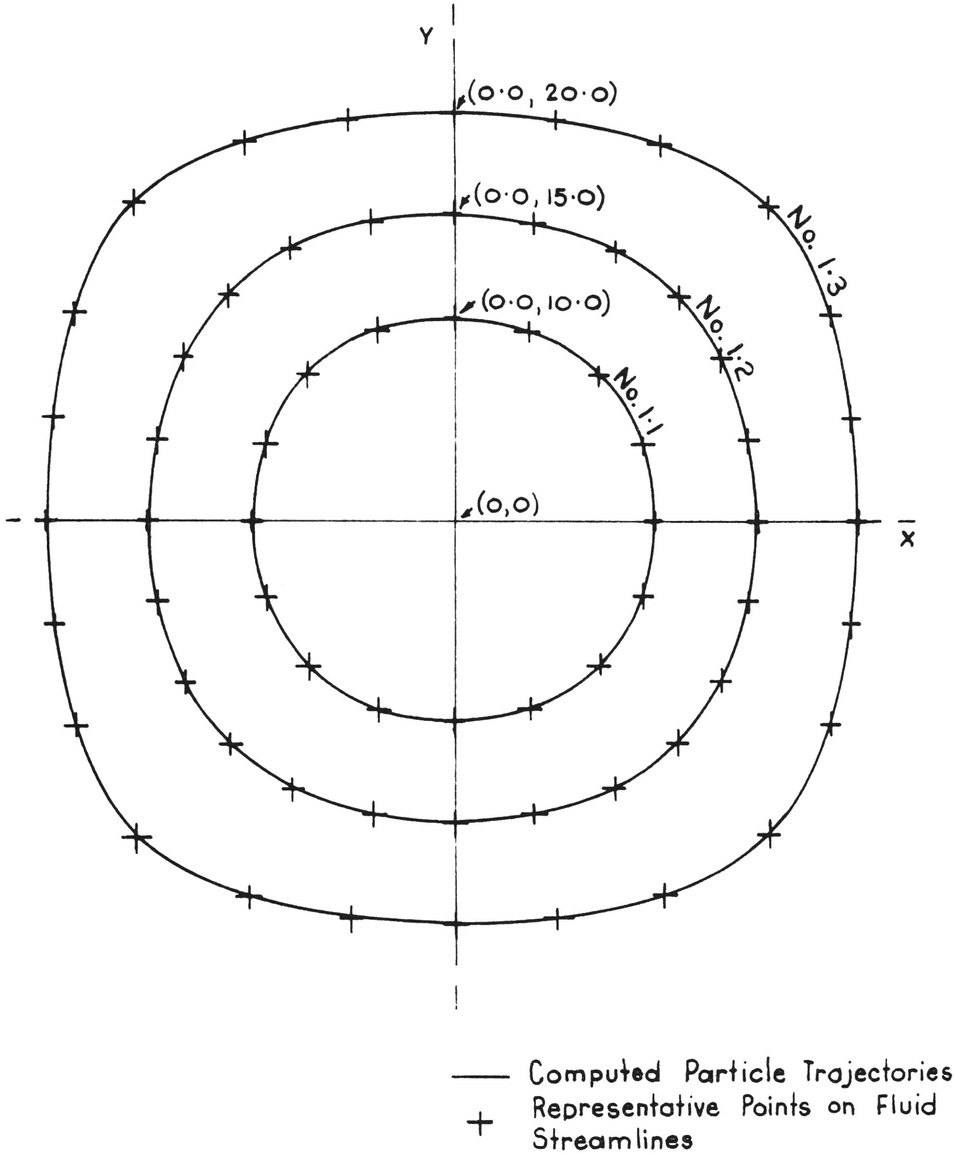

FIGURE 7 : COMPUTED TRAJECTORIES OF A NEUTRALLY-BUOYANT PARTICLE WITHIN THE MODEL EDDY FIELD - TRAJECTORIES NOS. 1.1, 1.2 AND 1.3.

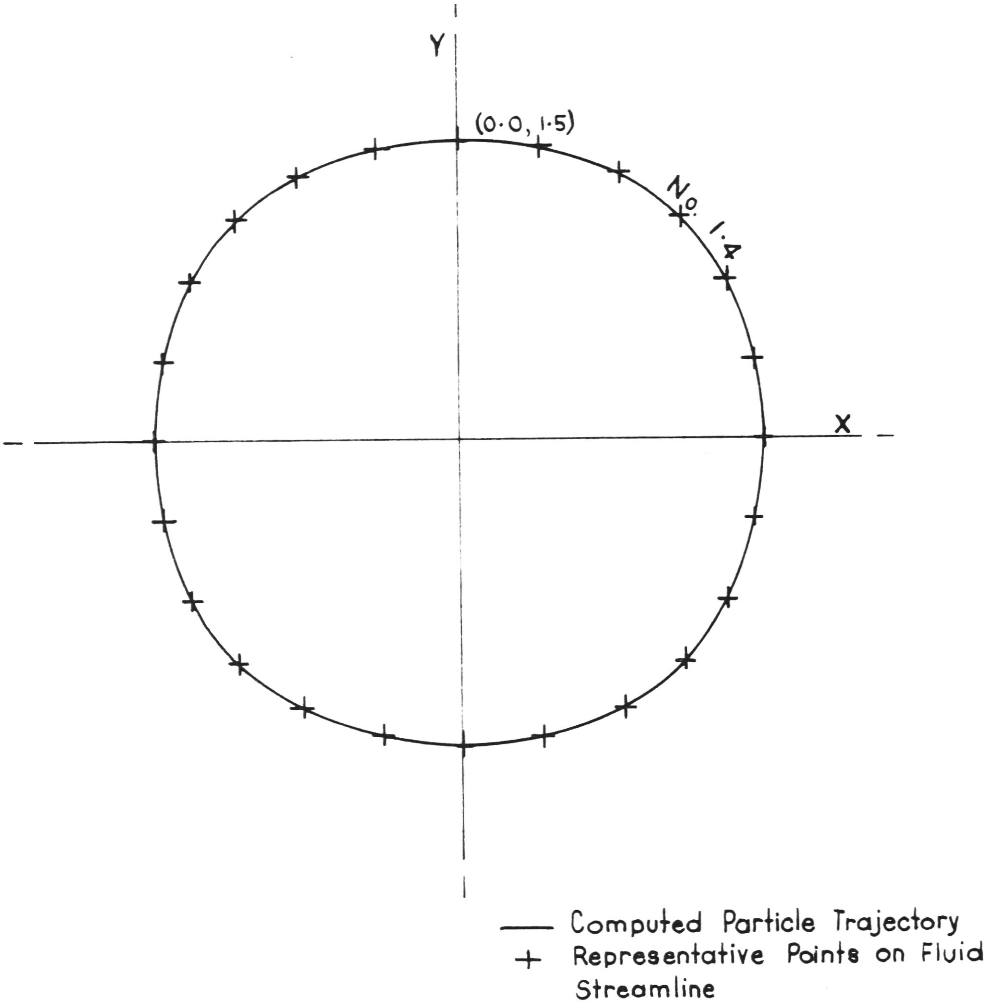

FIGURE 8 : COMPUTED TRAJECTORY OF A NEUTRALLY-BUOYANT PARTICLE WITHIN THE MODEL EDDY FIELD - TRAJECTORY NO. 1.4.

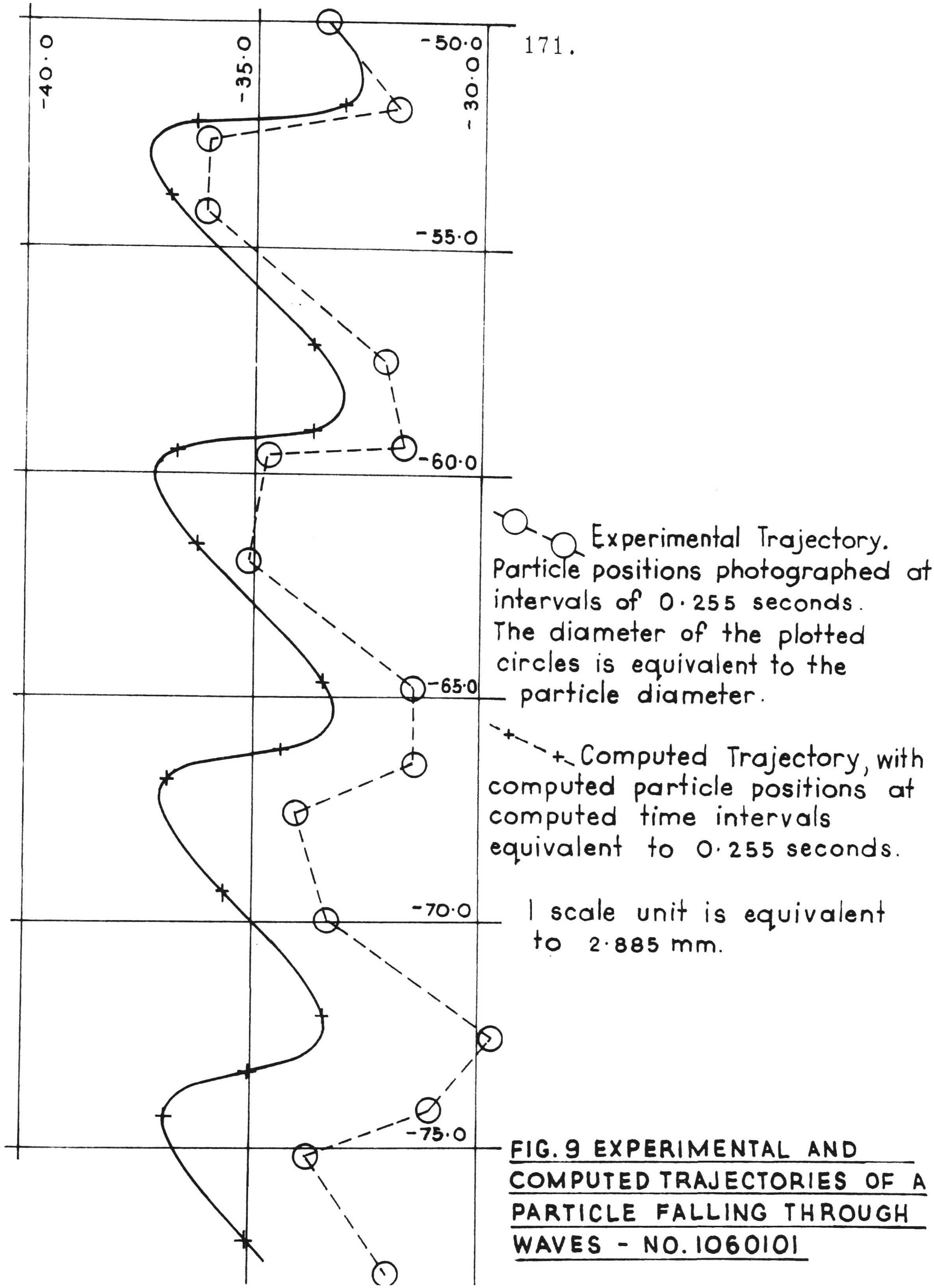

FIG. 9 EXPERIMENTAL AND COMPUTED TRAJECTORIES OF A PARTICLE FALLING THROUGH WAVES - NO. 1060101

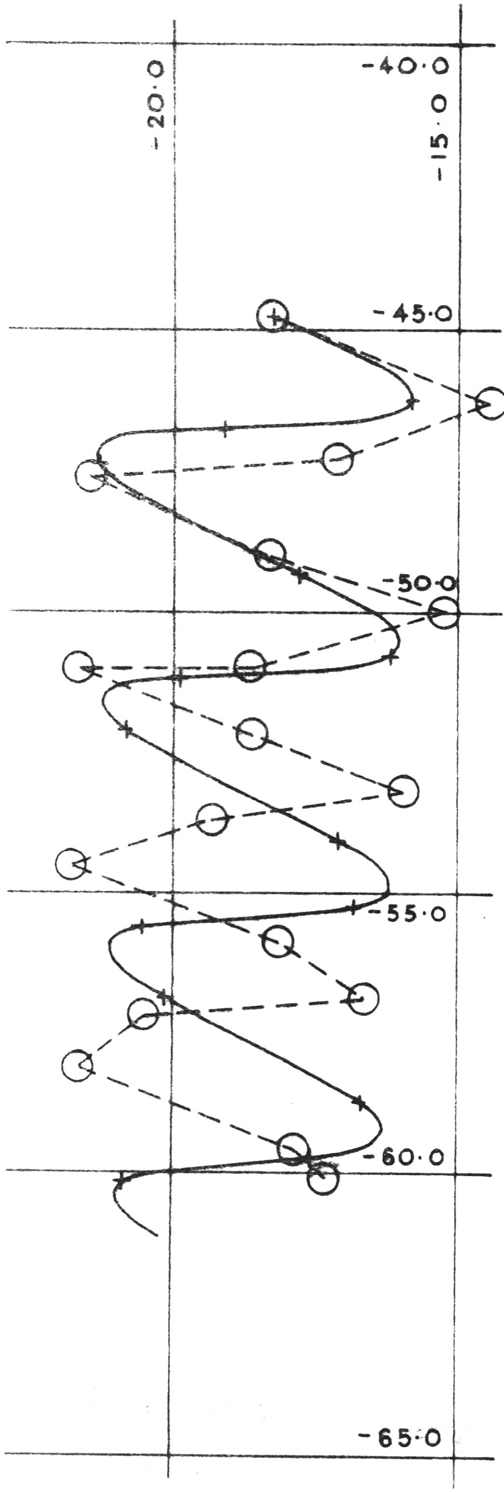

Experimental Trajectory. Particle positions photographed at intervals of 0·255 seconds. The diameter of the plotted circles is equivalent to the particle diameter.

Computed Trajectory, with computed particle positions at computed time intervals equivalent to 0·255 seconds.

1 scale unit is equivalent to 2·760 mm.

FIG. 10 : EXPERIMENTAL AND COMPUTED TRAJECTORIES OF PARTICLE FALLING THROUGH WAVES - NO. 1090101

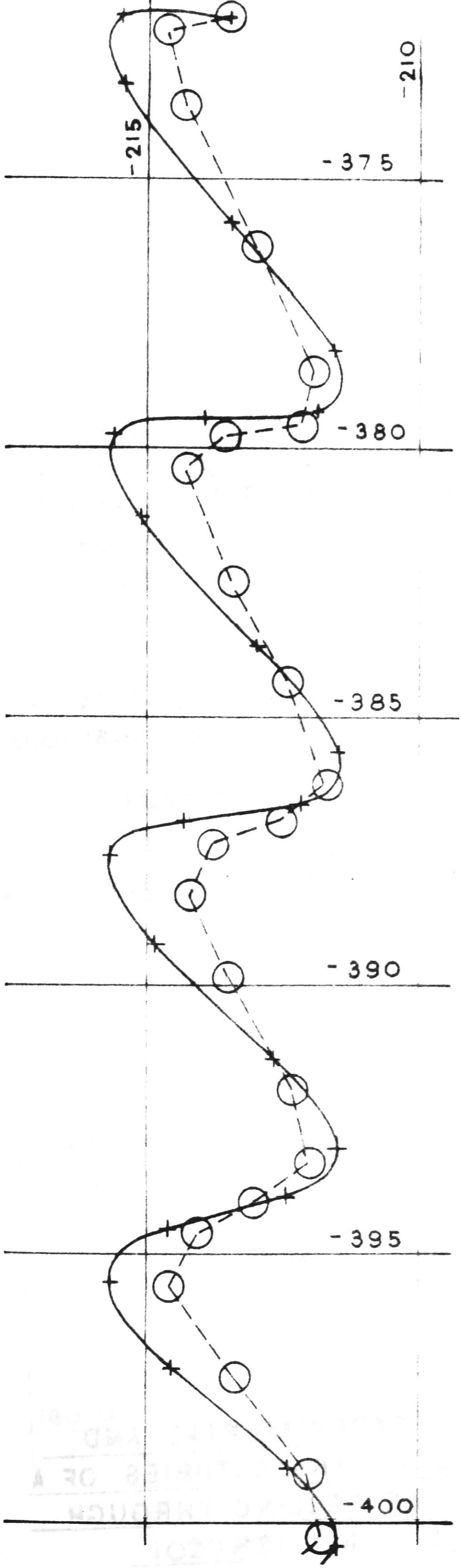

Experimental Trajectory. Particle positions photographed at intervals of 0·2 seconds The diameter of the plotted circles is equivalent to the particle diameter.

Computed Trajectory, with computed particle positions at computed time intervals equivalent to 0·2 seconds.

1 scale unit is equivalent to 1·835 mm.

FIG. 11: EXPERIMENTAL AND COMPUTED TRAJECTORIES OF A PARTICLE FALLING THROUGH WAVES - NO. 1120101

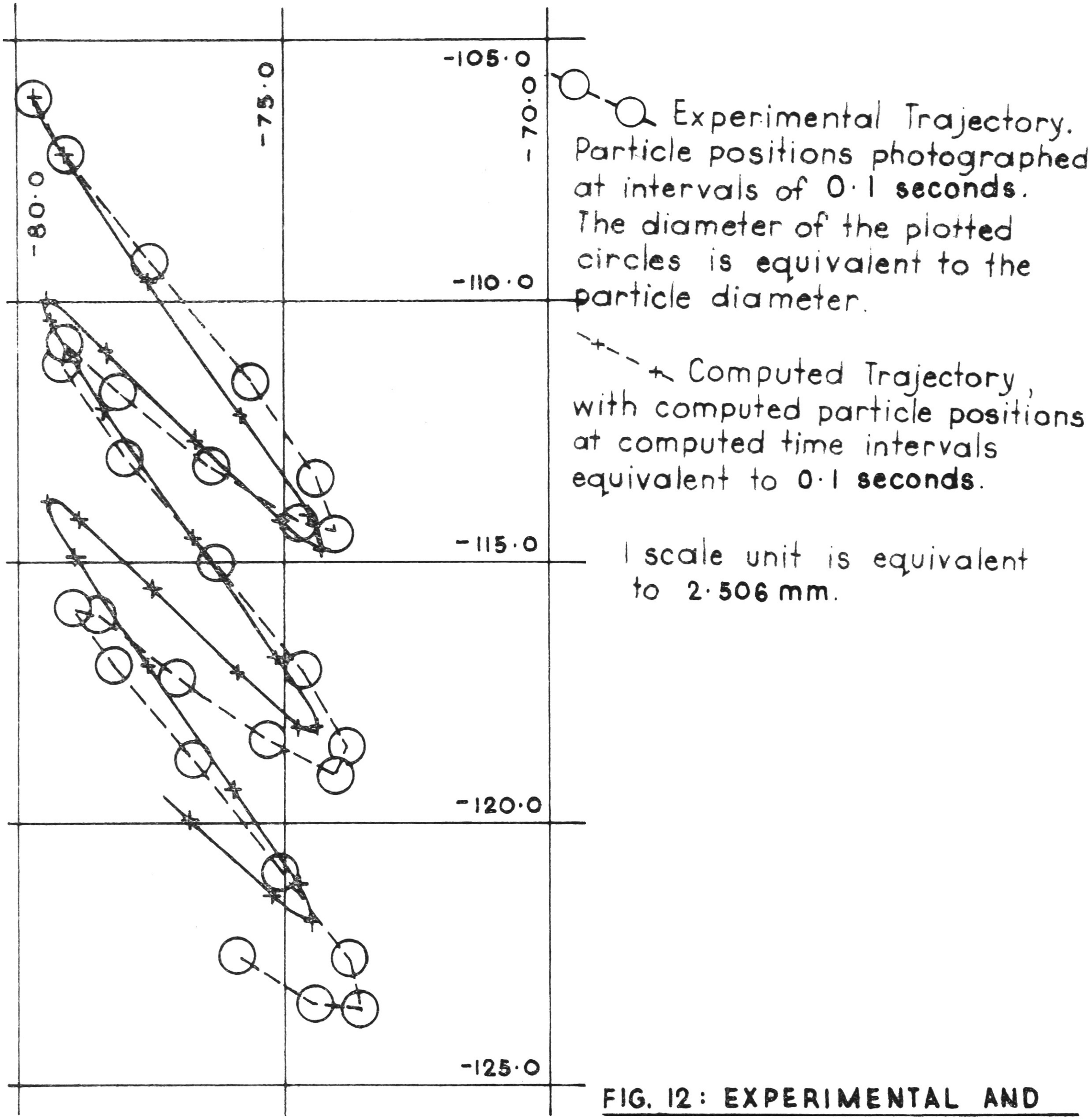

FIG. 12: EXPERIMENTAL AND COMPUTED TRAJECTORIES OF A PARTICLE FALLING THROUGH WAVES - NO. 1250201

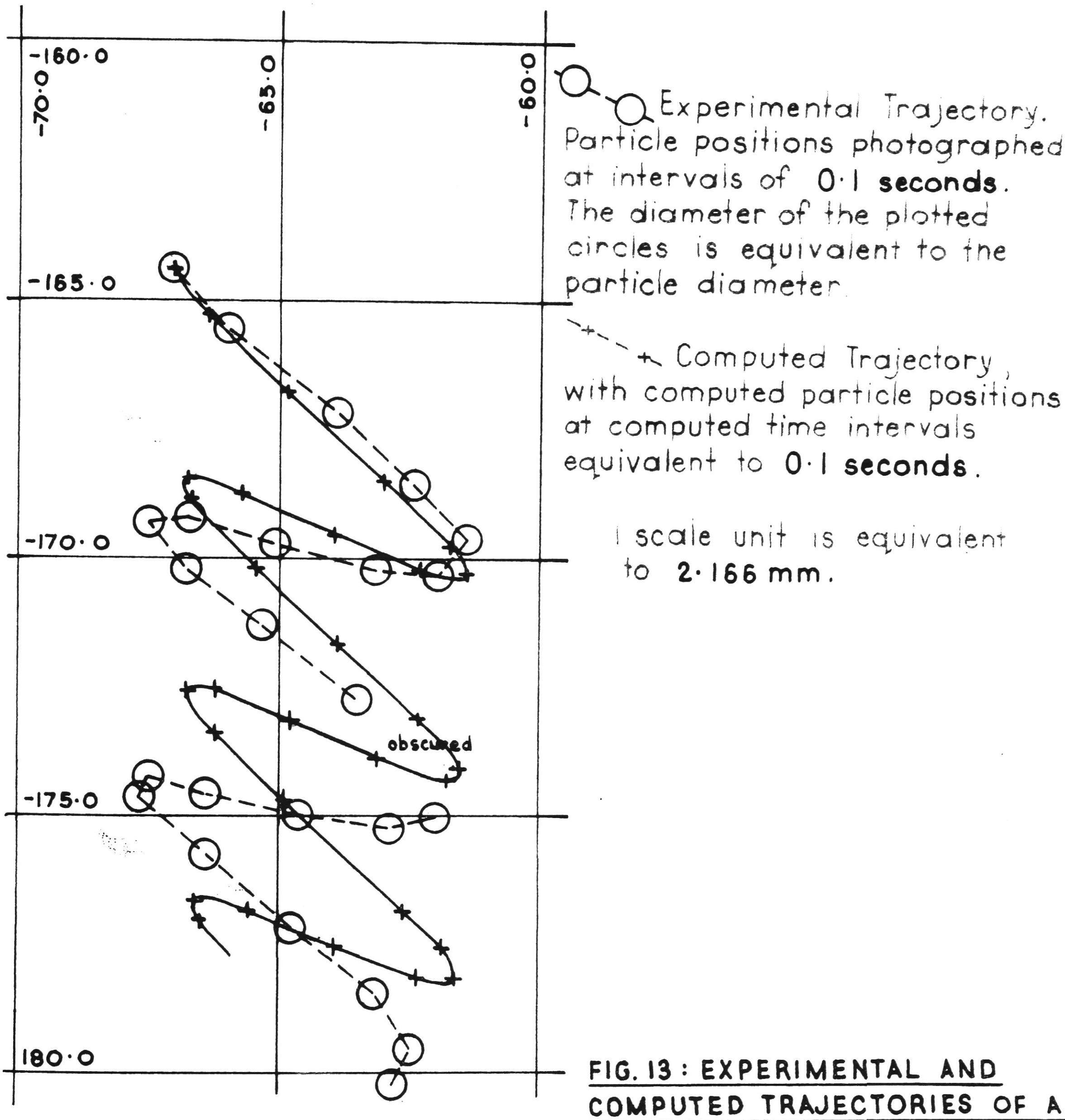

FIG. 13 : EXPERIMENTAL AND COMPUTED TRAJECTORIES OF A PARTICLE FALLING THROUGH WAVES - NO.1260101

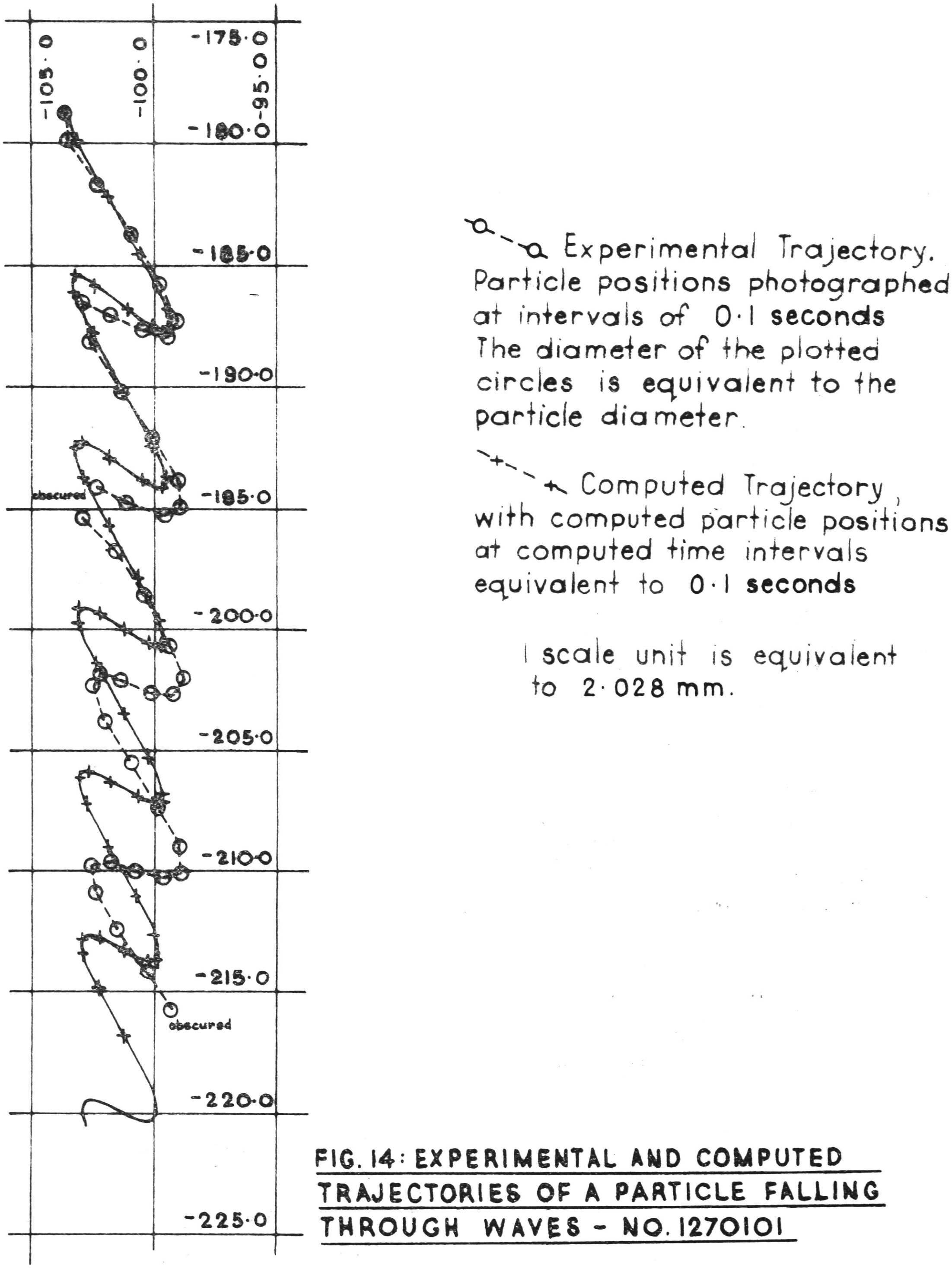

FIG. 14: EXPERIMENTAL AND COMPUTED TRAJECTORIES OF A PARTICLE FALLING THROUGH WAVES - NO. 1270101

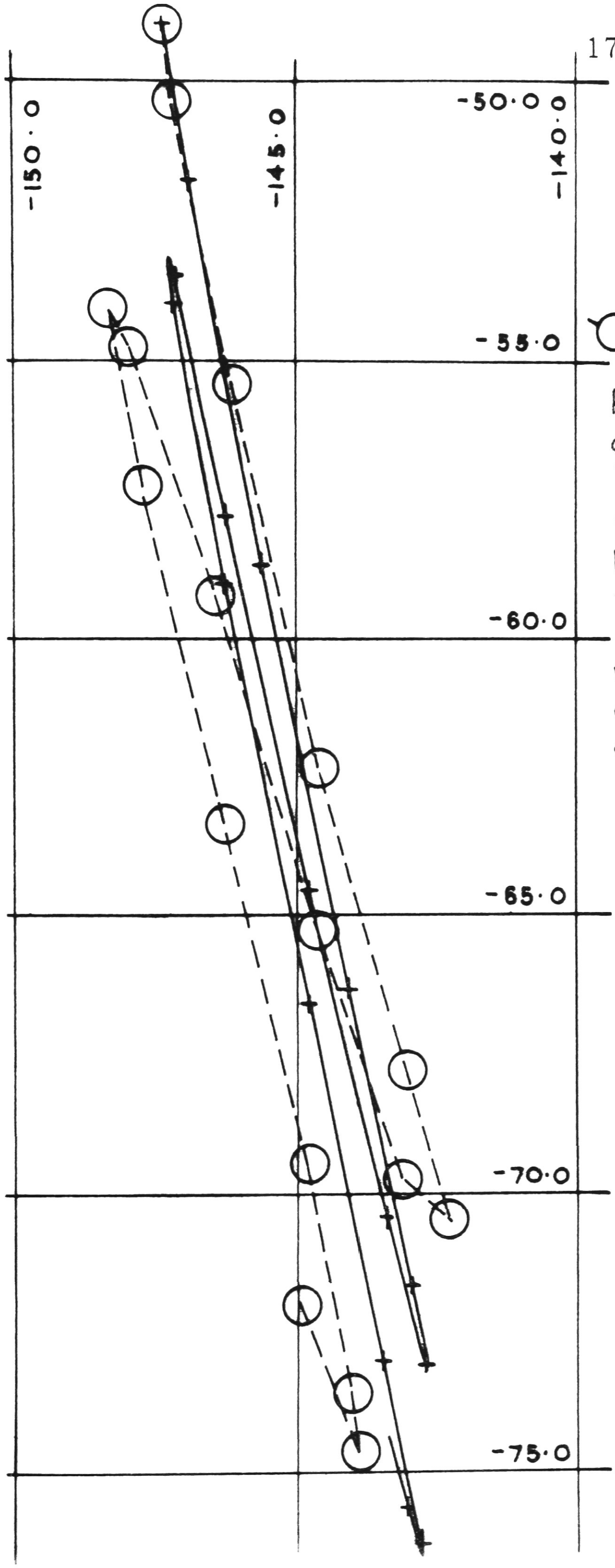

Experimental Trajectory. Particle positions photographed at intervals of 0·1 seconds. The diameter of the plotted circles is equivalent to the particle diameter.

Computed Trajectory, with computed particle positions at computed time intervals equivalent to 0·1 seconds.

1 scale unit is equivalent to 1·989 mm.

FIG. 15 : EXPERIMENTAL AND COMPUTED TRAJECTORIES OF A PARTICLE FALLING THROUGH WAVES - NO. 1280101

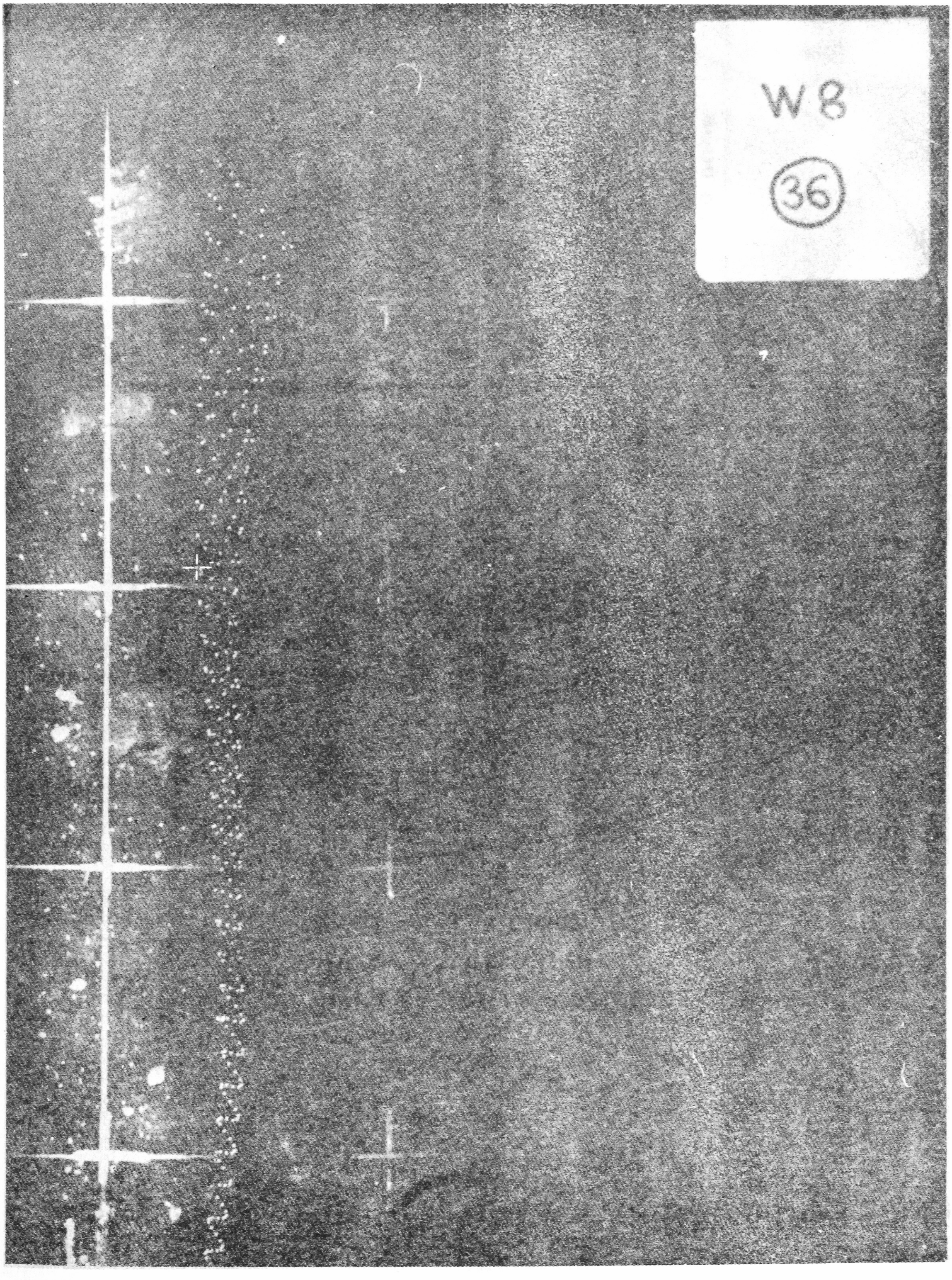

FIGURE 16: THE TRAJECTORY OF A PARTICLE FALLING THROUGH WAVES - RECORDED BY STROBOSCOPIC PHOTOGRAPHY.

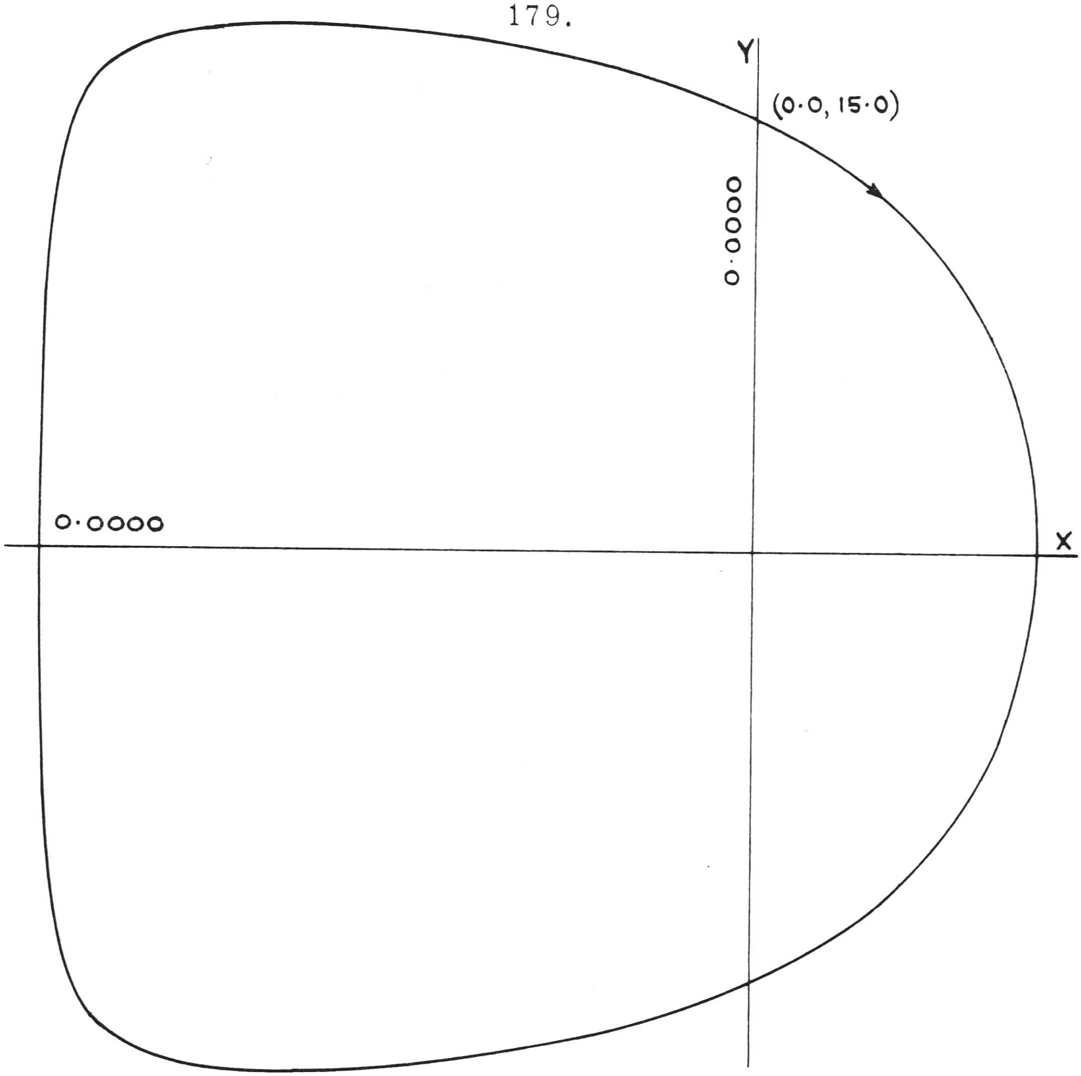

PART = $\sqrt{\frac{gd^3}{\nu}}$ = 1·1068

GRAV = (s - 1·0) = 1·00

XCNTR = YCNTR = 50·6250

UEDDY = 0·17

FIGURE 17 : COMPUTED PARTICLE TRAJECTORY 610101-620101
(NO. 2.16)

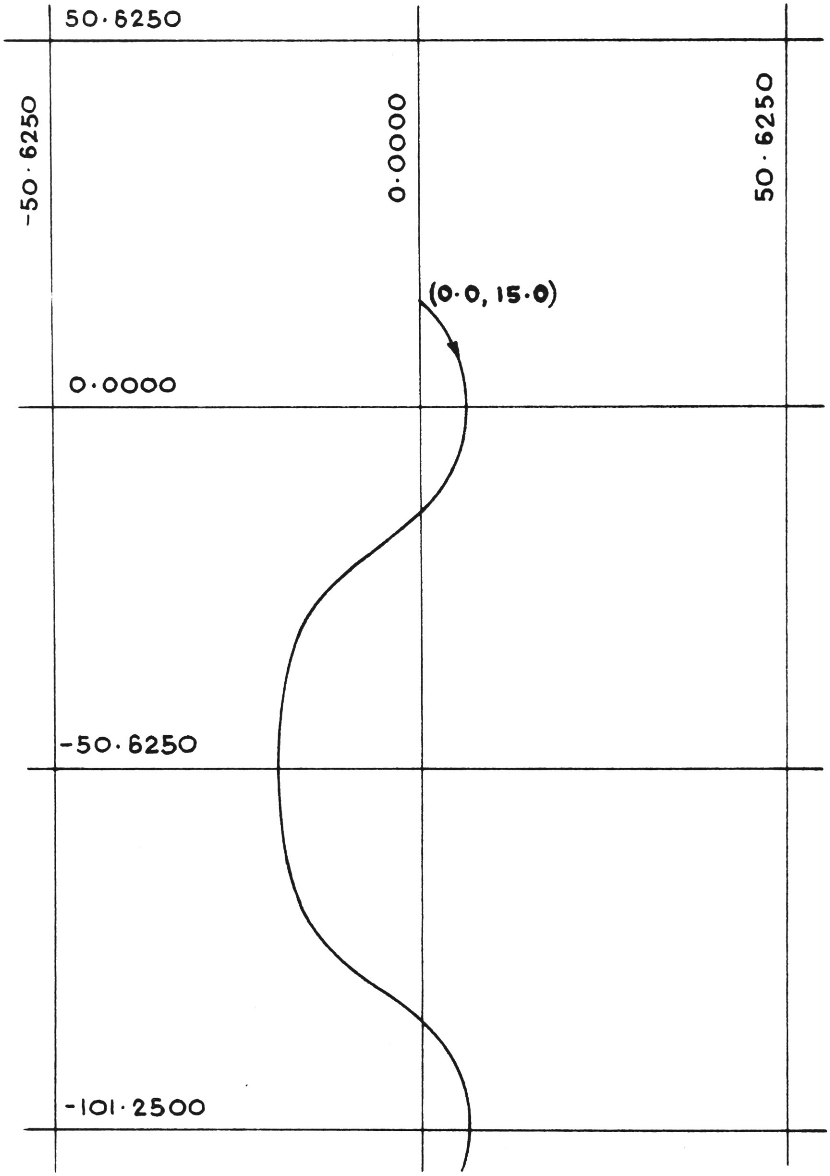

PART = $\frac{\sqrt{gd^3}}{\nu}$ = 1·1068

GRAV = (s - 1·0) = 1·00

XCNTR = YCNTR = 50·6250

UEDDY = 0·08

FIGURE 18: COMPUTED PARTICLE TRAJECTORY 380101 (No. 2·11)

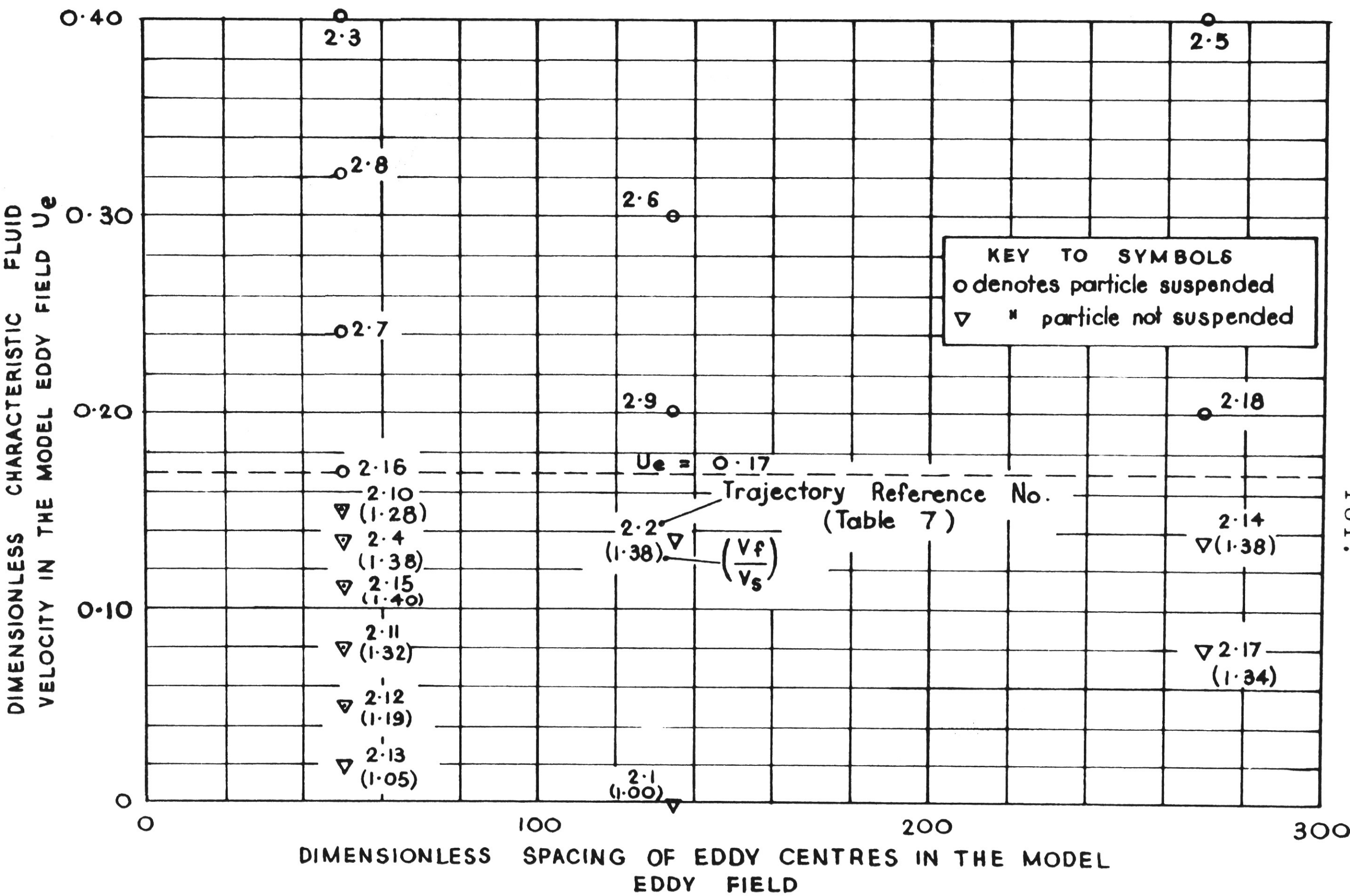

FIGURE 19 : CONDITIONS FOR THE SUSPENSION OF A PARTICLE WITHIN THE MODEL EDDY FIELD

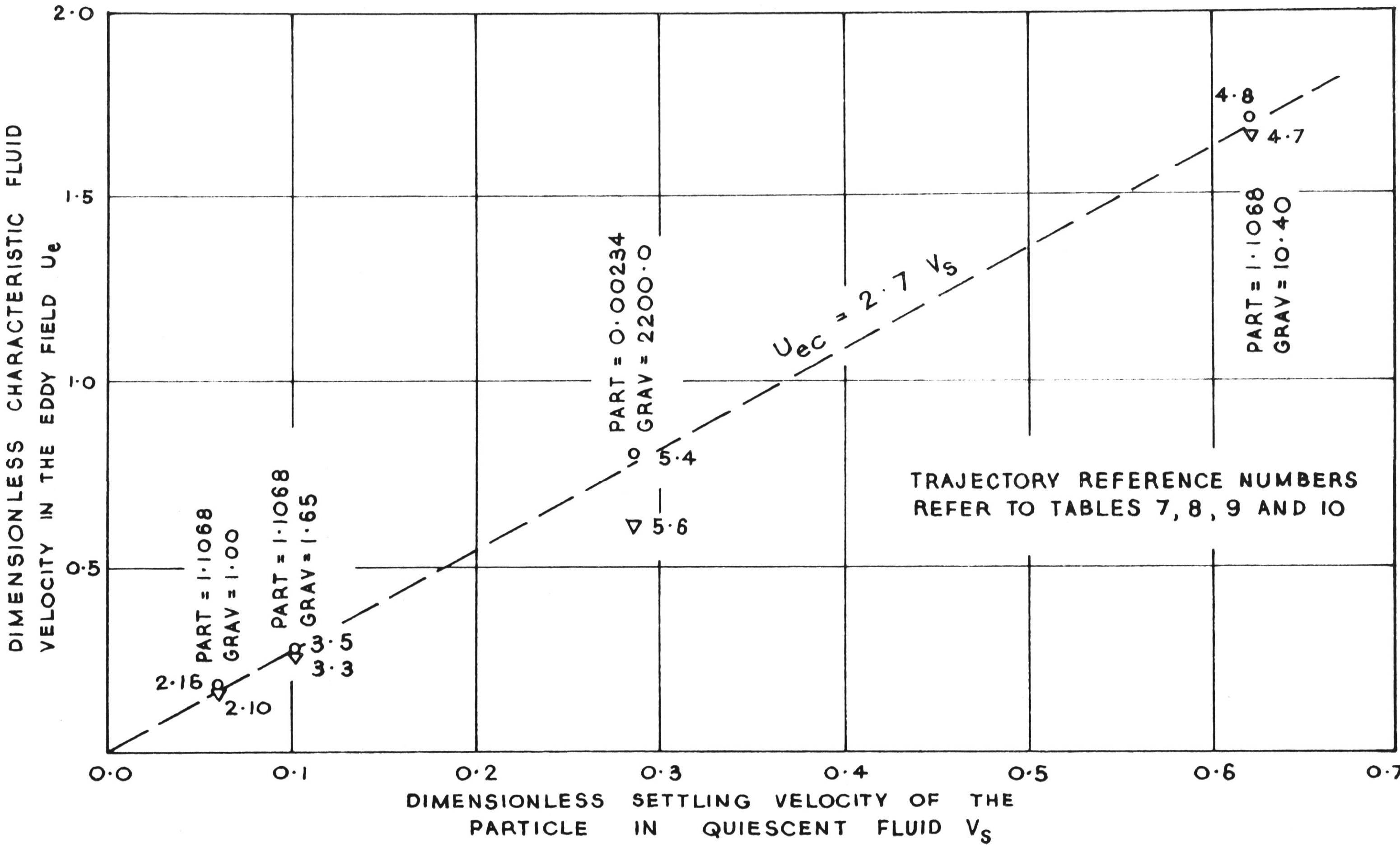

FIGURE 20 : CRITICAL VALUES OF THE CHARACTERISTIC FLUID VELOCITY FOR THE SUSPENSION OF PARTICLES WITHIN THE MODEL EDDY FIELD

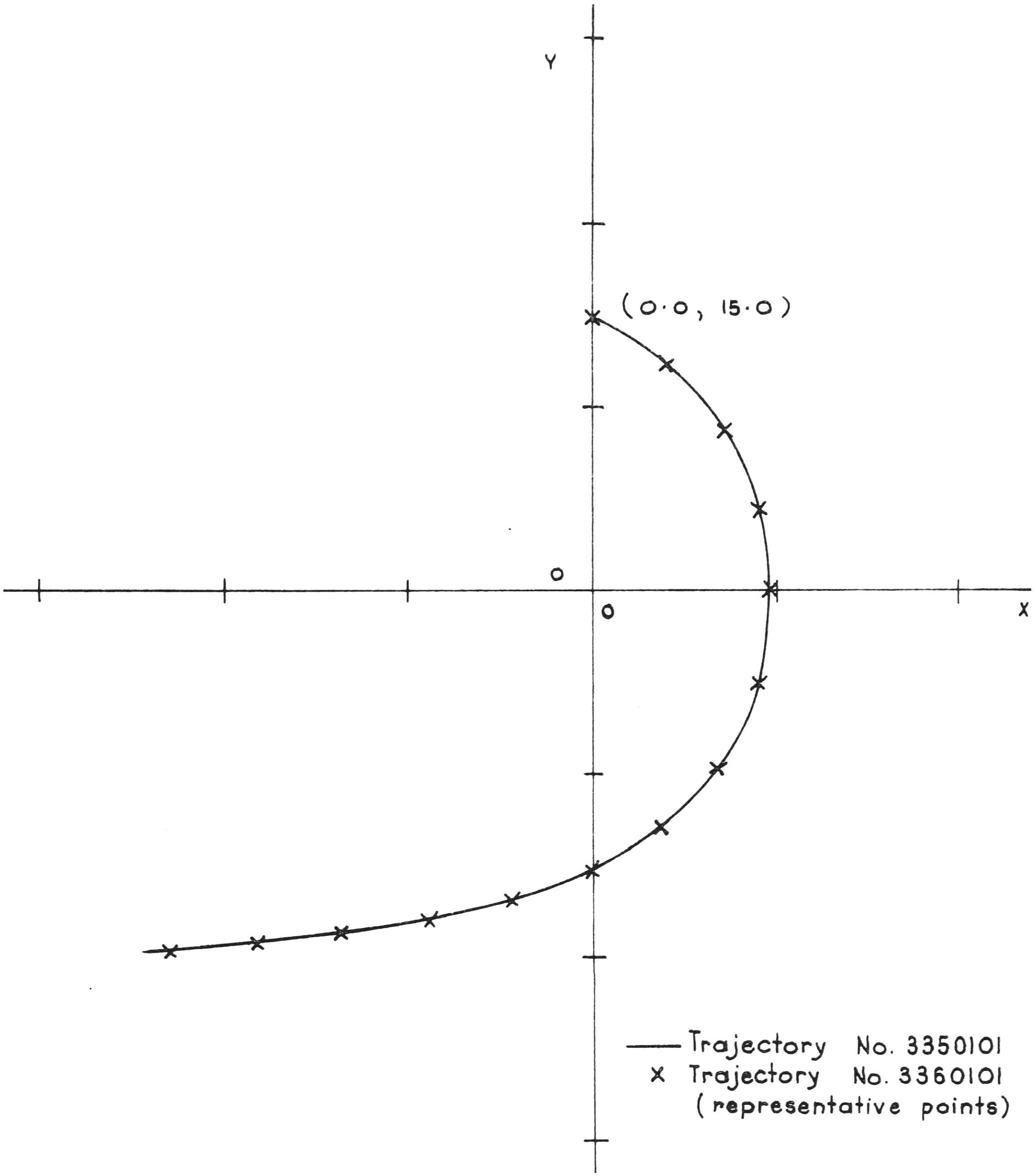

FIGURE 21 : A COMPARISON OF TWO COMPUTED PARTICLE TRAJECTORIES, WITH DIFFERENT CONDITIONS SPECIFIED AT THE STARTING POINT

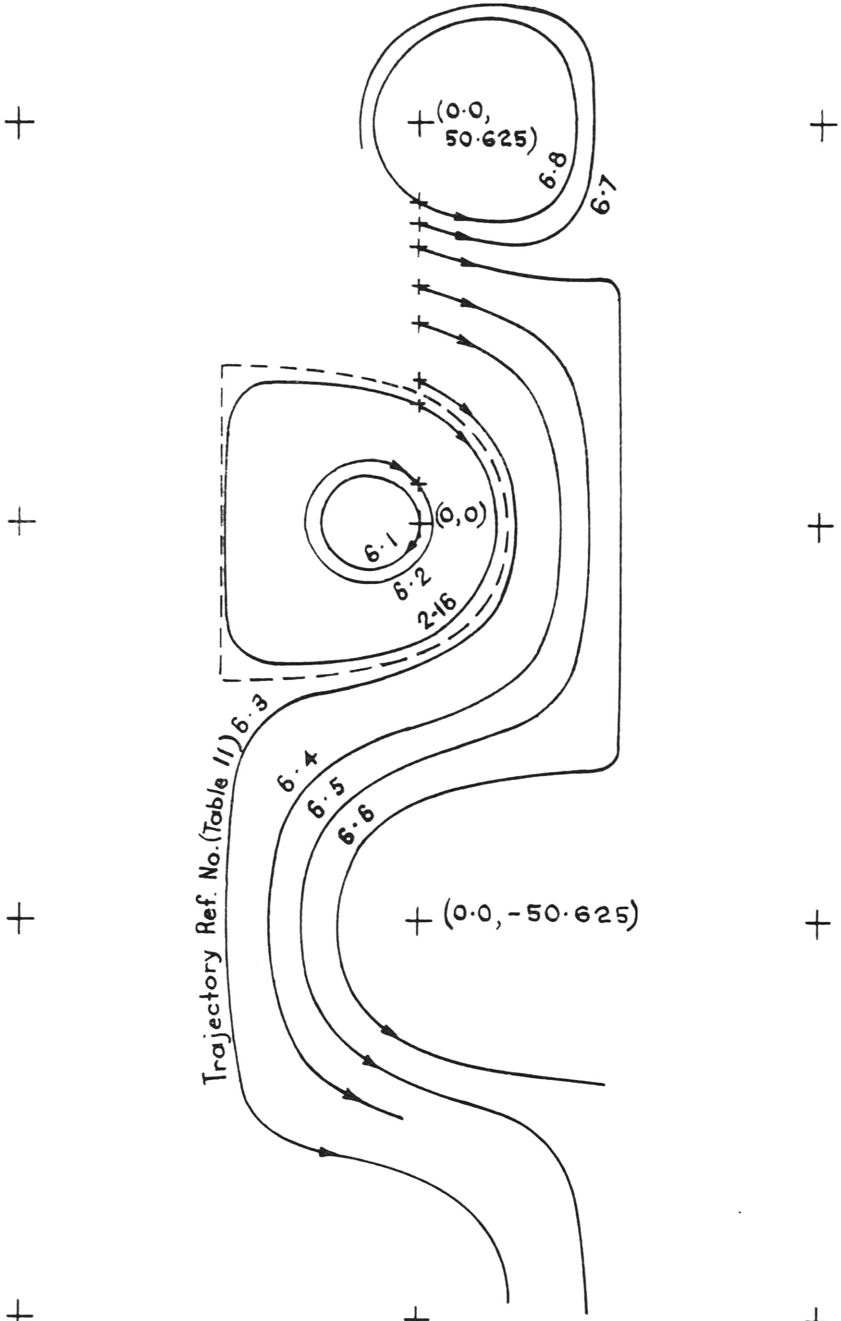

FIGURE 22: COMPUTED TRAJECTORIES OF A PARTICLE, WITH VARIOUS STARTING POINTS

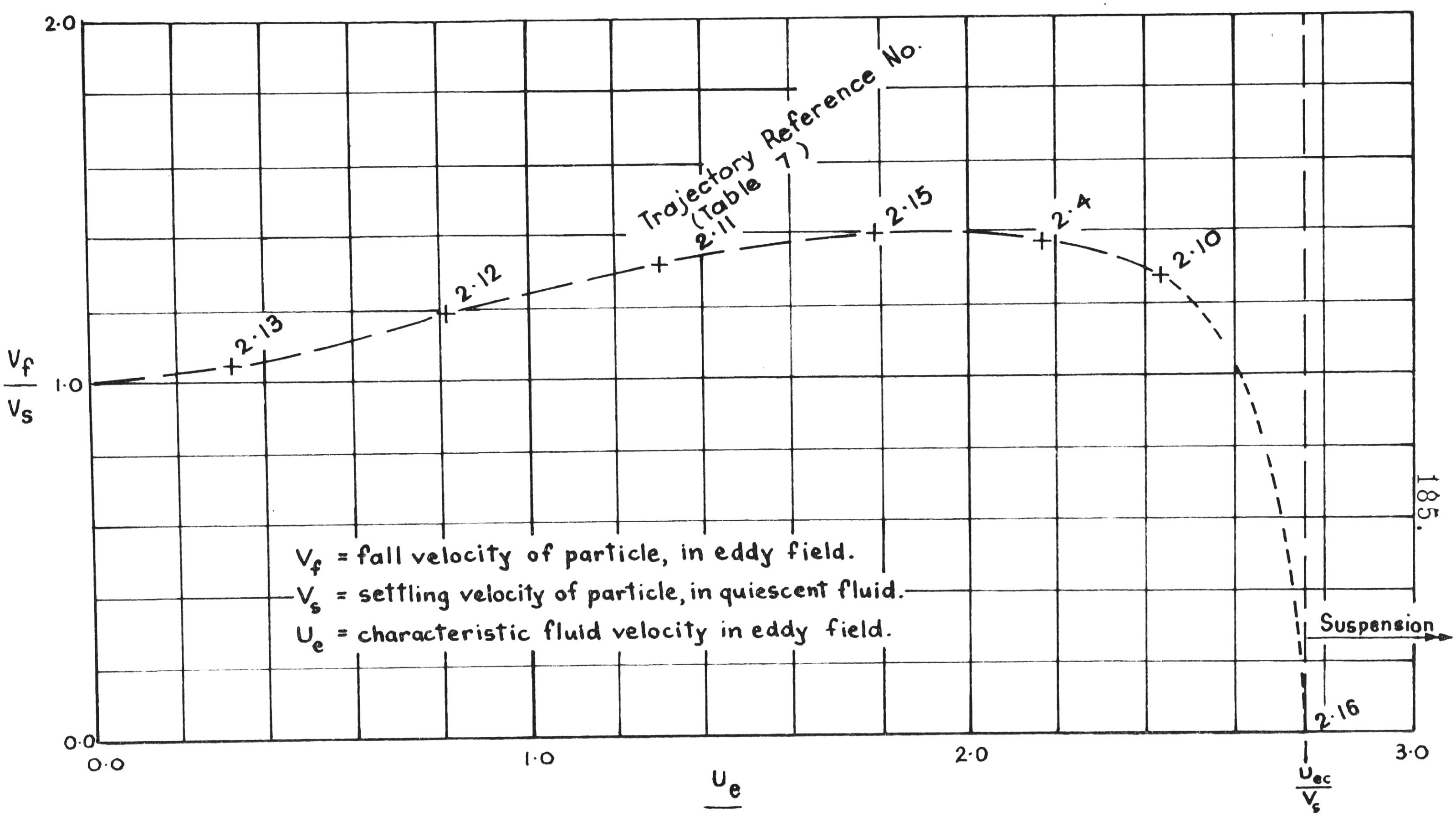

FIGURE 23 : THE FALL VELOCITY OF A PARTICLE FALLING THROUGH THE MODEL EDDY FIELD

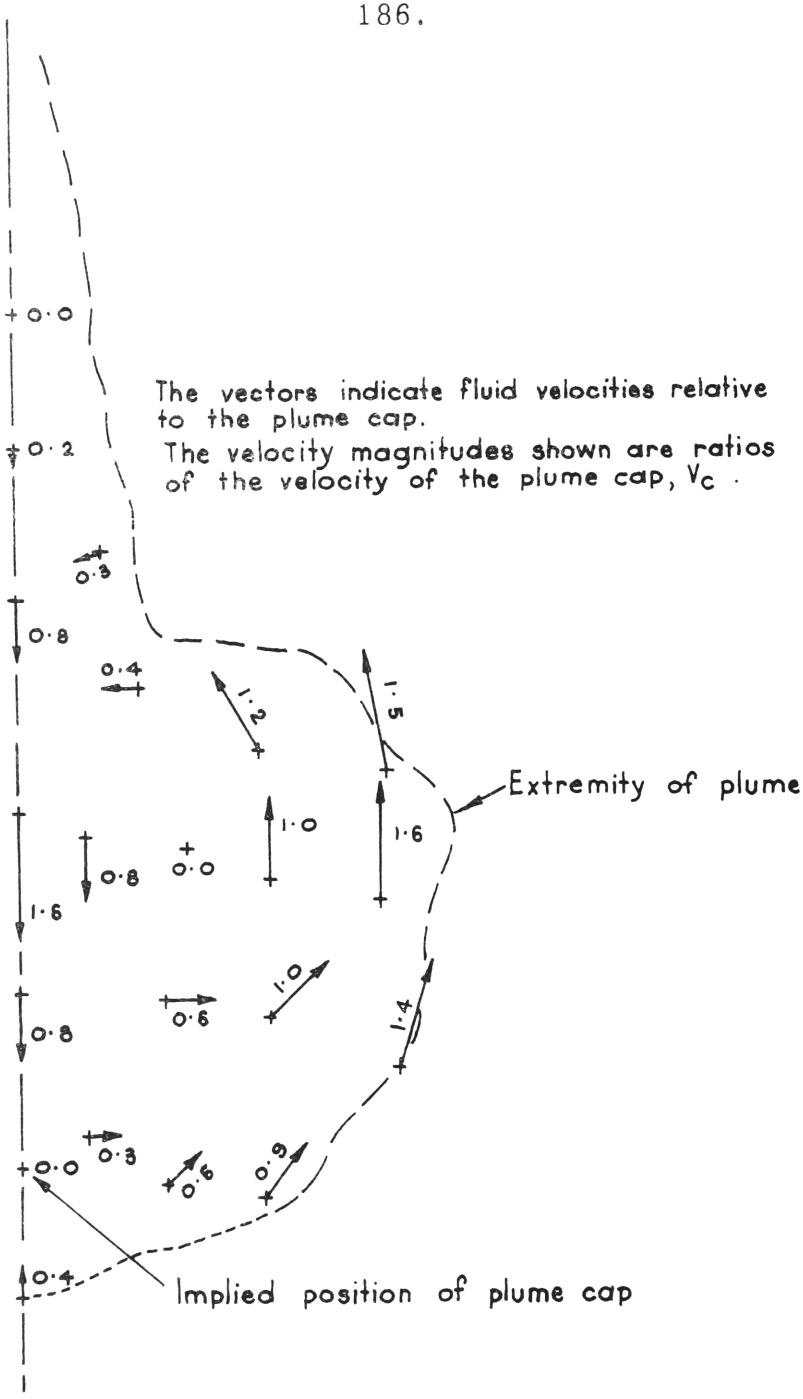

FIGURE 24: FLUID VELOCITIES WITHIN A TWO-DIMENSIONAL STARTING PLUME - FROM TSANG, REF (47).

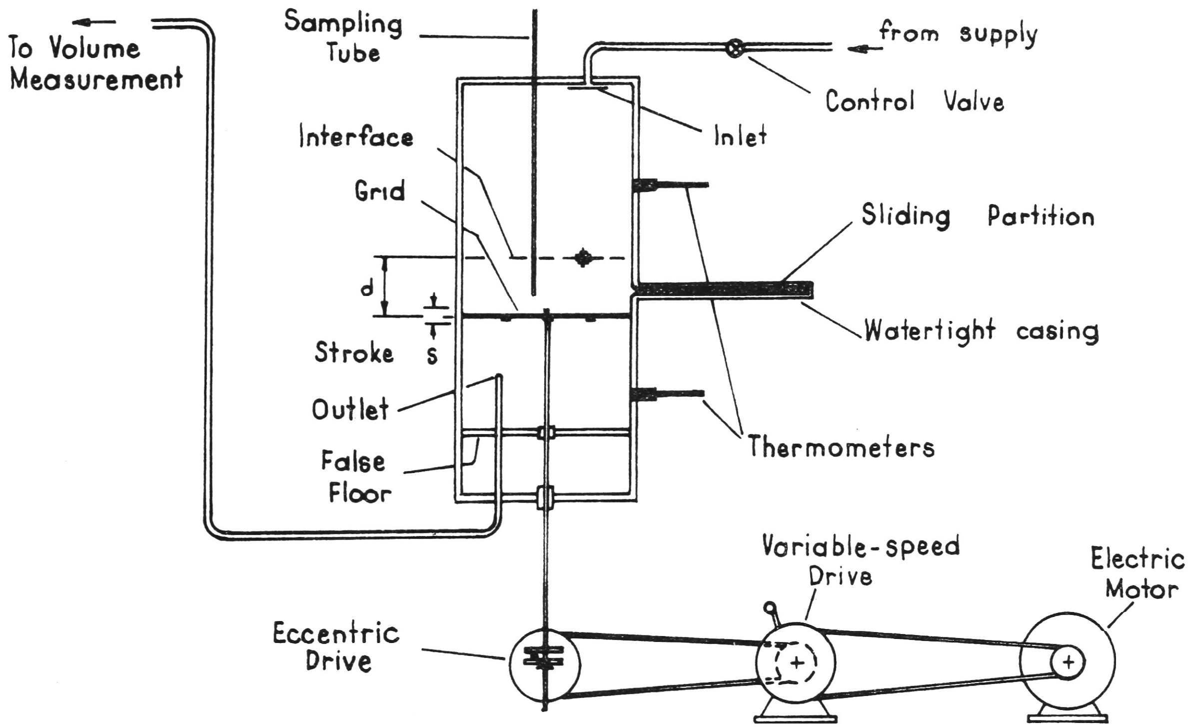

FIGURE 25 : EXPERIMENTAL APPARATUS FOR DETERMINATION OF RATES OF ENTRAINMENT ACROSS DENSITY DISCONTINUITIES

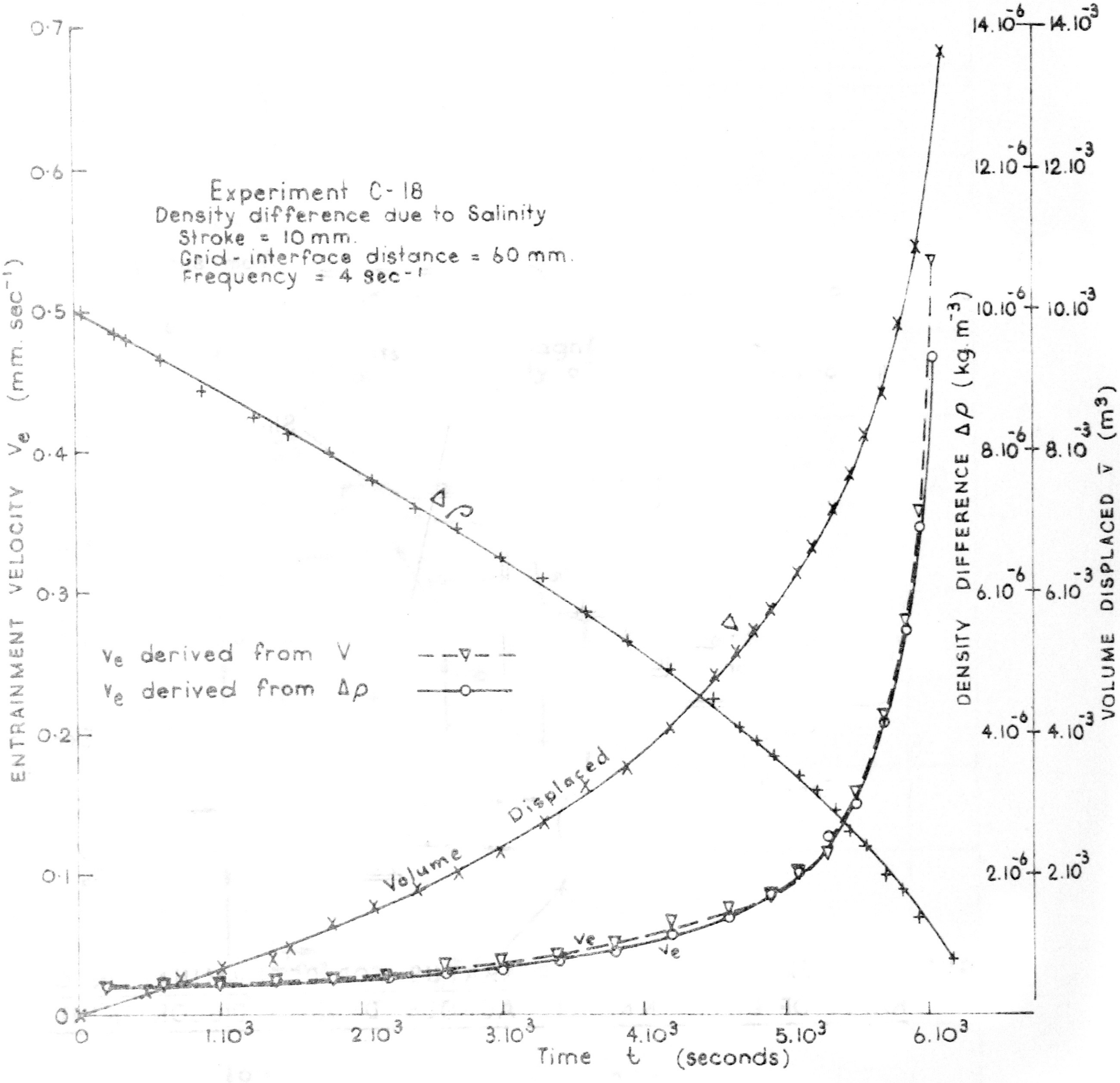

FIGURE 26: ENTRAINMENT VELOCITIES DETERMINED VOLUMETRICALLY AND DENSIMETRICALLY

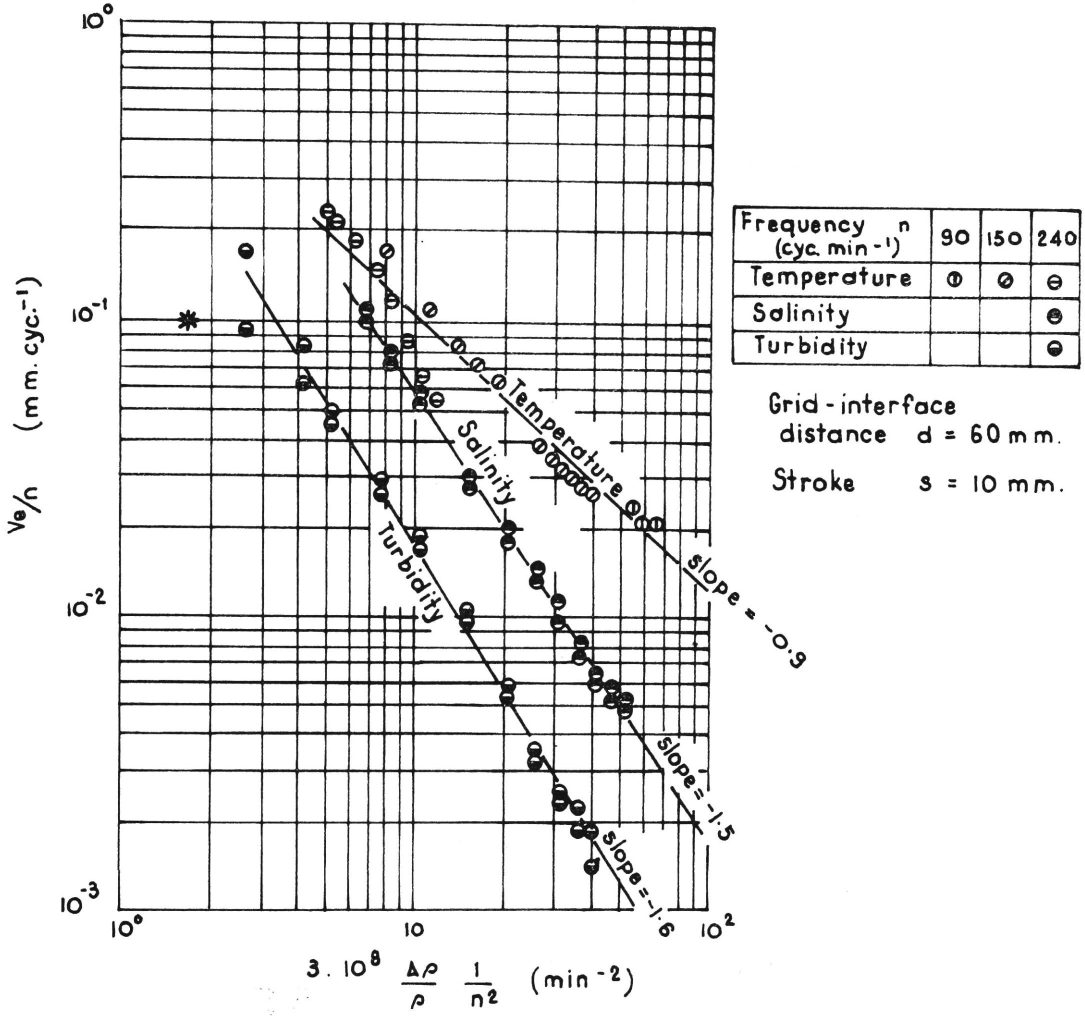

FIGURE 27 : ENTRAINMENT RATES FOR TEMPERATURE DIFFERENCES, SALINITY DIFFERENCES AND TURBIDITY

Table 1: Parameter Values in the Computations of Trajectories of Neutrally-Buoyant Particles in the Model Eddy Field

Trajectory Reference Number	Computation Number	Particle-Fluid Parameter PART = $\sqrt{gd^3}/\nu$	Gravitational Parameter GRAV = (s - 1.0)	Spacing of Eddy Centres XCNTR YCNTR	Starting Point XSTART	Starting Point YSTART	Starting Point TSTART	Starting Point KSTART	Characteristic Velocity in Eddy Field UEDDY	Step Limit STEP	Ordinate of Computed Trajectory after one circuit of Eddy Y1
1.1	4310101	1.1068	0.00	50.6250	0.0000	10.0000	0.0000	2	0.20	2.10^{-2}	10.0000
1.2	4300101	1.1068	0.00	50.6250	0.0000	15.0000	0.0000	2	0.20	2.10^{-2}	15.0000
1.3	4320101	1.1068	0.00	50.6250	0.0000	20.0000	0.0000	2	0.20	2.10^{-2}	20.0000
	4330101				-13.1597	17.3762	743.2387	1			
1.4	4270101	1.1068	0.00	5.0000	0.0000	1.5000	0.0000	2	0.20	2.10^{-3}	1.5000

The following parameter values are common to the computations tabulated above:

Added Mass Coefficient ADMASK = 0.5
Convergence Criterion DELSCR = 1.10^{-7}
Weighting Factor W = 2.0
Time Limit ITIME = 9
Punching Code KPUNCH = 1
IPUNCH = 20
IPRNT = 10

Table 2:- The Characteristics of the Experimental Standing Wave Systems - Wave Characteristics

Trajectory No.	Experiment No.	Length mm	Period sec	Amplitude mm	Water Depth mm	Dimensionless Parameters WLNG	WPER	WAMP	DPTH
1060101	W3	1460	0.968	13.5	630	506.0	45.5	4.68	218.5
1090101	W3	1460	0.968	13.5	630	529.0	46.8	4.89	228.0
1120101	W7	2000	1.167	60.0	760	1090.0	69.0	32.7	414.0
1250201	W8	1328	0.949	38.5	675	529.9	48.3	15.3	269.4
1260101	W8	1328	0.949	38.5	675	613.1	51.9	17.8	311.6
1270101	W8	1328	0.949	38.5	675	654.8	53.3	19.0	332.8
1280101	W8	1328	0.949	38.5	675	667.7	54.1	19.4	339.4

- Conditions at Starting Point

Trajectory No.	Coordinates (1) x_0 mm	y_0 mm	Dimensionless Parameters XSTART	YSTART	PHSE	UPTT	VPTT	Photographed by (d)
1060101	-96.6	-144.2	-33.5	-50.0	0.414(b)	0.133(b)	-0.156(b)	SSF
1090101	-50.6	-123.6	-18.3	-44.8	0.0(b)	0.310(b)	-0.120(b)	SSF
1120102	-392.0	-682.0	-213.5	-372.0	3.1416(b)	-0.220(b)	0.030(b)	N St2
1250201	(a)	(a)	- 79.7	-106.1	4.7124(b)	0.0(b)	- 0.076(c)	NSt1
1260101	(a)	(a)	- 67.0	-164.4	4.7124(b)	0.0(b)	-0.077(c)	NSt1
1270101	(a)	(a)	-103.5	-178.7	4.7124(b)	0.0(b)	-0.125(c)	NSt1
1280101	(a)	(a)	-147.4	- 48.8	4.7124(b)	0.0(b)	-0.070(c)	NSt1

(1) The origin of coordinates is: x=0 at a node of the wave system
y=0 at the undisturbed water level.

Notes:

(a) XSTART and YSTART were measured directly, from dimensionless plots of the experimental trajectory.

(b) estimated, from the experimental trajectory.

(c) equal to the (dimensionless) settling velocity of the particle in still water.

(d) SSF: Shackman Sequential-Frame camera.
NSt1: Nikon Camera and stroboscope, flash interval 0.1 seconds.
NSt2: " " " " " " 0.2 seconds.

Table 3: The Characteristics of the Experimental Particles.

Trajectory No.	Particle No.	Particle Characteristics: Still-Water Settling Velocity v_s mm. sec^{-1}	diameter d mm	density ratio s	Particle-Fluid Parameter PART=$\sqrt{gd^3}/\nu$	Gravitational Parameter GRAV=(s-1.0)	Added-mass coefficient ADMASK, k	Dimensional Ratios: $\frac{l}{L}=(s+k)d$ mm	$\frac{v}{V}=\sqrt{gd}$ mm. sec^{-1}	$\frac{t}{T}=(s+k)\sqrt{\frac{d}{g}}$ sec.
1060101	7	20.7	1.88	1.034	255.2	0.034	0.5	2.885	135.8	0.02125
1090101	12	12.5	1.82	1.017	243.0	0.017	0.5	2.760	133.6	0.02065
1120101	29	11.6	1.20	1.030	130.0	0.030	0.5	1.835	108.4	0.01695
1250201	36	9.7	1.66	1.013	235.37	0.013	0.5	2.506	127.4	0.01967
1260101	33	9.1	1.43	1.015	188.87	0.015	0.5	2.166	118.4	0.01830
1270101	35	14.3	1.32	1.032	168.26	0.032	0.5	2.028	113.9	0.01781
1280101	37	7.9	1.31	1.014	166.36	0.014	0.5	1.989	113.5	0.01753

Table 4: Comparison of the Computed and Experimentally-Determined Trajectories of Particles Falling through Waves.

Trajectory No.	Dimensionless Fall Velocity of Particle									Horizontal Excursions of Particle in Wave		
	In still water	In Wave				$\frac{V_c}{V_s}$	$\frac{V_e}{V_s}$	$\frac{V_c}{V_e}$		Computed	Experimental	$\frac{H_c}{H_e}$
		Computed		Experimental								
	V_s	V_c	n	V_e	n					H_c	H_e	
1060101	0.153	0.151	3	0.156	3	0.99	1.02	0.97		4.0	4.0	1.00
1090101	0.094	0.091	3	0.079	3	0.97	0.84	1.15		5.2	5.8	0.90
1120101	0.107	0.107	3	0.107	3	1.00	1.00	1.00		4.3	2.9	1.48
1250201	0.076	0.079	2	0.102	2	1.04	1.34	0.77		5.2	5.0	1.04
1260101	0.077	0.079	2	0.096	2	1.03	1.25	0.82		5.5	6.2	0.89
1270101	0.125	0.129	4	0.145	4	1.03	1.16	0.89		3.6	3.8	0.95
1280101	0.070	0.079	1	0.094	1	1.13	1.34	0.84		-	-	-

n = the number of wave periods over which the fall velocity has been calculated.

Expected page number is not in the original print copy.

Table 6: The Physical Spacing of Eddy Centres Corresponding to Certain Dimensionless Parameter Values.

Particle diameter d mm	Density ratio s	PART $= \frac{\sqrt{g d^3}}{\nu}$	GRAV $= (s - 1{\cdot}0)$	Dimensionless spacing of eddy centres					
				0.5000	10.6360	40.1780	50.6250	135.00	270.00
50.10^{-3}	2.00	1.1068	1.00	-	-	-	6.3mm	16.9mm	33.8mm
50.10^{-3}	2.65	1.1068	1.65	-	-	6.3mm	8.0mm	-	-
50.10^{-3}	11.40	1.1068	10.40	-	6.3mm	-	30.0mm	-	-
5.10^{-3}	2201	0.00234	2201	5.5mm	-	-	-	-	-

Table 7: Parameters in Computations of Particle Trajectories

Particle-Fluid Parameter PART = 1.1068
Gravitational Parameter GRAV = 1.00

Trajectory Reference Number	Computation Number	Characteristic Velocity UEDDY	Eddy Spacing XCNTR	Starting Point			Step Limit STEP	KSTART	IPRNT	IPUNCH	Remarks
				XSTART	YSTART	TSTART					
2.1	50101	0.000	135.00	0.0000	0.0000	0.0000	5.10^{-2}	2	25	200	Particle not suspended. $\frac{V_f}{V_s} = 1.00$
2.2	70101	0.135	135.00	0.0000	40.0000	0.0000	5.10^{-2}	2	25	200	Particle not suspended $\frac{V_f}{V_s} = 1.38$
	- 90101			7.9306	-34.6248	695.90	5.10^{-2}	1	25	200	
	-100101			-46.6597	-58.0083	0.0000	1.10^{-2}	1	25	200	
	-130101			-63.9470	-126.5874	0.0000	1.10^{-2}	1	25	200	
2.3	140102	0.400	50.6250	0.0000	15.0000	0.0000	2.10^{-2}	2	25	100	Particle suspended
2.4	140103	0.135	50.6250	0.0000	15.0000	0.0000	2.10^{-2}	2	25	100	Particle not suspended $\frac{V_f}{V_s} = 1.38$
2.5	160102	0.400	270.00	0.0000	80.0000	0.0000	1.10^{-1}	2	25	100	Particle suspended
2.6	170101	0.300	135.00	0.0000	40.0000	0.0000	5.10^{-2}	2	25	100	Particle suspended
2.7	190101	0.240	50.6250	0.0000	15.0000	0.0000	2.10^{-2}	2	25	100	Particle suspended
2.8	190102	0.320	50.6250	0.0000	15.0000	0.0000	2.10^{-2}	2	25	100	Particle suspended
2.9	200101	0.200	135.00	0.0000	40.0000	0.0000	5.10^{-2}	2	25	100	Particle suspended
	-230101			-36.2165	-44.6502	847.24	2.10^{-2}	1	25	100	
2.10	220101	0.150	50.6250	0.0000	15.0000	0.0000	2.10^{-2}	2	25	100	Particle not suspended $\frac{V_f}{V_s} = 1.28$
2.11	380101	0.080	50.6250	0.0000	15.0000	0.0000	2.10^{-2}	2	25	25	Particle not suspended $\frac{V_f}{V_s} = 1.32$
2.12	420101	0.050	50.6250	0.0000	15.0000	0.0000	2.10^{-2}	2	25	25	Particle not suspended $\frac{V_f}{V_s} = 1.19$

(continued)

Table 7 (cont'd.)

Trajectory Reference Number	Computation Number	Characteristic Velocity UEDDY	Eddy Spacing XCNTR	Starting Point			Step Limit STEP	KSTART	IPRNT	IPUNCH	Remarks
				XSTART	YSTART	TSTART					
2.13	430101	0.020	50.6250	0.0000	15.0000	0.0000	2.10^{-2}	2	25	25	Particle not suspended $\frac{V_f}{V_s} = 1.05$
	-440101			-7.7383	-52.6998	1054.30	2.10^{-2}	1	25	25	
2.14	450101	0.135	270.00	0.0000	80.0000	0.0000	2.10^{-2}	2	25	25	Particle not suspended $\frac{V_f}{V_s} = 1.38$
	-470101			-125.2601	-189.3791	3491.68	2.10^{-2}	1	25	25	
	-480101			-115.0718	-400.1977	4898.69	2.10^{-2}	1	25	25	
2.15	500101	0.110	50.6250	0.0000	15.0000	0.0000	2.10^{-2}	2	25	25	Particle not suspended $\frac{V_f}{V_s} = 1.40$
2.16	610101	0.170	50.6250	0.0000	15.0000	0.0000	2.10^{-2}	2	25	25	Particle suspended
	-620101			-24.5154	-6.0540	690.91	2.10^{-2}	1	25	25	
2.17	3400101	0.080	270.00	0.0000	80.0000	0.0000	2.10^{-2}	2	10	20	Particle not suspended $\frac{V_f}{V_s} = 1.34$
	-3410101			35.5070	4.4755	944.31	2.10^{-2}	1	10	20	
	-3420101			1.2088	-78.8433	1965.37	2.10^{-2}	1	10	20	
	-3430101			-45.0966	-115.5988	2638.72	2.10^{-2}	1	10	20	
	-3440101			-83.1833	-157.5186	3308.68	2.10^{-2}	1	10	20	
2.18	3500101	0.200	270.00	0.0000	80.0000	0.0000	2.10^{-2}	2	10	50	Particle suspended
	-3510101			42.3884	-47.6916	887.48	2.10^{-2}	1	10	50	
	-3520101			-76.0975	-88.6981	1727.32	2.10^{-2}	1	10	50	
	-3530101			-119.3368	-30.3446	2574.50	2.10^{-2}	1	10	50	
	-3540101			-104.8044	74.7311	3518.33	2.10^{-2}	1	10	50	
	-3550101			-6.0116	82.1554	4366.18	2.10^{-2}	1	10	50	

The following parameter values are common to the computations tabulated above:

Added Mass Coefft. ADMASK = 0.5
Convergence Criterion DELSCR = 1.10^{-7}
Weighting Factor W = 2.0
Punching Code KPUNCH = 1
Time Limit ITIME = 9

Table 8: Parameters in Computations of Particle Trajectories

Particle-Fluid Parameter PART = 1.1068
Gravitational Parameter GRAV = 1.65

Trajectory Reference Number	Computation Number	Characteristic Velocity UEDDY	Starting Point			KSTART	IPRNT	IPUNCH	Notes	Remarks
			XSTART	YSTART	TSTART					
3.1	2010101	0.17	0.0000	15.0000	0.0000	2	25	25		Particle not suspended.
3.2	2020101	0.22	0.0000	11.9000	0.0000	2	10	20	(1)	Particle not suspended.
3.3	3100101	0.25	0.0000	15.0000	0.0000	2	10	20		Particle not suspended.
3.4	3130101	0.30	0.0000	15.0000	0.0000	2	10	20		Incomplete. Suspension indicated.
3.5	3140101	0.27	0.0000	15.0000	0.0000	2	10	20		Particle suspended.
	- 3170101		-23.7245	-17.9401	356.6777	1	10	20		
	- 3180101		-24.4599	16.9100	730.5464	1	10	20		

Common Parameters:

Eddy Spacing XCNTR = 50.6250
YCNTR = 50.6250

Note (1): In 2020101 XCNTR = 40.1780
YCNTR = 40.1780

Added Mass Coefft. ADMASK = 0.5

Step Limit STEP = 2.10^{-2}

Convergence Criterion DELSCR = 1.10^{-7}

Weighting Factor W = 2.0

Punching Code KPUNCH = 1

Time Limit ITIME = 9

Table 9: Parameters in Computations of Particle Trajectories

Particle-Fluid Parameter PART= 1.1068
Gravitational Parameter GRAV = 10.40

Trajectory Reference Number	Computation Number	Characteristic Velocity UEDDY	Starting Point XSTART	Starting Point YSTART	Starting Point TSTART	KSTART	IPRNT	IPUNCH	Notes	Remarks
4.1	2030101	0.55	0.0000	3.1500	0.0000	2	10	20	(1)	Particle not suspended
4.2	3300101	1.70	0.0000	-15.0000	0.0000	1	10	20		Partial Trajectory - suspension indicated
4.3	3310101	1.60	0.0000	-15.0000	0.0000	1	10	20		Partial Trajectory - suspension not indicated
4.4	3320101	1.65	0.0000	-15.0000	0.0000	1	10	20		Partial Trajectory - suspension indicated
4.5	3330101	1.625	0.0000	-15.0000	0.0000	1	10	20		Partial Trajectory - suspension not indicated
4.6	3340101	1.64	0.0000	15.0000	0.0000	1	10	20		Particle not suspended
4.7	3360101	1.65	0.0000	15.0000	0.0000	2	10	20		Particle not suspended
4.8	3370101-	1.70	0.0000	15.0000	0.0000	2	10	20		Particle suspended
	-3380101		-24.5942	14.1944	100.42	1	10	20		

Common Parameters:

Eddy Spacing XCNTR = 50.6250
YCNTR = 50.6250

Note (1): In 2030101 XCNTR=10.6360
YCNTR= 10.6360

Added Mass Coefft. ADMASK = 0.5

Step Limit STEP=2.10^{-2}

Convergence Criterion DELSCR=1.10^{-7}

Weighting Factor W = 2.0

Punching Code KPUNCH = 1

Time Limit ITIME = 9

Table 10: Parameters in Computations of Particle Trajectories

Particle-Fluid Parameter PART = 0.00234

Gravitational Parameter GRAV = 2200.0

Trajectory Reference Number	Computation Number	Characteristic Velocity UEDDY	Starting Point			KSTART	IPRNT	IPUNCH	Notes	Remarks
			XSTART	YSTART	TSTART					
5.1	3600101	1.50	0.0000	0.1500	0.0000	2	10	20		Particle suspended
	-3610101		-0.1906	0.0347	0.6628	1	10	20		
5.2	3620101	1.20	0.0000	0.1500	0.0000	2	5	5		Incomplete. Suspension indicated.
	-3630101		-0.1368	-0.1509	0.5607	1	5	5		
5.3	3640101	1.00	0.0000	0.1500	0.0000	2	5	5		Incomplete. Suspension indicated.
	-3650101		-0.0737	-0.1654	0.5514	1	5	5		
5.4	3660101	0.80	0.0000	0.1500	0.0000	2	5	10		Particle suspended.
	-3670101		0.0338	-0.1315	0.4805	1	5	10		
	-3690101		-0.2073	-0.1749	0.9838	1	5	10		
	-3730101		-0.2423	-0.0830	1.4302	1	5	10		
5.5	3680101	0.60	0.0000	-0.1503	0.0000	1	5	10		Partial Trajectory. Suspension not indicated.
5.6	3700101	0.60	0.0000	0.1500	0.0000	2	5	10		Particle not suspended
	-3710101		0.0488	-0.1104	0.5238	1	5	10		

Common Parameters:

Eddy Spacing XCNTR = 0.5000

YCNTR = 0.5000

Added Mass Coefft ADMASK = 0.5

Step Limit STEP = 2.10^{-3}

Convergence Criterion DELSCR = 1.10^{-7}

Weighting Factor W = 2.0

Punching Code KPUNCH = 1

Time Limit ITIME = 9.

Table 11: Parameters in Computations of Particle Trajectories

Particle-Fluid Parameter PART = 1.1068
Gravitational Parameter GRAV = 1.00
Characteristic Fluid Velocity UEDDY = 0.17
Spacing of Eddy Centres XCNTR = 50.6250

Trajectory Reference Number	Computation Number	Starting Point XSTART	Starting Point YSTART	Starting Point TSTART	KSTART	IPRNT	IPUNCH
6.1	3820101	0.0000	0.0000	0.0000	2	10	20
	- 3830101	-10.2438	4.7479	432.68	1	10	20
	- 3840101	- 6.7784	-6.1305	836.96	1	10	20
6.2	3010101	0.0000	5.0000	0.0000	2	25	25
	- 3020101	- 12.7475	5.2711	496.60	1	25	25
6.3	3800101	0.0000	18.0000	0.0000	2	10	20
	- 3810101	-22.5738	-69.1607	717.63	1	10	20
6.4	3070101	0.0000	25.3125	0.0000	2	10	20
6.5	3080101	0.0000	30.0000	0.0000	2	10	20
	- 3090101	- 1.5103	-70.6515	825.85	1	10	20
6.6	3110101	0.0000	35.0000	0.0000	2	10	20
	- 3120101	24.5658	30.4343	386.55	1	10	20
	- 3150101	25.2856	0.7614	747.85	1	10	20
	- 3160101	24.5289	-30.4813	1120.8	1	10	20
	- 3190101	2.1594	-34.1658	1487.5	1	10	20
6.7	3200101	0.0000	38.0000	0.0000	2	10	20
6.8	3030101	0.0000	40.0000	0.0000	2	10	20
2.16	610101	0.0000	15.0000	0.0000	2	25	25
	-620101	-24.5154	-6.0540	690.91	1	25	25

Step Limit STEP = 2.10^{-2}
Added Mass Coefft ADMASK = 0.5
Convergence Criterion DELSCR = 1.10^{-7}
Weighting Factor W = 2.0
Punching Code KPUNCH = 1
Time Limit ITIME = 9

APPENDIX I

A Hypothesis Concerning Lift Forces on Spinning Particles

A component of force acting on an immersed body, in a direction perpendicular to that of the motion, relative to the body, of the surrounding fluid, is termed a lift force.

If the fluid is assumed to be inviscid, the Kutta-Joukowsky Circulation Theorem leads to an expression for the lift force acting on unit length of a long cylindrical body immersed in a one-dimensional flow:

$$F_L = \Gamma \rho_f u_f \tag{I.1}$$

where F_L = the lift force, per unit length of the cylinder

Γ = the circulation around the cylinder

ρ_f = the density of the fluid

u_f = the velocity of the fluid

The circulation Γ is defined as :

$$\Gamma = \oint v_t . ds \tag{I.2}$$

where v_t = the tangential component of fluid velocity, in the direction of the element ds of the boundary of the cylinder

and the symbol $\oint$ implies that the integration is to be carried out around the boundary of the cylinder.

It is known that lift forces will occur in viscous fluids, under appropriate circumstances:

Lewitt (I. 2) has described the voyages of the Flettner Rotor Ships, which were propelled by the transverse forces which acted on cylinders rotating (about vertical axes) in an airstream (the wind).

Chepil (I. 1) has described experiments in which experimental determinations were made of the pressure distributions on spherical particles immersed in a fluid in which a velocity gradient existed. The particles were fixed in position adjacent to the wall of a wind tunnel. The measurements indicated that a lift force was exerted on the particles.

It is accordingly evident that, in a viscous fluid, lift forces will occur:

(i) when a body is rotated, in a uniform flow, and

(ii) when a non-rotating body is situated in a flow in which a velocity gradient exists.

Both these situations are analogous to the existence of circulation in an inviscid fluid, as $\oint v_t . ds$ would be expected to be non-zero in each case. Rouse (I. 3) has pointed out that experimental determination (by Betz) of lift forces on cylinders rotating in viscous fluids has indicated that the extension of the circulation concept to viscous fluids yields results which are (at worst) of the correct order of magnitude.

This extension of the concept of circulation will now be applied in the examination of lift forces acting on a circular cylinder immersed in a flow in which a velocity gradient exists. The cylinder is assumed to be placed within the fluid with its axis perpendicular to the direction of the flow, which is assumed to be steady and two-dimensional, a velocity gradient existing (only) in the direction perpendicular to that of the axis of the cylinder. The cylinder is assumed to be free to rotate about its own axis - that is, to spin.

The variation in fluid velocities across the cylinder will impart to the cylinder a spinning motion, and the angular velocity (spin velocity) of the cylinder will attain an equilibrium value. The tangential velocity of the surface of the cylinder will be invariant, in magnitude and (angular) sense, from point to point on the surface of the cylinder. Accordingly, a given element of the cylinder surface will, in general, possess a non-zero velocity relative to the fluid adjacent to that element of the surface. At the condition of equilibrium, the net torque on the cylinder, arising from the drag forces associated with such relative velocities, will be zero.

The presence of the cylinder will cause the retardation of the fluid, in those regions in which the fluid velocity tends to be greater than the tangential velocity of the surface of the cylinder. Accordingly, the cylinder can be considered to impart to the fluid a "circulation" in the sense opposite to that of the rotation of the cylinder. At the condition of equilibrium, the net "circulation" will be zero, and hence it is to be expected that the net lift force on the cylinder will be zero.

The argument may be extended to the case of a sphere in a two-dimensional flow if the sphere be considered as an assembly of elemental cylinders of varying diameters: if the sphere is so small that the velocity gradient which would exist in the undisturbed flow may be considered invariant with distance across the diameter of the sphere, then it would be expected that the equilibrium angular velocity of a given elemental cylinder would be dependent upon the velocity gradient rather than upon the diameter of the cylinder. Under these circumstances, all the elemental cylinders comprising the sphere would have a single value of equilibrium angular velocity, and this would be the angular velocity of the sphere. Then, as the above argument indicates that the lift force on each of the elemental cylinders will be zero, it is expected that the lift force on the sphere will also be zero.

Young (I. 5) has described experiments involving the determination of the lift and drag force components acting on a spherical particle of nylon, initially resting on the bottom of a glass tube in which water was flowing. It was observed that the lift force apparently decreased sharply, once the particle had ceased to be in contact with the bottom of the tube. Having lifted clear of the rigid surface (that is, the bottom of the tube) the particle would then fall back to that surface, a "hopping" motion resulting.

If the reduction in the lift force component were due to the reduced steepness of the velocity gradient outside the region which is immediately adjacent to the rigid surface, it would be expected that the particle would tend to approach an equilibrium position in which the velocity gradient was such that the lift force would be of just sufficient magnitude to balance the effective weight of the particle. The reported "hopping" motion is consistent, on the other hand with the hypothesis that a reduction in the lift force occurs as a result of the acquisition by the particle of a spinning motion. This spinning motion (induced by the velocity gradient within the fluid), and the consequent reduction in the lift force, would persist until the particle again came into contact with the rigid surface. The spinning motion would then be substantially arrested by mechanical friction, and the magnitude of the lift force would be restored to the value which applied at the start of the "hop". Such a hypothesis is, however, at variance with the conclusions of Rubinow and Keller (I. 4), who have analysed the forces acting on a spinning sphere moving in a viscous fluid.

References Cited in Appendix I

(I. 1) Chepil W.S. "The Use of Spheres to Measure Lift and Drag on Wind-eroded Soil Grains" Soil Science Soc. of America, Proc. v. 25 1961 p. 243-245.

(I. 2) Lewitt E.H. "Hydraulics and the Mechanics of Fluids" Sir Isaac Pitman and Sons Ltd. London, 9th ed. 1956.

(I. 3) Rouse H. "Engineering Hydraulics" Rouse H. ed., John Wiley and Sons Inc. New York U.S.A. 1950.

(I. 4) Rubinow S.I., Keller J.B. "The Transverse Force on a Spinning Sphere Moving in a Viscous Fluid" J. of Fluid Mechanics v. 11 1961 pt. 3 p. 447-459.

(I. 5) Young D.F. "Drag and Lift on Spheres within Cylindrical Tubes" American Soc. of Civil Engineers Proc. v. 86 (J. of Hydraulics Divn.) n. HY6 June 1960 p. 47-57.

APPENDIX II

THE DRAG FORCE COEFFICIENT FOR A SPHERICAL PARTICLE

The values assigned to the dimensionless drag force coefficient C_D in Equation (2.8) - p. 31 - are based on the following salient values, which conform to the relationship presented by Rouse (II. 1;p. 122) for the case of a spherical particle:

REYNOLDS NUMBER $\mathbb{R} = \frac{u_{rel} d}{\nu}$	DRAG FORCE COEFFICIENT C_D
$< 10^{-1}$	$24.0/\mathbb{R}$
10^{-1}	240.0
10^{0}	25.0
10^{1}	4.2
10^{2}	1.1
10^{3}	0.45
$4 . 10^{3}$	0.40
10^{4}	0.42
10^{5}	0.50
$> 10^{5}$	0.50

Reynolds Number $\mathbb{R} = \frac{u_{rel} d}{\nu}$

where u_{rel} = the velocity of the fluid relative to the particle

d = the particle diameter

ν = the kinematic viscosity of the fluid

Reference: (II. 1) Rouse H., "Engineering Hydraulics" Rouse H. ed., John Wiley and Sons Inc. New York, U.S.A. 1950.

For intermediate values of Reynolds Number within the range $10^{-1} < \mathbb{R} < 10^{5}$, the corresponding values of the drag force coefficient are interpolated, on the assumption that a plot of log C_D against log $\mathbb{R}$ will consist of a series of straight lines, joining points with coordinates corresponding to the values tabulated above.

The relationship between Reynolds Number and the drag force coefficient is shown graphically in Figure II. 1.

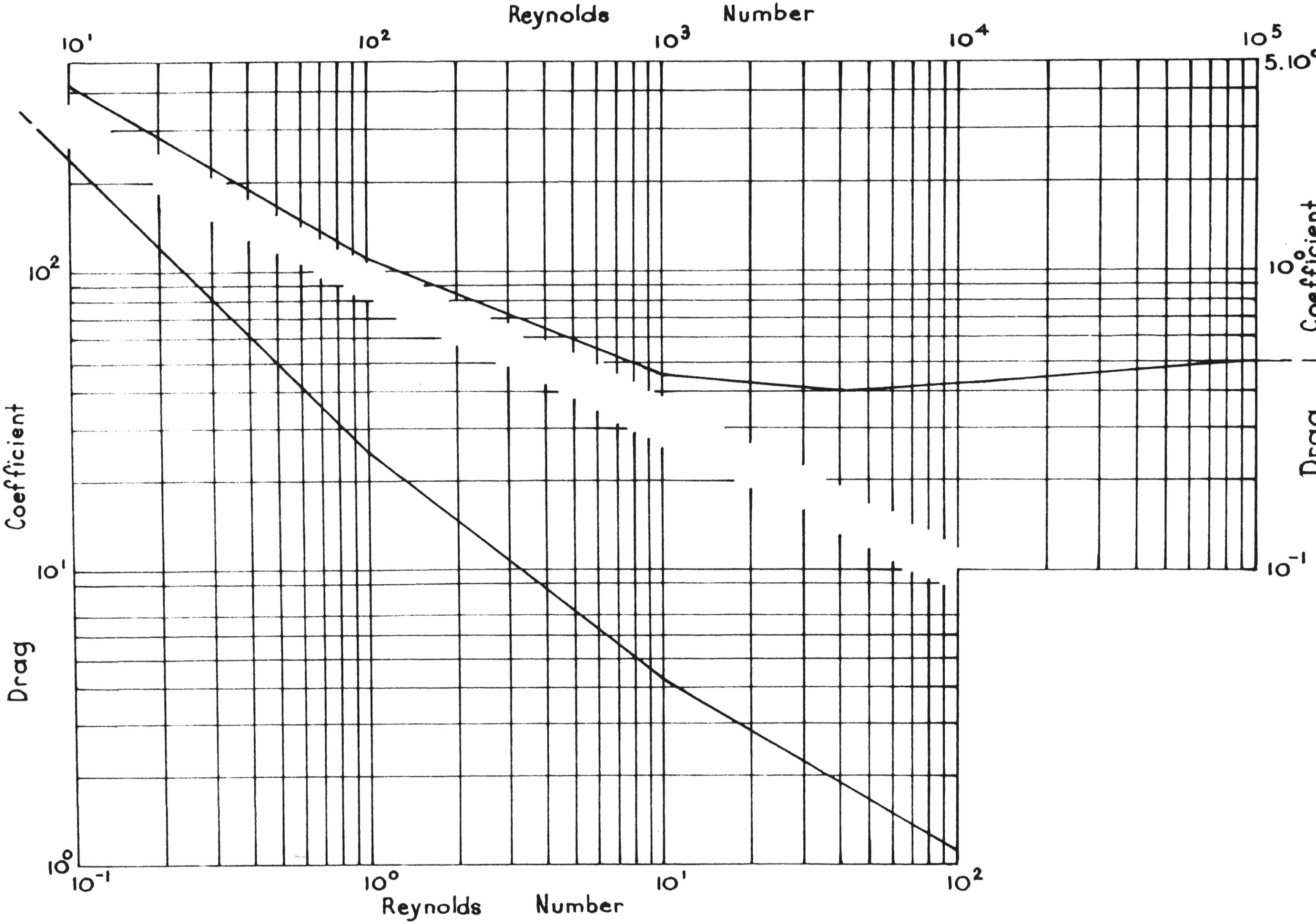

FIGURE II.1 : THE ASSUMED RELATIONSHIP BETWEEN REYNOLDS NUMBER AND THE DRAG COEFFICIENT FOR A SPHERICAL PARTICLE

APPENDIX III

The FORTRAN Computer Program for the Computation of the Trajectory of a Particle within the Model Eddy Field.

The sequence of operations within the program is described in Chapter 4.

This Appendix contains the following:

(v) Results of Particle-Trajectory Computation 4300101 p. III. 37-III. 39
(Position Coordinates only of computed points,
reproduced from the original printed output).

The FORTRAN Program for the Computation of the Trajectory of a Particle within the Model Eddy Field.

```
      IMPLICIT REAL*8(A-G,O-Z)
      LOGICAL DROP
      DIMENSION UEDDS(5)
      COMMON /COMM/XCNTR,YCNTR,UEDDY,PART,RNO,CD,FDRX,FDRY,UFL,VFL
      COMMON FFAX,FFAY,CONST1
      DATA NREAD/1/,NPUNCH/2/,NWRITE/3/
      WRITE (NWRITE,250)
  250 FORMAT ('1 THIS HAS BEEN RUN ON DECK NUMBER 6. ')
      READ (NREAD,200) IDENT,NSET,ITIME
  200 FORMAT (3I10)
      CALL TEME(ITIME,DROP)
      DO 999 NJ=1,NSET
      IDENS = (10000*IDENT)+(100*NJ)
      READ (NREAD,204) KSTART,KPUNCH
  204 FORMAT (2I10)
      READ (NREAD,207) XSTART,YSTART
  207 FORMAT (2D30.18)
      READ (NREAD,208) TSTART
  208 FORMAT (D30.18)
      READ (NREAD,202) PART,STEP,DELSCR,NSTEP,IPRNT,IPUNCH
  202 FORMAT (D20.4,D10.2,D10.2,I10,I10,I10)
      READ (NREAD,201) XCNTR,YCNTR,GRAV,ADMASK,W
  201 FORMAT (5D15.4)
      CONST1 = 1.00D+00+(GRAV/(1.00D+00+ADMASK))
      READ (NREAD,203) NV,(UEDDS(NN),NN=1,NV)
  203 FORMAT (I10,5D10.2)
      WRITE (NWRITE,223) IDENSS,NJ,NSET,IDENT
  223 FORMAT ('1 INPUT DATA FOR DATA SET ',I10,'  - THIS IS SET NUMBER '
     1,I5,' OF ',I5,' SET/S TO BE READ IN RUN ',I5)
      WRITE (NWRITE,224) PART,XCNTR,YCNTR,GRAV,XSTART,YSTART,TSTART
  224 FORMAT (///'  PARTICLE PARAMETER ',1PD20.8,///'  SPACING OF EDDY C
     1ENTRES - X ',D15.5,//27X,' Y ',D15.5,///'  GRAVITATIONAL PARAMETER
     2 ',D15.5,///'  STARTING POINT  -  X ',D30.18,//20X,' Y ',D30.18,//
     3'  STARTING TIME ',7X,D30.18)
      WRITE (NWRITE,225) NSTEP,STEP,DELSCR,ADMASK,W
  225 FORMAT (//'  NUMBER OF STEPS ',I10,///'  STEP LIMIT ',1PD10.2,///'
     1  CONVERGENCE CRITERION ',D10.2,///'  ADDED MASS COEFFICIENT ',0PD
     210.2,///'  WEIGHTING FACTOR ',1PD10.2)
      IF (KSTART.NE.1) GO TO 7
    6 READ (NREAD,205) UPTT,VPTT
  205 FORMAT (D30.18,D30.18)
```

```
      WRITE (NWRITE,214) UPTT,VPTT
  214 FORMAT (//'  PARTICLE VELOCITY COMPONENTS AT STARTING POINT HAVE B
     1EEN READ IN.    UPTT '.D25.18,/' ',69X,' VPTT ',D25.18)
      GO TO 8
    7 WRITE (NWRITE,215)
  215 FORMAT (//'  PARTICLE VELOCITY COMPONENTS WILL BE SET EQUAL TO THE
     1 FLUID VELOCITY COMPONENTS AT THE STARTING POINT. ')
    8 CONTINUE
      WRITE (NWRITE,212) (UEDDS(NN),NN=1,NV)
  212 FORMAT (//'  VELOCITY PARAMETERS ',D10.4,/(22X,D10.4))
      WRITE (NWRITE,213) IPRNT,IPUNCH
  213 FORMAT (//'  COORDINATES AND VELOCITIES ARE PRINTED FOR EACH OF TH
     1E FIRST  50 COMPUTED POINTS, AND THEN AFTER EVERY ',I5,' POINTS. '
     2//'  IF KPUNCH IS SET NE 0, A CARD IS PUNCHED AFTER EVERY ',I5,' C
     3OMPUTED POINTS. ')
      WRITE (NWRITE,226) KSTART,KPUNCH,ITIME
  226 FORMAT (////'  STARTING CODE  KSTART ',I5,'  - EQUALS 1 IF PARTICL
     1E VELOCITY COMPONENTS AT STARTING POINT ARE TO BE READ IN. '//'  P
     2UNCHING CODE  KPUNCH ',I5,'  - EQUALS 0 IF NO CARD OUTPUT IS REQUI
     3RED. '//'  TIME LIMIT PARAMETER  ITIME ',I5)
      DO 989 NU=1,NV
      IDENSS = IDENS+NU
      UEDDY = UEDDS(NU)
      WRITE (NWRITE,221) IDENSS,UEDDY
  221 FORMAT ('1'//////'  START OF RESULTS FOR DATA SUBSET ',I10,///////
     1'  VELOCITY PARAMETER  ',D12.5)
      CALL VELID
      IF (KPUNCH.EQ.0) GO TO 19
      WRITE (NPUNCH,230) PART,UEDDY,XCNTR,YCNTR,IDENSS
  230 FORMAT (D20.8,D10.3,2D20.8,I10)
      WRITE (NPUNCH,231) XSTART,YSTART,TSTART,IDENSS
  231 FORMAT (3D20.8,10X,I10)
      WRITE (NPUNCH,232) STEP,DELSCR,GRAV,W,IPUNCH,ADMASK,IDENSS
  232 FORMAT (4D10.2,I10,D10.2,10X,I10)
   19 CONTINUE
      IF (UEDDY.EQ.0.00D+00) GO TO 21
      DTBAS = STEP/UEDDY
      IF ((XCNTR/YCNTR).LT.1.00D00) DTBAS = DTBAS*XCNTR/YCNTR
      GO TO 22
   21 DTBAS = DSQRT(2.00D+00*STEP)
   22 DTBAS = DABS(DTBAS)
      TIM = TSTART
      NPAGE = 1
      NLINE = 0
      KOUNT = IPRNT
      NCARD = 0
      NTR = 0
```

```
      CALL VEL(XSTART,YSTART,TSTART)
      UFLT = UFL
      VFLT = VFL
      IF (KSTART.NE.2) GO TO 10
      UPTT = UFL
      VPTT = VFL
   10 CONTINUE
      CALL DRAG(UFLT,VFLT,UPTT,VPTT)
      XT = XSTART
      YT = YSTART
      XTO = XSTART
      YTO = YSTART
      WMSUM = 0.00D+00
      A = 1.00D+00
      FXSIGO = (FDRX+FFAX)*DSIGN(A,UPTT)
      FYSIGO = (FDRY+FFAY)*DSIGN(A,VPTT)
      DO 987 NL = 1,NSTEP
      IF (NL.EQ.1) GO TO 405
      IF (NL.LE.50) KOUNT = IPRNT
   11 NTR = 1
      DT = DTBAS
      IF (UPTT.NE.0.0D00) DT=DABS(STEP/UPTT)
      IF ((DABS(VPTT)).GT.(DABS(UPTT))) DT = DABS(STEP/VPTT)
      FXT = FDRX+FFAX
      FYT = FDRY+FFAY
   12 TEM = TIM+DT
      ACCX = FXT
      ACCY = FYT-GRAV
      D1X = UPTT*DT+0.50D00*ACCX*DT*DT
      D1Y = VPTT*DT+0.50D00*ACCY*DT*DT
      IF ((D1X**2+D1Y**2).GT.(STEP**2)) GO TO 800
      X1 = XT+D1X
      Y1 = YT+D1Y
      UPT1 = UPTT+ACCX*DT
      VPT1 = VPTT+ACCY*DT
   14 CALL VEL(X1,Y1,TEM)
      UFL1 = UFL
      VFL1 = VFL
      CALL DRAG(UFL1,VFL1,UPT1,VPT1)
      FX1 = FDRX+FFAX
      FY1 = FDRY+FFAY
      FX = (W*FXT+FX1)/(W+1.0D00)
      FY = (W*FYT+FY1)/(W+1.0D00)
      ACCX = FX
      ACCY = FY-GRAV
      D2X = UPTT*DT+0.50D00*ACCX*DT*DT
      D2Y = VPTT*DT+0.50D00*ACCY*DT*DT
      IF ((D2X**2+D2Y**2).GT.(STEP**2)) GO TO 800
```

```
      X2 = XT+D2X
      Y2 = YT+D2Y
      UPT2 = UPTT+ACCX*DT
      VPT2 = VPTT+ACCY*DT
      CALL VEL(X2,Y2,TEM)
      UFL2 = UFL
      VFL2 = VFL
      CALL DRAG(UFL2,VFL2,UPT2,VPT2)
      FX2 = FDRX+FFAX
      FY2 = FDRY+FFAY
   16 FX = (FXT+FX2)/2.0D+00
      FY = (FYT+FY2)/2.0D+00
      ACCX = FX
      ACCY = FY-GRAV
      D3X = UPTT*DT+0.50D00*ACCX*DT*DT
      D3Y = VPTT*DT+0.50D00*ACCY*DT*DT
      IF ((D3X**2+D3Y**2).GT.(STEP**2)) GO TO 800
      X3 = XT+D3X
      Y3 = YT+D3Y
      UPT3 = UPTT+ACCX*DT
      VPT3 = VPTT+ACCY*DT
      CALL VEL(X3,Y3,TEM)
      UFL3 = UFL
      VFL3 = VFL
      IF (NTR.EQ.1) GO TO 17
      DELXY = DSQRT((D3X-D2X)**2+(D3Y-D2Y)**2)
      IF (DELXY.LE.DELSCR) GO TO 15
   17 CALL DRAG(UFL3,VFL3,UPT3,VPT3)
      NTR = NTR+1
      FX1 = FX2
      FY1 = FY2
      FX2 = FDRX+FFAX
      FY2 = FDRY+FFAY
      X2 = X3
      Y2 = Y3
      D2X = D3X
      D2Y = D3Y
      GO TO 16
   15 TIM = TEM
      XTN = 0.50D+00*(X3+X2)
      YTN = 0.50D+00*(Y3+Y2)
      XM = 0.50D+00*(XT+XTN)
      YM = 0.50D+00*(YT+YTN)
      XT = XTN
      YT = YTN
```

```
      UPTT = 0.50D00*(UPT3+UPT2)
      VPTT = 0.50D00*(VPT3+VPT2)
      CALL VEL(XT,YT,TIM)
      UFLT = UFL
      VFLT = VFL
      CALL DRAG(UFLT,VFLT,UPTT,VPTT)
      FXSIGN = (FDRX+FFAX)*DSIGN(A,UPTT)
      FYSIGN = (FDRY+FFAY)*DSIGN(A,VPTT)
      DWX = 0.50D+00*(FXSIGO+FXSIGN)*DABS(XT-XTO)
      DWY = 0.50D+00*(FYSIGO+FYSIGN)*DABS(YT-YTO)
      FXSIGO = FXSIGN
      FYSIGO = FYSIGN
      XTO = XT
      YTO = YT
      DWM = (DWX+DWY)*DSQRT(XM**2+YM**2)
      WMSUM = WMSUM+DWM
      IF ((KOUNT.EQ.IPRNT).OR.(NL.EQ.NSTEP)) GO TO 406
      KOUNT = KOUNT+1
      GO TO 986
  406 IF (NLINE.NE.0) GO TO 400
  405 WRITE (NWRITE,101) IDENSS,PART,UEDDY,NPAGE,XCNTR,YCNTR,GRAV
  101 FORMAT ('1 DATA SUBSET ',I8,7X,' PARTICLE PARAMETER  ',1PD13.6,7X,
     1'       VELOCITY PARAMETER  ',0PD12.5,12X,' PAGE ',I3,//'     EDDY S
     2PACING -   IN X DIRECTION ',1PD12.5,'   IN Y DIRECTION ',D12.5,8X,
     3' GRAVITATIONAL PARAMETER  ',D11.4)
      WRITE (NWRITE,102)
  102 FORMAT (//'       TIME ',10X,' COORDINATES ',6X,' FLUID VELOCITY CO
     1OMPONENTS    PARTICLE VELOCITY COMPONENTS    REYNOLDS   WORK-MOMENT
     2 '//' ',19X,' X ',9X,' Y ',12X,' X ',9X,' Y ',14X,' X ',9X,' Y ',1
     30X,' NUMBER ',3X,' ON PARTICLE , TRIALS'/' ')
  400 CONTINUE
  402 WRITE (NWRITE,112) TIM,XT,YT,UFLT,VFLT,UPTT,VPTT,RNO,WMSUM,NTR
  112 FORMAT (' ',D12.5,1X,F11.4,1X,F11.4,5X,F10.4,2X,F10.4,7X,F10.4,2X,
     1F10.4,5X,D12.4,1X,D12.4,4X,I4)
  403 CONTINUE
      NLINE = NLINE+1
  407 IF (NLINE.GE.51) GO TO 404
      KOUNT = 1
      GO TO 986
  404 NPAGE = NPAGE+1
      NLINE = 0
      GO TO 406
  800 DT = DT*0.70D00
      GO TO 12
  986 CONTINUE
      IF (KPUNCH.EQ.0) GO TO 408
      IF ((NL.NE.1).AND.(NL.NE.(NCARD*IPUNCH))) GO TO 408
```

```
      WRITE (NPUNCH,240) IDENSS,NCARD,NL,TIM,XT,YT
  240 FORMAT (I10,I5,I10,3F15.4)
      NCARD = NCARD+1
  408 CONTINUE
      IF (DROP) GO TO 988
  987 CONTINUE
      NL = NSTEP
  988 CONTINUE
      WRITE (NWRITE,222) IDENSS,UEDDY
  222 FORMAT ('1'//////'  END OF RESULTS FOR DATA SUBSET ',I10,///////'
     1 VELOCITY PARAMETER ',D12.5)
      WRITE (NWRITE,216) NL,TIM ,XT,YT,UPTT,VPTT
  216 FORMAT (////'  LAST COMPUTED POINT ON TRAJECTORY  -  NUMBER ',I10,
     1//39X,' TIME ',1PD30.18,//39X,' POSITION COORDINATES  X ',D30.18,/
     261X,' Y ',D30.18,//39X,' PARTICLE VELOCITY COMPONENTS  X ',D30.18,
     3/69X,' Y ',D30.18)
      IF (KPUNCH.EQ.0) GO TO 989
      WRITE (NPUNCH,240) IDENSS,NCARD,NL,TIM,XT,YT
      WRITE (NPUNCH,207) XT,YT
      WRITE (NPUNCH,208) TIM
      WRITE (NPUNCH,205) UPTT,VPTT
  989 CONTINUE
  999 CONTINUE
      STOP
      END
```

```
      SUBROUTINE VELID
      DATA NWRITE/3/
      WRITE (NWRITE,5001)
 5001 FORMAT (//'  VELOCITY DISTRIBUTION -  INFINITE EDDY ARRAY. ')
      RETURN
      END
```

```
      SUBROUTINE VEL(XD,YD,TD)
      IMPLICIT REAL*8(A-G,O-Z)
      COMMON /COMM/XCNTR,YCNTR,UEDDY,PART,RNO,CD,FDRX,FDRY,UFL,VFL
      COMMON FFAX,FFAY,CONST1
      DATA DPI/3.1415926535898/
      XARG = XD*DPI/XCNTR
      YARG = YD*DPI/YCNTR
      UXY = DSIN(YARG)*DCOS(XARG)
      UFL = UXY*UEDDY
      VXY = -(YCNTR/XCNTR)*DSIN(XARG)*DCOS(YARG)
      VFL = VXY*UEDDY
      AFX = -DPI*((UFL*UFL*DTAN(XARG)/XCNTR)+(VFL*VFL*DCOTAN(XARG)*XCNTR
     1/(YCNTR*YCNTR)))
      AFY = -DPI*((VFL*VFL*DTAN(YARG)/YCNTR)+(UFL*UFL*DCOTAN(YARG)*YCNTR
     1/(XCNTR*XCNTR)))
      FFAX = AFX/CONST1
      FFAY = AFY/CONST1
      RETURN
      END
```

```
      SUBROUTINE DRAG(UFLD,VFLD,UPTD,VPTD)
      IMPLICIT REAL*8(A-H,O-Z)
      DIMENSION RN(8),C(8)
      COMMON /COMM/XCNTR,YCNTR,UEDDY,PART,RNO,CD,FDRX,FDRY,UFL,VFL
      COMMON FFAX,FFAY,CONST1
      DATA RN/1.0D-01,1.0D00,1.0D01,1.0D02,1.0D03,4.0D03,1.0D04,1.0D05/
      DATA C/2.4D02,2.5D01,4.2D00,1.1D00,4.5D-01,4.0D-01,4.2D-01,5.D-01/
      UREL = UFLD-UPTD
      VREL = VFLD-VPTD
      WREL = DSQRT((UREL**2)+(VREL**2))
      RNO = WREL*PART
      IF (RNO.NE.0.00D00) GO TO 1003
 1002 FDRX = 0.0D00
      FDRY = 0.0D00
      GO TO 1007
 1003 IF ((RNO.GT.1.0D-01).AND.(RNO.LT.1.0D+05)) GO TO 1004
      CD = 0.50D00
      IF (RNO.LE.1.0D-01) CD = 24.0D00/RNO
      GO TO 1006
 1004 DO 1005 N=2,8
      IF (RNO.GT.RN(N)) GO TO 1005
      DLNC = DLOG(C(N-1))+(DLOG(C(N))-DLOG(C(N-1)))*(DLOG(RNO)-DLOG(RN(N
     1-1)))/(DLOG(RN(N))-DLOG(RN(N-1)))
      CD = DEXP(DLNC)
      GO TO 1006
 1005 CONTINUE
 1006 CONTINUE
      FDRX = 0.75D00*CD*WREL*UREL
      FDRY = 0.75D00*CD*WREL*VREL
 1007 RETURN
      END
```

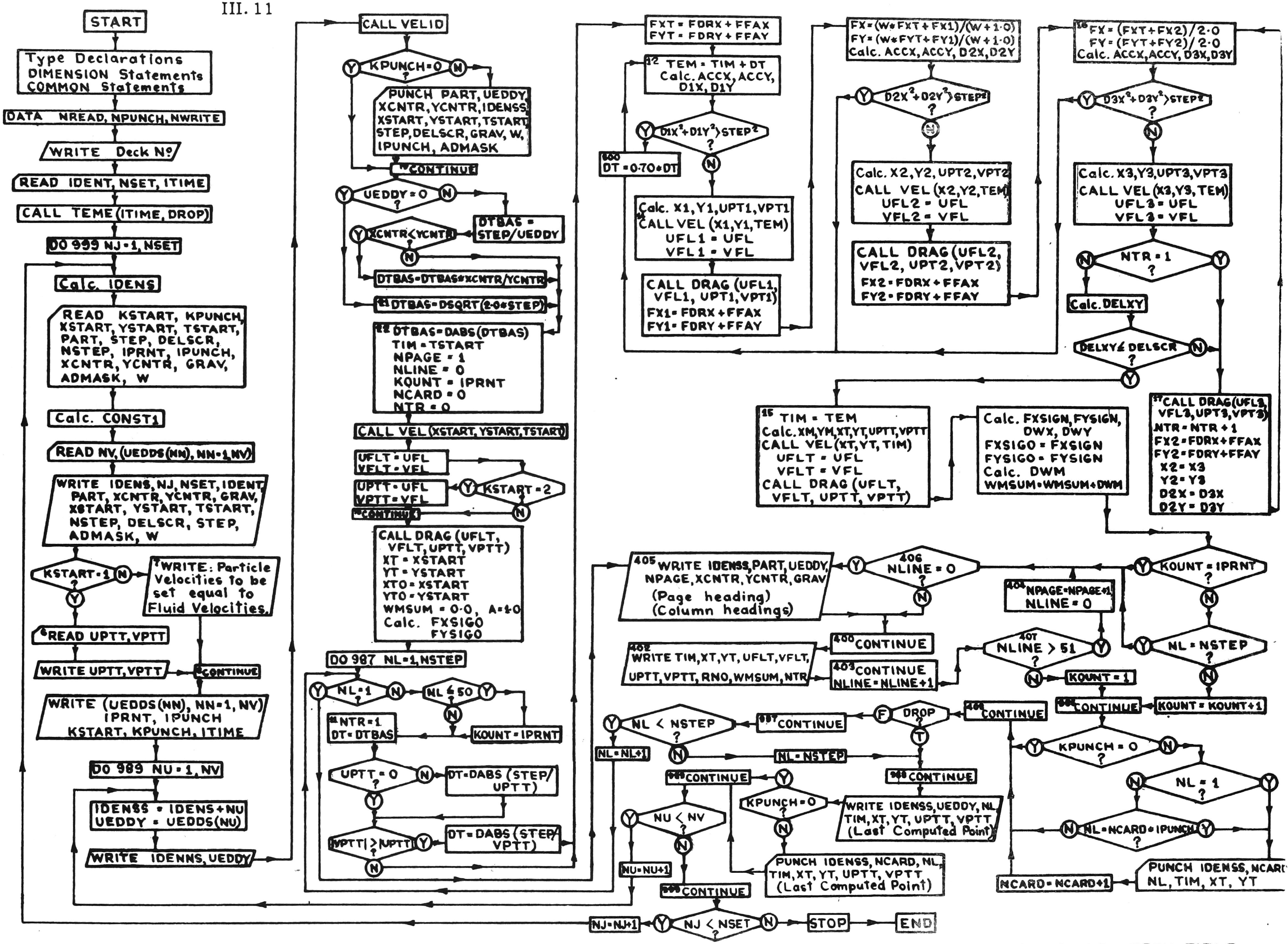

FIGURE III.1 FORTRAN PROGRAM FOR COMPUTATION OF THE TRAJECTORY OF A PARTICLE IN THE MODEL EDDY FIELD.

TABLE III.A

Variables to be Read as Data, in the Operation of the FORTRAN Program for the Computation of the Trajectory of a Particle in the Model Eddy Field.

Variable Name	Definition	Reference	Comments
IDENT		Section 4.5.2	Identification number of the machine run.
NSET		Section 4.5.2	The number of data sets in the machine run.
ITIME		Section 4.3 Note x.	Time control parameter
KSTART		Section 4.3 Note vii.	Starting Code: If KSTART=2, particle velocity components are set equal to fluid velocity components at the starting point. If KSTART=1, particle velocity components are to be read in as data.
KPUNCH		Section 4.5.1	Punched-Card Output Code: if KPUNCH=0, punched card output is supressed.
XSTART	$\frac{x_o}{(s+k)d}$	Section 4.3 Note vi.	Dimensionless x co-ordinate of the initial point on the trajectory.
YSTART	$\frac{y_o}{(s+k)d}$	Section 4.3 Note vi.	Dimensionless y co-ordinate of the initial point on the trajectory.
TSTART	$\frac{t_o}{(s+k)}\sqrt{\frac{g}{d}}$		Dimensionless time at which the particle passes through the initial point.
PART	$\frac{\sqrt{gd^3}}{\nu}$	Section 2.2.10	Particle-Fluid Parameter
STEP		Section 4.3 Note ii.	The maximum distance between two consecutive computed points on the particle trajectory

TABLE III. A (cont'd.)

Variable Name	Definition	Reference	Comments
DELSCR		Section 4.3 Note iii	A parameter which establishes a criterion for the termination of the prediction-correction procedure.
NSTEP			The number of trajectory points to be computed.
IPRNT		Section 4.5.1	Coordinates etc. are printed for each of the first 50 computed trajectory points, and at intervals of IPRNT points thereafter.
IPUNCH		Section 4.5.1	Output Cards are punched at intervals of IPUNCH computed trajectory points, if KPUNCH≠0.
XCNTR	$\frac{X}{(s+k)d}$		Dimensionless spacing of eddy centres, in the x coordinate direction.
YCNTR	$\frac{Y}{(s+k)d}$		Dimensionless spacing of eddy centres, in the y coordinate direction.
GRAV	(s-1.0)		Gravitational Parameter= (particle density/fluid density) - 1.0
ADMASK	k	Section 2.2.2	The Added-Mass Coefficient
W		Section 4.3 Note v.	A weighting factor.
NV		Section 4.5.2	The number of values of the Eddy Velocity Parameter UEDDY to be read within the data set. $1 \leq NV \leq 5$

TABLE III.A (cont'd.)

Variable Name	Definition	Reference	Comments
UEDDS(n) UEDDY	$\frac{U_e}{\sqrt{gd}}$	Section 3.2	The Eddy Velocity Parameter - the dimensionless characteristic velocity within the eddy field.
UPTT VPTT	$\frac{u_p}{\sqrt{gd}}$ $\frac{v_p}{\sqrt{gd}}$	Section 4.3 Note vii	Components of (dimensionless) particle velocity, in the x and y coordinate directions respectively, at the initial point on the particle trajectory-read in only if KSTART = 1

INPUT DATA FOR DATA SET 610100 - THIS IS SET NUMBER 1 OF 1 SET/S TO BE READ IN RUN 61

PARTICLE PARAMETER 1.10680000D 00

SPACING OF EDDY CENTRES - X 5.06250D 01
Y 5.06250D 01

GRAVITATIONAL PARAMETER 1.00000D 00

STARTING POINT - X 0.0
Y 1.500000000000000000D 01
STARTING TIME 0.0

NUMBER OF STEPS 10000

STEP LIMIT 2.00D-02

CONVERGENCE CRITERION 1.00D-07

ADDED MASS COEFFICIENT 0.50D 00

WEIGHTING FACTOR 2.00D 00

PARTICLE VELOCITY COMPONENTS WILL BE SET EQUAL TO THE FLUID VELOCITY COMPONENTS AT THE STARTING POINT.

VELOCITY PARAMETERS 0.1700D 00

COORDINATES AND VELOCITIES ARE PRINTED FOR EACH OF THE FIRST 50 COMPUTED POINTS, AND THEN AFTER EVERY 25 POINTS.

IF KPUNCH IS SET NE 0, A CARD IS PUNCHED AFTER EVERY 25 COMPUTED POINTS.

STARTING CODE KSTART 2 - EQUALS 1 IF PARTICLE VELOCITY COMPONENTS AT STARTING POINT ARE TO BE READ IN.

PUNCHING CODE KPUNCH 1 - EQUALS 0 IF NO CARD OUTPUT IS REQUIRED.

TIME LIMIT PARAMETER ITIME 9

START OF RESULTS FOR DATA SUBSET 610101

VELOCITY PARAMETER 0.17000D 00

VELOCITY DISTRIBUTION - INFINITE EDDY ARRAY.

DATA SUBSET 610101 PARTICLE PARAMETER 1.106800D 00 VELOCITY PARAMETER 0.17000D 00 PAGE 1

EDDY SPACING- IN X DIRN. 5.06250D 01 IN Y DIRN. 5.06250D 01 GRAVITATIONAL PARAMETER 1.0000D 00

TIME	COORDINATES		FLUID VELOCITY COMPONENTS		PARTICLE VELOCITY COMPONENTS		REYNOLDS NUMBER	WORK-MOMENT ON PARTICLE	
	X	Y	X	Y	X	Y			TRIALS
0.0	0.0	15.0000	0.1364	0.0	0.1364	0.0	0.0	0.0	0
0.10267D 00	0.0140	14.9971	0.1363	-0.0001	0.1363	-0.0507	0.5607D-01	-0.1778D-01	52
0.20535D 00	0.0280	14.9914	0.1363	-0.0002	0.1363	-0.0598	0.6594D-01	-0.9465D-01	43
0.30804D 00	0.0420	14.9852	0.1363	-0.0003	0.1363	-0.0614	0.6767D-01	-0.1863D 00	33
0.41077D 00	0.0560	14.9788	0.1362	-0.0004	0.1363	-0.0618	0.6797D-01	-0.2808D 00	24
0.51352D 00	0.0700	14.9725	0.1362	-0.0004	0.1362	-0.0619	0.6802D-01	-0.3759D 00	14
0.61630D 00	0.0840	14.9661	0.1361	-0.0005	0.1362	-0.0620	0.6803D-01	-0.4712D 00	4
0.71911D 00	0.0980	14.9597	0.1361	-0.0006	0.1361	-0.0621	0.6803D-01	-0.5667D 00	2
0.82196D 00	0.1120	14.9534	0.1361	-0.0007	0.1361	-0.0622	0.6803D-01	-0.6622D 00	2
0.92483D 00	0.1260	14.9470	0.1360	-0.0008	0.1360	-0.0623	0.6803D-01	-0.7579D 00	2
0.10277D 01	0.1400	14.9405	0.1360	-0.0009	0.1360	-0.0624	0.6803D-01	-0.8538D 00	2
0.11307D 01	0.1540	14.9341	0.1359	-0.0010	0.1360	-0.0624	0.6803D-01	-0.9497D 00	2
0.12336D 01	0.1680	14.9277	0.1359	-0.0011	0.1359	-0.0625	0.6803D-01	-0.1046D 01	2
0.13366D 01	0.1820	14.9212	0.1359	-0.0012	0.1359	-0.0626	0.6803D-01	-0.1142D 01	2
0.14397D 01	0.1960	14.9148	0.1358	-0.0012	0.1358	-0.0627	0.6803D-01	-0.1238D 01	2
0.15427D 01	0.2100	14.9083	0.1358	-0.0013	0.1358	-0.0628	0.6803D-01	-0.1335D 01	2
0.16458D 01	0.2240	14.9018	0.1357	-0.0014	0.1358	-0.0629	0.6803D-01	-0.1431D 01	2
0.17490D 01	0.2380	14.8953	0.1357	-0.0015	0.1357	-0.0630	0.6803D-01	-0.1528D 01	2
0.18521D 01	0.2520	14.8888	0.1356	-0.0016	0.1357	-0.0631	0.6803D-01	-0.1625D 01	2
0.19553D 01	0.2660	14.8823	0.1356	-0.0017	0.1356	-0.0632	0.6803D-01	-0.1722D 01	2
0.20586D 01	0.2800	14.8758	0.1356	-0.0018	0.1356	-0.0632	0.6803D-01	-0.1819D 01	2
0.21618D 01	0.2940	14.8693	0.1355	-0.0019	0.1355	-0.0633	0.6803D-01	-0.1916D 01	2
0.22651D 01	0.3080	14.8627	0.1355	-0.0020	0.1355	-0.0634	0.6803D-01	-0.2014D 01	2
0.23684D 01	0.3220	14.8562	0.1354	-0.0021	0.1354	-0.0635	0.6803D-01	-0.2111D 01	2
0.24718D 01	0.3360	14.8496	0.1354	-0.0021	0.1354	-0.0636	0.6803D-01	-0.2209D 01	2
0.25752D 01	0.3499	14.8430	0.1353	-0.0022	0.1354	-0.0637	0.6803D-01	-0.2306D 01	2
0.26786D 01	0.3639	14.8364	0.1353	-0.0023	0.1353	-0.0638	0.6803D-01	-0.2404D 01	2
0.27821D 01	0.3779	14.8298	0.1352	-0.0024	0.1353	-0.0639	0.6803D-01	-0.2502D 01	2
0.28856D 01	0.3919	14.8232	0.1352	-0.0025	0.1352	-0.0640	0.6803D-01	-0.2600D 01	2
0.29891D 01	0.4059	14.8166	0.1352	-0.0026	0.1352	-0.0641	0.6803D-01	-0.2699D 01	2
0.30927D 01	0.4199	14.8099	0.1351	-0.0027	0.1351	-0.0642	0.6803D-01	-0.2797D 01	2

DATA SUBSET 610101 PARTICLE PARAMETER 1.106800D 00 VELOCITY PARAMETER 0.17000D 00

EDDY SPACING- IN X DIRN. 5.06250D 01 IN Y DIRN. 5.06250D 01 GRAVITATIONAL PARAMETER 1.0000D 00

TIME	COORDINATES		FLUID VELOCITY COMPONENTS		PARTICLE VELOCITY COMPONENTS		REYNOLDS NUMBER	WORK-MOMENT ON PARTICLE	TRIALS
	X	Y	X	Y	X	Y			
0.30927D 01	0.4199	14.8099	0.1351	-0.0027	0.1351	-0.0642	0.6803D-01	-0.2797D 01	2
0.31963D 01	0.4339	14.8033	0.1351	-0.0028	0.1351	-0.0642	0.6803D-01	-0.2896D 01	2
0.32999D 01	0.4479	14.7966	0.1350	-0.0029	0.1350	-0.0643	0.6803D-01	-0.2994D 01	2
0.34036D 01	0.4619	14.7899	0.1350	-0.0030	0.1350	-0.0644	0.6803D-01	-0.3093D 01	2
0.35073D 01	0.4759	14.7833	0.1349	-0.0031	0.1349	-0.0645	0.6803D-01	-0.3192D 01	2
0.36110D 01	0.4899	14.7766	0.1349	-0.0031	0.1349	-0.0646	0.6803D-01	-0.3291D 01	2
0.37148D 01	0.5039	14.7699	0.1348	-0.0032	0.1349	-0.0647	0.6803D-01	-0.3390D 01	2
0.38186D 01	0.5179	14.7631	0.1348	-0.0033	0.1348	-0.0648	0.6803D-01	-0.3490D 01	2
0.39225D 01	0.5319	14.7564	0.1347	-0.0034	0.1348	-0.0649	0.6803D-01	-0.3589D 01	2
0.40264D 01	0.5459	14.7497	0.1347	-0.0035	0.1347	-0.0650	0.6803D-01	-0.3689D 01	2
0.41303D 01	0.5599	14.7429	0.1346	-0.0036	0.1347	-0.0651	0.6803D-01	-0.3788D 01	2
0.42343D 01	0.5739	14.7361	0.1346	-0.0037	0.1346	-0.0652	0.6803D-01	-0.3888D 01	2
0.43382D 01	0.5879	14.7293	0.1345	-0.0038	0.1346	-0.0653	0.6803D-01	-0.3988D 01	2
0.44423D 01	0.6019	14.7226	0.1345	-0.0039	0.1345	-0.0653	0.6803D-01	-0.4088D 01	2
0.45463D 01	0.6159	14.7157	0.1345	-0.0040	0.1345	-0.0654	0.6803D-01	-0.4189D 01	2
0.46505D 01	0.6299	14.7089	0.1344	-0.0041	0.1344	-0.0655	0.6803D-01	-0.4289D 01	2
0.47546D 01	0.6439	14.7021	0.1344	-0.0042	0.1344	-0.0656	0.6803D-01	-0.4389D 01	2
0.48588D 01	0.6579	14.6953	0.1343	-0.0042	0.1343	-0.0657	0.6803D-01	-0.4490D 01	2
0.49630D 01	0.6719	14.6884	0.1343	-0.0043	0.1343	-0.0658	0.6803D-01	-0.4591D 01	2
0.50673D 01	0.6859	14.6815	0.1342	-0.0044	0.1342	-0.0659	0.6803D-01	-0.4692D 01	2
0.76866D 01	1.0358	14.5059	0.1329	-0.0068	0.1329	-0.0683	0.6803D-01	-0.7261D 01	2
0.10333D 02	1.3857	14.3221	0.1315	-0.0092	0.1315	-0.0707	0.6803D-01	-0.9920D 01	2
0.13009D 02	1.7357	14.1296	0.1299	-0.0117	0.1300	-0.0732	0.6803D-01	-0.1267D 02	2
0.15719D 02	2.0856	13.9279	0.1282	-0.0142	0.1283	-0.0757	0.6803D-01	-0.1553D 02	2
0.18467D 02	2.4355	13.7163	0.1264	-0.0169	0.1264	-0.0783	0.6803D-01	-0.1849D 02	2
0.21256D 02	2.7854	13.4941	0.1244	-0.0196	0.1244	-0.0810	0.6803D-01	-0.2157D 02	2
0.24092D 02	3.1352	13.2603	0.1223	-0.0224	0.1223	-0.0838	0.6803D-01	-0.2478D 02	2
0.26979D 02	3.4851	13.0142	0.1200	-0.0252	0.1200	-0.0867	0.6802D-01	-0.2811D 02	2
0.29924D 02	3.8350	12.7546	0.1175	-0.0282	0.1176	-0.0896	0.6802D-01	-0.3159D 02	2
0.32933D 02	4.1848	12.4804	0.1149	-0.0312	0.1149	-0.0927	0.6802D-01	-0.3522D 02	2
0.36013D 02	4.5346	12.1901	0.1121	-0.0343	0.1121	-0.0958	0.6802D-01	-0.3902D 02	2

DATA SUBSET 610101 PARTICLE PARAMETER 1.106800D 00 VELOCITY PARAMETER 0.17000D 00 PAGE 3

EDDY SPACING- IN X DIRN. 5.06250D 01 IN Y DIRN. 5.06250D 01 GRAVITATIONAL PARAMETER 1.0000D 00

TIME	COORDINATES X	COORDINATES Y	FLUID VELOCITY COMPONENTS X	FLUID VELOCITY COMPONENTS Y	PARTICLE VELOCITY COMPONENTS X	PARTICLE VELOCITY COMPONENTS Y	REYNOLDS NUMBER	WORK-MOMENT ON PARTICLE	TRIALS
0.36013D 02	4.5346	12.1901	0.1121	-0.0343	0.1121	-0.0958	0.6802D-01	-0.3902D 02	2
0.39175D 02	4.8844	11.8821	0.1091	-0.0376	0.1091	-0.0990	0.6802D-01	-0.4300D 02	2
0.42428D 02	5.2342	11.5546	0.1059	-0.0409	0.1059	-0.1024	0.6802D-01	-0.4718D 02	2
0.45762D 02	5.5816	11.2077	0.1025	-0.0443	0.1025	-0.1058	0.6802D-01	-0.5155D 02	2
0.49021D 02	5.9102	10.8575	0.0990	-0.0476	0.0991	-0.1091	0.6802D-01	-0.5591D 02	2
0.52185D 02	6.2181	10.5073	0.0956	-0.0509	0.0956	-0.1123	0.6802D-01	-0.6021D 02	2
0.55260D 02	6.5069	10.1571	0.0921	-0.0540	0.0922	-0.1154	0.6802D-01	-0.6446D 02	2
0.58255D 02	6.7779	9.8069	0.0887	-0.0570	0.0888	-0.1184	0.6802D-01	-0.6866D 02	2
0.61177D 02	7.0323	9.4568	0.0853	-0.0598	0.0854	-0.1213	0.6802D-01	-0.7281D 02	2
0.64031D 02	7.2711	9.1066	0.0819	-0.0626	0.0820	-0.1241	0.6802D-01	-0.7691D 02	2
0.66823D 02	7.4953	8.7565	0.0786	-0.0653	0.0786	-0.1267	0.6802D-01	-0.8097D 02	2
0.69558D 02	7.7058	8.4063	0.0752	-0.0678	0.0753	-0.1293	0.6802D-01	-0.8498D 02	2
0.72241D 02	7.9032	8.0562	0.0719	-0.0703	0.0719	-0.1317	0.6803D-01	-0.8895D 02	2
0.74875D 02	8.0884	7.7061	0.0686	-0.0726	0.0686	-0.1341	0.6803D-01	-0.9288D 02	2
0.77465D 02	8.2619	7.3560	0.0653	-0.0749	0.0654	-0.1363	0.6803D-01	-0.9678D 02	2
0.80013D 02	8.4243	7.0058	0.0620	-0.0770	0.0621	-0.1384	0.6803D-01	-0.1006D 03	2
0.82524D 02	8.5761	6.6557	0.0588	-0.0790	0.0588	-0.1405	0.6803D-01	-0.1044D 03	2
0.84999D 02	8.7177	6.3057	0.0556	-0.0809	0.0556	-0.1424	0.6803D-01	-0.1082D 03	2
0.87442D 02	8.8497	5.9556	0.0524	-0.0827	0.0524	-0.1442	0.6803D-01	-0.1120D 03	2
0.89855D 02	8.9724	5.6055	0.0492	-0.0845	0.0492	-0.1459	0.6803D-01	-0.1157D 03	2
0.92240D 02	9.0861	5.2554	0.0460	-0.0861	0.0461	-0.1475	0.6803D-01	-0.1194D 03	2
0.94601D 02	9.1912	4.9053	0.0429	-0.0876	0.0429	-0.1490	0.6803D-01	-0.1230D 03	2
0.96939D 02	9.2879	4.5553	0.0398	-0.0890	0.0398	-0.1504	0.6804D-01	-0.1267D 03	2
0.99256D 02	9.3766	4.2052	0.0366	-0.0903	0.0367	-0.1517	0.6804D-01	-0.1303D 03	2
0.10155D 03	9.4573	3.8552	0.0335	-0.0915	0.0336	-0.1529	0.6804D-01	-0.1339D 03	2
0.10383D 03	9.5304	3.5051	0.0305	-0.0925	0.0305	-0.1540	0.6804D-01	-0.1374D 03	2
0.10610D 03	9.5961	3.1551	0.0274	-0.0935	0.0274	-0.1550	0.6804D-01	-0.1410D 03	2
0.10835D 03	9.6544	2.8050	0.0243	-0.0944	0.0244	-0.1559	0.6804D-01	-0.1445D 03	2
0.11059D 03	9.7055	2.4550	0.0213	-0.0952	0.0213	-0.1567	0.6804D-01	-0.1480D 03	2
0.11282D 03	9.7496	2.1050	0.0182	-0.0959	0.0183	-0.1573	0.6805D-01	-0.1515D 03	2
0.11504D 03	9.7868	1.7549	0.0153	-0.0964	0.0152	-0.1579	0.6805D-01	-0.1550D 03	2

EDDY SPACING- IN X DIRN. 5.06250D 01 IN Y DIRN. 5.06250D 01 GRAVITATIONAL PARAMETER 1.0000D 00

TIME	COORDINATES X	COORDINATES Y	FLUID VELOCITY COMPONENTS X	FLUID VELOCITY COMPONENTS Y	PARTICLE VELOCITY COMPONENTS X	PARTICLE VELOCITY COMPONENTS Y	REYNOLDS NUMBER	WORK-MOMENT ON PARTICLE	TRIALS
0.11504D 03	9.7868	1.7549	0.0153	-0.0964	0.0152	-0.1579	0.6805D-01	-0.1550D 03	2
0.11725D 03	9.8172	1.4049	0.0121	-0.0969	0.0122	-0.1584	0.6805D-01	-0.1585D 03	2
0.11946D 03	9.8407	1.0549	0.0091	-0.0973	0.0092	-0.1588	0.6805D-01	-0.1619D 03	2
0.12166D 03	9.8576	0.7049	0.0061	-0.0975	0.0061	-0.1590	0.6805D-01	-0.1654D 03	2
0.12386D 03	9.8678	0.3549	0.0031	-0.0977	0.0031	-0.1592	0.6805D-01	-0.1689D 03	2
0.12606D 03	9.8713	0.0049	0.0000	-0.0977	0.0001	-0.1592	0.6806D-01	-0.1723D 03	2
0.12826D 03	9.8682	-0.3451	-0.0030	-0.0977	-0.0029	-0.1592	0.6806D-01	-0.1758D 03	2
0.13046D 03	9.8584	-0.6951	-0.0060	-0.0975	-0.0059	-0.1590	0.6806D-01	-0.1792D 03	2
0.13266D 03	9.8420	-1.0451	-0.0090	-0.0973	-0.0090	-0.1588	0.6806D-01	-0.1827D 03	2
0.13487D 03	9.8189	-1.3951	-0.0121	-0.0969	-0.0120	-0.1584	0.6806D-01	-0.1862D 03	2
0.13708D 03	9.7890	-1.7451	-0.0151	-0.0965	-0.0150	-0.1580	0.6806D-01	-0.1896D 03	2
0.13930D 03	9.7522	-2.0951	-0.0181	-0.0959	-0.0181	-0.1574	0.6807D-01	-0.1931D 03	2
0.14153D 03	9.7086	-2.4450	-0.0212	-0.0952	-0.0211	-0.1567	0.6807D-01	-0.1966D 03	2
0.14377D 03	9.6579	-2.7950	-0.0242	-0.0945	-0.0242	-0.1560	0.6807D-01	-0.2001D 03	2
0.14602D 03	9.6000	-3.1449	-0.0273	-0.0936	-0.0272	-0.1551	0.6807D-01	-0.2037D 03	2
0.14828D 03	9.5349	-3.4949	-0.0304	-0.0926	-0.0303	-0.1541	0.6807D-01	-0.2072D 03	2
0.15056D 03	9.4623	-3.8449	-0.0334	-0.0915	-0.0334	-0.1530	0.6807D-01	-0.2108D 03	2
0.15285D 03	9.3821	-4.1948	-0.0365	-0.0903	-0.0365	-0.1518	0.6807D-01	-0.2144D 03	2
0.15517D 03	9.2940	-4.5447	-0.0397	-0.0890	-0.0396	-0.1505	0.6808D-01	-0.2180D 03	2
0.15750D 03	9.1979	-4.8947	-0.0428	-0.0876	-0.0427	-0.1492	0.6808D-01	-0.2216D 03	2
0.15986D 03	9.0934	-5.2446	-0.0459	-0.0861	-0.0459	-0.1477	0.6808D-01	-0.2253D 03	2
0.16224D 03	8.9803	-5.5945	-0.0491	-0.0845	-0.0490	-0.1461	0.6808D-01	-0.2289D 03	2
0.16465D 03	8.8583	-5.9444	-0.0523	-0.0828	-0.0522	-0.1444	0.6808D-01	-0.2327D 03	2
0.16709D 03	8.7271	-6.2944	-0.0555	-0.0810	-0.0554	-0.1425	0.6808D-01	-0.2364D 03	2
0.16956D 03	8.5862	-6.6443	-0.0587	-0.0791	-0.0586	-0.1406	0.6808D-01	-0.2402D 03	2
0.17207D 03	8.4352	-6.9942	-0.0619	-0.0771	-0.0619	-0.1386	0.6808D-01	-0.2440D 03	2
0.17461D 03	8.2737	-7.3441	-0.0652	-0.0750	-0.0651	-0.1365	0.6808D-01	-0.2479D 03	2
0.17720D 03	8.1011	-7.6939	-0.0685	-0.0727	-0.0684	-0.1343	0.6809D-01	-0.2518D 03	2
0.17983D 03	7.9169	-8.0438	-0.0718	-0.0704	-0.0717	-0.1319	0.6809D-01	-0.2557D 03	2
0.18250D 03	7.7206	-8.3937	-0.0751	-0.0680	-0.0750	-0.1295	0.6809D-01	-0.2597D 03	2
0.18523D 03	7.5113	-8.7435	-0.0784	-0.0654	-0.0784	-0.1269	0.6809D-01	-0.2637D 03	2

DATA SUBSET 610101 PARTICLE PARAMETER 1.106800D 00 VELOCITY PARAMETER 0.17000D 00 PAGE 5

EDDY SPACING- IN X DIRN. 5.06250D 01 IN Y DIRN. 5.06250D 01 GRAVITATIONAL PARAMETER 1.0000D 00

TIME	COORDINATES		FLUID VELOCITY COMPONENTS		PARTICLE VELOCITY COMPONENTS		REYNOLDS NUMBER	WORK-MOMENT ON PARTICLE	TRIALS
	X	Y	X	Y	X	Y			
0.18523D 03	7.5113	-8.7435	-0.0784	-0.0654	-0.0784	-0.1269	0.6809D-01	-0.2637D 03	2
0.18802D 03	7.2884	-9.0934	-0.0818	-0.0628	-0.0817	-0.1243	0.6809D-01	-0.2677D 03	2
0.19086D 03	7.0509	-9.4432	-0.0852	-0.0600	-0.0851	-0.1215	0.6809D-01	-0.2718D 03	2
0.19378D 03	6.7980	-9.7931	-0.0886	-0.0571	-0.0885	-0.1187	0.6809D-01	-0.2760D 03	2
0.19676D 03	6.5287	-10.1429	-0.0920	-0.0542	-0.0919	-0.1157	0.6809D-01	-0.2802D 03	2
0.19983D 03	6.2417	-10.4927	-0.0954	-0.0511	-0.0954	-0.1126	0.6809D-01	-0.2844D 03	2
0.20298D 03	5.9357	-10.8425	-0.0988	-0.0479	-0.0988	-0.1094	0.6809D-01	-0.2887D 03	2
0.20622D 03	5.6093	-11.1923	-0.1023	-0.0446	-0.1022	-0.1061	0.6809D-01	-0.2931D 03	2
0.20956D 03	5.2629	-11.5401	-0.1057	-0.0411	-0.1057	-0.1027	0.6809D-01	-0.2974D 03	2
0.21282D 03	4.9127	-11.8697	-0.1089	-0.0378	-0.1089	-0.0993	0.6809D-01	-0.3016D 03	2
0.21599D 03	4.5625	-12.1796	-0.1120	-0.0346	-0.1119	-0.0961	0.6809D-01	-0.3057D 03	2
0.21908D 03	4.2123	-12.4716	-0.1148	-0.0314	-0.1147	-0.0929	0.6809D-01	-0.3095D 03	2
0.22210D 03	3.8622	-12.7473	-0.1174	-0.0284	-0.1174	-0.0899	0.6809D-01	-0.3131D 03	2
0.22505D 03	3.5120	-13.0082	-0.1199	-0.0254	-0.1199	-0.0869	0.6809D-01	-0.3166D 03	2
0.22794D 03	3.1619	-13.2556	-0.1222	-0.0225	-0.1222	-0.0841	0.6809D-01	-0.3200D 03	2
0.23078D 03	2.8118	-13.4904	-0.1243	-0.0198	-0.1243	-0.0813	0.6809D-01	-0.3232D 03	2
0.23358D 03	2.4616	-13.7137	-0.1263	-0.0171	-0.1263	-0.0786	0.6809D-01	-0.3263D 03	2
0.23633D 03	2.1115	-13.9262	-0.1282	-0.0144	-0.1282	-0.0759	0.6808D-01	-0.3293D 03	2
0.23904D 03	1.7615	-14.1288	-0.1299	-0.0119	-0.1299	-0.0734	0.6808D-01	-0.3321D 03	2
0.24172D 03	1.4114	-14.3221	-0.1315	-0.0094	-0.1314	-0.0709	0.6808D-01	-0.3349D 03	2
0.24437D 03	1.0613	-14.5066	-0.1329	-0.0070	-0.1329	-0.0685	0.6808D-01	-0.3376D 03	2
0.24699D 03	0.7112	-14.6830	-0.1342	-0.0046	-0.1342	-0.0661	0.6808D-01	-0.3401D 03	2
0.24959D 03	0.3612	-14.8517	-0.1354	-0.0023	-0.1354	-0.0638	0.6808D-01	-0.3426D 03	2
0.25216D 03	0.0111	-15.0132	-0.1364	-0.0001	-0.1364	-0.0616	0.6808D-01	-0.3450D 03	2
0.25472D 03	-0.3389	-15.1679	-0.1374	0.0021	-0.1374	-0.0594	0.6808D-01	-0.3474D 03	2
0.25726D 03	-0.6890	-15.3161	-0.1382	0.0042	-0.1382	-0.0573	0.6808D-01	-0.3496D 03	2
0.25979D 03	-1.0390	-15.4582	-0.1389	0.0063	-0.1389	-0.0552	0.6808D-01	-0.3518D 03	2
0.26230D 03	-1.3890	-15.5945	-0.1395	0.0083	-0.1395	-0.0532	0.6808D-01	-0.3540D 03	2
0.26481D 03	-1.7391	-15.7253	-0.1400	0.0103	-0.1400	-0.0512	0.6807D-01	-0.3560D 03	2
0.26731D 03	-2.0891	-15.8509	-0.1403	0.0122	-0.1403	-0.0493	0.6807D-01	-0.3580D 03	2
0.26980D 03	-2.4391	-15.9715	-0.1406	0.0140	-0.1406	-0.0475	0.6807D-01	-0.3600D 03	2

DATA SUBSET 610101 PARTICLE PARAMETER 1.106800D 00 VELOCITY PARAMETER 0.17000D 00

EDDY SPACING- IN X DIRN. 5.06250D 01 IN Y DIRN. 5.06250D 01 GRAVITATIONAL PARAMETER 1.0000D 00

TIME	COORDINATES		FLUID VELOCITY COMPONENTS		PARTICLE VELOCITY COMPONENTS		REYNOLDS NUMBER	WORK-MOMENT ON PARTICLE	TRIALS
	X	Y	X	Y	X	Y			
0.26980D 03	-2.4391	-15.9715	-0.1406	0.0140	-0.1406	-0.0475	0.6807D-01	-0.3600D 03	2
0.27229D 03	-2.7891	-16.0873	-0.1408	0.0159	-0.1407	-0.0456	0.6807D-01	-0.3618D 03	2
0.27477D 03	-3.1391	-16.1986	-0.1408	0.0176	-0.1408	-0.0439	0.6807D-01	-0.3637D 03	2
0.27726D 03	-3.4891	-16.3055	-0.1408	0.0194	-0.1408	-0.0421	0.6807D-01	-0.3654D 03	2
0.27975D 03	-3.8391	-16.4082	-0.1406	0.0211	-0.1406	-0.0404	0.6807D-01	-0.3672D 03	2
0.28224D 03	-4.1891	-16.5069	-0.1404	0.0227	-0.1404	-0.0388	0.6807D-01	-0.3688D 03	2
0.28743D 03	-4.5391	-16.6017	-0.1400	0.0243	-0.1400	-0.0372	0.6807D-01	-0.3705D 03	2
0.28724D 03	-4.8890	-16.6928	-0.1396	0.0259	-0.1396	-0.0356	0.6807D-01	-0.3720D 03	2
0.28975D 03	-5.2390	-16.7803	-0.1390	0.0274	-0.1390	-0.0341	0.6807D-01	-0.3736D 03	2
0.29227D 03	-5.5890	-16.8644	-0.1384	0.0289	-0.1384	-0.0326	0.6806D-01	-0.3751D 03	2
0.29481D 03	-5.9390	-16.9451	-0.1377	0.0304	-0.1377	-0.0311	0.6806D-01	-0.3765D 03	2
0.29736D 03	-6.2889	-17.0225	-0.1369	0.0318	-0.1369	-0.0297	0.6806D-01	-0.3779D 03	2
0.29992D 03	-6.6389	-17.0968	-0.1360	0.0332	-0.1360	-0.0283	0.6806D-01	-0.3793D 03	2
0.30251D 03	-6.9888	-17.1681	-0.1350	0.0346	-0.1350	-0.0269	0.6806D-01	-0.3806D 03	2
0.30511D 03	-7.3388	-17.2364	-0.1339	0.0359	-0.1339	-0.0256	0.6806D-01	-0.3819D 03	2
0.30773D 03	-7.6887	-17.3018	-0.1327	0.0372	-0.1327	-0.0243	0.6806D-01	-0.3831D 03	2
0.31038D 03	-8.0386	-17.3643	-0.1315	0.0385	-0.1315	-0.0230	0.6806D-01	-0.3843D 03	2
0.31306D 03	-8.3886	-17.4241	-0.1302	0.0398	-0.1302	-0.0217	0.6806D-01	-0.3854D 03	2
0.31576D 03	-8.7385	-17.4812	-0.1288	0.0410	-0.1288	-0.0205	0.6806D-01	-0.3865D 03	2
0.31849D 03	-9.0884	-17.5356	-0.1273	0.0422	-0.1273	-0.0193	0.6806D-01	-0.3876D 03	2
0.32126D 03	-9.4383	-17.5874	-0.1257	0.0433	-0.1257	-0.0181	0.6805D-01	-0.3887D 03	2
0.32406D 03	-9.7882	-17.6366	-0.1241	0.0445	-0.1241	-0.0170	0.6805D-01	-0.3896D 03	2
0.32690D 03	-10.1381	-17.6833	-0.1223	0.0456	-0.1223	-0.0159	0.6805D-01	-0.3906D 03	2
0.32978D 03	-10.4880	-17.7274	-0.1205	0.0467	-0.1205	-0.0148	0.6805D-01	-0.3915D 03	2
0.33271D 03	-10.8379	-17.7691	-0.1187	0.0478	-0.1187	-0.0137	0.6805D-01	-0.3924D 03	2
0.33568D 03	-11.1878	-17.8082	-0.1167	0.0488	-0.1167	-0.0126	0.6805D-01	-0.3932D 03	2
0.33870D 03	-11.5377	-17.8448	-0.1147	0.0499	-0.1147	-0.0116	0.6805D-01	-0.3940D 03	2
0.34178D 03	-11.8876	-17.8790	-0.1127	0.0509	-0.1127	-0.0106	0.6805D-01	-0.3947D 03	2
0.34491D 03	-12.2374	-17.9106	-0.1105	0.0519	-0.1105	-0.0096	0.6805D-01	-0.3954D 03	2
0.34811D 03	-12.5873	-17.9397	-0.1083	0.0529	-0.1083	-0.0086	0.6805D-01	-0.3960D 03	2
0.35138D 03	-12.9371	-17.9662	-0.1060	0.0538	-0.1060	-0.0076	0.6805D-01	-0.3966D 03	2

DATA SUBSET 610101 PARTICLE PARAMETER 1.106800D 00 VELOCITY PARAMETER 0.17000D 00

EDDY SPACING- IN X DIRN. 5.06250D 01 IN Y DIRN. 5.06250D 01 GRAVITATIONAL PARAMETER 1.0000D 00

TIME	COORDINATES X	COORDINATES Y	FLUID VELOCITY COMPONENTS X	FLUID VELOCITY COMPONENTS Y	PARTICLE VELOCITY COMPONENTS X	PARTICLE VELOCITY COMPONENTS Y	REYNOLDS NUMBER	WORK-MOMENT ON PARTICLE	TRIALS
0.35138D 03	-12.9371	-17.9662	-0.1060	0.0538	-0.1060	-0.0076	0.6805D-01	-0.3966D 03	2
0.35471D 03	-13.2870	-17.9901	-0.1037	0.0548	-0.1037	-0.0067	0.6805D-01	-0.3972D 03	2
0.35812D 03	-13.6368	-18.0114	-0.1013	0.0557	-0.1013	-0.0058	0.6805D-01	-0.3976D 03	2
0.36162D 03	-13.9866	-18.0298	-0.0989	0.0566	-0.0989	-0.0048	0.6804D-01	-0.3981D 03	2
0.36520D 03	-14.3365	-18.0455	-0.0963	0.0576	-0.0964	-0.0039	0.6804D-01	-0.3984D 03	2
0.36978D 03	-14.7702	-18.0609	-0.0932	0.0587	-0.0932	-0.0028	0.6804D-01	-0.3988D 03	2
0.37445D 03	-15.1978	-18.0714	-0.0899	0.0598	-0.0899	-0.0017	0.6804D-01	-0.3991D 03	2
0.37923D 03	-15.6195	-18.0770	-0.0867	0.0608	-0.0867	-0.0006	0.6804D-01	-0.3992D 03	12
0.38419D 03	-16.0412	-18.0775	-0.0833	0.0619	-0.0833	0.0004	0.6804D-01	-0.3992D 03	2
0.38913D 03	-16.4449	-18.0728	-0.0801	0.0629	-0.0801	0.0015	0.6804D-01	-0.3991D 03	8
0.39412D 03	-16.8365	-18.0630	-0.0769	0.0639	-0.0769	0.0025	0.6804D-01	-0.3989D 03	11
0.39924D 03	-17.2222	-18.0478	-0.0736	0.0649	-0.0736	0.0035	0.6804D-01	-0.3985D 03	6
0.40368D 03	-17.5425	-18.0307	-0.0709	0.0658	-0.0709	0.0043	0.6804D-01	-0.3981D 03	2
0.40816D 03	-17.8545	-18.0095	-0.0682	0.0666	-0.0682	0.0051	0.6804D-01	-0.3975D 03	24
0.41289D 03	-18.1706	-17.9832	-0.0655	0.0675	-0.0655	0.0060	0.6804D-01	-0.3969D 03	2
0.41782D 03	-18.4867	-17.9515	-0.0627	0.0684	-0.0627	0.0069	0.6804D-01	-0.3961D 03	2
0.42263D 03	-18.7819	-17.9163	-0.0601	0.0692	-0.0601	0.0077	0.6804D-01	-0.3952D 03	19
0.42750D 03	-19.0686	-17.8765	-0.0575	0.0701	-0.0575	0.0086	0.6804D-01	-0.3941D 03	20
0.43253D 03	-19.3512	-17.8310	-0.0550	0.0710	-0.0550	0.0095	0.6804D-01	-0.3929D 03	2
0.43755D 03	-19.6211	-17.7810	-0.0525	0.0719	-0.0525	0.0104	0.6804D-01	-0.3916D 03	17
0.44240D 03	-19.8701	-17.7285	-0.0502	0.0727	-0.0502	0.0113	0.6804D-01	-0.3902D 03	16
0.44739D 03	-20.1149	-17.6701	-0.0479	0.0736	-0.0479	0.0122	0.6804D-01	-0.3887D 03	16
0.45262D 03	-20.3596	-17.6041	-0.0457	0.0746	-0.0457	0.0131	0.6804D-01	-0.3869D 03	14
0.45812D 03	-20.6044	-17.5291	-0.0434	0.0756	-0.0434	0.0141	0.6804D-01	-0.3849D 03	14
0.46391D 03	-20.8491	-17.4440	-0.0411	0.0767	-0.0411	0.0152	0.6804D-01	-0.3826D 03	12
0.47005D 03	-21.0938	-17.3469	-0.0387	0.0779	-0.0387	0.0164	0.6804D-01	-0.3799D 03	12
0.47560D 03	-21.3033	-17.2526	-0.0367	0.0790	-0.0367	0.0175	0.6804D-01	-0.3774D 03	25
0.48113D 03	-21.5010	-17.1525	-0.0348	0.0802	-0.0348	0.0187	0.6804D-01	-0.3746D 03	25
0.48661D 03	-21.6870	-17.0469	-0.0330	0.0813	-0.0330	0.0198	0.6804D-01	-0.3717D 03	24
0.49211D 03	-21.8642	-16.9343	-0.0313	0.0825	-0.0313	0.0211	0.6804D-01	-0.3686D 03	20
0.49752D 03	-22.0294	-16.8171	-0.0297	0.0838	-0.0297	0.0223	0.6804D-01	-0.3654D 03	40

EDDY SPACING- IN X DIRN. 5.06250D 01 IN Y DIRN. 5.06250D 01 GRAVITATIONAL PARAMETER 1.00000 00

TIME	COORDINATES		FLUID VELOCITY COMPONENTS		PARTICLE VELOCITY COMPONENTS		REYNOLDS NUMBER	WORK-MOMENT ON PARTICLE	
	X	Y	X	Y	X	Y			TRIALS
0.49752D 03	-22.0294	-16.8171	-0.0297	0.0838	-0.0297	0.0223	0.6804D-01	-0.3654D 03	40
0.50309D 03	-22.1904	-16.6895	-0.0282	0.0851	-0.0282	0.0236	0.6804D-01	-0.3618D 03	20
0.50859D 03	-22.3412	-16.5561	-0.0267	0.0864	-0.0267	0.0249	0.6804D-01	-0.3581D 03	34
0.51412D 03	-22.4848	-16.4144	-0.0253	0.0878	-0.0253	0.0263	0.6804D-01	-0.3542D 03	33
0.51963D 03	-22.6203	-16.2654	-0.0239	0.0892	-0.0239	0.0278	0.6804D-01	-0.3500D 03	36
0.52521D 03	-22.7503	-16.1061	-0.0226	0.0908	-0.0226	0.0293	0.6804D-01	-0.3456D 03	20
0.53072D 03	-22.8717	-15.9406	-0.0214	0.0923	-0.0214	0.0308	0.6804D-01	-0.3410D 03	20
0.53617D 03	-22.9855	-15.7680	-0.0203	0.0939	-0.0203	0.0324	0.6804D-01	-0.3361D 03	10
0.54160D 03	-23.0927	-15.5875	-0.0192	0.0956	-0.0192	0.0341	0.6804D-01	-0.3311D 03	25
0.54710D 03	-23.1956	-15.3952	-0.0182	0.0973	-0.0182	0.0358	0.6804D-01	-0.3258D 03	25
0.55266D 03	-23.2938	-15.1912	-0.0172	0.0991	-0.0172	0.0376	0.6804D-01	-0.3201D 03	12
0.55818D 03	-23.3861	-14.9783	-0.0162	0.1010	-0.0162	0.0395	0.6804D-01	-0.3142D 03	29
0.56373D 03	-23.4738	-14.7537	-0.0153	0.1029	-0.0153	0.0414	0.6804D-01	-0.3079D 03	13
0.56923D 03	-23.5559	-14.5202	-0.0145	0.1049	-0.0145	0.0434	0.6805D-01	-0.3015D 03	13
0.57468D 03	-23.6328	-14.2779	-0.0137	0.1069	-0.0137	0.0455	0.6805D-01	-0.2948D 03	14
0.57996D 03	-23.7031	-14.0327	-0.0130	0.1090	-0.0130	0.0475	0.6805D-01	-0.2880D 03	16
0.58521D 03	-23.7694	-13.7778	-0.0123	0.1110	-0.0123	0.0496	0.6805D-01	-0.2810D 03	2
0.59047D 03	-23.8321	-13.5116	-0.0116	0.1132	-0.0116	0.0517	0.6805D-01	-0.2737D 03	16
0.59560D 03	-23.8900	-13.2412	-0.0110	0.1153	-0.0110	0.0538	0.6805D-01	-0.2663D 03	16
0.60060D 03	-23.9434	-12.9666	-0.0104	0.1174	-0.0104	0.0560	0.6805D-01	-0.2588D 03	19
0.60556D 03	-23.9936	-12.6835	-0.0098	0.1196	-0.0098	0.0581	0.6805D-01	-0.2511D 03	19
0.61041D 03	-24.0401	-12.3963	-0.0093	0.1218	-0.0093	0.0603	0.6805D-01	-0.2433D 03	20
0.61530D 03	-24.0845	-12.0965	-0.0088	0.1239	-0.0088	0.0625	0.6805D-01	-0.2352D 03	2
0.62002D 03	-24.1250	-11.7967	-0.0084	0.1261	-0.0084	0.0646	0.6805D-01	-0.2271D 03	2
0.62471D 03	-24.1633	-11.4885	-0.0079	0.1283	-0.0079	0.0668	0.6805D-01	-0.2189D 03	2
0.62931D 03	-24.1988	-11.1761	-0.0075	0.1304	-0.0075	0.0689	0.6805D-01	-0.2105D 03	26
0.63390D 03	-24.2322	-10.8553	-0.0071	0.1326	-0.0071	0.0711	0.6805D-01	-0.2020D 03	26
0.63840D 03	-24.2634	-10.5303	-0.0067	0.1347	-0.0067	0.0732	0.6805D-01	-0.1934D 03	28
0.64289D 03	-24.2927	-10.1969	-0.0064	0.1368	-0.0064	0.0753	0.6805D-01	-0.1846D 03	2
0.64726D 03	-24.3198	--9.8635	-0.0060	0.1389	-0.0060	0.0774	0.6805D-01	-0.1758D 03	34
0.65156D 03	-24.3449	-9.5259	-0.0057	0.1409	-0.0057	0.0794	0.6805D-01	-0.1669D 03	2

DATA SUBSET 610101 PARTICLE PARAMETER 1.106800D 00 VELOCITY PARAMETER 0.17000D 00 PAGE 9

EDDY SPACING- IN X DIRN. 5.06250D 01 IN Y DIRN. 5.06250D 01 GRAVITATIONAL PARAMETER 1.0000D 00

TIME	COORDINATES X	COORDINATES Y	FLUID VELOCITY COMPONENTS X	FLUID VELOCITY COMPONENTS Y	PARTICLE VELOCITY COMPONENTS X	PARTICLE VELOCITY COMPONENTS Y	REYNOLDS NUMBER	WORK-MOMENT ON PARTICLE	TRIALS
0.65156D 03	-24.3449	-9.5259	-0.0057	0.1409	-0.0057	0.0794	0.6805D-01	-0.1669D 03	2
0.65581D 03	-24.3684	-9.1842	-0.0054	0.1429	-0.0054	0.0814	0.6805D-01	-0.1580D 03	2
0.65991D 03	-24.3898	-8.8466	-0.0051	0.1448	-0.0051	0.0833	0.6805D-01	-0.1492D 03	2
0.66397D 03	-24.4099	-8.5049	-0.0048	0.1466	-0.0048	0.0851	0.6805D-01	-0.1404D 03	2
0.66804D 03	-24.4288	-8.1547	-0.0045	0.1485	-0.0045	0.0870	0.6806D-01	-0.1313D 03	2
0.67202D 03	-24.4463	-7.8046	-0.0043	0.1502	-0.0043	0.0887	0.6806D-01	-0.1223D 03	2
0.67593D 03	-24.4624	-7.4544	-0.0040	0.1519	-0.0040	0.0904	0.6806D-01	-0.1134D 03	2
0.67977D 03	-24.4773	-7.1043	-0.0038	0.1535	-0.0038	0.0920	0.6806D-01	-0.1044D 03	2
0.68354D 03	-24.4910	-6.7542	-0.0035	0.1551	-0.0035	0.0936	0.6806D-01	-0.9551D 02	2
0.68725D 03	-24.5037	-6.4041	-0.0033	0.1566	-0.0033	0.0951	0.6806D-01	-0.8663D 02	2
0.69091D 03	-24.5154	-6.0540	-0.0031	0.1580	-0.0031	0.0965	0.6806D-01	-0.7777D 02	2

END OF RESULTS FOR DATA SUBSET 610101

VELOCITY PARAMETER 0.17000D 00

LAST COMPUTED POINT ON TRAJECTORY -

NUMBER 5075

TIME 6.909077752064339000D 02

POSITION COORDINATES X -2.451537050601946000D 01
Y -6.053980655875831000D 00

PARTICLE VELOCITY COMPONENTS X -3.084578750405562000D-03
Y 9.646066301329300000D-02

```
INPUT DATA FOR DATA SET  620100 - THIS IS SET NUMBER  1 OF  1 SET/S TO BE READ IN RUN  62

PARTICLE PARAMETER        1.10680000D 00

SPACING OF EDDY CENTRES - X      5.06250D 01
                          Y      5.06250D 01

GRAVITATIONAL PARAMETER     1.00000D 00

STARTING POINT -    X        -2.45153705060194600OD 01
                    Y        -6.0539806558758310000D 00
STARTING TIME                 6.9090777520643390000D 02

NUMBER OF STEPS      10000

STEP LIMIT    2.00D-02

CONVERGENCE CRITERION    1.00D-07

ADDED MASS COEFFICIENT    0.50D 00

WEIGHTING FACTOR     2.00D 00

PARTICLE VELOCITY COMPONENTS AT STARTING POINT HAVE BEEN READ IN.
                               UPTT -0.308457875040556100D-02
                               VPTT  0.964606630132930000D-01

VELOCITY PARAMETERS  0.1700D 00

COORDINATES AND VELOCITIES ARE PRINTED FOR EACH OF THE FIRST  50 COMPUTED POINTS, AND
THEN AFTER EVERY   25 POINTS.

IF KPUNCH IS SET NE 0, A CARD IS PUNCHED AFTER EVERY   25 COMPUTED POINTS.

STARTING CODE  KSTART   1  - EQUALS 1 IF PARTICLE VELOCITY COMPONENTS AT STARTING
POINT ARE TO BE READ IN.

PUNCHING CODE  KPUNCH   1  - EQUALS 0 IF NO CARD OUTPUT  IS REQUIRED.

TIME LIMIT PARAMETER  ITIME   9
```

START OF RESULTS FOR DATA SUBSET   620101

VELOCITY PARAMETER   0.17000D 00

VELOCITY DISTRIBUTION - INFINITE EDDY ARRAY.

DATA SUBSET 620101 PARTICLE PARAMETER 1.106800D 00 VELOCITY PARAMETER 0.17000D 00 PAGE 1

EDDY SPACING- IN X DIRN. 5.06250D 01 IN Y DIRN. 5.06250D 01 GRAVITATIONAL PARAMETER 1.0000D 00

TIME	COORDINATES X	COORDINATES Y	FLUID VELOCITY COMPONENTS X	FLUID VELOCITY COMPONENTS Y	PARTICLE VELOCITY COMPONENTS X	PARTICLE VELOCITY COMPONENTS Y	REYNOLDS NUMBER	WORK-MOMENT ON PARTICLE	TRIALS
0.69091D 03	-24.5154	-6.0540	-0.0031	0.1580	-0.0031	0.0965	0.6806D-01	0.0	0
0.69105D 03	-24.5158	-6.0400	-0.0031	0.1580	-0.0031	0.0965	0.6806D-01	0.3537D 00	2
0.69120D 03	-24.5163	-6.0260	-0.0031	0.1581	-0.0031	0.0966	0.6806D-01	0.7074D 00	2
0.69134D 03	-24.5167	-6.0120	-0.0031	0.1581	-0.0031	0.0966	0.6806D-01	0.1061D 01	2
0.69149D 03	-24.5171	-5.9980	-0.0031	0.1582	-0.0031	0.0967	0.6806D-01	0.1415D 01	2
0.69163D 03	-24.5176	-5.9840	-0.0030	0.1582	-0.0030	0.0967	0.6806D-01	0.1768D 01	2
0.69178D 03	-24.5180	-5.9700	-0.0030	0.1583	-0.0030	0.0968	0.6806D-01	0.2122D 01	2
0.69192D 03	-24.5185	-5.9560	-0.0030	0.1583	-0.0030	0.0968	0.6806D-01	0.2475D 01	2
0.69207D 03	-24.5189	-5.9419	-0.0030	0.1584	-0.0030	0.0969	0.6806D-01	0.2829D 01	2
0.69221D 03	-24.5193	-5.9279	-0.0030	0.1584	-0.0030	0.0969	0.6806D-01	0.3182D 01	2
0.69236D 03	-24.5198	-5.9139	-0.0030	0.1585	-0.0030	0.0970	0.6806D-01	0.3536D 01	2
0.69250D 03	-24.5202	-5.8999	-0.0030	0.1585	-0.0030	0.0971	0.6806D-01	0.3889D 01	2
0.69264D 03	-24.5206	-5.8859	-0.0030	0.1586	-0.0030	0.0971	0.6806D-01	0.4242D 01	2
0.69279D 03	-24.5211	-5.8719	-0.0030	0.1586	-0.0030	0.0972	0.6806D-01	0.4595D 01	2
0.69293D 03	-24.5215	-5.8579	-0.0030	0.1587	-0.0030	0.0972	0.6806D-01	0.4949D 01	2
0.69308D 03	-24.5219	-5.8439	-0.0030	0.1588	-0.0030	0.0973	0.6806D-01	0.5302D 01	2
0.69322D 03	-24.5223	-5.8299	-0.0029	0.1588	-0.0029	0.0973	0.6806D-01	0.5655D 01	2
0.69336D 03	-24.5228	-5.8159	-0.0029	0.1589	-0.0029	0.0974	0.6806D-01	0.6008D 01	2
0.69351D 03	-24.5232	-5.8019	-0.0029	0.1589	-0.0029	0.0974	0.6806D-01	0.6361D 01	2
0.69365D 03	-24.5236	-5.7879	-0.0029	0.1590	-0.0029	0.0975	0.6806D-01	0.6714D 01	2
0.69380D 03	-24.5240	-5.7739	-0.0029	0.1590	-0.0029	0.0975	0.6806D-01	0.7067D 01	2
0.69394D 03	-24.5245	-5.7599	-0.0029	0.1591	-0.0029	0.0976	0.6806D-01	0.7420D 01	2
0.69408D 03	-24.5249	-5.7459	-0.0029	0.1591	-0.0029	0.0976	0.6806D-01	0.7773D 01	2
0.69423D 03	-24.5253	-5.7319	-0.0029	0.1592	-0.0029	0.0977	0.6806D-01	0.8126D 01	2
0.69437D 03	-24.5257	-5.7179	-0.0029	0.1592	-0.0029	0.0977	0.6806D-01	0.8478D 01	2
0.69451D 03	-24.5261	-5.7039	-0.0029	0.1593	-0.0029	0.0978	0.6806D-01	0.8831D 01	2
0.69466D 03	-24.5265	-5.6899	-0.0029	0.1593	-0.0029	0.0978	0.6806D-01	0.9184D 01	2
0.69480D 03	-24.5269	-5.6759	-0.0029	0.1594	-0.0029	0.0979	0.6806D-01	0.9537D 01	2
0.69494D 03	-24.5273	-5.6619	-0.0028	0.1594	-0.0028	0.0979	0.6806D-01	0.9889D 01	2
0.69508D 03	-24.5277	-5.6479	-0.0028	0.1595	-0.0028	0.0980	0.6806D-01	0.1024D 02	2
0.69523D 03	-24.5282	-5.6339	-0.0028	0.1595	-0.0028	0.0980	0.6806D-01	0.1059D 02	2

DATA SUBSET 620101 PARTICLE PARAMETER 1.106800D 00 VELOCITY PARAMETER 0.17000D 00 PAGE 2

EDDY SPACING- IN X DIRN. 5.06250D 01 IN Y DIRN. 5.06250D 01 GRAVITATIONAL PARAMETER 1.0000D 00

TIME	COORDINATES		FLUID VELOCITY COMPONENTS		PARTICLE VELOCITY COMPONENTS		REYNOLDS NUMBER	WORK-MOMENT ON PARTICLE	TRIALS
	X	Y	X	Y	X	Y			
0.69523D 03	-24.5282	-5.6339	-0.0028	0.1595	-0.0028	0.0980	0.6806D-01	0.1059D 02	2
0.69537D 03	-24.5286	-5.6199	-0.0028	0.1596	-0.0028	0.0981	0.6806D-01	0.1095D 02	2
0.69551D 03	-24.5290	-5.6059	-0.0028	0.1596	-0.0028	0.0981	0.6806D-01	0.1130D 02	2
0.69566D 03	-24.5294	-5.5919	-0.0028	0.1597	-0.0028	0.0982	0.6806D-01	0.1165D 02	2
0.69580D 03	-24.5298	-5.5779	-0.0028	0.1597	-0.0028	0.0982	0.6806D-01	0.1200D 02	2
0.69594D 03	-24.5302	-5.5639	-0.0028	0.1598	-0.0028	0.0983	0.6806D-01	0.1236D 02	2
0.69608D 03	-24.5306	-5.5498	-0.0028	0.1598	-0.0028	0.0983	0.6806D-01	0.1271D 02	2
0.69623D 03	-24.5310	-5.5358	-0.0028	0.1599	-0.0028	0.0984	0.6806D-01	0.1306D 02	2
0.69637D 03	-24.5313	-5.5218	-0.0028	0.1599	-0.0028	0.0984	0.6806D-01	0.1341D 02	2
0.69651D 03	-24.5317	-5.5078	-0.0028	0.1600	-0.0028	0.0985	0.6806D-01	0.1377D 02	2
0.69665D 03	-24.5321	-5.4938	-0.0028	0.1600	-0.0028	0.0985	0.6806D-01	0.1412D 02	2
0.69679D 03	-24.5325	-5.4798	-0.0027	0.1601	-0.0027	0.0986	0.6806D-01	0.1447D 02	2
0.69694D 03	-24.5329	-5.4658	-0.0027	0.1601	-0.0027	0.0986	0.6806D-01	0.1482D 02	2
0.69708D 03	-24.5333	-5.4518	-0.0027	0.1602	-0.0027	0.0987	0.6806D-01	0.1517D 02	2
0.69722D 03	-24.5337	-5.4378	-0.0027	0.1602	-0.0027	0.0987	0.6806D-01	0.1553D 02	2
0.69736D 03	-24.5341	-5.4238	-0.0027	0.1603	-0.0027	0.0988	0.6806D-01	0.1588D 02	2
0.69750D 03	-24.5345	-5.4098	-0.0027	0.1603	-0.0027	0.0988	0.6806D-01	0.1623D 02	2
0.69765D 03	-24.5348	-5.3958	-0.0027	0.1604	-0.0027	0.0989	0.6806D-01	0.1658D 02	2
0.69779D 03	-24.5352	-5.3818	-0.0027	0.1604	-0.0027	0.0989	0.6806D-01	0.1693D 02	2
0.69793D 03	-24.5356	-5.3678	-0.0027	0.1605	-0.0027	0.0990	0.6806D-01	0.1729D 02	2
0.70144D 03	-24.5447	-5.0177	-0.0025	0.1616	-0.0025	0.1002	0.6806D-01	0.2607D 02	2
0.70492D 03	-24.5530	-4.6676	-0.0023	0.1627	-0.0023	0.1012	0.6806D-01	0.3483D 02	2
0.70836D 03	-24.5605	-4.3176	-0.0021	0.1638	-0.0021	0.1023	0.6806D-01	0.4357D 02	2
0.71177D 03	-24.5673	-3.9675	-0.0019	0.1647	-0.0019	0.1032	0.6806D-01	0.5230D 02	2
0.71515D 03	-24.5735	-3.6174	-0.0017	0.1656	-0.0017	0.1041	0.6806D-01	0.6100D 02	2
0.71850D 03	-24.5790	-3.2674	-0.0016	0.1663	-0.0016	0.1049	0.6806D-01	0.6969D 02	2
0.72182D 03	-24.5839	-2.9173	-0.0014	0.1671	-0.0014	0.1056	0.6806D-01	0.7837D 02	2
0.72513D 03	-24.5882	-2.5673	-0.0012	0.1677	-0.0012	0.1062	0.6806D-01	0.8703D 02	2
0.72842D 03	-24.5919	-2.2173	-0.0010	0.1682	-0.0010	0.1067	0.6806D-01	0.9568D 02	2
0.73169D 03	-24.5950	-1.8672	-0.0009	0.1687	-0.0009	0.1072	0.6806D-01	0.1043D 03	2
0.73495D 03	-24.5976	-1.5172	-0.0007	0.1691	-0.0007	0.1076	0.6806D-01	0.1129D 03	2

DATA SUBSET 620101 PARTICLE PARAMETER 1.106800D 00 VELOCITY PARAMETER 0.17000D 00 PAGE 3

EDDY SPACING- IN X DIRN. 5.06250D 01 IN Y DIRN. 5.06250D 01 GRAVITATIONAL PARAMETER 1.0000D 00

TIME	COORDINATES X	COORDINATES Y	FLUID VELOCITY COMPONENTS X	FLUID VELOCITY COMPONENTS Y	PARTICLE VELOCITY COMPONENTS X	PARTICLE VELOCITY COMPONENTS Y	REYNOLDS NUMBER	WORK-MOMENT ON PARTICLE	TRIALS
0.73495D 03	-24.5976	-1.5172	-0.0007	0.1691	-0.0007	0.1076	0.6806D-01	0.1129D 03	2
0.73820D 03	-24.5997	-1.1672	-0.0005	0.1694	-0.0005	0.1079	0.6806D-01	0.1216D 03	2
0.74144D 03	-24.6012	-0.8172	-0.0004	0.1696	-0.0004	0.1081	0.6806D-01	0.1302D 03	2
0.74467D 03	-24.6021	-0.4672	-0.0002	0.1698	-0.0002	0.1083	0.6806D-01	0.1388D 03	2
0.74790D 03	-24.6026	-0.1172	-0.0001	0.1698	-0.0001	0.1083	0.6806D-01	0.1474D 03	2
0.75163D 03	-24.6024	0.2868	0.0001	0.1698	0.0001	0.1083	0.6806D-01	0.1574D 03	5
0.75581D 03	-24.6014	0.7388	0.0003	0.1697	0.0003	0.1082	0.6806D-01	0.1685D 03	2
0.75999D 03	-24.5995	1.1908	0.0006	0.1694	0.0006	0.1079	0.6806D-01	0.1796D 03	2
0.76413D 03	-24.5968	1.6368	0.0008	0.1690	0.0008	0.1075	0.6806D-01	0.1906D 03	9
0.76835D 03	-24.5931	2.0887	0.0010	0.1684	0.0010	0.1069	0.6806D-01	0.2017D 03	2
0.77259D 03	-24.5885	2.5407	0.0012	0.1677	0.0012	0.1062	0.6806D-01	0.2129D 03	2
0.77680D 03	-24.5830	2.9866	0.0014	0.1669	0.0014	0.1054	0.6806D-01	0.2239D 03	9
0.78111D 03	-24.5764	3.4385	0.0016	0.1660	0.0016	0.1045	0.6806D-01	0.2351D 03	2
0.78545D 03	-24.5688	3.8904	0.0019	0.1649	0.0019	0.1034	0.6806D-01	0.2464D 03	2
0.78979D 03	-24.5601	4.3363	0.0021	0.1637	0.0021	0.1022	0.6806D-01	0.2575D 03	7
0.79424D 03	-24.5502	4.7882	0.0024	0.1624	0.0024	0.1009	0.6806D-01	0.2687D 03	2
0.79857D 03	-24.5395	5.2221	0.0026	0.1610	0.0026	0.0995	0.6806D-01	0.2796D 03	2
0.80211D 03	-24.5300	5.5720	0.0028	0.1597	0.0028	0.0983	0.6806D-01	0.2884D 03	2
0.80569D 03	-24.5196	5.9219	0.0030	0.1585	0.0030	0.0970	0.6806D-01	0.2972D 03	2
0.80933D 03	-24.5083	6.2718	0.0032	0.1571	0.0032	0.0956	0.6806D-01	0.3060D 03	2
0.81301D 03	-24.4960	6.6217	0.0034	0.1556	0.0034	0.0942	0.6806D-01	0.3149D 03	2
0.81676D 03	-24.4827	6.9716	0.0037	0.1541	0.0037	0.0926	0.6806D-01	0.3238D 03	2
0.82057D 03	-24.4682	7.3214	0.0039	0.1525	0.0039	0.0911	0.6806D-01	0.3327D 03	2
0.82445D 03	-24.4526	7.6713	0.0042	0.1509	0.0042	0.0894	0.6806D-01	0.3417D 03	2
0.82840D 03	-24.4357	8.0212	0.0044	0.1491	0.0044	0.0877	0.6806D-01	0.3506D 03	2
0.83243D 03	-24.4173	8.3710	0.0047	0.1473	0.0047	0.0859	0.6806D-01	0.3596D 03	2
0.83645D 03	-24.3980	8.7125	0.0050	0.1455	0.0050	0.0840	0.6806D-01	0.3685D 03	2
0.84056D 03	-24.3770	9.0539	0.0053	0.1436	0.0053	0.0821	0.6806D-01	0.3773D 03	2
0.84472D 03	-24.3545	9.3912	0.0056	0.1417	0.0056	0.0802	0.6806D-01	0.3861D 03	2
0.84897D 03	-24.3302	9.7284	0.0059	0.1397	0.0059	0.0782	0.6806D-01	0.3949D 03	2
0.85329D 03	-24.3041	10.0614	0.0062	0.1377	0.0062	0.0762	0.6806D-01	0.4037D 03	33

DATA SUBSET 620101 PARTICLE PARAMETER 1.10680D 00 VELOCITY PARAMETER 0.17000D 00 PAGE 4

EDDY SPACING- IN X DIRN. 5.06250D 01 IN Y DIRN. 5.06250D 01 GRAVITATIONAL PARAMETER 1.0000D 00

TIME	COORDINATES X	COORDINATES Y	FLUID VELOCITY COMPONENTS X	FLUID VELOCITY COMPONENTS Y	PARTICLE VELOCITY COMPONENTS X	PARTICLE VELOCITY COMPONENTS Y	REYNOLDS NUMBER	WORK-MOMENT ON PARTICLE	TRIALS
0.85329D 03	-24.3041	10.0614	0.0062	0.1377	0.0062	0.0762	0.6806D-01	0.4037D 03	33
0.85778D 03	-24.2754	10.3986	0.0066	0.1355	0.0066	0.0740	0.6806D-01	0.4125D 03	2
0.86234D 03	-24.2445	10.7316	0.0070	0.1334	0.0070	0.0719	0.6806D-01	0.4214D 03	29
0.86693D 03	-24.2117	11.0562	0.0074	0.1312	0.0074	0.0697	0.6806D-01	0.4300D 03	2
0.87153D 03	-24.1769	11.3724	0.0078	0.1291	0.0078	0.0676	0.6806D-01	0.4384D 03	2
0.87616D 03	-24.1400	11.6802	0.0082	0.1269	0.0082	0.0654	0.6806D-01	0.4466D 03	23
0.88094D 03	-24.0997	11.9880	0.0087	0.1247	0.0087	0.0632	0.6806D-01	0.4549D 03	2
0.88569D 03	-24.0575	12.2832	0.0091	0.1226	0.0091	0.0611	0.6806D-01	0.4629D 03	20
0.89054D 03	-24.0120	12.5742	0.0096	0.1204	0.0096	0.0589	0.6806D-01	0.4707D 03	18
0.89550D 03	-23.9629	12.8609	0.0102	0.1183	0.0102	0.0568	0.6806D-01	0.4783D 03	2
0.90050D 03	-23.9105	13.1393	0.0108	0.1161	0.0108	0.0546	0.6806D-01	0.4861D 03	16
0.90554D 03	-23.8548	13.4093	0.0114	0.1140	0.0114	0.0525	0.6806D-01	0.4935D 03	17
0.91071D 03	-23.7945	13.6751	0.0120	0.1119	0.0120	0.0504	0.6806D-01	0.5007D 03	15
0.91589D 03	-23.7306	13.9308	0.0127	0.1098	0.0127	0.0483	0.6807D-01	0.5078D 03	16
0.92107D 03	-23.6632	14.1756	0.0134	0.1078	0.0134	0.0463	0.6807D-01	0.5145D 03	16
0.92647D 03	-23.5887	14.4203	0.0142	0.1057	0.0142	0.0442	0.6807D-01	0.5213D 03	14
0.93214D 03	-23.5061	14.6651	0.0150	0.1037	0.0150	0.0422	0.6807D-01	0.5280D 03	14
0.93780D 03	-23.4186	14.8981	0.0159	0.1017	0.0159	0.0402	0.6807D-01	0.5345D 03	12
0.94329D 03	-23.3288	15.1135	0.0168	0.0998	0.0168	0.0383	0.6807D-01	0.5405D 03	10
0.94882D 03	-23.2331	15.3201	0.0178	0.0980	0.0178	0.0365	0.6807D-01	0.5462D 03	25
0.95438D 03	-23.1313	15.5178	0.0188	0.0962	0.0188	0.0347	0.6807D-01	0.5517D 03	25
0.95987D 03	-23.0249	15.7038	0.0199	0.0945	0.0199	0.0330	0.6807D-01	0.5569D 03	21
0.96528D 03	-22.9143	15.8781	0.0210	0.0929	0.0210	0.0314	0.6807D-01	0.5618D 03	23
0.97075D 03	-22.7963	16.0453	0.0222	0.0913	0.0222	0.0298	0.6807D-01	0.5664D 03	40
0.97629D 03	-22.6700	16.2064	0.0234	0.0898	0.0234	0.0283	0.6807D-01	0.5709D 03	19
0.98183D 03	-22.5365	16.3592	0.0248	0.0883	0.0248	0.0268	0.6807D-01	0.5752D 03	17
0.98735D 03	-22.3961	16.5033	0.0261	0.0869	0.0261	0.0254	0.6807D-01	0.5792D 03	32
0.99282D 03	-22.2492	16.6388	0.0276	0.0856	0.0276	0.0241	0.6807D-01	0.5830D 03	17
0.99847D 03	-22.0890	16.7710	0.0291	0.0842	0.0291	0.0227	0.6807D-01	0.5866D 03	19
0.10039D 04	-21.9255	16.8917	0.0307	0.0830	0.0307	0.0215	0.6807D-01	0.5900D 03	21
0.10094D 04	-21.7530	17.0058	0.0324	0.0818	0.0324	0.0203	0.6807D-01	0.5931D 03	22

DATA SUBSET 620101 PARTICLE PARAMETER 1.106800D 00 VELOCITY PARAMETER 0.17000D 00 PAGE 5

EDDY SPACING- IN X DIRN. 5.06250D 01 IN Y DIRN. 5.06250D 01 GRAVITATIONAL PARAMETER 1.0000D 00

TIME	COORDINATES X	COORDINATES Y	FLUID VELOCITY COMPONENTS X	FLUID VELOCITY COMPONENTS Y	PARTICLE VELOCITY COMPONENTS X	PARTICLE VELOCITY COMPONENTS Y	REYNOLDS NUMBER	WORK-MOMENT ON PARTICLE	TRIALS
0.10094D 04	-21.7530	17.0058	0.0324	0.0818	0.0324	0.0203	0.6807D-01	0.5931D 03	22
0.10148D 04	-21.5724	17.1126	0.0341	0.0806	0.0341	0.0191	0.6807D-01	0.5961D 03	25
0.10204D 04	-21.3772	17,2156	0.0360	0.0794	0.0360	0.0179	0.6807D-01	0.5989D 03	10
0.10259D 04	-21.1731	17.3115	0.0380	0.0783	0.0380	0.0168	0.6807D-01	0.6015D 03	10
0.10314D 04	-20.9573	17.4016	0.0400	0.0772	0.0400	0.0157	0.6807D-01	0.6040D 03	12
0.10370D 04	-20.7297	17.4858	0.0422	0.0762	0.0422	0.0147	0.6807D-01	0.6063D 03	12
0.10424D 04	-20.4933	17.5631	0.0444	0.0751	0.0444	0.0136	0.6807D-01	0.6084D 03	13
0.10478D 04	-20.2510	17.6331	0.0467	0.0742	0.0467	0.0127	0.6807D-01	0.6103D 03	14
0.10529D 04	-20.0057	17.6957	0.0489	0.0732	0.0489	0.0117	0.6807D-01	0.6119D 03	16
0.10578D 04	-19.7605	17.7510	0.0512	0.0724	0.0512	0.0109	0.6807D-01	0.6134D 03	16
0.10625D 04	-19.5153	17.7999	0.0535	0.0715	0.0535	0.0100	0.6807D-01	0.6147D 03	18
0.10676D 04	-19.2364	17.8486	0.0560	0.0706	0.0560	0.0091	0.6807D-01	0.6160D 03	16
0.10725D 04	-18.9534	17.8915	0.0585	0.0697	0.0585	0.0082	0.6807D-01	0.6171D 03	21
0.10774D 04	-18.6619	17.9296	0.0612	0.0689	0.0611	0.0074	0.6807D-01	0.6181D 03	20
0.10822D 04	-18.3621	17.9629	0.0638	0.0680	0.0638	0.0065	0.6807D-01	0.6190D 03	2
0.10867D 04	-18.0664	17.9906	0.0664	0.0672	0.0664	0.0057	0.6807D-01	0.6197D 03	24
0.10914D 04	-17.7498	18.0152	0.0691	0.0663	0.0691	0.0048	0.6807D-01	0.6203D 03	26
0.10959D 04	-17.4331	18.0351	0.0718	0.0655	0.0718	0.0040	0.6807D-01	0.6208D 03	2
0.11002D 04	-17.1165	18.0506	0.0745	0.0647	0.0745	0.0032	0.6807D-01	0.6212D 03	2
0.11045D 04	-16.7914	18.0632	0.0772	0.0638	0.0772	0.0023	0.6807D-01	0.6215D 03	2
0.11087D 04	-16.4622	18.0704	0.0799	0.0630	0.0799	0.0015	0.6807D-01	0.6217D 03	2
0.11128D 04	-16.1330	18.0747	0.0826	0.0622	0.0826	0.0007	0.6807D-01	0.6218D 03	38
0.11168D 04	-15.7912	18.0756	0.0853	0.0613	0.0853	-0.0002	0.6807D-01	0.6219D 03	2
0.11208D 04	-15.4451	18.0731	0.0880	0.0604	0.0880	-0.0011	0.6807D-01	0.6218D 03	2
0.11247D 04	-15.0949	18.0671	0.0907	0.0595	0.0907	-0.0020	0.6807D-01	0.6217D 03	2
0.11286D 04	-14.7447	18.0579	0.0933	0.0586	0.0933	-0.0029	0.6807D-01	0.6215D 03	2
0.11323D 04	-14.3945	18.0456	0.0959	0.0577	0.0959	-0.0038	0.6807D-01	0.6212D 03	2
0.11359D 04	-14.0444	18.0303	0.0984	0.0568	0.0984	-0.0047	0.6807D-01	0.6208D 03	2
0.11394D 04	-13.6942	18.0123	0.1009	0.0559	0.1009	-0.0056	0.6807D-01	0.6204D 03	2
0.11428D 04	-13.3440	17.9914	0.1033	0.0550	0.1033	-0.0065	0.6807D-01	0.6200D 03	2
0.11462D 04	-12.9939	17.9679	0.1057	0.0540	0.1056	-0.0075	0.6807D-01	0.6195D 03	2

DATA OF SORT 020101   PARTICLE PARAMETER 1.106800D 00   VELOCITY PARAMETER 0.17000D 00   PAGE 6

BODY SPACING- IN X DIRN. 5.06250D 01   IN Y DIRN. 5.06250D 01   GRAVITATIONAL PARAMETER 1.0000D 00

TIME	COORDINATES X	COORDINATES Y	FLUID VELOCITY COMPONENTS X	FLUID VELOCITY COMPONENTS Y	PARTICLE VELOCITY COMPONENTS X	PARTICLE VELOCITY COMPONENTS Y	REYNOLDS NUMBER	WORK-MOMENT ON PARTICLE	TRIALS
0.11462D 04	-12.9939	17.9679	0.1057	0.0540	0.1056	-0.0075	0.6807D-01	0.6195D 03	2
0.11494D 04	-12.6437	17.9418	0.1079	0.0530	0.1079	-0.0085	0.6806D-01	0.6189D 03	2
0.11526D 04	-12.2936	17.9131	0.1102	0.0521	0.1101	-0.0094	0.6806D-01	0.6183D 03	2
0.11558D 04	-11.9434	17.8819	0.1123	0.0511	0.1123	-0.0104	0.6806D-01	0.6176D 03	2
0.11589D 04	-11.5933	17.8481	0.1144	0.0501	0.1144	-0.0114	0.6806D-01	0.6169D 03	2
0.11619D 04	-11.2432	17.8118	0.1164	0.0490	0.1164	-0.0125	0.6806D-01	0.6161D 03	2
0.11649D 04	-10.8931	17.7731	0.1184	0.0480	0.1184	-0.0135	0.6806D-01	0.6153D 03	2
0.11678D 04	-10.5430	17.7318	0.1202	0.0469	0.1202	-0.0146	0.6806D-01	0.6145D 03	2
0.11707D 04	-10.1929	17.6880	0.1220	0.0458	0.1220	-0.0157	0.6806D-01	0.6136D 03	2
0.11736D 04	-9.8428	17.6418	0.1238	0.0447	0.1238	-0.0168	0.6806D-01	0.6126D 03	2
0.11764D 04	-9.4927	17.5929	0.1254	0.0435	0.1254	-0.0180	0.6806D-01	0.6116D 03	2
0.11792D 04	-9.1426	17.5415	0.1270	0.0424	0.1270	-0.0191	0.6806D-01	0.6106D 03	2
0.11819D 04	-8.7925	17.4875	0.1285	0.0412	0.1285	-0.0203	0.6806D-01	0.6096D 03	2
0.11846D 04	-8.4424	17.4308	0.1299	0.0400	0.1299	-0.0215	0.6806D-01	0.6085D 03	2
0.11873D 04	-8.0923	17.3715	0.1313	0.0387	0.1313	-0.0228	0.6805D-01	0.6073D 03	2
0.11899D 04	-7.7423	17.3093	0.1325	0.0374	0.1325	-0.0240	0.6805D-01	0.6062D 03	2
0.11926D 04	-7.3922	17.2224	0.1337	0.0361	0.1337	-0.0254	0.6805D-01	0.6049D 03	2
0.11952D 04	-7.0422	17.1766	0.1348	0.0348	0.1348	-0.0267	0.6805D-01	0.6037D 03	2
0.11978D 04	-6.6921	17.1058	0.1358	0.0334	0.1358	-0.0280	0.6805D-01	0.6024D 03	2
0.12003D 04	-6.3421	17.0320	0.1367	0.0320	0.1367	-0.0294	0.6805D-01	0.6010D 03	2
0.12029D 04	-5.9920	16.9550	0.1376	0.0306	0.1376	-0.0309	0.6805D-01	0.5996D 03	2
0.12054D 04	-5.6420	16.8749	0.1383	0.0292	0.1383	-0.0323	0.6805D-01	0.5982D 03	2
0.12079D 04	-5.2919	16.7914	0.1389	0.0277	0.1389	-0.0338	0.6805D-01	0.5967D 03	2
0.12105D 04	-4.9419	16.7044	0.1395	0.0261	0.1395	-0.0354	0.6805D-01	0.5952D 03	2
0.12130D 04	-4.5919	16.6139	0.1399	0.0246	0.1400	-0.0369	0.6805D-01	0.5936D 03	2
0.12155D 04	-4.2419	16.5917	0.1403	0.0230	0.1403	-0.0385	0.6804D-01	0.5920D 03	2
0.12180D 04	-3.8919	16.4217	0.1406	0.0213	0.1406	-0.0402	0.6804D-01	0.5904D 03	2
0.12204D 04	-3.5419	16.3197	0.1407	0.0196	0.1408	-0.0418	0.6804D-01	0.5887D 03	2
0.12229D 04	-3.1919	16.2135	0.1408	0.0179	0.1408	-0.0436	0.6804D-01	0.5869D 03	2
0.12254D 04	-2.8419	16.1030	0.1408	0.0161	0.1408	-0.0453	0.6804D-01	0.5851D 03	2
0.12279D 04	-2.4919	15.9880	0.1406	0.0143	0.1406	-0.0472	0.6804D-01	0.5832D 03	2

DATA SUBSET 620101 PARTICLE PARAMETER 1.106800D 00 VELOCITY PARAMETER 0.17000D 00 PAGE 7

EDDY SPACING- IN X DIRN. 5.06250D 01 IN Y DIRN. 5.06250D 01 GRAVITATIONAL PARAMETER 1.0000D 00

TIME	COORDINATES		FLUID VELOCITY COMPONENTS		PARTICLE VELOCITY COMPONENTS		REYNOLDS NUMBER	WORK-MOMENT ON PARTICLE	
	X	Y	X	Y	X	Y			TRIALS
0.12279D 04	-2.4919	15.9880	0.1406	0.0143	0.1406	-0.0472	0.6804D-01	0.5832D 03	2
0.12304D 04	-2.1419	15.8682	0.1404	0.0125	0.1404	-0.0490	0.6804D-01	0.5813D 03	2
0.12329D 04	-1.7919	15.7436	0.1400	0.0106	0.1400	-0.0509	0.6804D-01	0.5793D 03	2
0.12354D 04	-1.4419	15.6137	0.1396	0.0086	0.1396	-0.0529	0.6804D-01	0.5772D 03	2
0.12379D 04	-1.0919	15.4783	0.1390	0.0066	0.1390	-0.0549	0.6804D-01	0.5751D 03	2
0.12404D 04	-0.7420	15.3373	0.1383	0.0045	0.1383	-0.0569	0.6803D-01	0.5730D 03	2
0.12430D 04	-0.3920	15.1902	0.1375	0.0024	0.1375	-0.0590	0.6803D-01	0.5707D 03	2
0.12455D 04	-0.0421	15.0367	0.1366	0.0003	0.1366	-0.0612	0.6803D-01	0.5684D 03	2
0.12481D 04	0.3079	14.8765	0.1356	-0.0020	0.1356	-0.0634	0.6803D-01	0.5660D 03	2
0.12507D 04	0.6578	14.7092	0.1344	-0.0042	0.1344	-0.0657	0.6803D-01	0.5635D 03	2

Computed Trajectory No. 620101 continues to:

0.13869D 04 9.7302 -2.3711

```
END OF RESULTS FOR DATA SUBSET     620101

VELOCITY PARAMETER   0.17000D 00

LAST COMPUTED POINT ON TRAJECTORY  -
                     NUMBER        4873
                     TIME         1.38693505048092700OD 03
                     POSITION COORDINATES  X      9.73024655302867200OD 00
                                           Y     -2.37106316013538100OD 00
                     PARTICLE VELOCITY COMPONENTS  X     -2.04632031585159200OD-02
                                                   Y     -1.56980259683745600OD-01
```

COMPUTED PARTICLE TRAJECTORY No. 4300101 (No. 1.2, Table 1)

Note: In the original computer output, computed points on the trajectory were listed at intervals of 10 computed points - that is, position coordinates etc were printed for every tenth computed point. In order to reduce the length of this tabulation, points are tabulated herein at intervals of 20 computed points, except in the region in which the trajectory intersects the line X = 0.0 after one circuit of the eddy. In this region, points are tabulated at intervals of 10 computed points, as in the original output. Such intervals are identified by an asterisk (*).

COORDINATES		COORDINATES		COORDINATES		COORDINATES		COORDINATES	
X	Y	X	Y	X	Y	X	Y	X	Y
0.0000	15.0000	6.9909	13.7371	13.1944	8.1707	14.9683	1.1692	14.1508	-5.8361
0.2720	14.9983	7.2708	13.6203	13.3357	7.8906	14.9817	0.8892	14.0599	-6.1160
0.5520	14.9930	7.5507	13.4964	13.4689	7.6105	14.9914	0.6091	13.9632	-6.3959
0.8320	14.9840	7.8306	13.3649	13.5945	7.3304	14.9975	0.3291	13.8604	-6.6758
1.1120	14.9714	8.1104	13.2255	13.7129	7.0503	14.9999	0.0491	13.7513	-6.9558
1.3920	14.9551	8.3903	13.0776	13.8244	6.7702	14.9987	-0.2369	13.6353	-7.2356
1.6719	14.9350	8.6702	12.9207	13.9294	6.4901	14.9938	-0.5169	13.5123	-7.5155
1.9519	14.9113	8.9500	12.7542	14.0281	6.2100	14.9853	-0.7968	13.3819	-7.7954
2.2319	14.8837	9.2299	12.5773	14.1209	5.9299	14.9731	-1.0768	13.2434	-8.0753
2.5119	14.8523	9.5097	12.3894	14.2081	5.6498	14.9573	-1.3568	13.0966	-8.3552
2.7918	14.8169	9.7895	12.1895	14.2898	5.3698	14.9378	-1.6368	12.9409	-8.6350
3.0718	14.7775	10.0693	11.9768	14.3662	5.0897	14.9145	-1.9168	12.7756	-8.9149
3.3518	14.7341	10.3491	11.7499	14.4376	4.8096	14.8874	-2.1968	12.6001	-9.1947
3.6317	14.6865	10.6289	11.5078	14.5042	4.5296	14.8564	-2.4767	12.4136	-9.4746
3.9117	14.6345	10.9087	11.2488	14.5660	4.2495	14.8216	-2.7567	12.2153	-9.7544
4.1916	14.5782	11.1872	10.9725	14.6233	3.9695	14.7827	-3.0367	12.0042	-10.0342
4.4716	14.5174	11.4507	10.6923	14.6761	3.6894	14.7398	-3.3166	11.7792	-10.3140
4.7515	14.4519	11.6969	10.4120	14.7246	3.4094	14.6927	-3.5966	11.5391	-10.5938
5.0314	14.3815	11.9274	10.1318	14.7689	3.1293	14.6413	-3.8765	11.2823	-10.8736
5.3114	14.3062	12.1435	9.8517	14.8091	2.8493	14.5855	-4.1565	11.0077	-11.1528
5.5913	14.2256	12.3463	9.5715	14.8453	2.5693	14.5253	-4.4364	10.7274	-11.4186
5.8712	14.1397	12.5370	9.2913	14.8776	2.2892	14.4603	-4.7164	10.4472	-11.6669
6.1512	14.0481	12.7164	9.0112	14.9059	2.0092	14.3906	-4.9963	10.1670	-11.8993
6.4311	13.9507	12.8853	8.7310	14.9305	1.7292	14.3159	-5.2762	9.8868	-12.1171
6.7110	13.8471	13.0444	8.4509	14.9513	1.4492	14.2360	-5.5562	9.6066	-12.3216

COMPUTED PARTICLE TRAJECTORY 4300101 (continued)

COORDINATES X	COORDINATES Y	COORDINATES X	COORDINATES Y	COORDINATES X	COORDINATES Y	COORDINATES X	COORDINATES Y	COORDINATES X	COORDINATES Y
9.3265	-12.5137	0.9243	-14.9802	-7.4804	-13.5282	-14.0039	-6.2803	-14.8945	2.1265
9.0463	-12.6945	0.6443	-14.9904	-7.7603	-13.3987	-14.0982	-6.0002	-14.8645	2.4065
8.7662	-12.8647	0.3643	-14.9969	-8.0402	-13.2613	-14.1867	-5.7201	-14.8307	2.6864
8.4860	-13.0250	0.0843	-14.9998	-8.3201	-13.1155	-14.2698	-5.4401	-14.7928	2.9664
8.2059	-13.1760	-0.2017	-14.9991	-8.5999	-12.9609	-14.3475	-5.1600	-14.7509	3.2464
7.9258	-13.3184	-0.4817	-14.9946	-8.8798	-12.7969	-14.4202	-4.8799	-14.7049	3.5263
7.6456	-13.4526	-0.7617	-14.9866	-9.1596	-12.6227	-14.4879	-4.5999	-14.6546	3.8063
7.3655	-13.5792	-1.0417	-14.9749	-9.4395	-12.4376	-14.5509	-4.3198	-14.6000	4.0862
7.0854	-13.6984	-1.3217	-14.9595	-9.7193	-12.2409	-14.6093	-4.0398	-14.5408	4.3662
6.8053	-13.8108	-1.6017	-14.9404	-9.9991	-12.0314	-14.6633	-3.7597	-14.4771	4.6461
6.5252	-13.9165	-1.8816	-14.9176	-10.2789	-11.8083	-14.7128	-3.4797	-14.4086	4.9261
6.2452	-14.0161	-2.1616	-14.8910	-10.5587	-11.5701	-14.7582	-3.1996	-14.3351	5.2060
5.9651	-14.1096	-2.4416	-14.8605	-10.8385	-11.3155	-14.7994	-2.9196	-14.2566	5.4859
5.6850	-14.1975	-2.7216	-14.8261	-11.1181	-11.0428	-14.8366	-2,6396	-14.1727	5.7658
5.4049	-14.2798	-3.0015	-14.7878	-11.3862	-10.7626	-14.8698	-2.3595	-14.0833	6.0458
5.1249	-14.3569	-3.2815	-14.7454	-11.6366	-10.4824	-14.8992	-2.0795	-13.9881	6.3257
4.8448	-14.4290	-3.5615	-14.6988	-11.8709	-10.2022	-14.9247	-1.7995	-13.8868	6.6056
4.5647	-14.4961	-3.8414	-14.6480	-12.0905	-9.9220	-14.9464	-1.5195	-13.7793	6.8855
4.2847	-14.5585	-4.1214	-14.5928	-12.2966	-9.6418	-14.9644	-1.2394	-13.6651	7.1654
4.0046	-14.6163	-4.4013	-14.5331	-12.4903	-9.3616	-14.9787	-0.9594	-13.5439	7.4453
3.7246	-14.6697	-4.6812	-14.4687	-12.6724	-9.0815	-14.9893	-0.6794	-13.4153	7.7252
3.4445	-14.7188	-4.9612	-14.3996	-12.8439	-8.8013	-14.9963	-0.3994	-13.2790	8.0051
3.1645	-14.7636	-5.2411	-14.3255	-13.0054	-8.5212	-14.9997	-0.1194	-13.1343	8.2849
2.8845	-14.8043	-5.5210	-14.2463	-13.1576	-8.2410	-14.9994	0.1666	-12.9809	8.5648
2.6044	-14.8410	-5.8010	-14.1618	-13.3010	-7.9609	-14.9954	0.4466	-12.8180	8.8447
2.3244	-14.8737	-6.0809	-14.0716	-13.4362	-7.6808	-14.9878	0.7266	-12.6451	9.1245
2.0444	-14.9026	-6.3608	-13.9757	-13.5637	-7.4007	-14.9765	1.0066	-12.4615	9.4044
1.7643	-14.9276	-6.6407	-13.8737	-13.6838	-7.1206	-14.9616	1.2865	-12.2662	9.6842
1.4843	-14.9489	-6.9206	-13.7653	-13.7970	-6.8405	-14.9430	1.5665	-12.0585	9.9640
1.2043	-14.9664	-7.2005	-13.6503	-13.9036	-6.5604	-14.9207	1.8465	-11.8371	10.2438

COMPUTED PARTICLE TRAJECTORY 4300101 (continued)

COORDINATES		COORDINATES	
X	Y	X	Y
-11.6008	10.5236	-3.2348	14.7527
-11.3484	10.8034	-2.9547	14.7945
-11.0780	11.0831	-2.6747	14.8322
-10.7978	11.3536	-2.3947	14.8659
-10.5175	11.6061	-2.1146	14.8957
-10.2373	11.8424	-1.8346	14.9217
- 9.9571	12.0637	-1.5546	14.9439
-9.6770	12.2714	-1.2746	14.9623
-9.3968	12.4666	-0.9946	14.9771
-9.1166	12.6502	-0.7146	14.9882
-8.8365	12.8229	-0.4346	14.9956
-8.5563	12.9856	-0.2946	* 14.9980
-8.2762	13.1390	-0.1546	* 14.9994
-7.9961	13.2835	-0.0146	* 15.0000
-7.7160	13.4197	0.1314	* 14.9996
-7.4358	13.5481	0.2714	* 14.9983
-7.1557	13.6691	0.4114	* 14.9961
-6.8756	13.7832		
-6.5955	13.8906		
-6.3155	13.9916		
-6.0354	14.0867		
-5.7553	14.1759		
-5.4752	14.2597		
-5.1951	14.3381		
-4.9151	14.4113		
-4.6350	14.4797		
-4.3550	14.5433		
-4.0749	14.6022		
-3.7949	14.6567		
-3.5148	14.7069		

APPENDIX IV

THE FORTRAN COMPUTER PROGRAM FOR THE PLOTTING OF THE COMPUTED PARTICLE TRAJECTORIES.

The FORTRAN program listed on pages IV.3 - IV.10 was developed for the purpose of plotting the computed trajectories of particles in the model eddy field. The plotting was carried out on the "Calcomp" Plotter at the University of New South Wales Computing Centre.

The coordinates of the computed points on the particle trajectory are read from cards (which are punched during the computation of the trajectory, as described in Section 4.5.1) together with the values of the parameters defining the eddy field and particle characteristics and the values of the significant program-control parameters. This latter information is incorporated in the title which is written on the plotted sheet.

The data subset identification numbers (that is, the trajectory identification numbers) and the card identification numbers are checked for discontinuities, as the cards are read.

The plotting scale is determined by the program, with the criterion that the plotted trajectory should be as large as possible but must, together with the title and associated information, fit within a 15 inch by 10 inch format.

The mean fall velocity, based on the vertical displacement of each computed point relative to the starting point of the trajectory, is calculated for each computed point on the trajectory, and is printed in the printed output.

The position coordinates of each point at which the computed particle trajectory crosses an eddy axis (that is, a line passing through an eddy centre parallel to either of the two coordinate axes) are calculated, together with the associated time parameter. This information is included in the printed output.

A modified version of the listed program was employed in the plotting of the computed trajectories of particles falling through waves, as described in Chapter 5.

The subroutines called in the program are library subroutines which form part of the plotter operating system at the University of New South Wales Computing Centre.

The axes of the graph have been rotated through 90°, so that the longer dimension of the graph lies along the length of the plotting paper and hence is not restricted by the width of the paper. Accordingly, the x axis of the computed trajectory coincides with the y axis of the plotter.

FORTRAN PROGRAM FOR PLOTTING THE COMPUTED PARTICLE TRAJECTORIES

```
      DIMENSION XD(3000), YD(3000), ID(100),XCR(100), YCR(100),TCR(100)
      DIMENSION SC(3)
      DATA NCP/2/,XLIM/20.0/,YLIM/10.0/,POSN/0.0/
      DATA SC/0.5,1.0 ,2.0/
      DATA NREAD/1/, NWRITE/3/
      READ (NREAD, 230) PART, UEDDY, XCNTR, YCNTR
230   FORMAT (E20.8,E10.3,2E20.8)
      READ (NREAD, 231) XSTART, YSTART, TSTART
231   FORMAT (3E20.8)
      READ (NREAD, 232) STEP, DELSCR, GRAV, W, IPUNCH
232   FORMAT  (4E10.2,I10)
      NCR = 0
      NDISC1 = 0
      NDISC2 = 0
      NPAGE = 1
      WRITE (NWRITE, 200) NPAGE
200   FORMAT ('1 DATA INPUT PAGE ',I3,//' DATA SUBSET CARD POINT N
     1UMBER ',6X,' TIME ',13X,' X ',14X,' Y ',8X,' MEAN FALL VELOCITY ',
     2//' ' )
      READ (NREAD, 201) ID1, NCARD, NL, TT1, XT1, YT1
201   FORMAT (I10,I5,I10 ,3F15.4)
      WRITE (NWRITE, 203) ID1, NCARD, NL, TT1, XT1, YT1
203   FORMAT (' ',I8,5X,I5,3X,I8,4X,F15.4,2X,F15.4,2X,F15.4,12X,E12.4)
      NLINE = 1
      XT1D = XT1/XCNTR
      YT1D = YT1/YCNTR
      X1D  = 0.0
      X2D  = 0.0
      Y1D  = 0.0
      Y2D  = 0.0
      IF (XT1D.GT.0.0) X1D = XT1D
      IF (XT1D.LT.0.0) X2D = ABS(XT1D)
      IF (YT1D.GT.0.0) Y1D = YT1D
      IF (YT1D.LT.0.0) Y2D = ABS(YT1D)
      XD(1) = XT1D
      YD(1) = YT1D
      NEXP = NCARD+1
      NID = 1
      ID(NID) = ID1
      NA = 1
```

```
31   READ (NREAD,201,END=51) IDENSS,NCARD,NL,TT2,XT2,YT2
     XT2D = XT2/XCNTR
     YT2D = YT2/YCNTR
     NA = NA+1
     XD(NA) = XT2D
     YD(NA) = YT2D
     IF ((XT2D.GT.0.0).AND.(XT2D.GT.X1D)) X1D = XT2D
     XT2A = ABS(XT2D)
     IF ((XT2D.LT.0.0).AND.(XT2A.GT.X2D)) X2D = XT2A
     IF ((YT2D.GT.0.0).AND.(YT2D.GT.Y1D)) Y1D = YT2D
     YT2A = ABS(YT2D)
     IF ((YT2D.LT.0.0).AND.(YT2A.GT.Y2D)) Y2D = YT2A
     IF (IDENSS.EQ.ID(NID)) GO TO 33
     WRITE (NWRITE,204)
204  FORMAT ('    ****        **** ')
     NID = NID+1
     ID(NID) = IDENSS
     NDISC1 = NDISC1+1
     NLINE = NLINE+1
     GO TO 34
33   CONTINUE
     IF (NCARD.EQ.NEXP) GO TO 34
     WRITE (NWRITE,205)
205  FORMAT ('                **** ')
     NDISC2 = NDISC2+1
     NLINE = NLINE+1
34   NEXP = NCARD+1
     IF (((XT1D.LE.0.0).AND.(XT2D.GT.0.0)).OR.((XT1D.GE.0.0).AND.(XT2D.
    1LT.0.0))) GO TO 13
     IX1 = INT(XT1D)
     IX2 = INT(XT2D)
     IF (IX1.EQ.IX2) GO TO 16
     XCD = 0.50*FLOAT(IX1+IX2+1)
     IF (XT1D.LT.0.0) XCD = XCD-1.0
     XCI = XCD*XCNTR
     GO TO 14
13   XCI = 0.0
14   NCR = NCR+1
     XCR(NCR) = XCI
     YCR(NCR) = YT1+(YT2 - YT1)*(XCI-XT1)/(XT2-XT1)
     TCR(NCR) = TT1+(TT2-TT1)*(XCI-XT1)/(XT2-XT1)
     WRITE (NWRITE,206) TCR(NCR),XCR(NCR),YCR(NCR)
206  FORMAT (' ',14X,' AXIS CROSSED ',5X,F15.4,2X,F15.4,2X,F15.4)
     NLINE = NLINE+1
```

```
16  CONTINUE
    IF (((YT1D.GE.0.0).AND.(YT2D.LT.0.0)).OR.((YT1D.LE.0.0).AND.(YT2D.
   1GT.0.0))) GO TO 19
    IY1 = INT(YT1D)
    IY2 = INT(YT2D)
    IF (IY1.EQ.IY2) GO TO 22
    YCD = 0.50*FLOAT(IY1+IY2+1)
    IF (YT1D.LT.0.0) YCD=YCD-1.0
    YCI = YCD*YCNTR
    GO TO 20
19  YCI = 0.0
20  NCR= NCR+1
    YCR(NCR) = YCI
    XCR(NCR)= XT1+(XT2-XT1)*(YCI-YT1)/(YT2-YT1)
    TCR(NCR) = TT1+(TT2-TT1)*(YCI-YT1)/(YT2-YT1)
    WRITE (NWRITE,206) TCR(NCR), XCR(NCR), YCR(NCR)
    NLINE = NLINE+1
22  CONTINUE
    VFALL = 0.00
    DELT = TT2-TSTART
    IF (DELT.EQ.0.0) GO TO 25
    VFALL = (YT2-YSTART)/DELT
25  CONTINUE
    WRITE (NWRITE,203) IDENSS,NCARD,NL,TT2,XT2,YT2,VFALL
    NLINE = NLINE+1
    IF (NLINE.LT.50) GO TO 32
    NPAGE = NPAGE+1
    WRITE (NWRITE,200) NPAGE
    NLINE = 0
32  CONTINUE
    XT1D = XT2D
    YT1D = YT2D
    XT1 = XT2
    YT1 = YT2
    TT1 = TT2
    GO TO 31
51  CONTINUE
    NP = NA
    WRITE (NWRITE,214) NDISC2
214 FORMAT ('1 THE NUMBER OF DISCONTINUITIES IN THE CARD NUMBERS
   1WAS '   ,I5,/' ')
    WRITE (NWRITE,215) NDISC1
215 FORMAT (' THE NUMBER OF DISCONTINUITIES IN THE DATA SUBSET
   1NUMBERS   WAS ',I5,'.',//' ')
    WRITE (NWRITE,216) (ID(NK), NK=1,NID)
```

```
216   FORMAT (' THE FOLLOWING DATA SUBSETS ARE REPRESENTED
     1',//(' ', 10X,    I10))
      WRITE (NWRITE, 220)
220   FORMAT ('1   AXIS CROSSINGS '///' ',15X,' X',17X,' Y ',15X, ' TIM
     1E '/' ')
      DO 89 NJ=1,NCR
      WRITE (NWRITE,221) XCR(NJ), YCR(NJ), TCR(NJ)
 89   CONTINUE
221   FORMAT (' ',3F20.4)
      WTD = X1D+X2D
      HTD = Y1D+Y2D
      SD = 1.0
      WMAX = 10.0
      HMAX = 12.0
 50   DO 59 J=1,3
      SFT = SC(J)*SD/XCNTR
      WTI = WTD/SFT
      HTI = HTD/SFT
      IF ((WTI.LE.WMAX).AND.(HTI.LE.HMAX)) GO TO 52
 59   CONTINUE
      SD = SD*10.0
      GO TO 50
 52   SF =SFT
      WPD = WMAX*SF
      HPD = HMAX*SF
      DEL = 0.25*SF
      NX1 = INT(X1D)+1
      NX2 = INT(X2D)+1
      WGD = FLOAT(NX1+NX2)
      XMARD = WPD-WGD
      IF (XMARD.LT.0.0) GO TO 53
      XORD = 0.50*XMARD+FLOAT(NX2)
      NCX1 = NX1
      NCX2 = NX2
      XL1 = FLOAT(NCX1)+DEL
      XL2 = FLOAT(NCX2)+DEL
      GO TO 56
 53   FX1 = FLOAT(NX1) - X1D
      FX2 = FLOAT(NX2)-X2D
      IF (FX2.GT.FX1) GO TO 54
      WGD = FLOAT(NX2) + X1D
      XMARD = WPD-WGD
      IF (XMARD.LT.0.0) GO TO 55
      XORD = 0.50*XMARD+FLOAT(NX2)
```

```
      NCX1 = NX1-1
      NCX2 = NX2
      XL1 = X1D+DEL
      XL2 = FLOAT(NCX2)+DEL
      GO TO 56
54    WGD=FLOAT(NX1)+X2D
      XMARD = WPD-WGD
      IF (XMARD.LT.0.0) GO TO 55
      XORD = 0.50*XMARD+X2D
      NCX1 = NX1
      NCX2 = NX2-1
      XL1 = FLOAT(NCX1)+DEL
      XL2 = X2D+DEL
      GO TO 56
55    XMARD = WPD- WTD
      XORD = 0.50*XMARD+X2D
      NCX1 = NX1-1
      NCX2 = NX2-1
      XL1 = X1D+DEL
      XL2 = X2D+DEL
56    CONTINUE
      IF (XL1.GT.(WPD-XORD)) XL1 = WPD-XORD
      IF (XL2.GT.XORD) XL2 = XORD
      NY1 = INT (Y1D) + 1
      NY2 = INT(Y2D) + 1
      HGD = FLOAT(NY1+NY2)
      IF (HGD.GT.HPD) GO TO 61
      YORD = FLOAT(NY1)
      NCY1 = NY1
      NCY2 = NY2
      YL1 = FLOAT(NCY1)+DEL
      YL2 = FLOAT (NCY2)+DEL
      GO TO 65
61    FY1 = FLOAT(NY1)-Y1D
      FY2 = FLOAT(NY2)-Y2D
      IF (FY1.GT.FY2) GO TO 63
      HGD=FLOAT(NY1)+Y2D
      IF (HGD.GT.HPD) GO TO 64
      YORD = FLOAT(NY1)
      NCY1 = NY1
      NCY2 = NY2-1
      YL1 = FLOAT(NCY1)+DEL
      YL2 = Y2D+DEL
      GO TO 65
```

```
 63     HGD = FLOAT(NY2)+Y1D
        IF (HGD.GT.HPD) GO TO 64
        YORD = Y1D
        NCY1 = NY1-1
        NCY2 = NY2
        YL1 = Y1D+DEL
        YL2 = FLOAT(NCY2)+DEL
        GO TO 65
 64     YORD = Y1D
        HGD = Y1D +Y2D
        NCY1 = NY1-1
        NCY2 = NY2-1
        YL1 = Y1D+DEL
        YL2 = Y2D+DEL
 65     CONTINUE
        YMARD = HPD-HGD
        YMXD = 2.00*SF
        IF (YMARD.GT.YMXD) YMARD = YMXD
        YORD = YORD+(2.60*SF)+(0.50*YMARD)
        CALL NGRAPH(NCP,XLIM,YLIM,POSN)
        CALL SCALE(1.00,1.00)
        CALL ORIGNI(2.00,0.00)
        X = 0.00
        Y = 0.25
        CALL SYMBOL(Y,X,0.20, 'PARTICLE TRAJECTORY ',90.0,19)
        X = 0.15
        Y = 0.60
        DO 84 NK=1,6
        IF (NK.NE.4) GO TO 83
        X = 1.60
        Y = 0.60
 83     IDK = ID(NK)
        CALL NUMBRI(Y,X,0.20,IDK,90.0,-1)
        IF (NK.EQ.NID) GO TO  85
        Y = Y+0.32
        IF ((NK.EQ.5).AND.(NID.GT.6)) GO TO 86
 84     CONTINUE
        GO TO 85
 86     CONTINUE
        CALL SYMBOL(Y,X,0.18,'AND OTHERS',90.0,10)
 85     CONTINUE
        X = 3.70
        XN = 5.75
        Y = 0.16
        DY1 = 0.22
```

```
DY2 = 0.17
CALL SYMBOL(Y,X,0.12, 'EDDY SPACING X       ',90.0,21)
CALL NUMBRF(Y,XN,0.12,XCNTR,90.0,3)
Y = Y+DY2
CALL SYMBOL (Y,X,0.12,'                   Y       ',90.0,21)
CALL NUMBRF (Y,XN,0.12,YCNTR,90.0,3)
Y=Y+DY1
CALL SYMBOL(Y,X,0.12,'VELOCITY PARAMETER ',90.0,21)
CALL NUMBRF(Y,XN,0.12,UEDDY,90.0,4)
Y = Y+DY1
CALL SYMBOL (Y,X,0.12, 'PARTICLE PARAMETER ',90.0,21)
CALL NUMBRF (Y,XN,0.12,PART,90.0,4)
Y=Y+DY1
CALL SYMBOL(Y,X,0.12, ' GRAVITATIONAL PARAM.',90.0,21)
CALL NUMBRF (Y,XN,0.12,GRAV,90.0,4)
Y=Y+DY1
CALL SYMBOL(Y,X,0.12,'CONVERGENCE CRITERN.  ',90.0,21)
DELSC7 = DELSCR*(10.0**7)
CALL NUMBRF(Y,XN,0.12,DELSC7,90.0,2)
X=XN+0.50
CALL SYMBOL(Y,X,0.12,'.10',90.0,3)
X=X+0.30
Y=Y-0.08
CALL SYMBOL(Y,X,0.06,'-7',90.0,2)
X=7.00
XN = 9.05
Y=0.16
CALL SYMBOL(Y,X,0.12,'STARTING POINT    X        ',90.0,21)
CALL NUMBRF (Y,XN,0.12,XSTART,90.0,4)
Y=Y+DY2
CALL SYMBOL(Y,X,0.12,'                  Y        ',90.0,21)
CALL NUMBRF(Y,XN,0.12,YSTART,90.0,4)
Y=Y+DY2
CALL SYMBOL(Y,X,0.12,'                TIME       ',90.0,21)
CALL NUMBRF(Y,XN,0.12,TSTART,90.0,4)
Y=Y+DY1
CALL SYMBOL(Y,X,0.12, 'STEP LIMIT                ',90.0,21)
CALL NUMBRF(Y,XN,0.12,STEP,90.0,4)
Y=Y+DY1
CALL SYMBOL(Y,X,0.12, 'WEIGHTING FACTOR          ',90.0,21)
CALL NUMBRF(Y,XN,0.12,W,90.0,2)
Y=Y+DY1
CALL SYMBOL(Y,X,0.12,'PLOTTED AT EVERY          ',90.0,21)
CALL NUMBRI(Y,XN,0.12,IPUNCH,90.0,-1)
Y=Y+DY2
```

```
      CALL SYMBOL(Y,X,0.12,'   COMPUTED POINTS  ',90.0,21)
      CALL SCALE(SF,SF)
      CALL ORIGNV(YORD,XORD)
      YL1= -YL1
      NX=NCX1+NCX2+1
      NY=NCY1+NCY2+1
      DO 77 J=1,NX
      X=FLOAT(NCX1+1-J)
      XLAB = X*XCNTR
      XL = X-(0.05*SF)
      IF (X.LT.0.0) XL = X+(0.20*SF)
      YL = YL1-(0.10*SF)
      CALL NUMBRF(YL,XL,0.12,XLAB,180.0,4)
      CALL PLOT(YL1,X,1)
      CALL PLOT(YL2,X,0)
77    CONTINUE
      XL = (0.25*SF) - XL2
      XL2 = -XL2
      DO 78 J=1,NY
      Y = FLOAT(NCY1+1-J)
      YLAB=Y*YCNTR
      YL = Y+(0.05*SF)
      YL = -YL
      CALL NUMBRF(YL,XL,0.12,YLAB,90.0,4)
      Y=-Y
      CALL PLOT(Y,XL1,1)
      CALL PLOT(Y,XL2,0)
78    CONTINUE
      YD(1) = -YD(1)
      CALL PLOT (YD(1),XD(1),1)
      DO 91 NN=2,NP
      YD(NN) = -YD(NN)
      CALL PLOT (YD(NN),XD(NN),0)
91    CONTINUE
      CALL CLOSE
      STOP
      END
```

APPENDIX V.

Experimental Procedure for the Determination of the Trajectories of Non-buoyant Particles falling through Waves.

This appendix contains a description of the procedure followed in the determination of the experimental particle trajectories discussed in Section 5.3.

The experiments were carried out in a glass-sided wave flume at the University of New South Wales Water Research Laboratory, Manly Vale, New South Wales. The working length of the flume was about 11.9m. The width of the flume was 915 mm and the maximum available depth of water was approximately 1200 mm. Waves were generated by means of a motor-driven oscillating wave paddle. The waves travelled through a filter consisting of an array of rolls of fine wire mesh before entering the working zone. Initially, the examination of the trajectories of particles in a progressive wave train was contemplated; it was proposed that the waves should be absorbed on a non-reflecting beach at the far end of the flume. It was concluded, however, that difficulty would be experienced in effecting complete absorption of the incident waves, and that consequently the actual wave motion in the operating section of the flume might contain some reflected wave components in addition to the incident wave train. Accordingly, it was decided that a standing-wave system should be adopted, the standing-wave system being formed by reflection of the incident wave train.

In order to achieve conditions which approached (as closely as possible) complete reflection of the incident wave train, a vertical impervious bulkhead was fixed across the flume, perpendicular to the flume walls. In preparing for each experiment, water was admitted to the two sections of the flume (one each side of the bulkhead). Equalisation of the undisturbed water levels on the two sides of the bulkhead ensured that the force to be resisted by the bulkhead was limited to that due to wave action. The spaces between the edges of the bulkhead and the flume walls were sealed with modelling clay. The effectiveness of this sealing was confirmed by observations which indicated that no discernible motion of the water on the far side of the bulkhead was in evidence, with the wave generator in operation.

The longitudinal position within the flume of the reflecting bulkhead was dictated by structural considerations. The distance from the wave paddle to the bulkhead was approximately 11.9 m, of which approximately 3m adjacent to the bulkhead was available for observation and photography, through glass panels in the side of the flume.

In order to establish a velocity field which could be simply defined mathematically, it was desirable to operate under conditions which would satisfy the criterion for "deep-water" waves - that is, that the water depth should be equal to or greater than one-half the wave length. In practice, the range of conditions available which would satisfy (or nearly satisfy) this criterion was severely limited. The wave period was adjustable over a wide range, by means of a variable-speed unit in the drive train. The construction of the wave paddle was such, however, that it was not possible to reduce the amplitude of oscillation of the paddle below a certain minimum. It was necessary that the wave period (and the wave length) should be relatively short, in order that the deep-water criterion might be satisfied within the range of water depths which could be accommodated in the flume. Under these conditions (of short wave period), however, it was found that if the water depth were increased beyond a certain limit (of the order of 700 mm) breaking of the wave near the paddle occurred (even with the amplitude of oscillation of the paddle at its minimum) and the establishment of a well-formed system of stationary waves was not possible. The depth of water which could be employed was consequently limited. It was found, furthermore, that if the wave length were reduced below a certain value, transverse oscillations were set up within the flume. At wave lengths which were approximately equal to the width of the flume, the amplitude of the transverse oscillations became large (of the order of 150 mm, when the amplitude of the incident wave was of the order of 20 mm).

Accordingly, little opportunity existed for variation of the characteristics of the waves. Within these limitations, however, careful adjustment of the wave period permitted the establishment of a reasonably well-formed system of standing waves: nodes (points of zero vertical displacement and maximum horizontal displacement) and anti-nodes points of maximum vertical displacement and zero horizontal displacement) were clearly defined

at positions which

remained nearly stationary (although with some variation in position) throughout an experiment. The characteristics of the waves employed are listed in Table 2.

Wave lengths were measured by marking, on the side of the flume, the positions (as estimated by eye) of the nodes and antinodes of the wave system, and measuring the distances between the marks by means of a tape. The measurements were averaged, over a distance extending about one wave length in each direction from the zone of release of the particles. Wave heights (and hence amplitudes) were determined by marking (on the glass side of the flume) the limits of the vertical excursions of the water surface at an anti-node, and measuring the distance between the marks with a scale. Wave periods were determined by timing, with a stop-watch, 100 cycles of the wave generator.

In order to facilitate photography of the particle, it was necessary that the water within the flume should be as clear as possible. As the volume of water which was required precluded the use of distilled water, water drawn from the mains supply was used. The water was flocculated with potassium alum and allowed to stand within a large tank for several days. It was then filtered through a diatomaceous-earth filter before being placed in the flume.

The particles used in this series of experiments consisted of spheres of petroleum wax, each weighted with a single grain of quartz sand. As the density of the wax was less than that of water, suitable selection of the size of the sand grain and variation of the overall diameter of the particle would permit the preparation of buoyant, neutrally-buoyant or non-buoyant particles. In the present investigation, the objective was to prepare non-buoyant particles, with settling velocities (in quiescent water) of the order of 10-20 mm per second. In order to ensure that the particles could be conveniently photographed, it was specified that the particles should be about 1 mm - 2 mm in diameter. The wax was dyed yellow to facilitate the observation and photographing of the particles.

The particles were formed by hand: a single grain of sand was pressed into the approximate centre of a small body of wax, which was then rolled between a convex and concave glass surface (laboratory "watch-glasses") until it acquired a spherical form. The settling velocity (in quiescent water) of each particle was checked immediately it was made; particles having settling velocities of the order of 10 to 20 mm per second were retained, those with settling velocities considerably greater or less than this figure were rejected (as were any buoyant particles).

It became evident that the wax particles, when immersed, absorbed a certain amount of water. Accordingly, the selected particles were allowed to stand in distilled water for about one day after being manufactured. Each particle was then removed from the water and allowed to dry in a gentle air stream, until the film of moisture on the surface of the particle just disappeared. In this "surface-dry" condition the particle was then weighed on an analytic balance, to $\pm$ 0.00005g.

The diameter of each particle was measured by means of a 30 x microscope with a graticule scale, permitting measurement of the diameter to within ± 0.02mm (in the early stages of the investigation, some particles were measured with a 10 x magnifier to an accuracy of about ± 0.05 mm). At the same time, the sphericity of the particle was checked visually.

The particle was then again wetted, care being taken to remove any air bubbles from its surface by gently rolling the particle between the fingertips below the surface of distilled water. The settling velocity of the particle in quiescent water was then measured, by timing its fall over a measured distance (of approximately 300 mm) in distilled water. The measurement was repeated at least five times, obviously inconsistent results (occurring on occasions as a result of the particle's encountering a foreign body or an air bubble in the water) being rejected.

For a spherical particle settling through quiescent water, re-arrangement of the expression equating the fluid drag force and the net gravitational force on the particle leads to the relationship:-

$$(s-1) = 0.75\, C_D\, v_s^2/dg \qquad (V.1)$$

where s = the ratio of the density of the particle to the density of the surrounding fluid

v_s = the velocity of settlement of the particle

d = the particle diameter

g = the gravitational acceleration

C_D = the dimensionless drag coefficient

Substitution of the measured value of d, the experimental value of the settling velocity v_s, and the value of C_D (based upon the measured value of d, the experimental value of v_s and the drag coefficient curve for spherical particles of Fig. II. 1) permits the calculation of the value of s for the particle. Substitution of this value, together with the measured mass m of the particle, into the expression

$$d = \left[\frac{6\ m}{\pi\ s\ \rho_w} \right]^{1/3} \qquad (V.2)$$

where ρ_w = the density of the water, then yields a new estimate of d. This calculation was repeated using the new estimate of d to obtain a revised estimate of s from Equation (V. 1) and hence a further estimate of d from Equation (V. 2). This procedure was continued until no significant further variation occurred in d; the current values of d and s were then adopted as the properties of the particle. In the later phases of the investigation, a program was written which enabled this calculation to be carried out on an IBM "MATH" terminal which was available at this stage.

The variation between the initially-measured value of d and the finally-adopted value of d did not exceed $\pm$ 0.03 mm for any particle which was used in the experiments.

In a number of cases in which particles were salvaged from the bottom of the flume after their use in an experiment, the particles were re-examined with the object of detecting any change in their properties; no significant changes were observed.

In preliminary trials, particles were released above the surface of the water in the flume and allowed to drop through the water surface. It was concluded, however, that in order to prevent the attachment of air bubbles to the particle and to avoid the entanglement of the particle with small pieces of debris on the water surface, it would be necessary to have the particles continuously immersed in water during their release into the flume. The following procedure for the release of a particle was consequently developed: the wetted particle was inspected to ensure its freedom from attached air bubbles and debris, and was placed in a tube of rigid polyvinyl chloride, about 5 mm in internal diameter and about 1 m in length, closed at one end. The tube was then filled with water: in order to avoid the effects of temperature differences, the tube was filled with water which had immediately beforehand been withdrawn from the flume. The tube was held in a vertical position with its closed end downwards, and the particle was allowed to settle through the water within the tube until it was near the closed end of the tube. The tube was then quickly inverted and its open lower end placed beneath the surface of the water within the flume, the wave generator having previously been set in motion. The particle then settled through the water within the tube until it reached the open end of the tube, whereupon it emerged into the water within the flume. The release tube was then withdrawn, as soon as the particle had moved far enough away from the end of the tube to permit its withdrawal without causing undue disturbance to the motion of the particle. The photographic recording of the trajectory was not commenced until the particle had fallen to a point some distance below its point of release.

Particles were released at a distance of 100 mm from the outer surface of the glass side of the flume - that is, approximately 88 mm from the inner surface of the glass. This distance was controlled by holding a simple gauge-block between the inner face of the glass and the release tube. The essentially two-dimensional nature of the velocity field within the wave system was confirmed by observations which indicated that all the particles reached the bottom of the flume at distances between 50 mm and 150 mm from the outer face of the glass, after having fallen through a depth of water of about 700 mm.

The zone of release of the particles was approximately one wave length in front of the face of the reflecting bulkhead. The wave generator was operated for at least five minutes before the release of each particle, in order to allow the wave field to become fully established. It was observed that if the wave generator were operated continuously for more than about 30 minutes, a tendency existed for the development of extraneous longitudinal mass-transport currents. With an appropriate limitation on the duration of each period of operation of the wave generator, it was observed that the particles generally settled to the bed of the flume with little net translation in the longitudinal direction. Runs in which undue net translation in the longitudinal direction occurred were rejected.

In order to permit the calculation of the coordinates of the recorded particle positions, a square grid was marked on the outer face of the glass side of the flume. The value of the abscissa or ordinate, in the plane of motion of the particles, represented by the trace of each line of this grid was determined as follows: Prior to the start of each experiment, the camera which was to be used to record the particle trajectory was set up approximately opposite the centre of the grid, with its optical axis perpendicular to the plane of the glass wall of the flume. A sheet of clear acrylic plastic was temporarily set up inside the flume with its face in the plane of release of the particles (this plane is referred to below as the "particle plane"). This face of the plastic sheet carried a second grid of lines, at spacings of 100 mm in the horizontal and vertical directions. The plastic sheet was positioned in the flume so that the vertical grid lines were located at distances of 1600, 1700, 1800, 1900 and 2000 mm from the face of the bulkhead, while the horizontal grid lines were at elevations of 100, 200, 300 mm etc. above the bed of the flume. A photographic exposure was then made and the plastic sheet carrying the "particle plane" grid was removed from the flume. The resultant photograph showed two sets of grid lines: those marked on the glass side of the flume, and those marked on the plastic sheet and located in the "particle plane". (The two sets of lines were distinguished by marking small circles at the intersections of the lines on the plastic sheet in the "particle plane"). By proportioning the distances between the lines of the grid in the "particle plane", the coordinate (in the particle plane) corresponding to the trace of each line of the grid on the glass side of the flume could be established. The grid on the side of the flume appeared on each exposure made during the experiments.

Initially, particle trajectories were photographed by means of a Shackman Sequential-Frame Camera. This camera exposes a series of frames, approximately 25 mm square on standard 35 mm film, at nominal rates of up to 4 frames per second. This maximum rate of exposure was employed; the actual interval between exposures was determined to be 0.255 seconds. These experiments were conducted in daylight in the relatively subdued ambient lighting of the laboratory. Illumination consisted of one 1500 watt quartz-iodide lamp, suspended at a distance of approximately 500 mm above the water surface, immediately above the zone of release of the particles. The bed and rear wall of the flume were painted black, to minimise reflections. A typical exposure duration was 1/100 sec. at an aperture of f5.6, on Kodak Tri-X Pan Film.

After photographing the reference grid in the particle plane as described above, and without movement of the camera in the interim, the particle was released and the camera mechanism set in motion, the successive positions of the particle being recorded on successive frames of the film. On each frame of the processed film the coordinates of the particle position were measured, by means of a hand magnifier fitted with a measuring graticule, relative to the grid lines on the glass wall of the flume. On each frame, a measurement of the displacement of the water surface (at or near an anti-node) was also made, in order to establish the phase of the wave.

It was assumed that linear relationships existed between coordinates measured with respect to the grid on the glass wall of the flume and the corresponding coordinates on the particle plane, throughout the field of view (only small departures from linearity were in evidence). From measurements on the frame which depicted the grid on the glass wall of the flume and the grid in the particle plane (as described above) the appropriate relationships were derived, for the horizontal and vertical coordinates, by a Least-Squares Regression process. The relationships for horizontal and vertical coordinates were almost identical. These relationships were used to convert the coordinates measured from the negatives to the corresponding coordinates on the particle plane.

The compilation of the particle trajectory in this manner proved to be extremely tedious, and later experiments were photographed by means of a stroboscope.

The stroboscope employed was a Phillips PR9107, with a narrow-beam flash lamp. Early trials in which the light from the flash lamp was directed downwards through the water surface were unsuccessful. It was concluded that scattering of the light by the water was so great that the instantaneous positions of the particle were not registered on the photographic film by the individual flashes.

After some trials, a successful technique for stroboscopic photography was eventually developed. It was found necessary to work in darkness. The light emitted from the flash lamp was concentrated into a narrow beam by fitting to the front of the lamp a converging cone with a reflecting inner surface, terminating in a cylindrical tube of an inside diameter of approximately 10 mm and approximately 100 mm in length. The inner surface of the cylindrical tube had a non-reflective black surface. When this device was fitted, virtually all the light emitted from the flash lamp was contained within a beam with a nearly constant diameter of approximately 10 mm.

In order to photograph an experiment, the camera, a Nikon 35 mm with an 85 mm lens of f1.8 maximum aperture, was set up opposite the centre of the particle-release zone, with its optical axis perpendicular to the plane of the glass side of the flume. As described above, a reference grid in the "particle plane" - that is, the plane in which the particle was to be released - was photographed first. The actual experiment was photographed on a succeeding frame, without movement of the camera in the interim. The particle having been released as described above, the camera shutter was opened; the shutter was kept open until the particle approached the bed of the flume or until it was decided that a sufficient length of trajectory had been registered. As the diameter of the light beam was small in relation to the excursions of the particle, it was necessary for the experimenter to follow the particle with the light beam, endeavouring to ensure that the particle was at each flash illuminated by the beam. The tip of the tube at the front of the flash lamp was held close to the glass side of the flume, the lamp being held at such an angle that the light beam was as nearly perpendicular to the glass as possible, without the line of sight from the particle to the camera being obstructed by the flash lamp and its appurtenances. The "spot" of light formed where the light beam passed through the glass was concealed from the camera by means of a small shield fastened to the flash lamp.

In this way, successive positions of the particle were recorded (by successive flashes of the lamp) on a single frame of the film. Light from the flash lamp which was transmitted and reflected within the glass caused the registration on the film of some of the grid lines marked on the glass.

Flashing rates of five and ten flashes per second were employed, in various experiments.

A photograph of a typical trajectory recorded in this manner is reproduced as Figure 16. The flashing rate in this case was 10 flashes per second. The trajectory numbered 1250201 and described in Section 5.3 forms part of the trajectory illustrated in Figure 16.

The photographic records were converted to plots of the particle trajectory at the desired scale as follows: Positive transparencies were prepared from the negative film. The transparency which depicted the grid in the "particle plane" together with the grid on the glass side of the flume was placed in a slide projector and projected on to a screen. The distance between the projector and the screen, and the focus of the projector, were adjusted until a sharp image was obtained in which the distance between the lines of the "particle plane" grid was equal to the required distance - that is, to the actual grid spacing (100 mm) multiplied by the desired scale factor. The positions of the projected images of both sets of grid lines were then marked on a sheet of paper attached to the screen. This transparency was removed from the projector, and replaced by a transparency showing a particle trajectory (photographed from the same camera position as was the previous transparency). Slight adjustments of the direction of the optical axis of the projector, and to its focus (to compensate for differences in the positions of the transparencies within their mounts, and for differences in the positions of the mounts within the slide holder) permitted the projected images of the grid lines on the glass to be brought into coincidence with the corresponding positions previously marked on the screen. The successive particle positions were then marked on the paper in pencil. The result was a plot, to the desired scale, of the particle trajectory.

APPENDIX VI

The Computation of the Trajectories of Non-buoyant Particles Falling through Waves.

This appendix contains a description of the procedure followed in the computation of the computed trajectories which are described in Section 5.3.

The computer program used in the computation of the trajectories of particles in the standing wave system is essentially similar to the program which was developed for the computation of the trajectories of particles within the model eddy field and which is described in Chapter 4 and Appendix III. The computational structure of the programs is identical, and the modifications which were necessary to adapt the program for the purpose at present under discussion concerned, principally, the definition of the velocity field, and the input and output structures.

The material within this appendix is presented as follows:-

VI.1 The FORTRAN computer program for the computation of a particle trajectory within the standing wave system.

VI.1.1 The main program, and the subroutine DRAG.

VI.1.2 The subroutines VEL and VELID.

VI.2 The application of the computer program in the computation of a particle trajectory within the standing wave system.

VI.1 The FORTRAN Computer Program for the Computation of a Particle Trajectory within the Standing Wave System

VI.1.1 The Main Program and the Subroutine DRAG

As stated above, the main program is essentially similar to the program described in Chapter 4 and Appendix III. The following modifications were made:

(i) Input (READ) and Output (WRITE, on line printer or card punch) Statements were modified to accommodate the different data variables involved - the alterations in the data variables are discussed below.

(ii) Format statements were modified accordingly.

(iii) COMMON declaration statements were modified, as necessitated by the new data variables.

(iv) The maximum fluid velocity occurring within the wave system (UMAX) replaced the Eddy Velocity Parameter UEDDY in the calculation of the basic time step DTBAS.

(v) The loop structure causing the program to carry out the computation of a particle trajectory for each of the several (NV) values of the Eddy Velocity Parameter UEDDY was deleted.

(vi) Six parameters, CONST1, . . . , CONST6, are evaluated within the main program and are made accessible to the subroutine VEL (which defines the velocity distribution) by a COMMON Declaration Statement. The values of these parameters depend only upon the characteristics of the wave system and of the particle and are invariant with position and time.

Accordingly, they are evaluated once only, within the main program in order to avoid repeated (identical) evaluations each time the subroutine VEL is called. The parameters CONST1...CONST6 are defined in Section V1.1.2 below.

(vii) The variables which are read as data, in the operation of the program, are generally as listed in Table IILA with the omission of XCNTR, YCNTR, NV and UEDDY (which are associated with the definition of the velocity distribution within the model eddy field) and the substitution of the following:-

Dimensionless Wave Length WLNG = L = $\frac{\lambda}{(s+k)\ d}$ (VI.1)

Dimensionless Wave Period WPER = P = $\frac{\theta}{(s+k)}\sqrt{\frac{g}{d}}$ (VI.2)

Dimensionless Wave Amplitude WAMP = A = $\frac{a}{(s+k)d}$ (VI.3)

Dimensionless Water Depth DPTH = H = $\frac{h}{(s+k)d}$ (VI.4)

Phase Parameter PHSE = ϵ (VI.5)

where λ = the length of the wave

θ = the period of the wave

a = the amplitude of the wave

= $\frac{1}{2}$ the height (trough to crest) of the wave

h = the water depth

ϵ = a phase constant

s = the ratio of the density of the particle to the density of the surrounding fluid

k = the added mass coefficient

d = the diameter of the particle

g = the gravitational acceleration

The derivation of the dimensionless parameters from the corresponding dimensional quantities is in accordance with Equations (2.20), (2.21), (2.20) and (2.20) p. 40, respectively.

The calculation of the work done on (or by) the particle during its traverse of each segment of the trajectory (as described in Section 4.4) was retained within the modified program. The quantities which are evaluated are, however, of no significance within the present context.

No modification of the subroutine DRAG was required.

VI. 1.2 <u>The Subroutines VEL and VELID</u>

A new subroutine VEL was written to define the velocity distribution within the standing wave system. The velocity distribution was assumed to conform to the expressions presented by Wiegel (VI. 1) for the components of velocity within a standing wave of small amplitude:

$$u(x, y, t) = \frac{g.a.n}{\sigma} \cdot \frac{\cosh(n.(y+h))}{\cosh(n.h)} \cdot \cos(n.x).\cos(\sigma.t + \epsilon) \qquad \text{(VI. 6)}$$

$$v(x, y, t) = \frac{g.a.n}{\sigma} \cdot \frac{\sinh(n.(y+h))}{\cosh(n.h)} \cdot \sin(n.x).\cos(\sigma.t + \epsilon) \qquad \text{(VI. 7)}$$

where u (x, y, t) = the component, in the x coordinate direction, of the fluid velocity at the point (x, y) and at the time t

v(x, y, t) = the component, in the y coordinate direction, of the fluid velocity at the point (x, y) and at the time t

g = the gravitational acceleration

a = the amplitude of the wave

= $\frac{1}{2}$ the height (trough to crest) of the wave

n = the wave number

= $\dfrac{2\pi}{\lambda}$

λ = the length of the wave

h = the water depth

σ = the frequency of the wave

= $\dfrac{2\pi}{\theta}$

θ = the period of the wave

ϵ = a phase constant

x and y are position coordinates, with the origin at a node (a point of maximum horizontal motion and zero vertical motion) of the standing wave system, and at the elevation of the undisturbed water surface.

The term $\frac{g.a.n}{\sigma}$ in Equations (VI.6) and (VI.7) represents a velocity which is in fact the maximum velocity which occurs within the wave system:

$$u_{max} = \frac{g.a.n}{\sigma} = \frac{g.a.\theta}{\lambda} \qquad \text{(VI. 8)}$$

The associated dimensionless parameter U_{max} (to which corresponds the FORTRAN variable UMAX) may be derived, in accordance with Equation (2.18) p. 39 :

$$U_{max} = \frac{u_{max}}{\sqrt{dg}}$$

$$= \frac{g.a.\theta}{\lambda\sqrt{dg}}$$

$$= \frac{(s+k)\cdot\dfrac{a}{(s+k)d}\cdot\dfrac{\theta}{(s+k)}\cdot\sqrt{\dfrac{g}{d}}}{\dfrac{\lambda}{(s+k)\ d}}$$

$$= \frac{G.\ A.\ P}{L}$$

where G, A, P and L are the dimensionless parameters corresponding to g, a, θ and λ, in accordance with Equations (2.19), (2.20), (2.21) and (2.20)-p. 39 and 40 - respectively.

$$G = (s+k)\cdot\frac{g}{g} = (s+k)$$

$$A = \frac{a}{(s+k)d}$$

$$P = \frac{\theta}{(s+k)}\cdot\sqrt{\frac{g}{d}}$$

$$L = \frac{\lambda}{(s+k)\ d}$$

The conversion of length and time parameters to the corresponding dimensionless parameters in accordance with Equations (2.20) and (2.21) - or in accordance with any consistent system - will not affect the values of the trigonometric and hyperbolic functions, and hence Equations (VI. 6) and (VI. 7) may be written in terms of dimensionless parameters as follows:-

$$U_{(X,Y,T)} = (s+k)\,.\frac{A.P}{L}\cdot\frac{\cosh(N\ (Y\ +H)\ )}{\cosh(N.H)}\cdot\cos(N.X)\cos\left(2\pi\frac{T}{P} + \epsilon\right) \quad (VI. 9)$$

$$V_{(X,Y,T)} = (s+k) \cdot \frac{A.P}{L} \cdot \frac{\sinh(N\,(Y+H))}{\cosh(N.H)} \cdot \sin(N.X)\cos\left(2\pi\frac{T}{P}+\epsilon\right) \qquad \text{(VI. 10)}$$

where U and V are the components, in the two coordinate directions, of the dimensionless fluid velocity,

X and Y are dimensionless position coordinates

T = a dimensionless time

N = the dimensionless wave number

A = the dimensionless wave amplitude

P = the dimensionless wave period

L = the dimensionless wave length

H = the dimensionless water depth

ϵ = a phase constant

s = the ratio of the density of the particle to the density of the surrounding fluid

k = the added mass coefficient.

The components, in the two coordinate directions, of the fluid acceleration are:

$$a_{fx} = a_{fx}\,(x,y,t)$$

$$= \frac{\partial u}{\partial t}\Big|_{(x,y,t)} + u.\frac{\partial u}{\partial x}\Big|_{(x,y,t)} + v.\frac{\partial u}{\partial y}\Big|_{(x,y,t)} \text{ where } \begin{matrix} u=u(x,y,t) \\ v=v(x,y,t) \end{matrix}$$

$$= \frac{u}{\cos(\sigma.t+\epsilon)}.(-1).\sigma.\sin(\sigma.t+\epsilon) + u.\frac{u}{\cos(n.x)}.(-1).n.\sin(n.x) + v.\frac{u.n.\sinh(n(y+h))}{\cosh(n(y+h))}$$

$$= -u.\sigma.\tan(\sigma.t+\epsilon) - u^2.n.\tan(n.x) + u.v.n.\tanh(n(y+h))$$

$$= -u\left\{\sigma.\tan(\sigma.t+\epsilon) + n\left[u.\tan(n.x) - v.\tanh(n(y+h))\right]\right\}$$

and $a_{fy} = a_{fy}(x,y,t)$

$$= \frac{\partial v}{\partial t}\bigg|_{(x,y,t)} + u.\frac{\partial v}{\partial x}\bigg|_{(x,y,t)} + v.\frac{\partial v}{\partial y}\bigg|_{(x,y,t)} \qquad \text{where } \begin{array}{l} u=u(x,y,t) \\ v=v(x,y,t) \end{array}$$

$$= \frac{v}{\cos(\sigma.t+\epsilon)}.(-1).\sigma.\sin(\sigma.t+\epsilon) + u.\frac{v}{\sin(nx)}.n.\cos(nx) + v.\frac{v.n.\cosh(n(y+h))}{\sinh(n(y+h))}$$

$$= -v.\sigma.\tan(\sigma.t+\epsilon) + \frac{u.v.n}{\tan(nx)} + \frac{v^2.n}{\tanh(n(y+h))}$$

$$= -v\left\{\sigma.\tan(\sigma.t+\epsilon) - n\left[\frac{u}{\tan(nx)} + \frac{v}{\tanh(n(y+h))}\right]\right\}$$

In terms of the dimensionless parameters, the components of fluid acceleration are

$$A_{fx}(X,Y,T) = -U\left\{\frac{2\pi}{P}.\tan\left(\frac{2\pi T}{P}+\epsilon\right)+N\left[U.\tan(NX)-V.\tanh(N(Y+H))\right]\right\} \qquad \text{(VI.11)}$$

$$A_{fy}(X,Y,T) = -V\left\{\frac{2\pi}{P}.\tan\left(\frac{2\pi T}{P}+\epsilon\right) - N\left[\frac{U}{\tan(NX)} + \frac{V}{\tanh(N(Y+H))}\right]\right\} \qquad \text{(VI.12)}$$

In the following description, the FORTRAN variable names which occur correspond to those used in the program; the description employs, however, the ordinary notation of algebra rather than the notation of the FORTRAN language.

The following six parameters are evaluated within the main program, shortly after the commencement of the computation of a particle trajectory and before the subroutine VEL is called for the first time:

$$\text{CONST 1} = \frac{s+k}{1+k} = 1 + \frac{s-1}{1+k} = 1 + \frac{\text{GRAV}}{1+\text{ADMASK}}$$

$$\text{CONST 2} = N = \frac{2\pi}{L} = \frac{2\pi}{\text{WLNG}}$$

$$\text{CONST 4} = \frac{2\pi}{P} = \frac{2\pi}{\text{WPER}}$$

$$\text{CONST 5} = (s+k) \cdot \frac{AP}{L} \cdot \frac{1}{\cosh(NH)} = (\text{GRAV}+1.0+\text{ADMASK}) \frac{\text{WAMP.WPER}}{\text{WLNG.cosh (CONST3)}}$$

$$\text{CONST 6} = \epsilon = \text{PHSE}$$

The values of the above parameters are dependent only upon the characteristics of the wave system and the characteristics of the particle; they are invariant with position and time. Accordingly, they are conveniently evaluated (once only) within the main program, in order to avoid the calculation of identical values in each execution of the subroutine VEL. The values of the parameters are made available within the subroutine VEL by a COMMON Declaration Statement.

The subroutine VEL, as modified for the computation of the trajectory of a particle within the standing wave system, is as follows:

```
SUBROUTINE VEL (XD, YD, TD)
IMPLICIT REAL*8(A-G, O-Z)
COMMON PART, RNO, CD, UFL, VFL, FDRX, FDRY, FFAX, FFAY
COMMON CONST1, CONST2, CONST3, CONST4, CONST5, CONST6
ARG1 = (CONST2*YD)+CONST3
ARG2 = (CONST2*XD)
ARG3 = (CONST4*TD)+CONST6
SNH1 = DSINH(ARG1)
CSH1 = DCOSH(ARG1)
TNH1 = DTANH(ARG1)
SIN2 = DSIN(ARG2)
COS2 = DCOS(ARG2)
TAN2 = DTAN(ARG2)
SIN3 = DSIN(ARG3)
COS3 = DCOS(ARG3)
TAN3 = DTAN(ARG3)
UFL  = CONST5*CSH1*COS2*COS3
VFL  = CONST5*SNH1*SIN2*COS3
```

```
AFX  = -UFL*((CONST4*TAN3)+CONST2*((UFL*TAN2)-(VFL*TNH1)))
AFY  = -VFL*((CONST4*TAN3)-CONST2*((UFL/TAN2)+(VFL/TNH1)))
FFAX=  AFX/CONST1
FFAY = AFY/CONST1
RETURN
END
```

A subroutine VELID, which causes the printing of an appropriate identification, is associated with the subroutine VEL.

VI. 2 The Application of the Computer Program in the Computation of a Particle Trajectory within the Standing Wave System

In the computation of the trajectory of a particle within the standing wave system, by means of the computer program described in Section VI. 1 above, the following procedure was adopted.

(i) From the experimentally measured characteristics of the wave system and properties of the particle, the dimensionless parameters WLNG, WPER, WAMP and DPTH were evaluated.

(ii) By examination of the photographic record of the experimentally determined particle trajectory, a suitable section of the trajectory was selected. The criteria for suitability included:-

(a) Visibility of the particle, and the absence of unduly large gaps in the recorded trajectory. As discussed in Appendix V, it was found necessary to confine the light from the stroboscope lamp into a narrow beam, and to follow the excursions of the particle with this beam. Occasionally, the light beam would fail to illuminate the particle during one or more flashes of the lamp, resulting in gaps in the recorded trajectory.

(b) Freedom from undue drift - that is, from undue net horizontal motion of the particle in the direction of the length of the flume.

(iii) The dimensionless coordinates (XSTART, YSTART) of the starting point of the selected section of the trajectory were determined. These parameters were evaluated either by converting (in accordance with Equation (2, 20), p. 40) the dimensional coordinates, or directly from dimensionless plots of the experimentally determined trajectories. In all cases, the first node to the right of the starting point was selected as the origin of the coordinate system. The parameter TSTART was invariably assigned a value of zero.

(iv) The value to be assigned to the phase parameter PHSE was estimated as follows:-

(a) In the case of a trajectory recorded by means of the Shackman Sequential-Frame Camera, the elevation of the water surface on a selected vertical line (at or near a point of maximum vertical displacement) within the field of view was measured, on the frame which showed the particle at the selected starting point, on a number of frames which preceded this frame and on a number of frames which followed this frame. These measurements yielded a plot of water surface elevation (at the selected vertical) versus time, and from this plot the phase relationship at the starting point was estimated.

(b) In the case of a trajectory recorded by means of the stroboscope, the phase relationship at the selected starting point was estimated, by examination of the relative positions of the selected starting point and preceding and succeeding recorded points on the particle trajectory.

(v) The values to be assigned to the components (UPTT and VPTT) of the particle velocity at the starting point were estimated,

(a) by measuring the components of the displacement, relative to the starting point, of the succeeding recorded particle position. The magnitudes of these displacement components, together with the known time interval between the photographic records, yielded an estimate of the components of particle velocity at the starting point.

(b) in those cases in which the phase relationship at the selected starting point indicated that the horizontal component of the fluid velocity at the starting point would approach zero, the horizontal component of particle velocity at the starting point (UPTT) was assigned a value of zero, and the vertical component of particle velocity at the starting point (VPTT) was assigned a value corresponding, in magnitude and sense, to the dimensionless settling velocity, in quiescent water, of the particle.

(vi) From the experimentally determined properties of the particle, the particle-fluid parameter PART and the gravitational parameter GRAV were evaluated.

The specific values assigned to the parameters discussed above, in the computation of the trajectories under discussion, are listed in Tables 2 and 3.

It was found that the efficiency of the computation tended to be greater, in the case of the computation of the trajectories of the experimental particles, than in the case of the computation of the trajectories of the(hypothetical) neutrally-buoyant particles in the model eddy field as described in Section 5.2. The experimental particles were of considerably greater diameter and mass than would be the neutrally-buoyant particles of Section 5.2. If a given change occurs in the force impressed on a particle, then the consequent effect on the form of the particle trajectory will be less in the case of a particle of greater mass than in the case of a particle of lesser mass. The enhanced efficiency of the computation in the case of the experimental particles is therefore attributed to the effect of increased particle mass in reducing the sensitivity of the form of the particle trajectory to a given change in the forces acting on the particle. In the execution of the computation as described in Section 4.2, variations in the estimated magnitudes of the average force components acting on the particle during its traverse of a segment of the trajectory will have comparatively little effect on the form of the trajectory segment, in the case of the experimental particles. Accordingly, the convergence criterion established by a given value of the parameter DELSCR will be satisfied after the computation of a relatively small number of trial trajectory points. In the computation of the trajectories of the experimental particles, the parameter DELSCR has been assigned a value of 10^{-7}, and the criterion thus established has apparently usually been satisfied after the computation of two trial points, this being the minimum number permitted within the structure of the program.

A computer program was developed for the purpose of plotting the computed trajectories of particles in the wave field, by modification of the program previously developed for the plotting of particle trajectories in the model eddy field.

Reference Cited in Appendix VI.

(VI. 1) Wiegel R.L. "Oceanographical Engineering" Prentice-Hall Inc., Englewood Cliffs N.J., U.S.A. 1964.

APPENDIX VII

The Interchange of Energy between a Suspended Particle and the Surrounding Fluid.

This appendix contains the results of the calculation of the interchange of energy between particle and fluid, for a number of computed particle trajectories. The provisions made in the computer program for the examination of the energy interchange are described in Section 4.4. The implications of the results are discussed in Section 6.3.6.

In accordance with the sign convention specified in Section 2.2.9 and Section 4.4, the transfer of an element of energy from the fluid to the particle has been assigned a positive sense. Conversely, the transfer of energy from the particle to the fluid has been assigned a negative sense.

In the course of the development of the computer program, the evaluation of the integral $\oint$ F.ds was carried out, in the computation of the particle trajectory numbered 600101. F represents the force exerted on the particle by the fluid during the traverse by the particle of the element ds of its trajectory, and each elemental product F.ds is assigned a sense in accordance with the convention outlined above.

Trajectory No. 600101 is shown in Figure VII.1. Table VII.A shows values of the integral $\int_{(X_o, Y_o)}^{(X, Y)}$ F.ds evaluated between the starting point (X_o, Y_o) and the arbitrarily-selected points whose co-ordinates (X, Y) are tabulated. Also tabulated are values of $(Y - Y_o)$, the vertical displacements of the particle with respect to its starting point.

Examination of Table VII. A indicates that -

(i) the value of $\oint$ F. ds integrated around one circuit of the trajectory from the starting point $(0.0, Y_O)$ to the point $(0.0, Y_O + \Delta Y)$, is very nearly equal to zero;

(ii) the interchange of energy between the particle and the fluid is associated primarily with variations in the potential energy of the particle.

These results are in conformity with expectations: the particle, after executing one circuit of the eddy, returns (virtually) to its starting point, with a velocity which differs very little from its velocity at the starting point, and consequently it is to be expected that the net transfer of energy between the particle and the fluid throughout one circuit of the eddy should be virtually zero. Also, the variations in the velocity of the particle which occur during the particle's traverse of its trajectory are relatively small, and consequently the variations in the kinetic energy of the particle are small, in comparison with the variations in the potential energy of the particle.

The predominance of the particle potential energy in the interchange of energy between the particle and the fluid is demonstrated by the close correspondence between the values of $\int_{(X_O, Y_O)}^{(X, Y)}$ F. ds and the values of (Y-Yo) in Table VII. A. In the computation of the trajectory at present under consideration (No. 600101) the gravitational parameter

(GRAV) was assigned a value of 1.0, corresponding to a ratio of 2,0 between the density of the particle and the density of the fluid. When this ratio has this particular value, a numerical equivalence exists between the dimensionless units of (potential) energy and the dimensionless units of elevation, as demonstrated in the following paragraphs.

The potential energy of a non-buoyant spherical particle which is submerged in a fluid may be expressed as

$$e = \frac{\pi d^3}{6} (\rho_p - \rho_f) gy \tag{VII.1}$$

where

e = the potential energy of the particle, with respect to an arbitrary datum plane,

d = the diameter of the particle

ρ_p = the density of the particle

ρ_f = the density of the fluid

g = the gravitational acceleration

y = the elevation of the particle, above the datum plane.

In the formulation of the equation of motion - Equation (2,17), p.39 - on which the computation of the particle trajectories has been based, terms with the dimensions of a force have been made dimensionless by dividing by the weight of a fluid element having a volume equal to that of the particle - that is, by dividing by $\frac{\pi d^3}{6} \rho_f g$

Equation (VII.1) consequently leads to the following relationship between the dimensionless units of energy (E) and the dimensionless units of elevation (Y):

$$E = (s-1.0)Y$$

where s = the ratio of the density of the particle to the density of the fluid.

Accordingly, in the particular case of a particle for which the value of s is 2.0, a numerical equivalence exists between the dimensionless units of energy and the dimensionless units of elevation.

In the computation of the trajectory 610101-620101, which is illustrated in Figure 17, the "Moment of Work" has been computed as described in Section 4.4. As defined by Equation (4.5) p. 67 the "Moment of Work" is evaluated as

$$M = \oint R(F.ds)$$

where R is the radial distance from the eddy centre, as (more strictly) defined below Equation (4.5).

The results of this computation are shown in Appendix III. In a restarted computation (as in this case) the accumulated value of the Moment of Work has not been automatically transferred from the initial computation to the subsequent computation. Accordingly, the values of Moment of Work in Computation 620101 must be adjusted, by a value corresponding to the sum accumulated up to the final point of Computation 610101.

Some representative results are shown in Table VII.B. The tabulated values, for a number of arbitrarily-selected points on the computed trajectory, comprise the position co-ordinates X and Y, the radial distance R from the eddy centre to the computed point, and M(X, Y), the moment of work integrated from the starting point (X_O, Y_O) to the point (X, Y)

$$M\ (X, Y) \quad = \quad \oint_{(X_O, Y_O)}^{(X, Y)} \qquad R(F, ds)$$

Interpolating between the last two points tabulated in Table VII. B, the value of M, integrated around the trajectory traversed by the particle in executing one circuit of the eddy, is estimated to be + 490. The sense and magnitude of this quantity are to be interpreted as described below.

As the radial distance R and the length of the trajectory segment ds are, by definition, positive in sense, each element of the integral has the sign corresponding to the sense of the associated transfer of energy, as specified in Section 4.4. Throughout one circuit of the eddy, the net transfer of energy to the particle is zero, as pointed out in the discussion (above) of the trajectory 600101. Consequently, if $\oint R(F, ds)$, evaluated around one circuit of the eddy, has a positive sense, it is implied that the transfer of energy to the particle from the fluid (a transfer in this sense having been assigned a positive sense) has, on the average, occurred at a greater distance from the eddy centre than has the transfer of energy from the particle to the fluid. Accordingly, if $\oint R(F. ds)$ has a positive sign, as in the case at present under consideration, it is implied that energy has been transferred towards the centre of the eddy from the more outlying zones traversed by the particle trajectory. The occurrence of a negative sign would, conversely, imply an outward transfer of energy.

In examining the magnitude of $\oint R(F.ds)$ it is convenient to assume that all the energy involved in the particle-fluid energy interchange can be accounted for as potential energy of the particle. This assumption is justified in the light of the discussion above of the results for the trajectory 600101. The trajectory at present under discussion (610101-620101) has been computed for a particle having a density ratio s of 2.0 and hence, as pointed out above, a numerical equivalence exists between the dimensionless units of potential energy and the dimensionless units of elevation. Table VII.B indicates that the magnitude of the vertical excursion of the particle, between the vertical extremities of its trajectory, is (18.0775 + 18.0756) units or, that is, 36.1531 units. (The points tabulated in Table VII.B include those two points, of the computed points for which results have been printed, which have extreme values of Y). Accordingly, within those segments of its trajectory in which the vertical component of the particle velocity has a negative sense, the particle will contribute to the fluid a total quantity of energy ΔE equivalent to 36.15 units (rounding-off the above figure). Within the "rising" segments of its trajectory, the particle will acquire from the fluid an equal quantity of potential energy.

The mean change in radius associated with the transfer of this quantity of energy is given by

$$\Delta R = \frac{\oint R\,(F.ds)}{\Delta E}$$

$$= \frac{490}{36.15} \doteqdot 13.6 \quad \text{Units}$$

Table VII. C shows the results of some calculations, similar to that outlined above, for a number of computed trajectories of suspended particles. The magnitude of ΔR (the mean interval of radial distance over which the transfer of energy occurs) appears to be dependent upon the specific characteristics of the trajectory, as might be expected. In the case of the first five trajectories tabulated in Table VII. C, however, the magnitude of ΔR relative to the spacing of eddy centres tends to be fairly constant, in spite of variations in the parameters which define the properties of the particle and of the eddy field. The starting point of each of these five trajectories is at the same relative position within the eddy field (X_O = 0.0, Y_O = 0.3 Yc), and the trajectories are generally similar in overall form. In the case of the final two trajectories in Table VII. C, the relative positions of the starting points within the eddy field differ from that associated with the first five trajectories, and the forms of the trajectories differ somewhat from those of the first five - as indicated in Figure 22, in which the forms of these trajectories may be compared with that of Trajectory No. 2.16 (610101-620101). The values of ΔR (relative to the spacing of eddy centres) associated with these two trajectories are somewhat less than those associated with the first five trajectories, but are nevertheless of the same order of magnitude - namely, of the order of one-fifth of the spacing of the eddy centres. In all cases the sense of the net transfer of energy is inward - that is, toward the eddy centre.

The above results are specific to the conditions applying in the particular computations involved, and no general quantitative conclusion can be drawn. The computations have demonstrated, however, that the suspension of a particle within an eddy can cause a net transfer of energy between different zones of an eddy

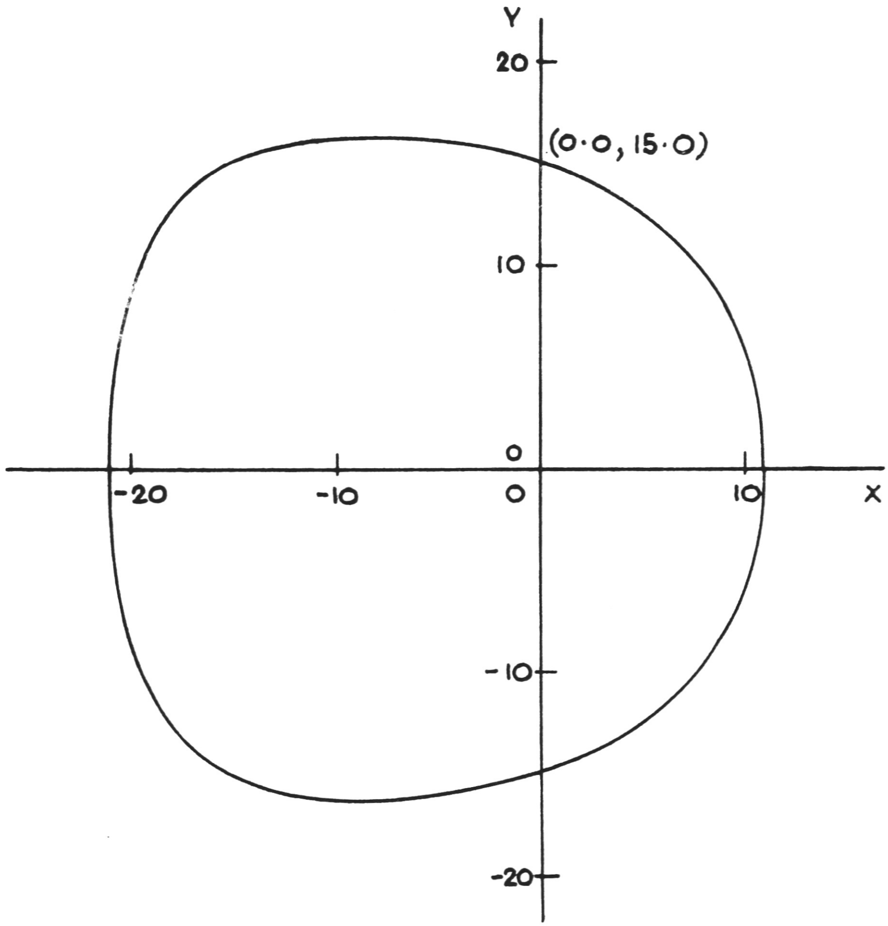

FIGURE VII.1: PARTICLE TRAJECTORY 600101

Table VII.A Computed Points on Particle Trajectory 600101

X	Y	$\int_{(X_0Y_0)}^{(X,Y)} F.ds$	$Y - Y_0$
0.0000	15.0000	0.0000	0.0000
3.1354	13.7152	- 1.283	- 1.2848
6.2841	11.5693	- 3.430	- 3.4307
8.6563	8.8012	- 6.198	- 6.1988
9.9142	6.3503	- 8.647	- 8.6497
10.8058	3.1997	-11.80	-11.8003
11.0884	0.0495	-14.95	-14.9505
10.8279	-3.1003	-18.10	-18.1003
9.9645	-6.2497	-21.25	-21.2497
8.7394	-8.6988	-23.70	-23.6988
6.4175	-11.4783	-26.48	-26.4783
3.2661	-13.6776	-28.68	-28.6776
0.1155	-14.9995	-30.00	-29.9995
- 2.3346	-15.6553	-30.65	-30.6553
-5.1345	- 16.1051	-31.10	-31.1051
-8.1379	- 16.2693	-31.27	-31.2693
-12.1844	- 15.8959	-30.90	-30.8959
-14.9828	- 15.0112	-30.02	-30.0112
-18.5362	- 12.0009	-27.01	-27.0009
-20.1805	- 8.1486	-23.16	-23.1486
-20.8979	- 3.9475	- 18.95	-18.9475
-21.0826	- 0.0972	- 15.10	-15.0972
-20.8786	4.1625	- 10.84	-10.8375
-20.2219	8.0114	- 6.997	- 6.9886
-18.4087	12.2089	- 2.802	- 2.7911
-15.1404	14.9579	- 0.05266	- 0.0421
-12.3388	15.8845	0.8769	0.8845
- 8.1373	16.2896	1.287	1.2896
- 5.3368	16.1476	1.148	1.1476
- 2.1866	15.6465	0.6483	0.6465
- 0.0867	15.0903	0.09238	0.0903
0.2633	14.9775	-0.02044	-0.0225

Table VII. B Computed Points on Particle Trajectory 610101-620101.

X	Y	R	$\int_{(X_o, Y_o)}^{(X, Y)} R(F.ds)$
0.0000	15.0000	15.0000	0.0000
3.1352	13.2603	13.6258	-24.78
5.5816	11.2077	12.5207	-51.55
7.9032	8.0562	11.2855	-88.95
8.9724	5.6055	10.5794	-115.7
9.6544	2.8050	10.0536	-144.5
9.8713	0.0049	9.8713	-172.3
9.6579	-2.7950	10.0542	-200.1
8.9803	-5.5945	10.5804	-228.9
7.9169	-8.0438	11.2863	-255.7
5.2629	-11.5401	12.6835	-297.4
3.1619	-13.2556	13.6275	-320.0
0.0111	-15.0132	15.0132	-345.0
-6.2889	-17.0225	18.1471	-377.9
-11.8876	-17.8790	21.4703	-394.7
-16.0142	-18.0775	24.1506	-399.2
-18.1706	-17.9832	25.5649	-396.9
-22.3412	-16.5561	27.8071	-358.1
-23.5559	-14.5202	27.6716	-301.5
-24.1250	-11.7967	26.8548	-227.1
-24.4099	-8.5049	25.8491	-140.4
-24.5261	-5.7039	25.1806	-68.94
-24.5882	-2.5673	24.7219	9.26
-24.6026	-0.1172	24.6029	69.6
-24.5885	2.5407	24.7194	135.1
-24.5196	5.9219	25.2246	219.4
-24.3980	8.7125	25.9070	290.7
-24.1400	11.6802	26.8173	368.8
-23.5061	14.6651	27.7056	450.2
-22.3961	16.5033	27.8199	501.4
-19.5153	17.7999	26.4137	536.9
-18.0664	17.9906	25.4962	541.9
-15.7912	18.0756	24.0019	544.1
-13.3440	17.9914	22.3998	542.2
-11.2432	17.8118	21.0635	538.3
-9.1426	17.5415	19.7811	532.8
-5.9920	16.9550	17.9827	521.8
-2.8419	16.1030	16.3519	507.3
-0.0421	15.0367	15.0368	490.6
0.3079	14.8765	14.8797	488.2

Table VII.C The Interchange of Energy between Suspended Particles and the Surrounding Fluid.

Trajectory Reference Number	Particle-Fluid Parameter PART	Gravitational Parameter GRAV	Spacing of Eddy Centres XCNTR	Ordinate of Starting Point YSTART	Vertical Extremities of Trajectory Y_{max} Y_{min}	Vertical Excursion of Particle Y_{ex}	$(s-1.0)Y_{ex}$	Moment of Work $\oint R\, F.ds$	$\Delta R = \frac{\oint R\, F.ds}{(s-1.0)Y_{ex}}$	$\frac{\Delta R}{XCNTR}$
2.16	1.1068	1.00	50.625	15.00	18.0756 -18.0775	36.1531	36.15	+490	13.6	0.268
2.18	1.1068	1.00	270.00	80.00	90.1198 -90.1189	180.2387	180.24	+10,520	58.4	0.216
3.5	1.1068	1.65	50.625	15.00	18.6497 -18.6532	37.3029	61.55	+ 881	14.3	0.283
4.8	1.1068	10.40	50.625	15.00	18.6199 - 18.5929	37.2128	387.01	+5429	14.0	0.277
5.4	0.00234	2200	0.500	0.15	0.1805 - 0.1804	0.3609	793.98	+ 88	0.111	0.222
6.2	1.1068	1.00	50.625	5.00	8.1049 - 8.1040	16.2089	16.21	+148	9.1	0.180
6.1	1.1068	1.00	50.625	0.00	6.1294 - 6.1298	12.2592	12.26	+101	8.2	0.163

APPENDIX VIII

The Spiral Form of the Computed Trajectories of Non-buoyant Particles

The spiral form of the computed trajectories of non-buoyant particles suspended within the model eddy field has been described in Section 6.3.7. The magnitude of the spiral effect, in the computed trajectories of a number of suspended particles, is indicated in Table VIII.A. The tabulated quantities S' and S represent the increase in the radial distance from the eddy centre to the particle trajectory, as compared with the corresponding distance at the starting point, when the angular displacement of the particle from its starting point (with the point (0.0, 0.0) as origin) is π and 2π radians respectively. These quantities are defined in the diagram which accompanies Table VIII.A. In the case of Trajectory 6.1, the starting point is at the eddy centre (0.0, 0.0) and S is the abscissa of the point in which the particle trajectory, after executing one circuit of the eddy, intersects the line Y = 0.0.

The trajectories listed in Table VIII.A generally differ somewhat in form, one from another, and so precise comparisons are not possible. The general trend of the effect of the density of the particle, relative to that of the suspending fluid, is shown in Figure VIII.1, in which the values of S for Trajectories 2.16, 3.5 and 4.8 are plotted against the values of (s-1.0) where s is the ratio of the density of the particle to the density of the suspending fluid. In the computations of these three trajectories, all parameters had constant values, with the exception of the gravitational parameter (s-1.0) and the characteristic fluid velocity within the eddy field.

It is of interest to note that in Table VIII. A the values of S' tend to be relatively close to the corresponding values of S. This trend implies that most of the spiral effect occurs in that section of the trajectory between $\theta = 0$ and $\theta = \pi$. In each case, this section of the trajectory is shorter than is the section between $\theta = \pi$ and $\theta = 2\pi$, and accordingly it is implied that the rate of spiralling is not uniform along the length of the trajectory. The former section of the trajectory $(0 \leq \theta \leq \pi)$ traverses a zone which is relatively close to the eddy centre, and in which the curvature of the streamlines is relatively sharp. In the case of Trajectory 2.16, S' is slightly greater than S; no explanation of this phenomenon is available.

The final column of Table VIII. A shows, for each trajectory, the magnitude of S relative to the overall height (between vertical extremities) of the computed particle trajectory. It is evident that the values of S are small, in relation to the overall dimensions of the computed trajectories, as is borne out in the plotted trajectories (as, for example, in Figure 17).

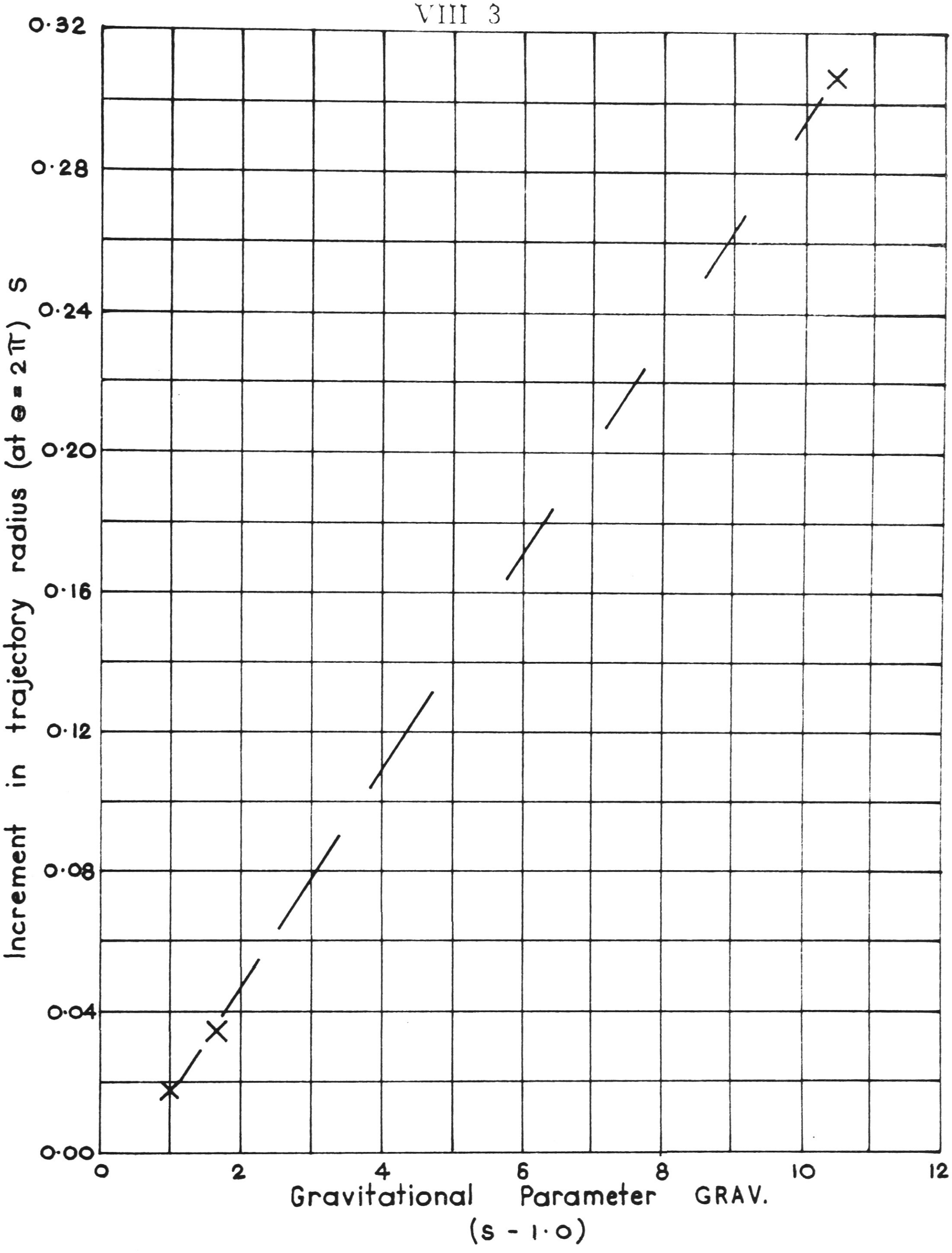

FIGURE VIII.1: THE SPIRAL FORM OF COMPUTED PARTICLE TRAJECTORIES : EFFECT OF VARIATION IN THE PARAMETER GRAV.

Table VIII.A The Spiral Form of Computed Particle Trajectories.

Definitions:

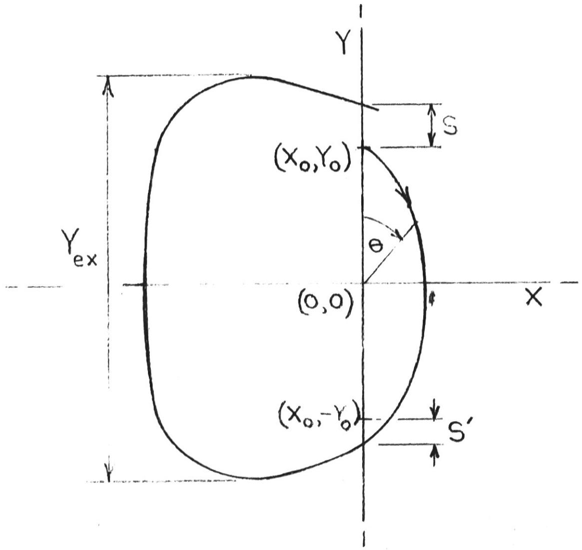

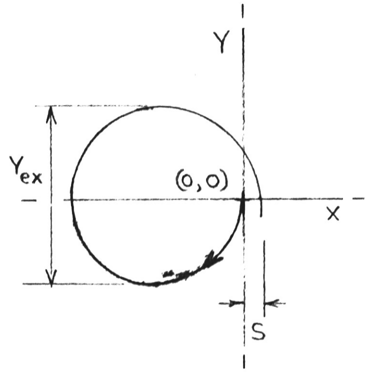

Trajectory Ref. N° 6.1

Trajectory		Starting Point θ = 0		θ = π			θ = 2π			Y_{ex}	$\frac{S}{Y_{ex}}$
Ref. No.	Tble.	Xo	Yo	X	Y	S'	X	Y	S		
2.16	7	0.0000	15.0000	0.0000	-15.0182	0.0182	0.0000	15.0178	0.0178	36.15	.00049
2.9	7	0.0000	40.0000	0.0000	-40.0314	0.0314	0.0000	40.0504	0.0504	90.19	.00056
2.18	7	0.0000	80.0000	0.0000	-80.0196	0.0196	0.0000	80.0225	0.0225	180.24	.00012
3.5	8	0.0000	15.0000	0.0000	-15.0317	0.0317	0.0000	15.0322	0.0322	37.30	.00086
4.8	9	0.0000	15.0000	0.0000	-15.2450	0.2450	0.0000	15.3068	0.3068	37.21	.0082
5.4	10	0.0000	0.1500	0.0000	-0.1503	0.0003	0.0000	0.1504	0.0004	0.36	.0011
6.2	11	0.0000	5.0000	0.0000	-5.0105	0.0105	0.0000	5.0197	0.0197	16.21	.0012
6.1	11	0.0000	0.0000				0.0081	0.0000	0.0081	12.26	.00066

APPENDIX IX.

The Symmetry of the Computed Particle Trajectories

In Section 6.3.8, attention is drawn to the existence of certain symmetries in the computed particle trajectories. Consecutively-traversed sections of the trajectory, located within quadrants which are on a given side of the line X = 0.0, form symmetrical pairs.

In discussing the symmetry of sections of the particle trajectory, it is convenient to consider a pair of trajectory sections, one of which is located in the first quadrant ($X \geq 0$, $Y \geq 0$) and the other of which is located in the second quadrant ($X \geq 0$, $Y < 0$). For this pair of trajectory sections, the axis of symmetry will be the line Y = 0.0. The discussion will, however, be applicable to any pair of consecutively-traversed sections of the trajectory, provided that both are on a given side of the line X = 0.0.

The direction (relative to the coordinate axes) of the particle trajectory at any point depends upon the ratio of the components, parallel to the respective coordinate axes, of the velocity of the particle at that point. If the sections of the trajectory located within the first and second quadrants are symmetrical (in geometric form) about the line Y = 0.0, it is implied that the particle, having passed through a point (X, Y) in the first quadrant, will subsequently pass through the point (X, -Y) in the second quadrant, with the following relationship being satisfied:-

$$-\frac{U_p\,(X, Y)}{U_p\,(X, -Y)} = \frac{V_p\,(X, Y)}{V_p\,(X, -Y)} = r$$

where U_p (X, Y) and V_p (X, Y) are the components, in the x and y co-ordinate directions respectively, of the velocity of the particle at the point (X, Y), and r is a constant, for all pairs of points (X, Y), (X, - Y).

Examination of the results of the computations of particle trajectories - as typified by the results of the computation of the trajectory identified as No. 610101 - 620101 (Figure 17 and Appendix III, p. III.15-III.36) - indicates that these conditions are substantially satisfied. Furthermore, when the components of particle velocity at a point (X, Y) are compared with the corresponding velocity components at the computed point (for which results are printed) which is closest to the point (X, - Y) then it is evident that the somewhat more restrictive condition, that the value of r should be unity, is substantially satisfied. This implies that the distribution with distance (measured, from the line Y = 0.0, along the two sections of the trajectory) of the magnitudes of the particle velocity components must be identical, along the two sections of the trajectory. It is also implied that the time required for the particle to traverse that section of its trajectory which lies within the first quadrant should be equal to that required for its traverse of the section which lies within the second quadrant, the two sections being equal in length. The results indicate that this condition is substantially fulfilled.

The conditions for the existence of symmetry of geometric form, and of symmetry of particle velocities (as observed to exist in the computed trajectories) may be expressed in terms of particle accelerations:

$$A_{px}(X, Y) = A_{px}(X, -Y)$$

$$A_{py}(X, Y) = -A_{py}(X, -Y)$$

where $A_{px}(X, Y)$ and $A_{py}(X, Y)$ are the components, in the x and y co-ordinate directions respectively, of the particle acceleration at the point (X, Y),

provided that continuity of the particle velocity exists at the intersection of the particle trajectory with the line $Y = 0.0$.

The existence of symmetry of the particle trajectory about the line $Y = 0.0$ implies that the particle trajectory must cross this line orthogonally. The computed trajectories satisfy this condition. This is to be expected, since at the line $Y = 0.0$ the horizontal component of the fluid velocity is zero, and consequently the velocity of the particle tends to be in the direction of the gravitational vector (that is, vertically downwards).

For the existence of symmetry about the line $X = 0.0$, it would be necessary that the particle trajectory should cross the line $X = 0.0$ orthogonally. It has been observed, however, that at all points on its trajectory a non-buoyant particle tends to have a sensibly invariant, non-zero vertical component of velocity relative to the surrounding fluid. The fluid streamlines cross the line $X = 0.0$ orthogonally, and hence the existence of such a component of relative velocity precludes the particle trajectory's crossing this line orthogonally. The computed trajectories of non-buoyant particles indicate considerable asymmetry about the line $X = 0.0$.